

Regulation of protein synthesis during doxorubicin-induced toxicity

Thesis submitted for the degree of
Doctor of Philosophy
at the University of Leicester

By

Robert Harvey BSc

Medical Research Council Toxicology Unit
University of Leicester

September 2016

Abstract

Regulation of protein synthesis during doxorubicin-induced toxicity

By Robert Harvey

In response to DNA damage, cells decrease global rates of protein synthesis to conserve energy and selectively translate mRNAs of proteins involved in the DNA damage response.

Doxorubicin is a widely used chemotherapeutic that induces double strand DNA breaks. It might be expected that doxorubicin-induced DNA damage would rapidly inhibit global protein synthesis through the phosphorylation of eIF2 α , as has been observed in response to UVB-induced DNA damage. However, in MCF10A cells, a delay of 9 hours was observed between DNA damage recognition and protein synthesis inhibition. Furthermore, eIF2 α phosphorylation was not observed until 12 hours, and global protein synthesis inhibition was subsequently shown to be independent of eIF2 α phosphorylation status.

An alternative regulator of translation initiation is the mTORC1 target protein 4E-BP1. Doxorubicin-induced mTORC1 inhibition preceded eIF2 α phosphorylation and correlated with the inhibition of global protein synthesis, suggesting that the DDR signalled through mTOR to regulate protein synthesis. Experiments using p53^{-/-} MCF10A cells suggested that doxorubicin-induced mTORC1 inhibition was mediated by p53 activity, and p53^{-/-} cells were shown to be more sensitive to doxorubicin-induced cell death.

Interestingly, doxorubicin-and catalytic-inhibition of mTORC1 activity mediated the phosphorylation of eIF2 α in a signalling mechanism that may be dependent on PP6, DNA-PKcs and GCN2 or PERK. Importantly, eIF2 α phosphorylation was absent in response to doxorubicin in p53^{-/-} cells, whereas catalytic inhibition of mTORC1 activity enhanced eIF2 α phosphorylation. These data suggested a mechanism where p53-mediated mTORC1 inhibition signalled to enhance the phosphorylation of eIF2 α .

Acknowledgements

First, I would like to thank my supervisor, Anne Willis, for giving me the opportunity to complete a PhD within her laboratory and for her support, advice and general positivity throughout my PhD.

A very big thank you to all past and present members of the Willis group who have helped me through the past 4 years, especially Tuija Pöyry and Mark Stoneley, who have both supported me in the lab and always made time to help me make sense of my data. I am also particularly grateful to Lindsay Wilson, who was kind enough to help me find everything when I first joined the lab, and Jashu Meisuria, without whom the lab would grind to a halt. A specially thank you to Lucia Pinon for her help and support with everything related to FACS. Your time, knowledge and advice has been invaluable.

Thank you to all my family, especially my parents Ken and Marion, who have always believed in me, been there to support me, and taught me that hard work pays off. Finally, I must thank my wife, Naomi, who did not complain (too much) about the long hours I spent in the lab during my final months, I could not have done this without you.

Table of Contents

Abstract	i
Acknowledgements	ii
Table of Contents	iii
List of Tables	ix
List of Figures	x
List of abbreviations	xii
1 Introduction	1
1.1 mRNA processing	1
1.2 Cap-dependent translation.....	1
1.2.1 Translation Initiation.....	2
1.2.1.1 Assembly of the 43S pre-initiation complex	2
1.2.1.2 Recruitment of the 43S pre-initiation complex	5
1.2.1.3 Ribosomal scanning of the 5' UTR.....	5
1.2.1.4 Start codon recognition	6
1.2.1.5 Assembly of the 80S ribosome	7
1.2.2 Translation elongation	7
1.2.3 Translation termination	10
1.3 Cap-independent translation	10
1.4 Regulation of translation initiation.....	10
1.4.1 Regulation of ternary complex	11
1.4.1.1 eIF2 α kinases.....	13
1.4.1.1.1 GCN2.....	13
1.4.1.1.2 PKR	13
1.4.1.1.3 PERK.....	14
1.4.1.1.4 HRI.....	14
1.4.1.2 Selective translation of mRNA	15
1.4.1.3 eIF2 α dephosphorylation	17
1.5 mTOR signalling.....	18
1.5.1 mTORC1.....	18
1.5.1.1 Regulation of mTORC1 activity	19
1.5.1.2 mTORC1 regulation of protein synthesis	23
1.5.1.2.14E-BP	24

1.5.1.2.2	p70 S6K.....	26
1.5.1.2.3	5' terminal oligopyrimidine mRNA	27
1.5.1.2.4	Ribosome biogenesis	27
1.5.1.3	Feedback mechanisms regulating mTORC1 activity	28
1.5.2	mTORC2.....	29
1.5.2.1	Regulation of mTORC2 activity	29
1.5.2.2	mTORC2 dependent cellular processes	30
1.5.3	mTORC1-mTORC2 crosstalk signalling	30
1.5.4	Dysregulation of mTOR in cancer.....	31
1.6	DNA damage.....	32
1.6.1	Endogenous DNA damage	32
1.6.2	Exogenous DNA damage	32
1.7	Topoisomerase enzymes	33
1.7.1	Type I topoisomerase	33
1.7.2	Type II topoisomerase	34
1.7.2.1	Catalytic mechanism of topoisomerase II	34
1.7.3	Therapeutic targeting of topoisomerases	37
1.7.3.1	Doxorubicin	37
1.7.3.1.1	Doxorubicin-dependent inhibition of topoisomerase II.....	37
1.7.3.1.2	Doxorubicin generates reactive oxygen species	38
1.7.3.1.3	Cardiotoxicity limits the effectiveness of doxorubicin	38
1.8	DNA damage response signalling.....	39
1.8.1	ATM	41
1.8.2	ATR.....	42
1.8.3	DNA-PKcs.....	43
1.9	p53.....	45
1.9.1	Stabilisation and activation of p53	45
1.9.2	p53 activation in response to DNA damage	47
1.9.2.1	Cell cycle regulation	47
1.9.2.2	p53 dependent regulation of the cell cycle	50
1.9.2.2.1	G1/S cell cycle arrest.....	50
1.9.2.2.2	G2/M cell cycle arrest	50
1.9.2.3	p53 mediated apoptosis	51
1.9.2.4	p53 mediated regulation of mTOR signalling	51

1.10	Aims of thesis.....	54
2	Materials and methods	56
2.1	Chemicals and reagents.....	56
2.1.1	Buffers.....	56
2.2	Cell culture techniques.....	57
2.2.1	Cell lines	57
2.2.2	Cell maintenance	57
2.2.2.1	MCF10A p53 ^{+/+} cells	57
2.2.2.2	MCF10A p53 ^{-/-} cells.....	57
2.2.2.3	Synchronisation of MCF10A cells	57
2.2.2.4	Cryopreservation of cell lines	59
2.2.2.5	Reviving frozen cell stocks	59
2.2.3	Cell transfection	59
2.2.3.1	Plasmid DNA transfection	59
2.2.3.2	siRNA transfection.....	59
2.2.4	Treatment with doxorubicin.....	62
2.2.5	Treatment with small molecule inhibitors	62
2.2.6	Flow cytometry.....	64
2.2.6.1	Cell death analysis	64
2.2.6.2	Cell cycle analysis of live cells	64
2.2.6.3	Ethanol fixation of cells	64
2.2.6.4	Cell cycle analysis of fixed cells	64
2.2.6.5	Quantification of S-phase cells.....	65
2.2.6.6	Quantification of reactive oxygen species	67
2.2.6.7	Analysis of flow cytometry data	67
2.2.7	Low resolution, high content fluorescent microscopy	69
2.2.8	β-Galactosidase senescence staining	69
2.2.9	Microscopy.....	69
2.3	Protein techniques.....	70
2.3.1	Preparation of protein samples.....	70
2.3.1.1	Whole cell lysis.....	70
2.3.1.2	Protein quantification.....	70
2.3.2	Western blotting.....	70

2.3.2.1	Protein sample preparation	70
2.3.2.2	SDS-polyacrylamide gel electrophoresis	72
2.3.2.3	Protein transfer to PVDF membrane	72
2.3.2.4	Ponceau staining.....	72
2.3.2.5	Primary antibody incubation	72
2.3.2.6	Secondary antibody incubation and ECL detection	73
2.3.2.7	Secondary antibody incubation and LI-COR detection	73
2.3.2.8	Removal of antigens from PVDF membranes.....	77
2.3.2.9	Quantification of band intensity	77
2.3.3	Radiolabelling	77
2.3.3.1	^[35] S methionine incorporation	77
2.3.3.2	^[3] H uridine incorporation	77
2.3.3.3	Radioisotope precipitation and quantification.....	77
2.3.3.4	Normalisation of spectral counts	78
2.3.4	Polysome profiling	78
2.3.4.1	Preparation of cell lysate	78
2.3.4.2	Sucrose density centrifugation	78
2.3.5	Statistical analysis	79
2.4	Bacterial Techniques	80
2.4.1	Bacterial cell transformation	80
2.4.2	Bacterial culture	80
2.4.3	Bacterial glycerol stocks	80
3	Doxorubicin-induced eIF2α phosphorylation and inhibition of translation initiation	81
3.1	Introduction	81
3.1.1	eIF2 α dependent regulation of protein synthesis.....	81
3.1.2	DNA damage dependent protein synthesis inhibition	81
3.1.3	Inhibition of Topoisomerase II by doxorubicin	82
3.1.4	Aims	82
3.2	Results	84
3.2.1	Optimisation of doxorubicin treatment in MCF10A cells	84
3.2.2	Doxorubicin induced G2/M cell cycle arrest.....	88

3.2.3	Doxorubicin inhibited global protein synthesis and translation initiation	91
3.2.4	Combination of eIF2 kinases may regulate doxorubicin-induced eIF2 α phosphorylation.....	95
3.2.5	eIF2 α phosphorylation was not required for doxorubicin-induced inhibition of protein synthesis	99
3.3	Discussion	104
4	Doxorubicin-induced inhibition of mTORC1 signalling.....	107
4.1	Introduction	107
4.1.1	Regulation of mTORC1 signalling	107
4.1.2	mTORC1 regulation of protein synthesis.....	109
4.1.3	Regulation of mTORC1 by cellular stress.....	109
4.1.4	Aims	110
4.2	Results	111
4.2.1	Doxorubicin inhibited mTOR signalling	111
4.2.2	Doxorubicin induced crosstalk signalling between mTOR and eIF2	117
4.2.3	Treatment with doxorubicin induced a senescence-like phenotype	123
4.2.4	Doxorubicin did not induce substantial ROS generation	127
4.3	Discussion	132
5	Doxorubicin-induced inhibition of mTORC1 signalling was mediated by p53	135
5.1	Introduction	135
5.1.1	DNA damage signalling	135
5.1.2	p53 dependent DNA damage cell cycle checkpoints.....	136
5.1.3	Aims	136
5.2	Results	137
5.2.1	Doxorubicin-induced eIF2 α phosphorylation and mTOR inhibition was not dependent on cell cycle state	137
5.2.2	The role of DNA damage signalling pathways in doxorubicin-induced mTOR inhibition was unclear.....	144
5.2.3	Doxorubicin-induced mTORC1 inhibition was mediated by p53	150

5.2.4	p53 ^{-/-} cells were less sensitive to doxorubicin-induced inhibition of translation initiation	152
5.2.5	Doxorubicin-induced eIF2α phosphorylation was dependent on p53 mediated mTORC1 inhibition	155
5.2.6	Knockdown of endogenous p53 recapitulated the response in p53 ^{-/-} cells	158
5.2.7	p53 was required for doxorubicin-induced G1 arrest.....	160
5.3	Discussion	163
6	Discussion	166
6.1	Proposed model for doxorubicin-induced protein synthesis inhibition.....	166
6.2	Role of eIF2α in doxorubicin-induced toxicity	169
6.3	Doxorubicin-induced protein synthesis inhibition was likely mediated by mTORC1 inhibition	170
6.4	Doxorubicin-induced mTORC1 inhibition was mediated by p53 activity	172
6.5	Crosstalk signalling from mTORC1 inhibition mediated eIF2α phosphorylation.....	174
	References	177

List of Tables

Table 2-1. MCF10A cell culture media	58
Table 2-2. siRNA target sequences	61
Table 2-3. Small molecule inhibitors	63
Table 2-4. EdU reaction cocktail	66
Table 2-5. Recipes for SDS-PAGE gels	71
Table 2-6. Primary antibodies for non-phosphorylated target proteins	74
Table 2-7. Primary antibodies for phosphorylated target proteins.....	75
Table 2-8. Secondary antibodies.....	76

List of Figures

Figure 1-1. Translation initiation	4
Figure 1-2. Translation elongation.....	9
Figure 1-3. Regulation of ternary complex	12
Figure 1-4. Re-initiation model of ATF4 mRNA translation	16
Figure 1-5. Activation of mTORC1 at the surface of lysosome	20
Figure 1-6. Schematic representation of mTOR signalling.....	22
Figure 1-7. mTORC1 dependent regulation of 4E-BP1 and protein synthesis..	25
Figure 1-8. Catalytic cycle of topoisomerase II	36
Figure 1-9. Schematic representation of the DNA damage response	40
Figure 1-10. Stabilisation of p53.....	46
Figure 1-11. Regulation of cell cycle progression	49
Figure 1-12. p53 dependent regulation of mTOR signalling.....	53
Figure 2-1. Gating of FACS analysis	68
Figure 3-1. DNA damage response in MCF10A cells	85
Figure 3-2. Lower concentrations of doxorubicin induced G2/M arrest but not cell death	87
Figure 3-3. Doxorubicin induced G2/M arrest	89
Figure 3-4. Reduction of S-phase cells in response to doxorubicin	90
Figure 3-5. Doxorubicin inhibited global protein synthesis	92
Figure 3-6. Doxorubicin inhibited translation initiation in MCF10A cells.....	94
Figure 3-7. Depletion of individual eIF2 α kinases had a modest effect on eIF2 α phosphorylation induced by doxorubicin	96
Figure 3-8. Depletion of multiple eIF2 α kinases reduced eIF2 α phosphorylation induced by doxorubicin.....	98
Figure 3-9. ISRIB rescued thapsigargin induced protein synthesis inhibition .	101
Figure 3-10. ISRIB did not rescue protein synthesis inhibition induced by doxorubicin	103
Figure 4-1. Regulation of TSC and mTOR signalling	108
Figure 4-2. Doxorubicin inhibited mTORC1 signalling	112
Figure 4-3. Depletion of TSC2 did not rescue doxorubicin-induced protein synthesis inhibition	114
Figure 4-4. Partial depletion of 4E-BP1/4E-BP2 did not rescue doxorubicin- induced protein synthesis inhibition.....	116

Figure 4-5. Catalytic inhibition of mTOR enhanced eIF2 α phosphorylation	118
Figure 4-6. Depletion of PP6c diminished doxorubicin and AZD8055 induced eIF2 α phosphorylation	120
Figure 4-7. Double and triple knockdown of eIF2 α kinases diminished AZD8055 induced eIF2 α phosphorylation	122
Figure 4-8. MCF10A cells did not immediately recover from doxorubicin treatment	124
Figure 4-9. Doxorubicin rapidly induced a senescence-like phenotype	126
Figure 4-10. Quantification of reactive oxygen species using low resolution, high content fluorescent microscopy	128
Figure 4-11. FACS quantification of reactive oxygen species after treatment with doxorubicin	131
Figure 5-1. Synchronisation of MCF10A cells	138
Figure 5-2. Doxorubicin inhibited cell cycle progression following release from synchronisation	140
Figure 5-3. eIF2 α phosphorylation and mTORC1 inhibition were observed in synchronised cells treated with doxorubicin	142
Figure 5-4. DNA damage signalling inhibitors did not alleviate mTOR inhibition or eIF2 α phosphorylation.....	145
Figure 5-5. Analysis of doxorubicin-induced mTOR inhibition and eIF2 α phosphorylation following depletion of ATM and DNA-PKcs.....	148
Figure 5-6. Doxorubicin did not inhibit mTORC1 signalling or induce eIF2 α phosphorylation in MCF10A p53 ^{-/-} cells.....	151
Figure 5-7. Doxorubicin inhibited translation initiation in p53 ^{-/-} cells less robustly than in p53 ^{+/+} cells	154
Figure 5-8. p53 mediated mTORC1 inhibition and eIF2 α phosphorylation in response to doxorubicin	156
Figure 5-9. siRNA depletion of p53 recapitulated the response observed in p53 ^{-/-} cells	159
Figure 5-10. p53 mediated doxorubicin-induced G1 cell cycle arrest	161
Figure 5-11. p53 ^{-/-} cells were more sensitive to doxorubicin-induced cell death	162
Figure 6-1. Proposed model of doxorubicin-induced mTORC1 inhibition and eIF2 α phosphorylation.....	168

List of abbreviations

43S PIC: 43S pre-initiation complex

4E-BP: Eukaryotic initiation factor 4E binding protein

5' TOP: 5' Terminal oligopyrimidine tract

A: Adenine

aa tRNA: Amino-acyl-tRNA

A-site: Aminoacyl site in ribosome

AMP: Adenosine monophosphate

AMPK: AMP activated protein kinase

ATF4: Activating transcription factor 4

ATP: Adenosine triphosphate

ATM: Ataxia telangiectasia mutated

ATR: Ataxia telangiectasia and Rad3 related

APS: Ammonium persulphate

BrdU: 5-bromo-2'-deoxyuridine

BSA: Bovine serum albumin

Cdk: Cyclin-dependent kinases

Chk1: Checkpoint 1 kinase

Chk2: Checkpoint 2 kinase

DCFH-DA: 2',7'-dichlorofluorescein diacetate

DDR: DNA damage response

DMEM: Dulbecco's modified eagle medium

DNA: Deoxyribonucleic acid

DNA-PKcs: DNA-dependent protein kinase catalytic component

Dox: Doxorubicin

DSB: Double strand DNA break

dsRNA: Double-stranded RNA

DTT: Dithiothreitol

E-Site: Exit site in the ribosome

EDTA: Ethylenediaminetetraacetic acid

EdU: 5-ethynyl-2'-deoxyuridine

eEF: Eukaryotic elongation factor

eEF2k: Eukaryotic elongation factor 2 kinase

eIF: Eukaryotic initiation factor

eIF2k: Eukaryotic initiation factor 2 kinase

ER: Endoplasmic reticulum

eRF: Eukaryotic release factor

ERK: Extracellular signal-regulated kinase

G: Guanine

GADD34: Growth arrest and DNA damage-inducible protein

GAP: GTPase activating protein

GCN2: General control non-derepressible-2

GDP: Guanosine diphosphate

GEF: Guanine nucleotide exchange factor

GTP: Guanosine triphosphate

HEPES: 4-(2-hydroxyethyl)-1-piperazineethanesulfonic acid

HRI: Heme-regulated inhibitor

IMS: Industrial methylated spirit

IR: Ionising radiation

IRES: Internal ribosome entry site

ISR: Integrated stress response

NHEJ: Non-homologous end joining

MAPK: Mitogen-activated protein kinase

MDM2: Mouse double minute 2 homolog

MDM4: Mouse double minute 4 homolog

MEF: Mouse embryo fibroblast

MEK: Mitogen-activated protein kinase kinase

Met-tRNAⁱ: Methionyl transfer RNA

mRNA: Messenger RNA

mTOR: Mammalian/mechanistic target of rapamycin

mTORC1: Mammalian/mechanistic target of rapamycin complex 1

mTORC2: Mammalian/mechanistic target of rapamycin complex 2

ORF: Open reading frame

P-site: Peptidyl site in the ribosome

p70 S6K: p70 Ribosomal S6 kinase

PABP: Poly(A) binding protein

PBS: Phosphate buffered saline

PDK1: Phosphoinositide dependent kinase 1

PERK: PKR-like ER kinase

PI3K: Phosphoinositide 3-kinase

PIC: Pre-initiation complex

PKC: Protein kinase C

PKR: Protein kinase double-stranded RNA-dependent

PP: Protein phosphatase

PTEN: Phosphatase and tensin homolog on chromosome 10

Rag: RAS-related GTP-binding protein

Rheb: Ras homolog enriched in brain

RNA: Ribonucleic acid

RPS6: Ribosomal protein S6

ROS: Reactive oxygen species

rRNA: Ribosomal RNA

RSK: p90 Ribosomal S6 kinase

SDS: Sodium dodecyl sulphate

SDS-PAGE: SDS-polyacrylamide gel electrophoresis

Ser: Serine

SGK1: Serum and glucocorticoid induced kinase 1

siRNA: Small interfering ribonucleic acid

ssDNA: Single strand DNA

SSB: Single strand DNA break

T: Thymidine

TC: Termination complex

TCA: Trichloroacetic acid

TEMED: Tetramethylethylenediamine

Thr: Threonine

Top1: Type 1 topoisomerase

Top2: Type 2 topoisomerase 2

TOR: Target of rapamycin

tRNA: Transfer RNA

TSC: Tuberous sclerosis complex

uORF: Upstream open reading frame

U: Uridine

UPR: Unfolded protein response

UTR: Untranslated region

UV: Ultraviolet light

1 Introduction

The central dogma of all biology is that DNA is transcribed into mRNA, which is in turn translated into a polypeptide that folds into a functional protein.

1.1 mRNA processing

After transcription and splicing, a 7-methylguanosine cap is added to the first transcribed nucleotide of an mRNA, generating an m⁷GpppN cap structure (Shatkin 1976). Capping is an extremely important process because most cellular mRNAs are translated in a cap-dependent manner, during which the initiation complexes form at the cap site. The cap also increases mRNA stability and protects mRNA from degradation by cellular exonucleases (reviewed in (Cowling 2010)).

At the 3' end of an mRNA, a series of adenine residues are added by the process of polyadenylation, to create a poly-A tail. In mammalian mRNA, poly-A tails are typically in excess of 200 nucleotides in length. A poly-A tail protects mRNA from degradation, provides a platform for the circularisation of mRNA, stimulates the binding of eIF4F complex, and is required for mRNA export to the cytoplasm (Dreyfus & Régnier 2002; Proudfoot 2011).

In the nucleus, the 5' cap binds to the cap binding complex (CBC) and the mRNA is exported through the nuclear pore complex (NPC), via transcription coupled export (TREX) (reviewed in (Köhler & Hurt 2007; Culjkovic-Kraljacic & Borden 2013)).

1.2 Cap-dependent translation

Cap-dependent translation is a highly regulated process, in which an mRNA is decoded into a polypeptide sequence that will fold into a functional protein. Cap-dependent translation consists of 3 steps. First, initiation, where initiation factors enable the assembly of an 80S ribosome complex that will decode mRNA. Secondly, elongation, during which an 80S ribosome proceeds along the mRNA, producing a decoded, nascent polypeptide sequence. Thirdly, termination, in which after encountering a stop codon, the ribosome complex dissociates, releasing the nascent polypeptide and ribosomal subunits.

1.2.1 Translation Initiation

The role of translation initiation is to produce an elongation-competent 80S ribosomal subunit, with the methionyl-tRNA_i (Met-tRNA_i) positioned at the AUG start codon. Initiation by the scanning mechanism proceeds in a number of key steps, and this process is dependent on canonical eukaryotic initiation factors (eIFs) (Figure 1-1). All stages of translation are highly regulated, but it has been proposed that initiation is the rate limiting step of cap-dependent translation (Jackson et al. 2010; Kong & Lasko 2012; Aitken & Lorsch 2012; Hinnebusch 2014). However, the control of translation elongation has also emerged as an important regulator of protein synthesis (Faller et al. 2014; Richter & Collier 2015).

1.2.1.1 Assembly of the 43S pre-initiation complex

The current model of translation initiation suggests that the 43S pre-initiation complex (43S PIC) assembles prior to recruitment to mRNA (Sonnenberg & Hinnebusch 2009). The 43S PIC is a scanning competent ribosomal complex, composed of two core complexes, eIF2 ternary complex, and the 40S small ribosomal subunit (with associated eIFs) (Figure 1-1A).

eIF2 ternary complex consists of the Met-tRNA_i bound to eIF2-GTP. The function of the ternary complex is to deliver the Met-tRNA_i to the peptidyl site (P-site) of the ribosome. eIF2 is a heterotrimeric protein complex, comprised of α , β and γ subunits, and binds to the Met-tRNA_i when eIF2 is bound to GTP (Figure 1-1A). eIF2-GDP also binds Met-tRNA_i, but at least in yeast, the affinity of eIF2-GDP for Met-tRNA_i was lower (Kapp & Lorsch 2004). During start codon recognition, eIF2-GTP is hydrolysed to eIF2-GDP. To ensure that eIF2 can continue to deliver Met-tRNA_i to the 43S PIC, eIF2-GDP is recycled to eIF2-GTP, by the guanine nucleotide exchange factor (GEF), eIF2B (Webb & Proud 1997) (Figure 1-1E). A Met-tRNA_i is recruited to every mRNA undergoing cap-dependent translation, thus, recruitment of the Met-tRNA_i is a rate limiting step for translation initiation, and is the subject of extensive regulation. The regulation of eIF2 in response to cellular stress is the subject of a subsequent chapter (1.4.1 Regulation of ternary complex).

eIF2 ternary complex assembles with the 40S ribosome and eIFs, including eIF1, eIF1A, eIF3 and eIF5, to facilitate the formation of the 43S PIC (Asano et al. 2000) (Figure 1-1A). eIF1 binds near the P-site of the 40S ribosomal subunit, maintaining the 40S ribosome in an open conformation (Rabl et al. 2011), and is essential for the formation of a scanning competent 43S PIC (Pestova et al. 1998). eIF1A binds near the A-site of the 40S ribosome, promoting the formation of the 43S PIC (Pestova et al. 1998) and stabilising the binding of ternary complex (Yu et al. 2009). eIF3 binds to the solvent face of the 40S ribosome, acting as a molecular scaffold (Siridechadilok et al. 2005), and facilitates the recruitment of ternary complex, eIF1, and eIF1A (Sokabe & Fraser 2014). eIF5 interacts with eIF3 and eIF2, mediating the GTP hydrolysis of eIF2-GTP during start codon recognition (Paulin et al. 2001). In yeast, eIF5B has also been shown to stabilise the 43S PIC in a closed conformation on the mRNA (Saini et al. 2014).

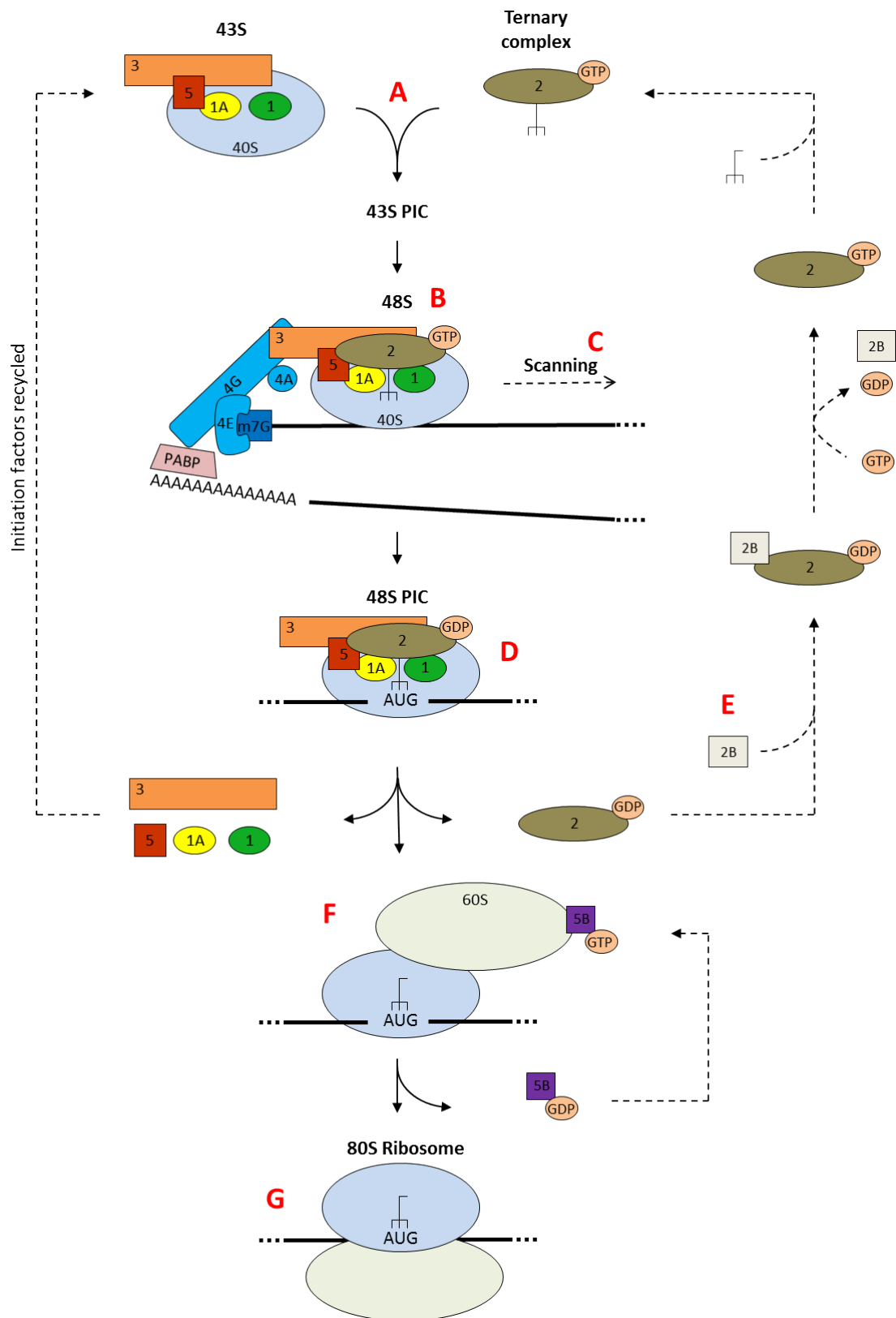


Figure 1-1. Translation initiation

Schematic representation of translation initiation. Broken arrows indicate initiation factor recycling.

1.2.1.2 Recruitment of the 43S pre-initiation complex

eIF4F is a cap binding complex that plays a central role in the recruitment of the 43S PIC to the mRNA (Figure 1-1B). eIF4F is a trimeric protein complex, consisting of eIF4E, eIF4A and eIF4G. eIF4E recognises, and binds to, the 5' cap structure of the mRNA (Sonenberg et al. 1979), acting as an anchor for the rest of the complex. eIF4A, a DEAD-box RNA helicase, unwinds cap proximal secondary structure of mRNA to enhance the recruitment of the 43S PIC (Rozen et al. 1990). eIF4G is a large scaffold protein that binds to both eIF4E and eIF4A (Imataka & Sonenberg 1997), enhancing the helicase activity of eIF4A (Oberer et al. 2005). eIF4G also binds Poly (A) binding protein (PABP), a protein that binds to the mRNA 3' poly-A tail (Imataka et al. 1998). This interaction brings the 5' and 3' ends of the mRNA together, forming a closed-loop mRNA (Wells et al. 1998).

The recruitment of the 43S PIC to a closed-loop mRNA is primarily mediated by eIF4F. eIF4G (within eIF4F) directly binds to eIF3 (within the 43S PIC), facilitating the recruitment of the 43S PIC to the 5' cap site (LeFebvre et al. 2006). However, mutating eIF3 binding sites on eIF4G has no effect on translation (Hinton et al. 2007), thereby suggesting that the recruitment of the 43S PIC proceeds via multiple interactions. The helicase activity of eIF4A also resolves cap proximal mRNA secondary structure within the 5' UTR, to create a landing platform for the 43S PIC.

eIF4F is essential for cap-dependent translation, so it is unsurprising that this complex is a major regulatory target. eIF4F is regulated at two main points. First, eIF4E-binding proteins (4E-BPs) bind eIF4E, preventing eIF4E binding to eIF4G, and inhibit eIF4F formation (Haghighat et al. 1995). Secondly, eIF4B can associate with eIF4F, stimulating eIF4A's helicase activity (Rogers et al. 2001). Both of these proteins are regulated in response to mTOR signalling, and are the subject of a subsequent chapter (1.5.1.2 mTORC1 regulation of protein synthesis).

1.2.1.3 Ribosomal scanning of the 5' UTR

After recruitment to the mRNA, the 43S PIC is held in an open conformation, allowing it to scan the mRNA for the AUG start codon (Figure 1-1C). Base by

base, linear scanning, occurs in a 5' to 3' direction. The mRNA is threaded through the mRNA-binding channel within the 40S ribosome, to enable the Met-tRNA_i to search for the start site from the first nucleotide (Kumar et al. 2016). Many of the factors already recruited to the complex via their roles in 43S PIC formation play key roles in ribosome scanning. eIF1 and eIF1A induce a 43S PIC scanning competent conformation (Passmore et al. 2007), and through their interactions with 40S ribosome proteins, ensure the mRNA is correctly orientated for scanning to occur (Lomakin & Steitz 2013). In addition, eIF1 enables the 43S PIC to discriminate against incorrect start codons, and those in poor context (Pestova et al. 1998). In order for scanning to occur, mRNA 5' UTR secondary structure must be unwound by RNA helicases, and helicase activity is most likely responsible for the 5' to 3' direction of scanning. The primary helicase, eIF4A, is a relatively weak helicase, but its activity is enhanced by eIF4G (Oberer et al. 2005), eIF4B (Rogers et al. 2001) and eIF4E (Feoktistova et al. 2013). However, more structured 5' UTR require additional helicases, such as DHX29 (Pisareva et al. 2008), to facilitate more efficient processing of 5' UTR secondary structure.

1.2.1.4 Start codon recognition

The 43S PIC identifies the appropriate AUG start codon, frequently located within the Kozak sequence (5'-(A/G)NNAUGG-3') (Kozak 1987). Mutation of residues within the Kozak sequence have been shown to enhance leaky scanning, whereby the 43S PIC bypasses the AUG codon and initiates at a downstream start codon (reviewed in (Kozak 1991)). Upon AUG recognition, codon-anticodon base pairing induces a myriad of conformational changes within the 43S PIC.

The key step of committing the ribosome to the start codon is the GTP hydrolysis of eIF2-GTP (Figure 1-1D). eIF1 inhibits premature eIF2-GTP hydrolysis (Unbehauen et al. 2004), however, upon start codon recognition, conformational rearrangements within the 43S PIC displace eIF1 (Maag et al. 2006). Subsequently, the GTPase-activating protein (GAP), eIF5, induces the hydrolysis of eIF2-GTP (Chakrabarti & Maitra 1991; Paulin et al. 2001). Hydrolysis reduces the affinity of eIF2 for the Met-tRNA_i, leading to the dissociation of eIF2 (Kapp & Lorsch 2004). These structural changes generate

a closed conformation, 48S initiation complex, stabilising the interaction between mRNA and the Met-tRNA_i. The 48S complex is bound to the mRNA, with the anticodon loop of the Met-tRNA_i paired with the start codon, in the P-site of the ribosome.

1.2.1.5 Assembly of the 80S ribosome

The final stage of initiation is recruitment of a 60S ribosomal subunit to the 48S initiation complex, assembling an elongation competent 80S ribosome (Figure 1-1F). Recruitment of the 60S ribosome is mediated by the GTPase, eIF5B (Pestova et al. 2000). Upon the recruitment of the 60S ribosome to the 48S initiation complex, eIF5B undergoes GTP hydrolysis, as part of a checkpoint that monitors 80S ribosome formation (Shin et al. 2002). This process facilitates further conformational rearrangements, reducing the affinity of eIF5B for the complex and results in the dissociation of all initiation factors (Pestova et al. 2000). The resulting complex is an elongation competent 80S ribosome (Figure 1-1G).

1.2.2 Translation elongation

Elongation is the phase of translation where the mRNA is decoded into a nascent polypeptide sequence, one codon at a time. The assembly of a polypeptide chain is mediated by the ribosome, and assisted by eukaryotic elongation factors (eEFs). This process can be separated into two phases (Figure 1-2). First, recruitment of amino-acyl-tRNA (aa-tRNA) to the A-site of the ribosome, followed by peptide bond formation between the amino acid in the A- and P-sites (Figure 1-2A), and secondly, ribosome translocation (Figure 1-2B).

eEF1A, bound to GTP (eEF1A-GTP), delivers an aa-tRNA to the A-site of the ribosome. Upon correct codon-anticodon pairing, the ribosome mediates eEF1A-GTP hydrolysis. eEF1A-GDP has a much lower affinity for the aa-tRNA, facilitating the release of eEF1A. eEF1A-GDP is rapidly recycled by the GEF, eEF1B, to ensure that eEF1A continues to deliver aa-tRNAs to elongating ribosomes (Hershey 1991; Browne & Proud 2002).

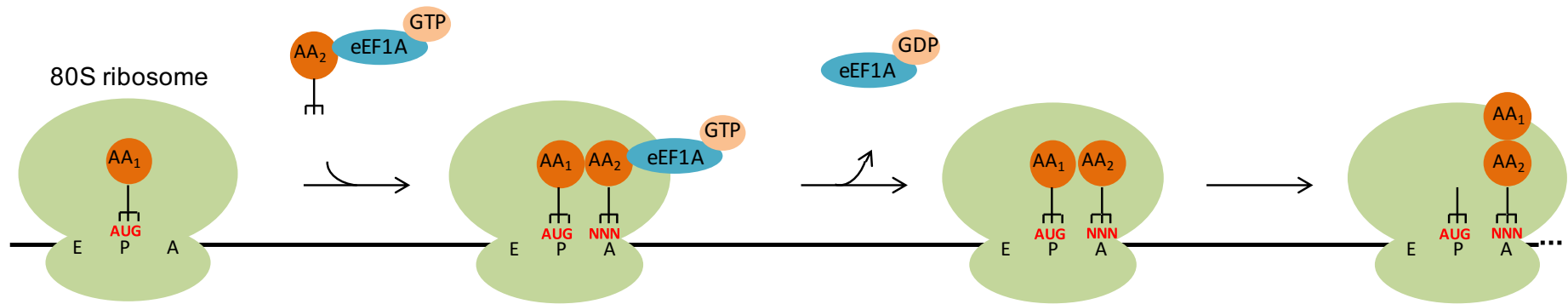
Upon the delivery of the aa-tRNA to the A-site of the ribosome, a peptide bond forms between the amino acid in the A-site and the adjacent amino acid in the P-site. Peptide bond formation is catalysed by ribosomal RNA (rRNA) within the

peptidyl transferase centre, located within the 60S ribosome subunit (Rodnina 2013) (Figure 1-2A).

After peptide bond formation, the ribosome translocates along the mRNA to the next codon. Ribosome translocation involves the movement of the peptidyl-tRNA·mRNA, from the A-and P-site of the ribosome, to the P-and E-site, allowing the next aa-tRNA to be recruited to the free A-site (Kaul et al. 2011). eEF2-GTP is recruited to the ribosome, and it is the hydrolysis of eEF2-GTP that directly stimulates the translocation of the ribosome (Spahn et al. 2004) (Figure 1-2B).

This sequence of aa-tRNA delivery, peptide formation, and ribosome translocation, continues until a stop codon is reached, triggering the termination of elongation.

A



B

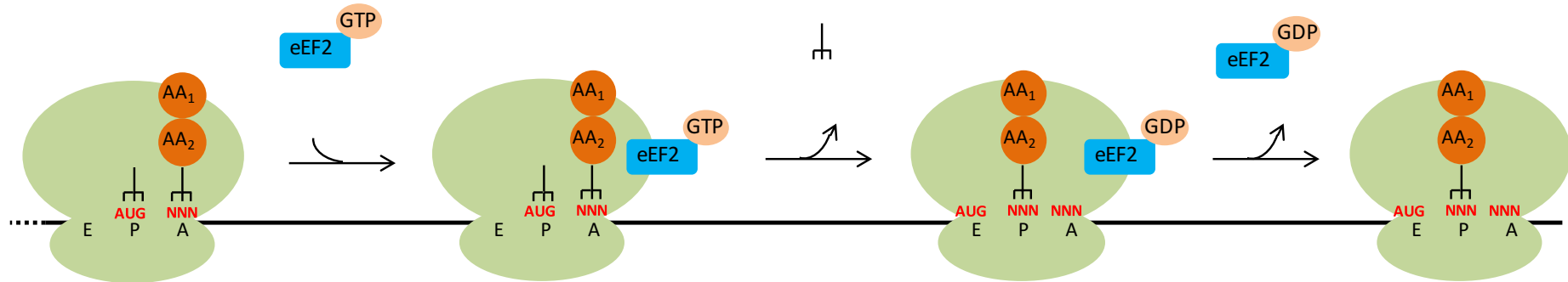


Figure 1-2. Translation elongation

Schematic representation of translation elongation.

1.2.3 Translation termination

Termination of translation occurs when a stop codon (UAA, UAG or UGA) is recognised within the A-site of a translating ribosome (reviewed in (Jackson et al. 2012)). Termination requires two eukaryotic release factors (eRFs), eRF1 and eRF3. eRF1 recognises the stop codon within the A-site, whereas eRF3 is a ribosome dependent GTPase that stimulates the termination reaction. eRF1, eRF2, and GTP form a stable complex that binds to the A-site of the ribosome, forming a pre-termination complex (pre-TC). The 80S ribosome and eRF1 are required for eRF3 mediated GTP hydrolysis, triggering peptidyl-tRNA hydrolysis and release of the nascent polypeptide. (Zhouravleva et al. 1995; Jackson et al. 2012).

1.3 Cap-independent translation

Although the majority of translation in eukaryotic organisms is cap-dependent, a small amount of translation initiates independent of the cap site, through internal ribosome entry sites (IRES). IRESs are sections of highly structured RNA found within the 5' UTR of mRNA, which are able to recruit eIFs and ribosomal subunits in absence of eIF4F. IRESs were first identified in viruses that efficiently translated mRNA in the absence of a 5' cap site. In poliovirus, it was shown that the structure of 5' UTR recruited translational components independently of a cap structure (Pelletier & Sonenberg 1988). The first cellular IRES was identified in the mRNA of the immunoglobulin heavy-chain-binding-protein (Macejak & Sarnow 1991). The benefit of IRESs to the cell is that they enable the translation of specific mRNA to be maintained when cap dependent translation is inhibited, such as during cellular stress (Spriggs et al. 2008).

1.4 Regulation of translation initiation

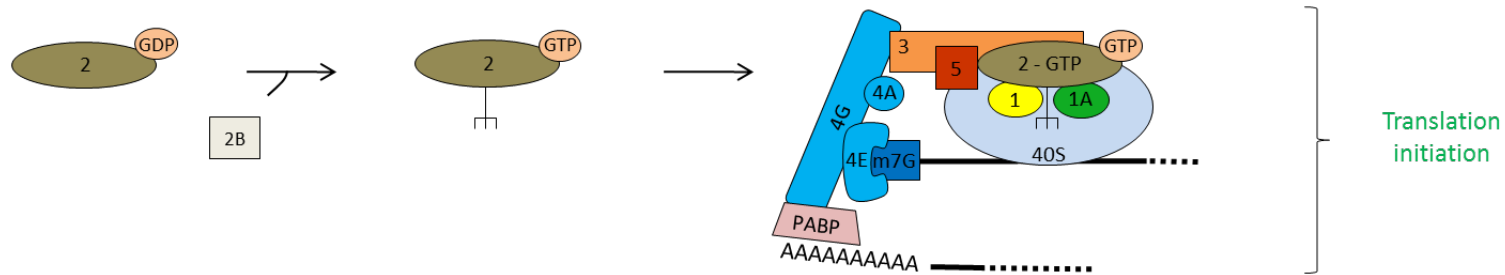
By regulating mRNA translation, a cell can modulate protein synthesis in response to intra- and extra-cellular cues, including cellular stress. Translation initiation is a rate limiting step of translation, and as such is a highly regulated process. Inhibition of translation is mediated through the regulation of two proteins, eIF2 and eIF4E, that regulate ternary complex availability and eIF4F complex formation respectively.

1.4.1 Regulation of ternary complex

As explained previously, eIF2 recruits the Met-tRNA_i to the 40S ribosome during 43S-PIC assembly (1.2.1.1 Assembly of the 43S pre-initiation complex).

Recruitment of a Met-tRNA_i is essential for start site recognition, and hence is a rate limiting step of 43S-PIC assembly. During the process of initiation, eIF2 undergoes GTP hydrolysis, releasing eIF2-GDP after start codon recognition. eIF2 has a greater affinity for the Met-tRNA_i when bound to GTP. eIF2-GDP is recycled by its GEF, eIF2B, to eIF2-GTP, so it is able to bind more Met-tRNA_i and participate in subsequent rounds of translation initiation. In response to a wide variety of cellular stresses, eIF2 is phosphorylated at serine 51 within the α subunit (eIF2 α). Phosphorylation of eIF2 α inhibits translation initiation by enhancing the affinity of eIF2-GDP for eIF2B, subsequently inhibiting eIF2B's GEF activity, and thereby decreasing the availability of ternary complex forming eIF2-GTP. In mammalian cells, eIF2B is present at much lower concentrations than eIF2, hence, a modest level of eIF2 phosphorylation can inhibit eIF2B function, resulting in the inhibition of translation initiation (Figure 1-3).

No Stress:



Cellular Stress:

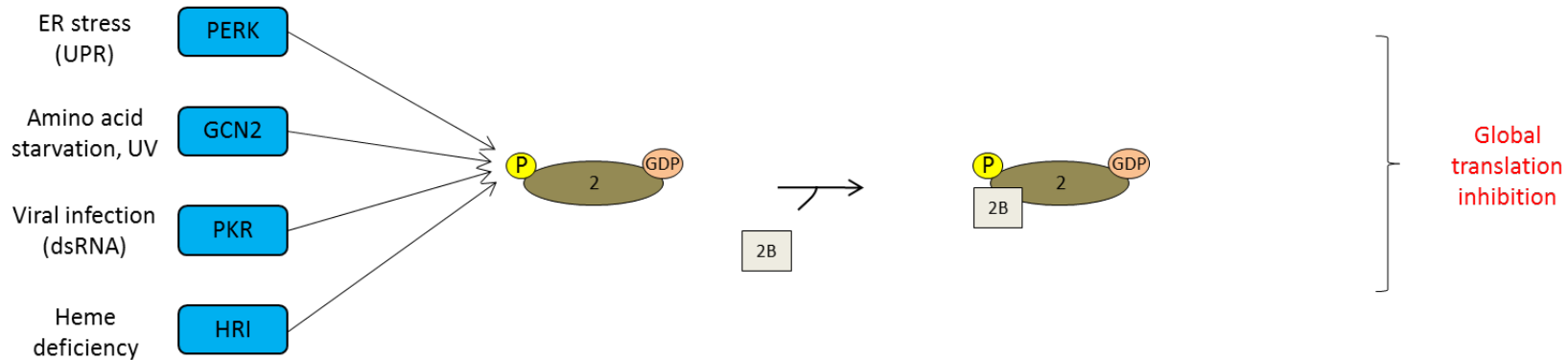


Figure 1-3. Regulation of ternary complex

Schematic representation of the regulation of ternary complex and global translation initiation during cellular stress.

1.4.1.1 eIF2 α kinases

The family of protein kinases responsible for eIF2 α phosphorylation are the eIF2 kinases (eIF2K). In mammalian cells, four eIF2Ks have been identified: GCN2 (general control non-derepressible-2); PKR (protein kinase double-stranded RNA-dependent); PERK (PKR-like ER kinase); and HRI (heme-regulated inhibitor). eIF2Ks share a conserved activation mechanism, whereby upon receiving the appropriate stress signal, eIF2Ks become activated following dimerisation and auto-phosphorylation (Donnelly et al. 2013). eIF2Ks phosphorylate eIF2 α in response to different cellular stress stimuli, contributing to the regulation of the integrated stress response (ISR). The primary consequence of eIF2 α phosphorylation is the inhibition of global protein synthesis, however, the phosphorylation of eIF2 α also enables the selective reprogramming of mRNA translation (Harding et al. 2000; Powley et al. 2009). It has been suggested that the translation of some mRNA are either repressed, or resistant, to eIF2 α phosphorylation (Baird et al. 2014).

1.4.1.1.1 GCN2

GCN2 was originally shown to be activated in response to amino acid starvation, balancing global protein synthesis with amino acid availability. GCN2 binds uncharged tRNA through interactions with a histidyl-tRNA synthase related domain (HisRS) that facilitates dimerisation and kinase activation (Dong et al. 2000; Qiu et al. 2001; Zhang et al. 2002). Additional cell stresses that activate GCN2 include UV induced DNA damage, and the subsequent phosphorylation of eIF2 α was identified to be the primary inhibitor of protein synthesis (Deng et al. 2002). GCN2 induced eIF2 α phosphorylation also facilitates translational reprogramming to selectively translate mRNA involved in the DNA damage response (DDR) (Powley et al. 2009).

1.4.1.1.2 PKR

PKR has been identified to be predominantly activated in response to double strand RNA (dsRNA) during viral infection. PKR is localised in the cytosol and nucleus, and contains a dsRNA binding domain. It has been suggested that the binding of dsRNA facilitates PKR activation through dimerisation and auto-phosphorylation (Vattem et al. 2001). PKR induced eIF2 α phosphorylation

inhibits global protein synthesis to repress the translation of viral mRNA. However, PKR has also been shown to be activated by a range of stimuli, including ER stress (Nakamura et al. 2010) and DNA damage (Bergeron et al. 2000). Furthermore, in response to metabolic stress, PKR was shown to interact with DICER (Nakamura et al. 2015), and PKR induced eIF2 α phosphorylation has been shown to contribute to apoptosis (Srivastava et al. 1998; Peidis et al. 2011).

1.4.1.1.3 PERK

PERK is an endoplasmic reticulum (ER) transmembrane protein, and forms one arm of the unfolded protein response (UPR). The N-terminal region of PERK is localised within the ER lumen, where it binds to the ER chaperone, immunoglobulin binding protein (BiP). The C-terminal region of PERK is cytosolic and contains the kinase domain. PERK is activated in response to unfolded proteins, which lead to the dissociation of BiP and subsequent dimerisation and auto-phosphorylation of PERK (Bertolotti et al. 2000). First, PERK serves to balance the amount of unfolded proteins in the ER with chaperone availability by phosphorylating eIF2 α and inhibiting global protein synthesis (Harding et al. 1999). Secondly, PERK induced eIF2 α phosphorylation attenuates ternary complex availability, triggering the selective translation of mRNAs, such as activating transcription factor 4 (ATF4) (Harding et al. 2000). ATF4 is itself a transcription factor, regulating the expression of many different pro-survival genes involved in amino acid metabolism, autophagy, and apoptosis. ATF4 mediated expression serves to restore ER function and homeostasis (reviewed extensively in (Ron & Walter 2007; Ron & Harding 2012; Hetz 2012).

1.4.1.1.4 HRI

HRI is found at high levels in red blood cells (Crosby et al. 1994) where it regulates globin synthesis in response to heme levels. When heme levels are high, HRI is bound by heme, inhibiting HRI activity. However, when heme levels are low, heme does not bind HRI, leading to the activation of HRI by auto-phosphorylation (Rafie-Kolpin et al. 2003). For many years, the role of HRI was thought to be exclusive to erythroid cells, however, HRI has been shown to play

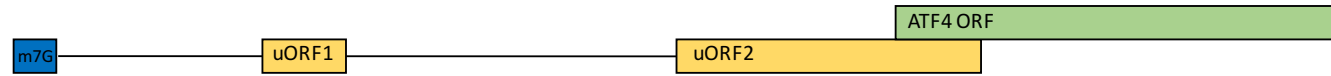
a role in other cell types, and more importantly, in response to other stimuli. HRI has been suggested to regulate ER homeostasis in liver (Acharya et al. 2010), as well mediate the response to arsenite in MEFs (McEwen et al. 2005).

1.4.1.2 Selective translation of mRNA

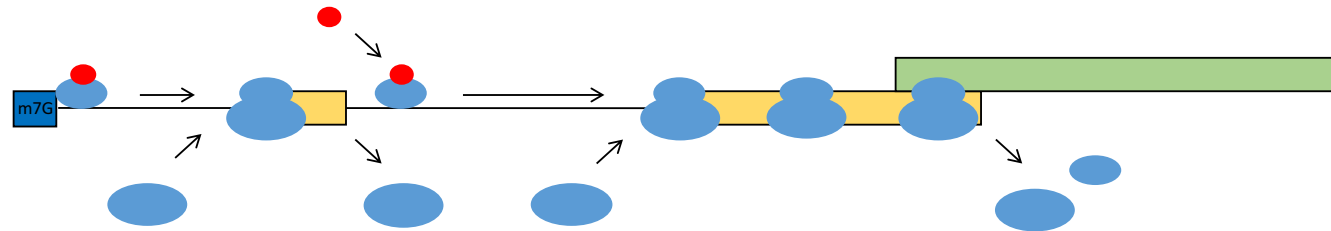
The translation of some mRNA are actually enhanced in response to eIF2 α phosphorylation, at a time when global translation is inhibited. The best described mammalian mRNA to use this regulatory mechanism is ATF4.

ATF4 expression has mostly been studied in response to ER stress and amino acid deprivation, through the activation of PERK and GCN2 respectively. One model for the selective translation of ATF4 involves a re-initiation mechanism at two upstream open reading frames (uORFs) (Vattem & Wek 2004) (Figure 1-4A). When ternary complex availability is high, uORF1 is translated by ribosomes, and these ribosomes re-initiate on the inhibitory uORF2. uORF2 is out-of-frame with the ATF4 coding region, resulting in limited ATF4 expression (Figure 1-4B). However, under stressed conditions, when eIF2 α is phosphorylated and ternary complex availability is low, the scanning ribosome does not re-initiate at uORF2. The ribosome proceeds to re-initiate at the start of the ATF4 coding region, resulting in an increase in ATF4 translation (Figure 1-4C).

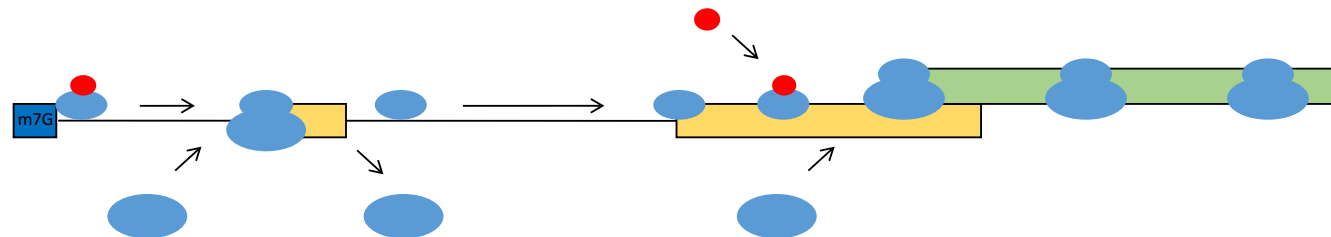
A ATF4 mRNA



B No stress – high level of eIF2-GTP



C Cellular stress – low level of eIF2-GTP







Key:  = 80S  = 60S  = 40S  = eIF2-GTP

Figure 1-4. Re-initiation model of ATF4 mRNA translation

Schematic representation of the re-initiation model for ATF4 translation. Figure adapted from Jackson et al. 2010.

1.4.1.3 eIF2 α dephosphorylation

As discussed previously, eIF2 α is phosphorylated in response cellular stress to inhibit global protein synthesis. For example, GCN2 induced eIF2 α phosphorylation co-ordinates protein synthesis rates with nutrient availability. However, when the availability of nutrients increase, protein synthesis must resume. This process is mainly conducted by eIF2 α phosphatases, such as protein phosphatase 1 (PP1), which restores eIF2B activity by removing the phosphorylation site within eIF2 α (Novoa et al. 2001; Novoa et al. 2003). The expression of GADD34 is enhanced in response to eIF2 α phosphorylation. Interestingly, GADD34 forms part of a negative feedback mechanism to restore protein synthesis (Novoa et al. 2001), as it directly mediates the recruitment of PP1 to eIF2 α , facilitating de-phosphorylation (Choy et al. 2015).

1.5 mTOR signalling

Target of rapamycin (TOR) is a highly conserved serine/threonine protein kinase found in all eukaryotes. TOR was originally discovered in yeast and was found to mediate the inhibitory effect of rapamycin on cell growth (Heitman et al. 1991; Kunz et al. 1993). A single mammalian/mechanistic TOR (mTOR) kinase was identified shortly after (Brown et al. 1994; Sabatini et al. 1994) and belongs to the phosphoinositide 3-kinase (PI3K) family of kinases, which also includes DNA damage sensors ATM, ATR and DNA-PKcs.

mTOR signalling integrates a vast array of stimuli including growth factor stimulation; amino acid levels; energy levels; genotoxic stress; and oxygen levels. In response to these stimuli, mTOR regulates cell growth, proliferation, metabolism, autophagy and survival. mTOR forms two functionally distinct, multi-protein complexes, mTORC1 and mTORC2. Both mTOR complexes include a core of mTOR, mLST8, DEPTOR and Tti1/Tel2. mTORC1 is distinguished by additionally containing PRAS-40 and raptor, whereas mTORC2 is distinguished by including rictor, mSin1 and protor1/2 (Laplane & Sabatini 2009; Efeyan & Sabatini 2010; Laplane & Sabatini 2012).

TOR was originally identified as a target of rapamycin. Rapamycin binds to FKBP12, and this complex binds near the catalytic site of mTOR, allosterically inhibiting its kinase activity (Brown et al. 1994; Chen et al. 1995). For reasons yet to be identified, rapamycin only inhibits mTOR within mTORC1, whereas mTOR within mTORC2 is generally insensitive to rapamycin. Different sensitivities to rapamycin indicate that mTORC1 and mTORC2 function as distinctly separate complexes. mTORC1 is activated in response to energy status, nutrients and growth factors, whereas mTORC2 activity appears to be primarily mediated by growth factors (Efeyan & Sabatini 2010; Laplane & Sabatini 2012).

1.5.1 mTORC1

mTORC1 has been extensively studied since its identification due to its role as a central regulator of cell growth and proliferation. Dysregulation of mTOR signalling has been heavily implicated in human disease, including cancer; obesity; and type 2 diabetes (Sabatini 2006; Efeyan & Sabatini 2010; Laplane

& Sabatini 2012). Importantly, mTORC1 signalling is repressed during times of stress, such as under starvation conditions, hypoxia, and genotoxic stress, subsequently inhibiting protein synthesis.

1.5.1.1 Regulation of mTORC1 activity

Complete activation of mTORC1 is dependent on two key, independent steps regulated by two small GTPases, RAS-related GTP-binding protein (Rag) and Ras homolog enriched in brain (Rheb) (Figure 1-5).

Rag proteins enhance mTORC1 translocation to the surface of the lysosome. Rag proteins were initially identified to upregulate mTORC1 activity in response to amino acid stimulation, and function as heterodimers of RagA or RagB with RagC or RagD. Amino acid levels are sensed by the vacuolar H⁺-ATPase (v-ATPase)/ragulator complex, and the amino acid transporter, SLC38A9, at the surface of the lysosome (Zoncu et al. 2011; Wang et al. 2015). Ragulator functions as the GEF for RagA or RagB (Bar-Peled et al. 2012), activating the Rag heterodimer. Activation of Rag stimulates the binding of mTORC1 through interactions with raptor (Sancak et al. 2008), translocating mTORC1 to the surface of the lysosome (Sancak et al. 2010). An important negative regulator of the Rag proteins is GATOR 1, which has inhibitory GAP activity toward RagA and RagB (Bar-Peled et al. 2013). GATOR 1 is negatively regulated by GATOR 2, thereby enhancing Rag activity. Importantly, the activity of GATOR2 is inhibited in response to p53 induced sestrin expression, subsequently inhibiting Rag activity and mTORC1 activation (Parmigiani et al. 2014).

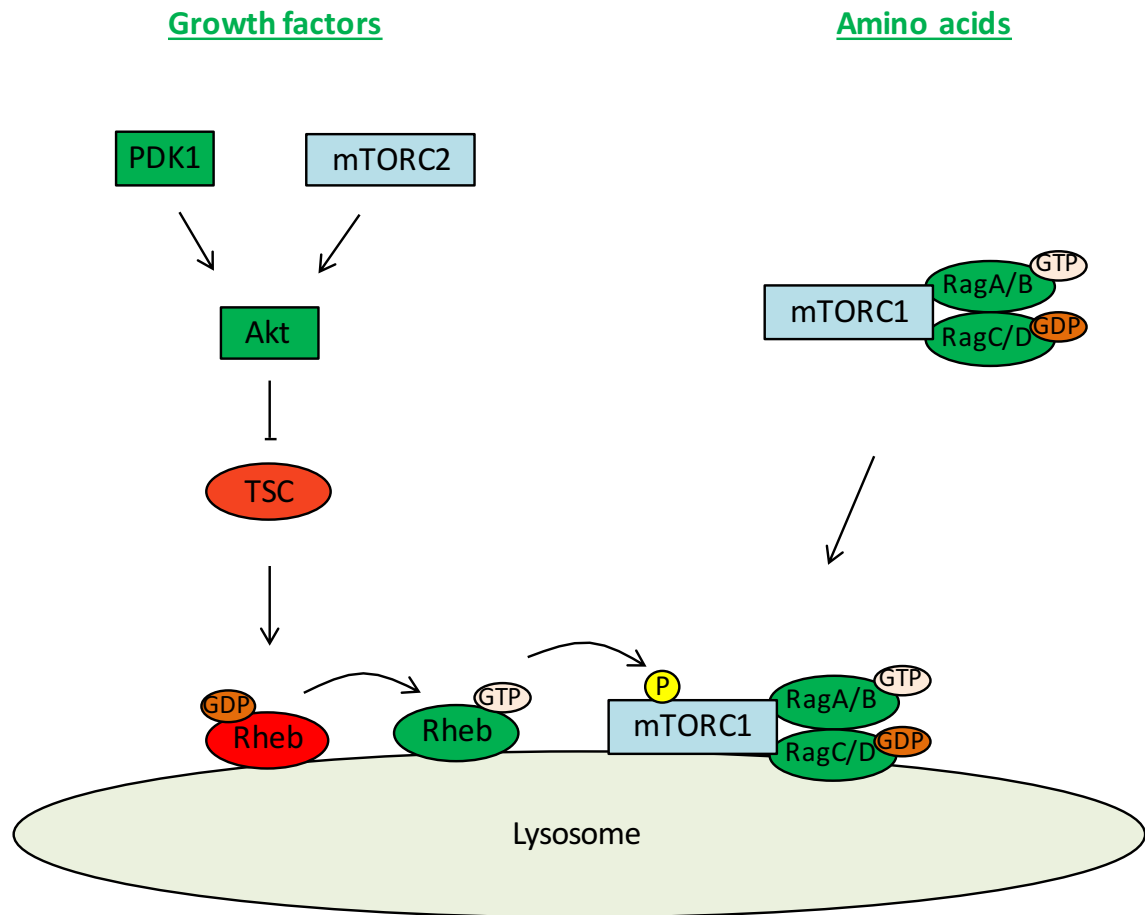


Figure 1-5. Activation of mTORC1 at the surface of lysosome

Schematic representation of mTORC1 activation at the lysosome in response to growth factor and amino acid stimulation. Green boxes indicate activators of mTORC1 activity, whereas red boxes indicate inhibitors of mTORC1 activity.

Rheb is loaded with GTP and activated at the surface of the lysosome. Upon mTORC1 translocation to the lysosome, Rheb binds mTORC1 through interactions with LST8 and the catalytic domain of mTOR, enhancing mTORC1 kinase activity (Long et al. 2005). Although the exact mechanisms of Rheb activation, and subsequent mTORC1 activation are not clear, Rheb has been identified to be negatively regulated by tuberous sclerosis complex (TSC). TSC is comprised of a heterodimer of tuberous sclerosis 1 (known as TSC1 or hamartin) and tuberous sclerosis 2 (known as TSC2 or tuberin). TSC is a negative regulator of mTORC1 activity, via the inhibition of Rheb activity. TSC exhibits GAP activity toward Rheb, hydrolysing Rheb-GTP to Rheb-GDP, preventing the activation of mTORC1 (Inoki, Li, et al. 2003). TSC functions as a major sensor within mTORC1 signalling, mediating signals from an array of cellular pathways in response to varied stimuli. These stimuli phosphorylate TSC, either enhancing or inhibiting its activity (Figure 1-6).

TSC is inactivated by the serine/threonine protein kinase Akt, stimulating mTORC1 signalling (Inoki et al. 2002; Manning et al. 2002). In addition, TSC activity has been shown to be inhibited in response to MAPK/ERK activation, through phosphorylation by RSK (She et al. 2010) and ERK (Ma et al. 2005) (Figure 1-6). Conversely, TSC activity can be enhanced in response to cellular stress, inhibiting mTORC1 activity. Stimulation of TSC activity is predominantly mediated by adenosine monophosphate-activated protein kinase (AMPK). In response enhanced AMP/ATP ratio, AMPK directly phosphorylates TSC and inhibits mTORC1 activity (Inoki, Zhu, et al. 2003). AMPK has also been identified to be activated in response to additional stimuli, such as genotoxic stress (Feng et al. 2005) and reactive oxygen species (ROS) (Alexander et al. 2010). Interestingly, AMPK also inactivates mTORC1 independently of TSC by directly phosphorylating raptor (Gwinn et al. 2008). TSC activity is also enhanced in response to the direct phosphorylation by glycogen synthase kinase 3 (GSK3). Through this mechanism, Wnt signalling upregulates mTORC1 activity by inhibiting GSK3 (Inoki et al. 2006) (Figure 1-6).

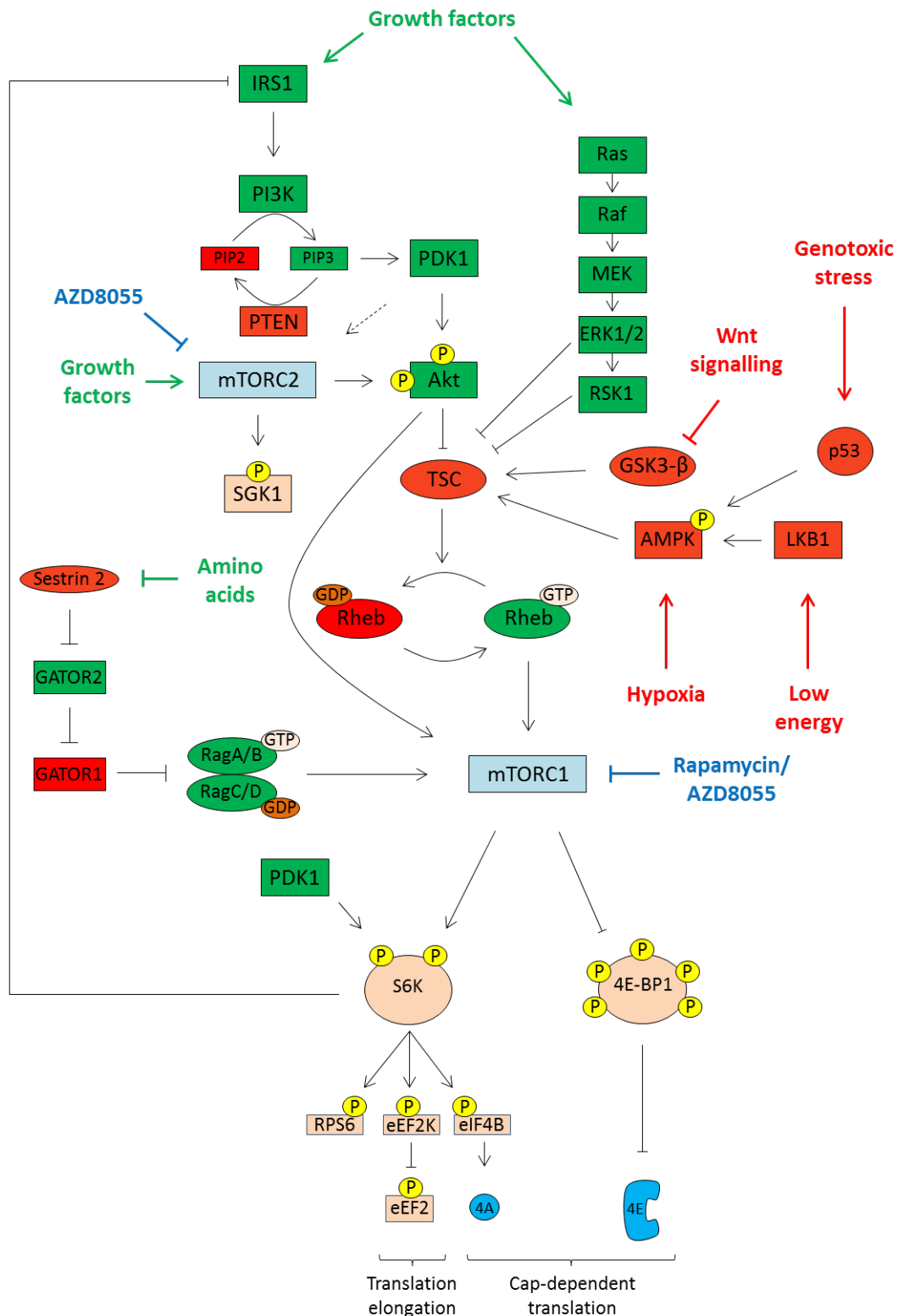


Figure 1-6. Schematic representation of mTOR signalling

Arrows indicate activators of the downstream protein, whereas blocked arrows indicate an inhibitor of the protein. Green boxes and arrows indicate activators of mTORC1 signalling, red boxes and arrows indicate inhibitors of mTORC1 signalling. Blue blocked arrows indicate catalytic inhibitors of mTOR signalling.

A major inhibitory kinase of TSC is Akt, a downstream effector of phosphoinositide 3-kinase (PI3K) signalling. The PI3K pathway is activated in response to stimulation by insulin and insulin-like growth factor 1 (IGF1). PI3K catalyses the formation of phosphatidylinositol (3,4,5) triphosphate (PIP3) from phosphatidylinositol (4,5) biphosphate (PIP2), promoting the translocation of Akt to the plasma membrane. At the plasma membrane, Akt is phosphorylated at Thr 308 by phosphoinositide-dependent kinase 1 (PDK1) (Stephens et al. 1998). Complete activation of Akt also requires phosphorylation at Ser 473, in a process dependent on mTORC2 activity (Figure 1-6). It has been suggested that phosphorylation at Ser 473 enhances the phosphorylation by PDK1 at Thr 308 (Sarbasov et al. 2005). PI3K activity is counteracted by phosphatase and tensin homolog on chromosome 10 (PTEN), which dephosphorylates PIP3 back to PIP2, inhibiting Akt activation. PTEN functions as an upstream inhibitor of mTORC1 signalling and has been identified as a tumour suppressor. Many inactivating PTEN mutations have been identified in various types of cancer (Li et al. 1997), leading to an upregulation of Akt activity, and mTORC1 signalling.

Growth factors activate two key signalling pathways in parallel, PI3K signalling and mitogen-activated protein kinase/extracellular signal-regulated kinase (MAPK/ERK) signalling (Figure 1-6). PI3K and MAPK/ERK converge to inhibit TSC activity, enhancing Rheb-GTP and activation of mTORC1 at the surface of the lysosome. However, for complete activation, mTORC1 must also translocate to the surface of the lysosome, in close proximity of Rheb. Translocation of mTORC1 to the lysosome is mediated by amino acids, and together with growth factor signalling, these two independent processes ensure that growth pathways are only activated when both amino acids and growth factors are in plentiful supply.

1.5.1.2 mTORC1 regulation of protein synthesis

Downstream targets of mTORC1 regulate cell growth and proliferation. In particular, mTORC1 controls protein synthesis by the phosphorylation of eIF4E-binding proteins (4E-BPs) and ribosomal protein S6 kinase (p70 S6K). Through the modulation of these targets, mTORC1 regulates cap-dependent translation initiation and translation elongation.

1.5.1.2.1 4E-BP

As described earlier (1.2.1.2 Recruitment of the 43S pre-initiation complex), cap-dependent translation requires the formation of the eIF4F complex at the 5' cap structure of mRNA, to facilitate the recruitment of the 43S ribosome to the mRNA. Formation of eIF4F is dependent on interactions between the 5' cap-binding component, eIF4E, and the scaffold component, eIF4G. eIF4E is regulated by a family of 4E-BPs that compete with eIF4G for a single binding site on eIF4E (Mader et al. 1995). Through this mechanism, 4E-BPs prevent eIF4F complex formation and inhibit cap-dependent translation. In mammalian cells, three 4E-BP isoforms have been identified. 4E-BP1 is highly expressed in most cell types; 4E-BP2 is the primary isoform in the brain, although it is expressed at lower levels in many other cell types; and 4E-BP3 is expressed primarily in colon and liver tissue (Tsukiyama-Kohara et al. 2001). The capacity of 4E-BP to bind eIF4E is regulated by mTORC1 dependent phosphorylation (Figure 1-7). When nutrients and growth factors are limiting, mTORC1 is inactive and 4E-BP is hypo-phosphorylated. In its hypo-phosphorylated state, 4E-BP interacts with eIF4E, preventing eIF4F formation and inhibiting cap-dependent translation. Conversely, in response to mTORC1 activation, 4E-BP is hyper-phosphorylated, stimulating 4E-BP dissociation from eIF4E and enhancing cap-dependent translation (Figure 1-7) (reviewed in (Hay & Sonenberg 2004)). The mechanism of 4E-BP regulation by mTORC1 is conserved across all three isoforms. Dissociation of 4E-BP from eIF4E is dependent on the sequential phosphorylation of four conserved residues. Phosphorylation at Thr 37 and Thr 46 primes 4E-BP for the subsequent phosphorylation at Thr 70, and finally Ser 65 (Gingras et al. 1999; Gingras et al. 2001). Interestingly, Thr 37, Thr 46 and Ser 70 have been shown to be insensitive to rapamycin, and Ser 65 may be rapamycin sensitive (Wang et al. 2005; Thoreen et al. 2009). It has been suggested that phosphorylation at Ser 70 and Ser 65 are the most critical for 4E-BP dissociation from eIF4E (Gingras et al. 2001) and provide a greater indication of mTORC1 activity.

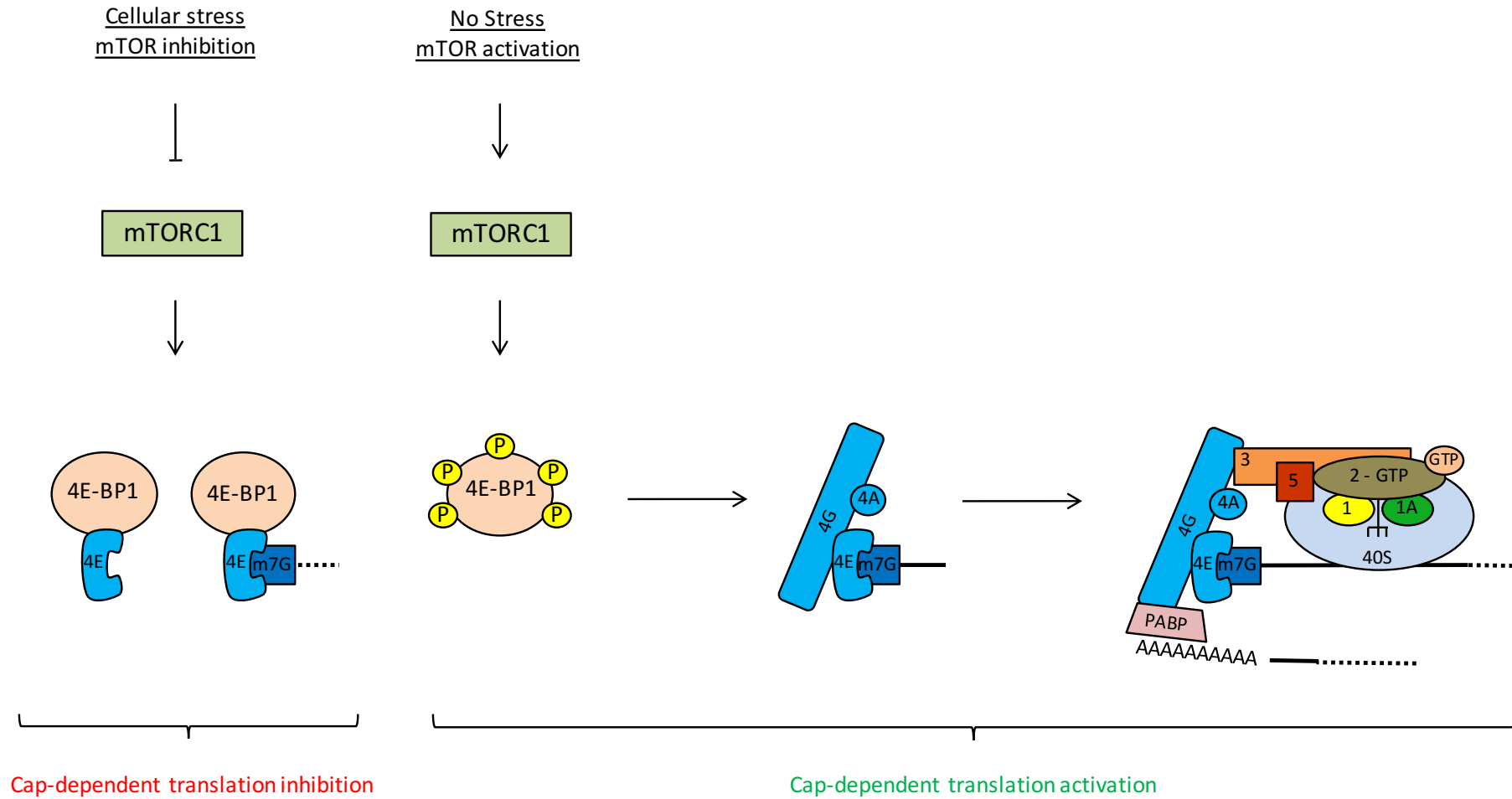


Figure 1-7. mTORC1 dependent regulation of 4E-BP1 and protein synthesis

Schematic representation of the regulation of protein synthesis mediated by 4E-BP1 in response to mTORC1 signalling.

1.5.1.2.2 p70 S6K

Two p70 S6K isoforms, S6K1 and S6K2, have been identified in mammalian cells, sharing conserved functions and phosphorylation sites. For the remainder of this thesis, S6K1 is referred to as p70 S6K.

p70 S6K is a downstream target of mTORC1. mTORC1 phosphorylates p70 S6K at Thr 389 generating a docking site for PDK1. PDK1 associates with p70 S6K, and the subsequent phosphorylation at Thr 229 is required for complete kinase activation (Pullen et al. 1998). Downstream targets of p70 S6K phosphorylation include eukaryotic elongation factor 2 kinase (eEF2K), eIF4B and ribosomal protein 6 (RPS6) (Figure 1-6).

As discussed earlier (1.2.2 Translation elongation), eEF2 mediates the translocation of the ribosome during translation elongation. eEF2 is phosphorylated within the GTP-binding domain, inhibiting its ability to bind to the ribosome (Carlberg et al. 1990). Phosphorylation of eEF2 is mediated by eEF2K, a calcium/calmodulin-dependent kinase. eEF2K is regulated by p70 S6K and inactivated by phosphorylation at Ser 366 (Xuemin Wang et al. 2001). However, the regulation of eEF2K is more complex and two additional inhibitory phosphorylation sites have been identified (Ser 78 and Ser 359). Although the exact mechanisms are not clear, these phosphorylation sites are regulated in an mTORC1 dependent, p70 S6K independent manner (Knebel et al. 2001; Browne & Proud 2004).

eIF4B is an RNA binding protein that has been shown to bind eIF3 (Méthot et al. 1996) and PABP (Bushell et al. 2001), and assist in the assembly of the 48S translation initiation complex (Dmitriev et al. 2003). However, the primary role of eIF4B is to stimulate the activity of the DEAD box RNA helicase, eIF4A, within the eIF4F complex (Rozen et al. 1990). eIF4B enhances ATP binding to eIF4A, stimulating its helicase activity to promote the unwinding secondary mRNA structure during translation initiation (Rogers et al. 1999). Phosphorylation of eIF4B at Ser 422 is central to the stimulation of eIF4A, and is mediated in response to mTORC1 signalling by p70 S6K (Raught et al. 2004); and MAPK/ERK signalling by RSK (Shahbazian et al. 2006).

The regulation of eEF2K and eIF4B provides a mechanism for mTORC1 to enhance both translation elongation and initiation. Regulation of both processes ensures a co-ordinated upregulation of protein synthesis in response to growth factors and nutrients.

RPS6 is a protein component of the 40S ribosomal subunit, and is phosphorylated at multiple residues by p70 S6K in response to mTORC1 activation (Chung et al. 1992). In addition, RPS6 is phosphorylated by p90 S6K (RSK) in response to MAPK/ERK signalling (Roux et al. 2007). The physiological role of RPS6 phosphorylation is still unclear, however, RPS6 phosphorylation has been implicated as a regulator of cell growth and cell size, as well as insulin production (Ruvinsky et al. 2005). The phosphorylation of RPS6 has also been implicated in the control of the ribosome biogenesis, regulating the transcription of nucleolar proteins required for rRNA synthesis (Chauvin et al. 2014).

1.5.1.2.3 5' terminal oligopyrimidine mRNA

5' TOP mRNA are distinguished by a 5' oligopyrimidine tract and are preferentially translated in response to mTORC1 activation (Jefferies et al. 1994). These mRNAs include components of the translation machinery and ribosomal proteins (Thoreen et al. 2012). It was originally suggested that 40S ribosomes containing phosphorylated RPS6 selectively regulated 5' TOP mRNA. This hypothesis was based on the coincidental reduction of RPS6 phosphorylation and 5' TOP mRNA down regulation in response to rapamycin (Jefferies et al. 1994). The regulation of 5' TOP mRNA were shown to be independent of p70 S6K and RPS6 (Pende et al. 2004; Ruvinsky et al. 2005), and it has been suggested that 5' TOP mRNA are regulated in a 4E-BP1 dependent manner (Thoreen et al. 2012), however this hypothesis remains controversial (Gandin, Masvidal, Hulea, et al. 2016).

1.5.1.2.4 Ribosome biogenesis

Ribosome biogenesis is dependent on the synthesis of ribosomal RNA (rRNA) and ribosomal proteins, which form the 40S and 60S ribosomal subunits. Although the mechanisms of ribosome biogenesis are beyond the scope of this thesis, it is important to appreciate the level of regulation exerted by mTORC1.

rRNA is synthesised by RNA polymerase I (Pol I), except for rRNA 5S that is synthesised by RNA polymerase III (Pol III). In addition to the regulation of rRNA by RPS6, mTORC1 positively regulates the activity of two Pol I factors, transcription initiation factor 1A (TIF-1A) (Mayer et al. 2004); and upstream binding factor (UBF) (Hannan et al. 2003). Inhibition of mTORC1 signalling suppresses the activity of both TIF-1A and UBF, inhibiting rRNA synthesis, as well as disrupting rRNA processing (Iadevaia et al. 2012). mTORC1 also regulates the expression of ribosomal proteins. Many ribosomal proteins are 5' TOP mRNA, and as eluded to earlier, their translation is heavily regulated by 4E-BP1 and mTORC1 signalling (Thoreen et al. 2012).

mTORC1 enhances ribosome biogenesis simultaneously with enhancing cap-dependent translation, co-ordinating increased levels of protein synthesis with increased availability of ribosomes.

1.5.1.3 Feedback mechanisms regulating mTORC1 activity

Negative feedback inhibition has been reported to play an important role in the regulation of mTORC1 signalling. Prolonged activation of mTORC1 (by the knockout of upstream negative regulators) or prolonged stimulation (by nutrients or growth factors) results in the down regulation of receptors that activate PI3K and MAPK/ERK signalling.

Insulin receptor substrate (IRS) is directly phosphorylated by p70-S6K, reducing the stability of IRS and altering its cellular localisation (Harrington et al. 2004; Shah et al. 2004; Takano et al. 2001). Growth factor receptor-bound protein 10 (Grb10) binds to activated receptor tyrosine kinases, such as insulin receptor (INSR), suppressing signalling from the receptor. Grb10 is directly phosphorylated by mTORC1, leading to the stabilisation of Grb10 and suppression of signalling to PI3K and MAPK/ERK (Yu et al. 2011; Hsu et al. 2011). The expression of platelet-derived growth factor receptor (PDGFR) is also reduced in response to mTORC1 signalling, limiting the activation PI3K and MAPK/ERK signalling (Zhang et al. 2007). These mechanisms combine to reduce PI3K and MAPK/ERK activation of mTORC1 signalling to limit mTORC1 activity and control growth and proliferation.

In addition to feedback signalling in response to constitutive mTORC1 activity, there is evidence supporting feedback mechanisms after mTORC1 inhibition. Rapamycin induced mTORC1 inhibition has been shown to activate MAPK/ERK signalling, in a mechanism dependent on p70 S6K, PI3K, and RAS signalling (Carracedo et al. 2008). Feedback control is not only exerted on receptors of upstream signalling. p70 S6K has been suggested to directly phosphorylate mTOR kinase at Ser 2448 (Holz & Blenis 2005; Chiang & Abraham 2005), however the exact role of this modification has yet to be elucidated.

1.5.2 mTORC2

mTORC2 is distinguished from mTORC1 by the presence of rictor and Sin1, and by being predominantly insensitive to rapamycin (Sarbasov et al. 2004). However, prolonged exposure to rapamycin has been reported to inhibit the assembly of mTORC2 in a number of cell types (Sarbasov et al. 2006).

1.5.2.1 Regulation of mTORC2 activity

The exact mechanism of mTORC2 insensitivity to rapamycin is unclear, but it indicates that mTORC1 and mTORC2 have distinct roles within the cell. The extensive use of rapamycin has meant that much more is known about the regulation of mTORC1, and the regulation of mTORC2 remains less clear. Whereas mTORC1 is activated by growth factors, nutrients and energy status, mTORC2 appears to be predominantly regulated in response to growth factors, such as insulin and IGF1. Growth factor activation of mTORC2 also indicates that it may be dependent on PI3K signalling (Frias et al. 2006; García-Martínez & Alessi 2008; Huang et al. 2008).

Although the exact mechanism of PI3K activation of mTORC2 has yet to be identified, insulin has been shown to enhance interactions between mTORC2 and the ribosome, and this interaction was shown to be essential for mTORC2 kinase activity (Zinzalla et al. 2011). Additionally, mTORC2 localises to the ER, an organelle rich with ribosomes, supporting the notion that mTORC2 may be regulated by the ribosome (Boulbles et al. 2011). TSC is a negative regulator of mTORC1 activity, however, TSC was also shown to associate with rictor. In response to growth factors, TSC binding to rictor was required for complete activation of mTORC2. TSC activation of mTORC2 was also independent of

Rheb-GAP activity, indicating this is a separate role to that observed in mTORC1 activation (Huang et al. 2008).

1.5.2.2 mTORC2 dependent cellular processes

mTORC2 has been shown to exhibit kinase activity toward two related proteins, Akt and serum- and glucocorticoid-induced protein kinase 1 (SGK1).

As described earlier (1.5.1.1 Regulation of mTORC1 activity), complete Akt activation requires phosphorylation within the kinase domain by both PDK1 (Thr 308) and mTORC2 (Ser 473). Interestingly, mTORC2 dependent Akt phosphorylation has been suggested to facilitate PDK1 dependent phosphorylation (Sarbasov et al. 2005), implicating mTORC2 as a positive regulator of mTORC1 signalling.

SGK1, has overlapping roles with other kinases, such as Akt. Two well described roles for SGK1 include the negative regulation the forkhead box O (FOXO) transcription factors (Brunet et al. 2001), and the stimulation of ion channels (Lang & Shumilina 2013). mTORC2 mediates the activation of SGK1 in response to growth factor activation of PI3K signalling. SGK1 is phosphorylated within its hydrophobic motif by mTORC2, facilitating the recruitment of PDK1 and subsequent phosphorylation within SGK1's kinase domain (García-Martínez & Alessi 2008).

mTORC2 has also been shown to regulate the organisation of the cytoskeleton, independently of mTORC1, by directly regulating paxillin, Rho, Rac and PKC α (Jacinto et al. 2004; Sarbasov et al. 2004).

1.5.3 mTORC1-mTORC2 crosstalk signalling

Although mTORC1 and mTORC2 are independent complexes, their signalling pathways are interlinked and can regulate one another. As described previously, mTORC2 regulates mTORC1 through the modulation of Akt activity. However, mTORC1 can also influence mTORC2 activity. p70 S6K has been shown to negatively regulate mTORC2 through feedback mechanisms to regulate mTORC1 activity. p70 S6K directly phosphorylates rictor and Sin1, two exclusive components of mTORC2, in a rapamycin sensitive fashion. Phosphorylation of rictor reduces mTORC2 dependent Akt phosphorylation. It

has been shown that the phosphorylation of rictor does not inhibit mTOR kinase activity, or disrupt mTORC2, but rictor mutant cells lacking this phosphorylation site display enhanced Akt phosphorylation (Dibble et al. 2009; Julien et al. 2010). Sin1 is also phosphorylated on multiple residues by p70 S6K, leading to the dissociation of Sin1 from mTORC2 and subsequently inhibiting mTORC2 kinase activity. In response to Sin1 phosphorylation, mTORC2 becomes insensitive to growth factor stimulation and mTORC2 dependent Akt phosphorylation is inhibited (Liu et al. 2013).

1.5.4 Dysregulation of mTOR in cancer

As a key regulator of cell growth and proliferation, it is unsurprising that mTOR signalling has been shown to be dysregulated in a number of disease states. Tumour suppressors, such as p53 and PTEN, are mutated in many different cancers, leading to increased signalling through mTOR (Hollstein et al. 1991; Li et al. 1997). p53 has been identified as a regulator of 4E-BP-dependent transformation. Mice lacking p53 and 4E-BPs showed enhanced levels of tumorigenesis, whereas mice lacking only 4E-BPs were resistant to oncogene driven transformation (Petroulakis et al. 2009). Furthermore, 4E-BPs have been shown to negatively regulate cell proliferation (Dowling et al. 2010). These studies suggest that the constitutive activation of mTORC1 enhances transformation through 4E-BP and the regulation of protein synthesis. The regulatory role of mTOR in proliferation has made it an extensive target for cancer therapy. Initially rapamycin analogues (rapalogues) were used, however, the clinical effect of these were minimal. The limited therapeutic effect of rapamycin can be attributed to the fact that rapamycin only partially inhibits mTORC1 dependent 4E-BP phosphorylation (Choo et al. 2008). mTORC1 negative feedback signalling also complicated the use of rapamycin, as mTORC1 inhibition lead to the activation of Akt, protecting cells from apoptosis (O'Reilly et al. 2006).

Catalytic mTOR inhibitors, targeting both mTORC1 and mTORC2, have now been developed. Catalytic inhibitors block 4E-BP phosphorylation and inhibit cap-dependent translation far more efficiently than rapamycin (Chresta et al. 2010).

1.6 DNA damage

It has been estimated that a cell within the human body is subjected to thousands of DNA lesions per day (Lindahl & Barnes 2000). DNA strand breaks are typically single strand breaks (SSBs) or double strand breaks (DSBs). DSBs are more dangerous for a cell because it does not leave a complementary strand for the repair of the break, and can lead to the loss of genetic material. However, SSBs block DNA replication, and critically, when the DNA replication apparatus encounters a SSB, it can generate a DSB (Jackson & Bartek 2009). These DNA lesions are generated by many different endogenous and exogenous sources.

1.6.1 Endogenous DNA damage

Endogenous DNA damage, often referred to as spontaneous DNA damage, arises naturally within the cell in response to normal metabolism and DNA replication. Spontaneous DNA damage can be induced by DNA mismatches or as a consequence of metabolic processes. One such metabolic process is oxidative phosphorylation. Reactive oxygen species (ROS) are generated as a by-product of oxidative phosphorylation, and ROS induce SSBs through the direct oxidation of DNA bases and the phosphodiester backbone (Cooke et al. 2003; Dizdaroglu & Jaruga 2012).

1.6.2 Exogenous DNA damage

Exogenous DNA damage includes environmental stimuli, such as solar ultraviolet light (UV) and ionising radiation (IR); as well as chemical stimuli, such as chemotherapeutics.

UV radiation is almost unavoidable and induces two types of DNA lesions, cyclopyrimidine dimers (CPDs) and 6-4 pyrimidine photoproducts (6-4PPs) (Rastogi et al. 2010). CPDs and 6-4PPs induce DNA breaks by distorting the DNA helix, inhibiting replication and transcription by blocking DNA polymerase and RNA polymerase II (Pol II) (Donahue et al. 1994). UV also induces the generation of ROS (Wang & Kochevar 2005), which induce SSBs through the same mechanism as endogenous ROS damage.

Exposure to IR can be from artificial and natural sources. Artificial sources of IR include medical treatments, such X-rays and radiotherapy, whereas natural

sources include cosmic radiation. IR induces DSBs through the direct ionisation of DNA, and additionally induces SSBs through the generation of ROS (Close et al. 2013).

Many chemotherapeutic drugs target cancer cells by inducing DNA damage. These DNA damage inducing drugs include bifunctional alkylating agents, such as cisplatin and mitomycin C, which generate DNA damage through inter- and intra-strand crosslinks; replication inhibitors, such as aphidicolin; and topoisomerase inhibitors, such as etoposide and anthracyclines (Jackson & Bartek 2009).

1.7 Topoisomerase enzymes

During replication and transcription, DNA is unwound and DNA strands are separated to allow access for DNA and RNA polymerases. Due to the helical structure of DNA, unwinding of DNA generates a topological strain on the DNA molecule, leading to supercoiling. Positive supercoiling is generated upstream of the replication or transcription site, and negative supercoiling generated downstream of the site. DNA supercoiling is detrimental to replication and transcription because it blocks the progress of polymerases.

Topoisomerases are enzymes that relieve the topological strain on DNA, through the introduction of transient DNA breaks. Two classes of topoisomerase are present in mammalian cells, type I (Top1), which generate a transient break in one strand of DNA; and type II (Top2), which generate a transient break in both strands of DNA simultaneously. (Reviewed extensively in (Ghilarov & Shkundina 2012; Wang 2002; Champoux 2001)).

1.7.1 Type I topoisomerase

Top1 functions as monomer and catalyses the relaxation of supercoiling through the induction of a SSB (Pommier 2006; Ghilarov & Shkundina 2012). A SSB is induced by nucleophilic attack of the DNA backbone, by a tyrosine residue within the enzymes catalytic site. This tyrosine residue covalently binds to the broken DNA stand, enabling the unbroken stand to pass through the break, relieving the supercoiling (Pommier 2006). After the reaction is complete, the broken stand is re-ligated within the enzyme and DNA is released. The reaction does not require any ATP because the energy is provided through the

tension of supercoiled DNA. However, magnesium is required to ensure the non-covalently bound end of cleaved DNA is maintained in the correct orientation. (Reviewed extensively in (Wang 2002; Pommier 2006; Ghilarov & Shkundina 2012))

Due to differences in their mechanism of action, Top1s are further subdivided into type IA (Top1A) and type IB (Top1B). Type1A targets only negatively supercoiling, whereas type1B relieves both positive and negative supercoiling (Pommier et al. 2010).

1.7.2 Type II topoisomerase

Top2 also relieves DNA supercoiling in response to replication and transcription. However, after the completion of replication, two interlinked DNA circles (catenanes) must be separated to allow the segregation of new chromosomes. This process, known as decatenation, is essential for all eukaryotic cells, and is primarily mediated by Top2. However, decatenation has also been suggested to be carried out by Top1B (Brown & Cozzarelli 1981).

Mammalian cells express two Top2 enzymes, Top2 α and Top2 β . Top2 α is essential for the separation of replicated chromosomes (Carpenter & Porter 2004), and relieves positive supercoiling more efficiently than negative supercoiling (McClendon et al. 2005). Top2 β is equally efficient towards both positive and negative DNA supercoiling (McClendon et al. 2005), and has also been shown to be dispensable in some cell types (Nitiss 2009a).

1.7.2.1 Catalytic mechanism of topoisomerase II

Top2 functions as homodimer and catalyses the cleavage of both DNA strands, generating a DSB. The DSB induced by Top2 is extremely transient, and does not induce the DDR because the broken DNA ends are protected by the enzyme (Figure 1-8) (Nitiss 2009a). ATP binding is required for this reaction to take place, facilitating a closed clamp structure around the DNA prior to DNA cleavage. The mechanism of DNA cleavage by Top2 is similar to that of Top1, as a tyrosine residue within the enzymes catalytic site is used to attack the phosphodiester backbone in the presence of magnesium. After catalysing the break, the enzyme forms a phosphotyrosine linkage with the 5' phosphate of the broken strand. As Top2 operates as a homodimer, Top2 cleaves both DNA

strands simultaneously. Each Top2 subunit individually targets opposite DNA strands, four bases apart, and binds to the 5' phosphate of the broken DNA strand. The DNA strand cleaved by Top2 is termed the gate segment (G segment), and the DNA duplex passed through the cleavage site is termed the transported segment (T segment). Cleavage of the DNA allows the T segment to be passed through the G segment, to relieve supercoiling or separating replicated chromosomes. After the T segment exits the enzyme, DNA breaks are re-ligated within the enzyme (Figure 1-8). The energy from the initially cleaved phosphodiester bond is maintained within the phosphotyrosine bond, allowing the enzyme to re-ligate DNA without a co-factor. ATP hydrolysis is required to open the clamp structure of Top2, releasing the re-annealed DNA duplex. (Top2 mechanism has been reviewed extensively in (Champoux 2001; Nitiss 2009a; Pommier et al. 2010; Ghilarov & Shkundina 2012)).

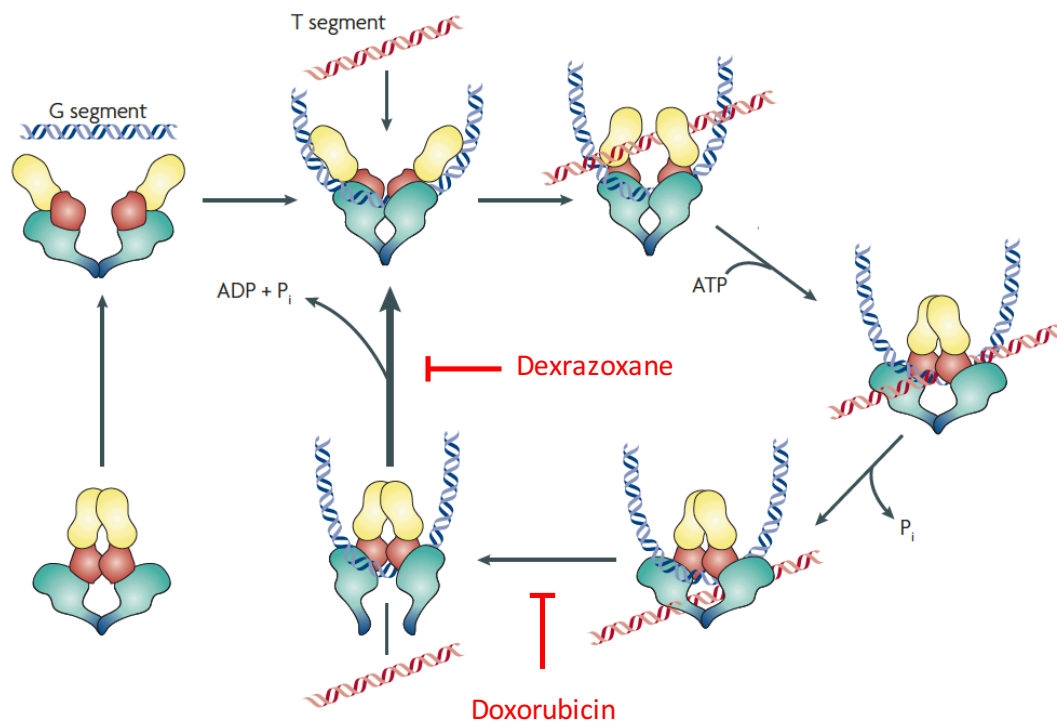


Figure 1-8. Catalytic cycle of topoisomerase II

Schematic representation of the catalytic cycle of topoisomerase II. Points of inhibition by doxorubicin (Top2 poison) and dexamethasone (Top2 catalytic inhibitor) are shown in red. This figure is adapted from Nitiss, 2009.

1.7.3 Therapeutic targeting of topoisomerases

Topoisomerase enzymes have become important chemotherapeutic targets, due to their ability to create transient DNA breaks through their normal reaction cycle. Many Top1 and Top2 inhibitors generate DNA damage by taking advantage of the transient DNA breaks induced by the enzymes, and are now in clinical use. The consequence of a DSB is potentially catastrophic, so Top2 is targeted within tumours to induce cell death.

Compounds that target Top2 activity generally do so by acting as either a Top2 poison, or a Top2 inhibitor. Top2 poisons covalently bind Top2 to the DNA, stabilising the complex after DNA cleavage, inducing a DSB. Conversely, Top2 inhibitors act by catalytically inhibiting enzymatic activity after re-ligation of DNA, and thus do not induce DSBs.

1.7.3.1 Doxorubicin

Doxorubicin (also known as Adriamycin) is an anthracycline antibiotic compound, derived from the bacterium, *Streptomyces peucetius*. Doxorubicin, and its derivatives, are extremely efficient chemotherapeutics used to treat a range of different cancers including breast, lung, liver and oesophageal cancers; as well as leukaemia and lymphomas. Although doxorubicin is a very effective chemotherapeutic, the exact mechanism of its action is not fully understood. Doxorubicin primarily induces cell death through the induction of DNA damage (Tewey et al. 1984), however, both ROS generation and DNA adduct formation have been implicated in doxorubicin toxicity (Gewirtz 1999; Yang et al. 2014).

1.7.3.1.1 Doxorubicin-dependent inhibition of topoisomerase II

Doxorubicin is a Top2 poison, and as mentioned previously the primary cellular response to doxorubicin is the induction of DSBs (Tewey et al. 1984; Burgess et al. 2008). Doxorubicin, as with all anthracyclines, intercalates within DNA. Under normal conditions, Top2 would bind DNA and induce a transient DSB. Cleavage of DNA is followed by rapid re-ligation after strand passage. Doxorubicin stabilises the cleavage intermediate and therefore inhibits re-ligation. Stabilisation by doxorubicin covalently traps Top2 to the DNA, leading to the formation of a stable Top2-DNA complex that blocks transcription and

replication. Although re-ligation is inhibited by doxorubicin, the DSB is confined to within the Top2 enzyme and consequently the DDR is not initiated. However, trapped Top2-DNA complexes are removed from DNA in a process mediated by the proteasome. It is the processing of these complexes that results in the generation of DSBs (Mao et al. 2001; Fan et al. 2008). By this mechanism, concentrations of doxorubicin in excess of 400 nM poisons every Top2 protein in the cell, generating enzyme mediated DNA damage (Nitiss 2009b).

Importantly, doxorubicin does not inhibit the enzymatic activity of Top2. In fact, it has been suggested that doxorubicin requires Top2 to be catalytically active to induce DSBs, by stabilising the subsequent cleavage intermediate. Catalytic inhibition of Top2 has been shown to desensitise cells to another Top2 poison, etoposide (Jenen & Sehested 1997). Furthermore, tumour cells that are resistant to doxorubicin-induced cell death have distinctly lower levels of Top2 (Burgess et al. 2008).

1.7.3.1.2 Doxorubicin generates reactive oxygen species

All anthracyclines contain a quinone moiety within their chemical structure. This quinone undergoes reduction into a semiquinone radical, through the action of the mitochondrial electron transport chain (Doroshov & Davies 1986). In the presence of iron, doxorubicin undergoes redox cycling back to a quinone, generating vast amounts of ROS, particularly hydroxyl free radicals (Doroshov & Davies 1986; Rajagopalan et al. 1988; Benchekroun et al. 1993). Hydroxyl radicals are extremely reactive and are capable of inducing DNA damage (Cooke et al. 2003; Dizdaroglu & Jaruga 2012). Through these mechanisms, it has been suggested that doxorubicin may influence its chemotherapeutic effect through ROS mediated damage.

1.7.3.1.3 Cardiotoxicity limits the effectiveness of doxorubicin

The use of doxorubicin has been limited somewhat by the induction of cardiotoxicity in patients. Cardiac tissue is rich in mitochondria, and studies in mice and rats have suggested that the cardio-toxic side effect of doxorubicin is mediated by the generation of ROS (Rajagopalan et al. 1988; Benchekroun et al. 1993; Zhou et al. 2001). This hypothesis has been further supported by pre-treatment with the iron-chelator, dexrazoxane, reducing doxorubicin-induced

ROS generation and cardiotoxicity (Ichikawa et al. 2014), however, this response has not been reported with other iron chelators. It is important to note that dexrazoxane is also an inhibitor of Top2 enzymatic activity, inhibiting ATP hydrolysis after DNA re-ligation. Through this mechanism, dexrazoxane traps Top2 on the DNA without generating a DSB (Overholtzer et al. 2003). To induce DSBs, doxorubicin requires Top2 to be enzymatically active. Thus, inhibition of Top2 activity by dexrazoxane may abrogate doxorubicin-induced DNA damage, by reducing the number of Top2-DNA covalent complexes. Additionally, a similar mechanism has been proposed for dexrazoxane to protect the cell from DNA damage induced by another Top2 inhibitor, etoposide. (Jenen & Sehested 1997). Furthermore, it has been suggested that dexrazoxane depletes Top2 within the cell, and it is this mechanism that protects cells from doxorubicin-induced DNA damage and cardiotoxicity (Deng et al. 2014).

1.8 DNA damage response signalling

All DNA damage poses a substantial risk to genomic stability, as it can interfere with normal DNA transcription and replication. In addition, if strand breaks are not adequately repaired, DNA damage can generate DNA mutations or chromosomal aberrations. Due to the high risk associated with DNA damage, mammalian cells have developed a range of connected cellular networks, collectively known as the DNA damage response (DDR). A number of different proteins regulate the DDR, and are categorised as DNA damage sensors, transducers, mediators, or effectors. DNA damage sensors recognise DNA damage and recruit transducer proteins. Transducer proteins signal through mediator proteins to activate effector proteins, which regulate cell cycle checkpoints and enable repair of the DNA (Figure 1-9) (Jackson & Bartek 2009; Polo & Jackson 2011).

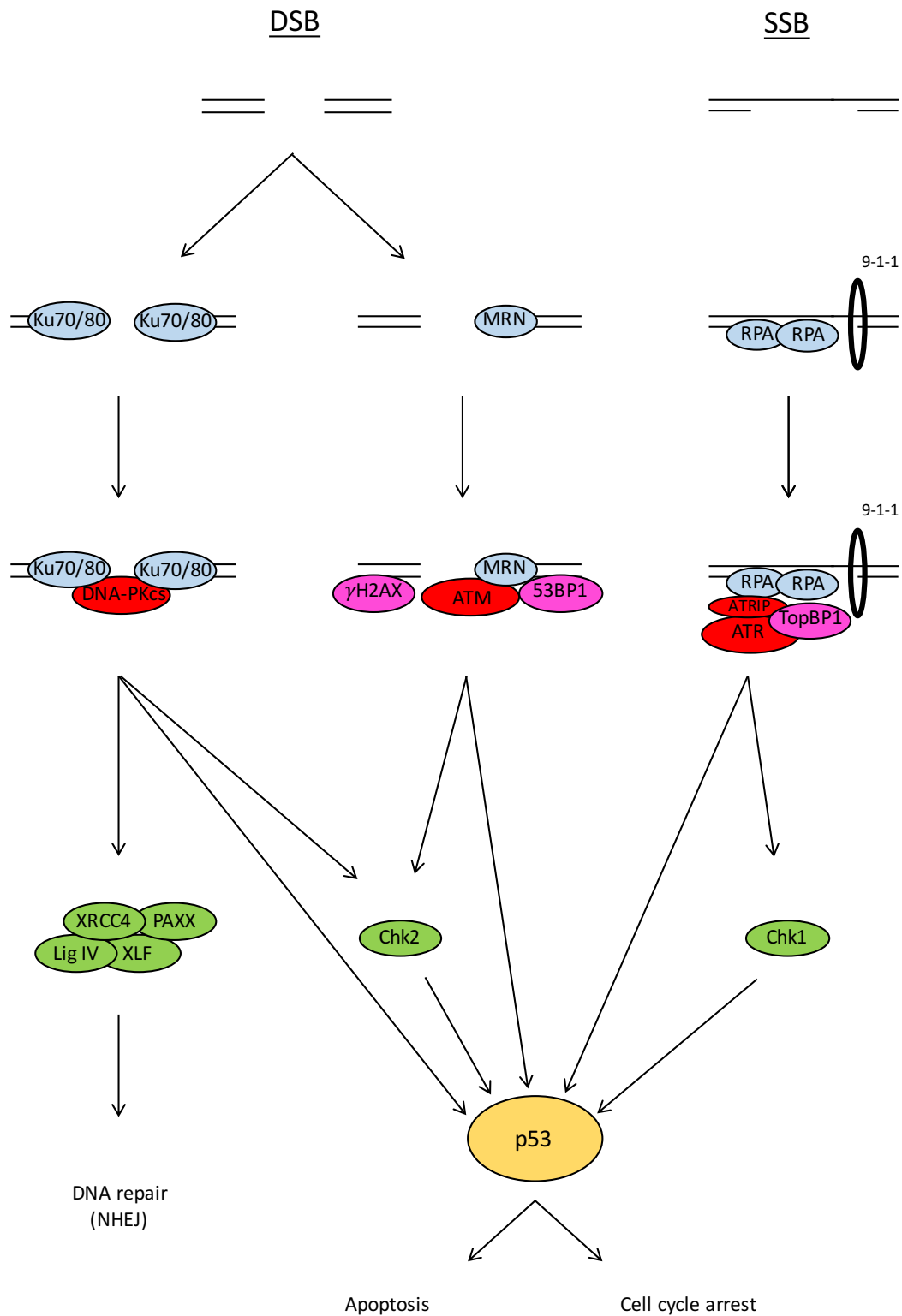


Figure 1-9. Schematic representation of the DNA damage response

Schematic representation of the DDR in response to single strand breaks (SSB) and double strand breaks (DSB). DNA damage sensors are in blue, mediators are in pink, transducers are in red, and effectors are in green.

The DDR is primarily mediated by three, functionally similar, PI3K serine/threonine protein kinases, Ataxia telangiectasia mutated (ATM), Ataxia telangiectasia and Rad3 related (ATR), and DNA-dependent protein kinase (DNA-PK). ATM, ATR and DNA-PK share a conserved response to the recognition of DNA damage. All three kinases are recruited to DNA breaks through interactions with their respective DNA damage sensors, within a conserved domain (Falck et al. 2005).

ATM and ATR are categorised as DNA damage signalling transducers, whereas DNA-PK is a DNA repair protein. However, all three are directly recruited to DNA breaks, and play key roles in DDR signalling. ATM and DNA-PKcs are primarily activated in response to DSBs, whereas ATR is primarily activated in response to SSBs and replication stress. A key role of the DDR is to induce cell cycle arrest in response to DNA damage, to enable the cell to repair the damage. Conversely, if the damage is deemed unreparable, downstream DDR effectors are capable of inducing cell death pathways.

1.8.1 ATM

In undamaged cells, ATM is found as an inactive homodimer. Following DNA damage, ATM undergoes auto-phosphorylation, leading to dimer dissociation and activation of an ATM monomer (Bakkenist & Kastan 2003). Although the exact mechanism of ATM activation in response to DSBs is not clear, it is known that ATM is recruited to DSBs through interactions with the MRE11-RAD50-NBS1 (MRN) complex (Uziel et al. 2003) (Figure 1-9). The MRN complex acts as a sensor of DNA damage, bridging the DSB, and is one of the first complexes to bind to the break site. Upon recruitment to the break, ATM phosphorylates the histone variant, H2AX (γ H2AX) (Burma et al. 2001). γ H2AX localises in the nucleosomes around the DSB, creating a platform for the recruitment of repair complexes, and the activation of ATM substrates (Bonner et al. 2008). Such target proteins include the DDR effector, checkpoint 2 kinase (Chk2). ATM was shown to phosphorylate and activate Chk2 (Matsuoka et al. 1998), and Chk2 subsequently phosphorylates the tumour suppressor, p53 (Shieh et al. 2000) (Figure 1-9). p53 is stabilised and activated upon phosphorylation, leading to various p53 dependent processes, such as the induction of p53 dependent gene expression and activation DNA damage cell

cycle checkpoints (Meek 2009). In addition, ATM regulates p53 activity through the direct phosphorylation of Ser 15, leading to its stabilisation (Canman et al. 1998; Banin et al. 1998). The exact mechanism of p53 activation, and its subsequent downstream signalling, are described in detail within a later section.

In addition to its role within the DDR, ATM has also been implicated in the indirect regulation of protein synthesis pathways. In response to hypoxia and ROS, ATM signalling was shown to lead to the inhibition of mTORC1 signalling through the regulation of AMPK (Alexander et al. 2010; Guo et al. 2010; Ji et al. 2010).

1.8.2 ATR

ATR is activated in response to a range of different DNA damage. However, it is predominantly activated by SSBs that are generated during DNA replication (Cimprich & Cortez 2008). Replication protein A (RPA) detects and binds to all single stranded regions of DNA (ssDNA). RPA coated ssDNA subsequently recruits ATR interacting protein (ATRIP) and ATR to the SSB (Zou & Elledge 2003). Although ATR is recruited to the break site, it is not fully activated. Complete activation requires the RAD17-replication factor C (RFC) mediated recruitment of RAD9-RAD1-HUS1 (9-1-1) complex, which is stimulated by RPA (Figure 1-9). The 9-1-1 complex subsequently recruits topoisomerase-binding protein-1 (TOPBP1), leading to the full activation of ATR (Kumagai et al. 2006).

ATR has a number of downstream effectors, such as checkpoint kinase 1 (Chk1) (Liu et al. 2000) (Figure 1-9). The primary role of Chk1 is the regulation of cell cycle progression. Entry into mitosis is governed by the activation of cdc2-cyclin B, by cdc25. However, Chk1 prevents progression into mitosis through the inhibitory phosphorylation of cdc25C (Sanchez et al. 1997). Chk1 also phosphorylates and activates p53 (Figure 1-9), in a similar mechanism to Chk2 (Shieh et al. 2000). In addition, ATR has been shown to directly phosphorylate p53 (Tibbetts et al. 1999). Interestingly, ATR regulates DNA damage checkpoints, and functions in a similar manner as ATM, regarding the regulation of p53 activity.

1.8.3 DNA-PKcs

It is imperative that a cell repairs damaged DNA to avoid mutations or chromosomal aberrations. The repair of DSBs in mammalian cells is carried out by two independent pathways, homologous recombination (HR), and non-homologous end joining (NHEJ). DNA repair by HR is limited to S-phase and G2, whereas NHEJ operates throughout the cell cycle, and does not require template DNA. Because of these characteristics, NHEJ is the major repair pathway for DSBs (Lieber 2008).

DNA-PK is a large kinase composed of a Ku70/Ku80 heterodimer and DNA-PK catalytic subunit (DNA-PKcs), which is activated in response to DSBs (Figure 1-9). DNA-PKcs has been identified as a key component of the NHEJ pathway and is essential for DNA repair (Kurimasa et al. 1999). Upon the induction of DSBs, Ku70/Ku80 heterodimer acts as a DNA damage sensor, binding to exposed DNA ends. The binding of Ku70/Ku80 to DNA stimulates the recruitment of DNA-PKcs to the break site through a direct interaction with Ku70/Ku80. Within the Ku:DNA-PKcs complex, conformational rearrangements enable DNA-PKcs to contact the DNA ends, leading to DNA-PKcs auto-phosphorylation and kinase activation (Gottlieb & Jackson 1993). Repair of DNA is mediated by DNA ligase IV, that is recruited to the break site as part of a complex with x-ray cross-complementing protein 4 (XRCC4), XRCC4-like factor (XLF) and paralog of XRCC4 and XLF (PAXX) (Figure 1-9). XRCC4 and PAXX directly bind to Ku70/Ku80 and DNA-PKcs, mediating the recruitment of DNA ligase IV. XRCC4, XLF and PAXX are all required for stabilisation of NHEJ protein assembly at the break site, and promote the efficient repair of DNA (Ahnesorg et al. 2006; Roy et al. 2015; Ochi et al. 2015).

In addition to its role in DNA repair, DNA-PKcs also mediates signalling within the DDR. Much like ATM, DNA-PKcs phosphorylates and activates Chk2 (Li & Stern 2005), subsequently upregulating p53 activity. (Figure 1-9) DNA-PKcs also mirrors ATM and ATR activity by directly activating p53, through the phosphorylation of Ser 15 (Lees-Miller et al. 1992). DNA-PKcs dependent regulation of the DDR and NHEJ takes place within the nucleus. However, DNA-PKcs has been shown to be present in the cytoplasm (Frasca et al. 2001), particularly at lipid rafts (Lucero et al. 2003), and has been shown to regulate

the activation of Akt at the plasm membrane (Feng et al. 2004). Additionally, DNA-PKcs has been shown to down regulate mTORC1 dependent phosphorylation of p70 S6K, in response to DNA damage (Cam et al. 2014). Furthermore, DNA-PKcs regulates the inhibition of protein synthesis through the activation of GCN2 in response to UV induced DNA damage. DNA-PKcs facilitated the reprogramming of mRNA translation to preferentially translate mRNAs involved in DNA repair (Powley et al. 2009). It should also be noted that DNA-PKcs has been shown to have a protective role in the maintenance of telomeres (Bailey et al. 1999).

1.9 p53

p53 plays an essential role in tumour suppression and is mutated a vast number of different cancers (Hollstein et al. 1991). p53 is a transcription factor that is activated in response to a range of cellular stresses, including DNA damage, replication stress, hypoxia, and nutrient deficiency (Lavin & Gueven 2006). As a transcription factor, p53 regulates the expression of many different genes, regulating cell cycle arrest, apoptosis, autophagy, and mTOR signalling (Brady & Attardi 2010; Riley et al. 2008).

1.9.1 Stabilisation and activation of p53

Activation of p53 dependent gene expression requires the stabilisation of p53; the binding of p53 to specific target genes; and finally, the activation of those target genes (Zilfou & Lowe 2009).

In unstressed cells, the level of p53 is low due to its relatively short half-life. p53 is subjected to a complex regulatory mechanism, mediated by MDM2, and culminating in the degradation of p53 by the proteasome (Figure 1-10). MDM2 is an E3 ubiquitin ligase (Honda et al. 1997), which binds and ubiquitinates p53 within the transactivation domain (TAD). MDM2 mediated ubiquitination facilitates the nuclear export of p53, and enhances its degradation, in a mechanism dependent on the proteasome (Kubbutat et al. 1997; Haupt et al. 1997). Therefore, during unstressed conditions, the level of p53 within the cell is determined by the rate of its degradation (Lavin & Gueven 2006). MDM2 is stabilised by MDM4 (also known as MDMX), protecting MDM2 from auto-ubiquitination and degradation (Gu et al. 2002). In addition, MDM4 directly inhibits p53 by blocking p53 transactivation (Finch et al. 2002).

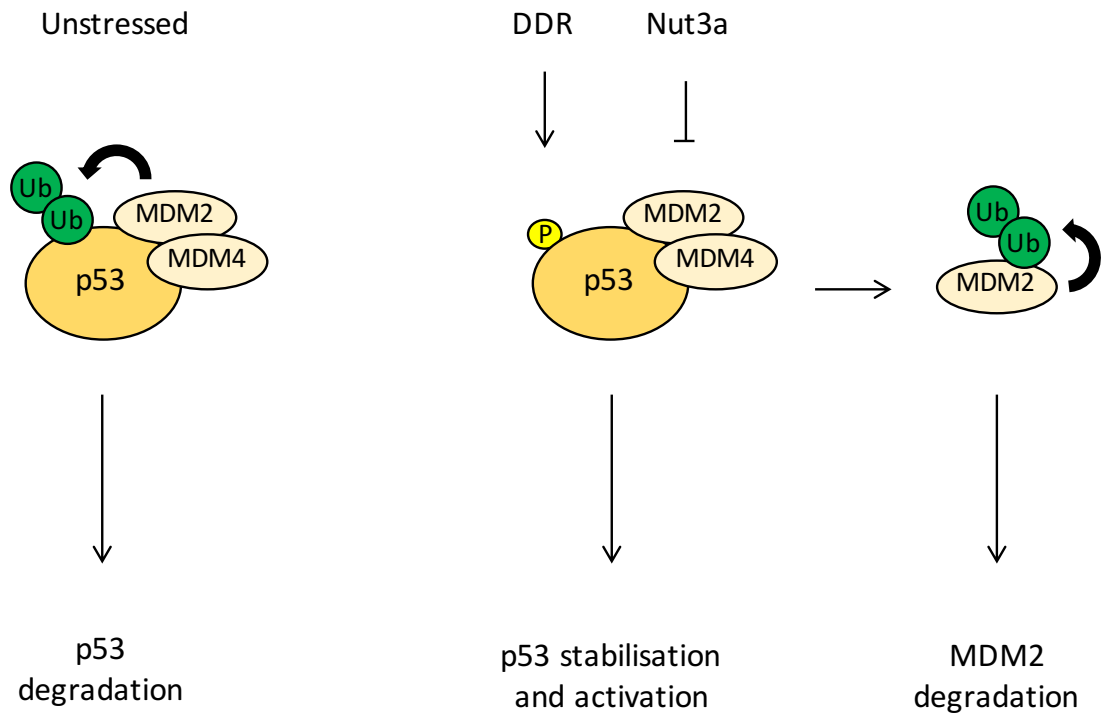


Figure 1-10. Stabilisation of p53

Schematic representation of p53 degradation and stabilisation.

In response to cellular stress, p53 and MDM2 are subjected to a range of post-translational modifications. These modifications, such as phosphorylation of p53 in response to DNA damage, disrupt the interaction between MDM2-MDM4 and p53 (Shieh et al. 1997). Phosphorylation of MDM2 also limits the capacity of MDM2 to shuttle p53 to the cytoplasm for degradation (Maya et al. 2001). Upon dissociation from p53, MDM2 becomes destabilised, leading to auto-ubiquitination and degradation (Stommel & Wahl 2004) (Figure 1-10). In the absence of MDM2 mediated ubiquitination, p53 is stabilised and forms an active tetramer. Activated p53 recruits co-activators and histone modifying enzymes to regulate the transcription of target genes (Brady & Attardi 2010).

1.9.2 p53 activation in response to DNA damage

p53 is extensively phosphorylated in response to DNA damage. Three residues within its TAD (Ser 15, Thr 18, and Ser 20) have been identified to be critical in the stabilisation of p53.

In response to DNA damage, such as that induced by IR and UV, p53 is rapidly phosphorylated at Ser 15. All three key DDR kinases directly phosphorylate p53 at Ser 15, destabilising the interaction with MDM2 (Banin et al. 1998; Tibbetts et al. 1999; Lees-Miller et al. 1992). Chk2, activated by ATM and DNA-PKcs, and Chk1, activated by ATR, also phosphorylate p53 at Ser 20 (Shieh et al. 2000), and ATM directly phosphorylates MDM2 (Maya et al. 2001). These modifications combine to weaken the interaction between p53 and MDM2, and provide robust stabilisation and activation of p53 in response to DNA damage.

Activated p53 regulates the transcription of a range of genes that determine cell fate. p53 mediates cell survival and repair of DNA damage, through the induction of DNA damage cell cycle checkpoints. However, if the damage is irreparable, p53 induces programmed cell death by enhancing the transcription of pro-apoptotic factors.

1.9.2.1 Cell cycle regulation

The development and survival of an organism requires cells to divide. The cell cycle is a complex set of cellular events that regulates DNA replication and cell division. The cell cycle has four stages, G1, S-phase, G2, and mitosis. G1 and G2 are gap phases, where the cell grows prior to DNA replication and mitosis.

Importantly, G1 and G2 play essential roles in cell cycle progression, in the form of cell cycle checkpoints, ensuring the cell is ready to progress into S-phase or mitosis (Figure 1-11).

The cell cycle is regulated by cyclin proteins that mediate cell cycle progression through the regulation of cyclin-dependent kinases (cdks). Cyclins are differentially expressed through the cell cycle, and bind to their respective cdk, activating its kinase activity. It is the activation of the cyclin kinase that triggers cell cycle progression.

Cyclin D (G1 cyclin) and cyclin E (G1/S-phase cyclin) phosphorylate, and inactivate, retinoblastoma protein (Rb). Decreased Rb leads to an upregulation of EF2 dependent gene expression, triggering progression from G1 into S-phase (Dyson 1998) (Figure 1-11). Cyclin A (S-phase cyclin) activates proteins involved in DNA replication and phosphorylates FoxM1. Phosphorylation of FoxM1 relieves auto-inhibition and stimulates the recruitment of CREB binding protein (CBP), thereby upregulating FoxM1 dependent gene expression (Major et al. 2004) (Figure 1-11). An important FoxM1 transcriptional target is cyclin B (mitosis cyclin), a cyclin that is required for progression from G2 into M-phase (Figure 1-11). (Reviewed extensively in (Giacinti & Giordano 2006; Satyanarayana & Kaldis 2009; Lim & Kaldis 2013)).

Cdk/cyclin complexes are negatively regulated by Cdk inhibitors (CKIs), blocking kinase activity and preventing cell cycle progression in response to cellular stress. Two families of inhibitors have been characterised. Firstly, INK4 family which bind only Cdk4 and Cdk6; and secondly, Cip/Kip family (including p21, p27 and p57), which primarily bind Cdk1 and Cdk2 (Sherr & Roberts 1999).

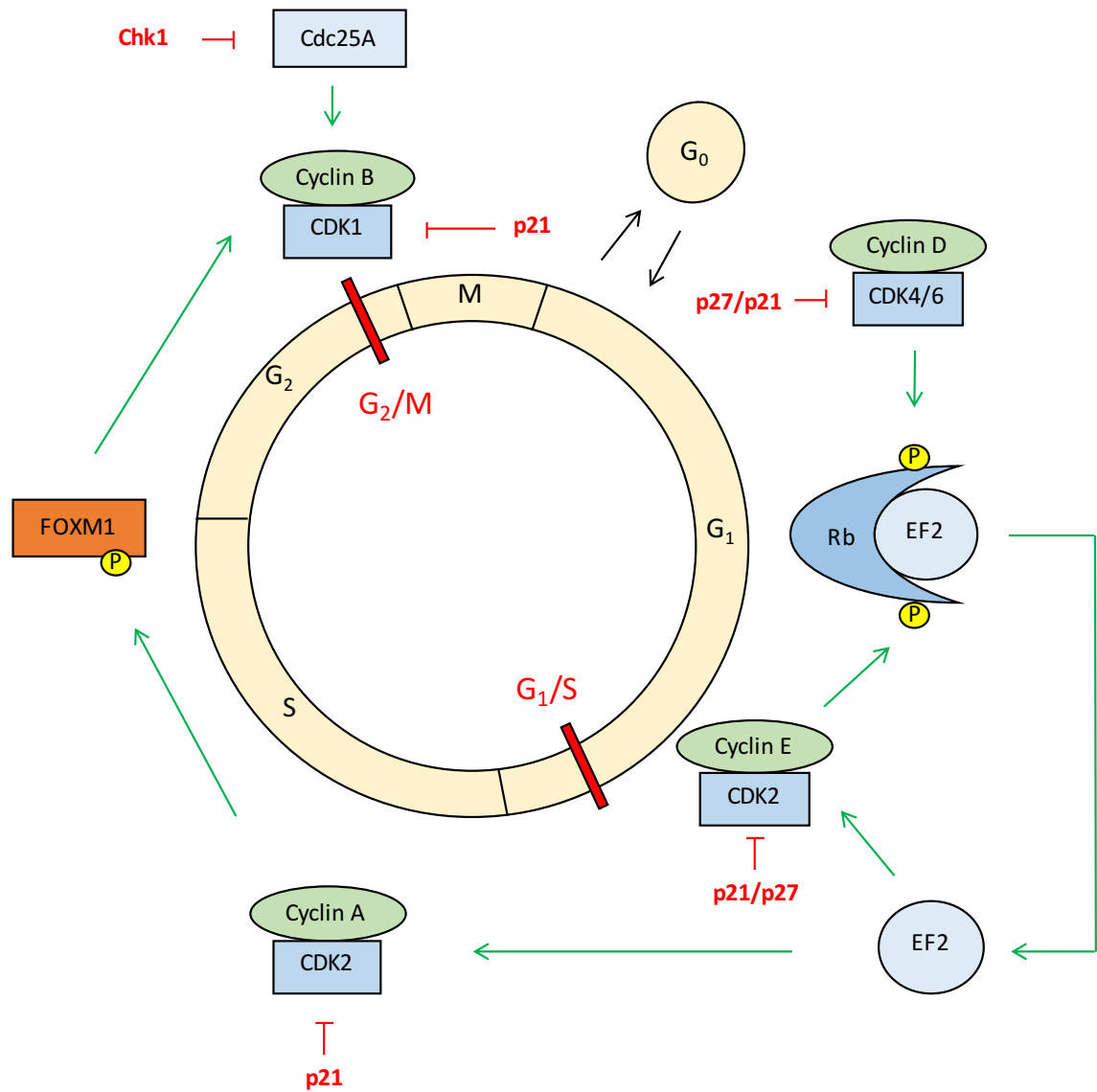


Figure 1-11. Regulation of cell cycle progression

Schematic representation of the regulation of the cell cycle. Cyclin/cdk dependent steps mediating cell cycle progression are marked by green arrows. G₂/M and G₂/S DNA damage cell cycle checkpoints are marked by red blocked arrows. Points of cyclin/cdk inhibition are also marked in red.

1.9.2.2 p53 dependent regulation of the cell cycle

In response to DNA damage, the cell cycle is inhibited by the activation of checkpoints prior to S-phase (G1/S checkpoint) and mitosis (G2/M checkpoint).

1.9.2.2.1 G1/S cell cycle arrest

Cell cycle arrest at the G1/S checkpoint is primarily mediated in a p53 dependent manner. p21 is an inducible cell cycle inhibitor and a target gene of p53 (El-Deiry et al. 1993). The expression of p21 was first shown to be enhanced after DNA damage induced p53 stabilisation (Dulic et al. 1994). p21 induces cell cycle arrest in G1 by inhibiting G1 cyclin complexes (cyclin D, cyclin E and cyclin A) containing Cdk2, Cdk4, and Cdk6 (Wade Harper et al. 1993; Waldman et al. 1995) (Figure 1-11). This mechanism inhibits the phosphorylation of Rb, and represses EF2 mediated transcription, thereby preventing progression into S-phase. Additionally, p21 inhibits DNA synthesis by binding to proliferating-cell nuclear antigen (PCNA) and suppressing DNA polymerase (Waga et al. 1994).

1.9.2.2.2 G2/M cell cycle arrest

G2/M cell cycle arrest is mediated by the regulation of the protein phosphatase cdc25C. Cdc25C removes an inhibitory phosphorylation site on cdc2, activating its kinase activity and enabling progression in mitosis (Figure 1-11). However, in response to activation of the DDR, Chk1 phosphorylates cdc25C at Ser 216, and enhances binding to 14-3-3 proteins (Sanchez et al. 1997). This interaction inhibits the phosphatase activity of cdc25C, preventing entry into mitosis. G2/M arrest is largely considered to be independent of p53 activity, however, 14-3-3 proteins are transcriptionally upregulated by p53 following DNA damage (Hermeking et al. 1997). In addition, p53 and p21 have been identified to be required for sustained G2 cell cycle arrest in response to DNA damage (Bunz et al. 1998). These studies suggest that p53 may play a key role in both checkpoints, however, the role of p53 in G2/M may be cell type dependent.

These mechanisms enable the DDR to slow the cell cycle, and prevent DNA synthesis or mitosis, until the cell has had time to repair the damage.

1.9.2.3 p53 mediated apoptosis

If DNA damage is irreparable, p53 induces programmed cell death to preserve genomic integrity. p53 has been shown to be essential for radiation induced apoptosis (Lowe et al. 1993). p53 regulates apoptosis in transcription dependent, and independent mechanisms, activating both the extrinsic, and intrinsic, apoptosis pathways (Haupt et al. 2003; Zilfou & Lowe 2009).

The induction of apoptosis is a complex series of events that are beyond the scope of this thesis. However, it is important to understand the regulatory role played by p53, particularly in the induction of the intrinsic apoptosis pathway. In the nucleus, p53 enhances the expression a number of pro-apoptotic factors including, PUMA (p53-up-regulated modulator of apoptosis), Bax, and Noxa (Nakano & Vousden 2001; Miyashita & Reed 1995; Oda et al. 2000). In the cytosol, p53 localises in the mitochondria, binding Bcl-X_L and Bcl2, inducing permeabilisation of the outer mitochondrial membrane, and the release of cytochrome c (Mihara et al. 2003). PUMA also plays a key role in the permeabilisation of the mitochondria outer membrane. PUMA enters the mitochondria and binds to Bcl-X_L, releasing p53 to activate Bax, and subsequently induce permeabilisation of the membrane (Chipuk et al. 2005).

p53 also regulates the extrinsic apoptosis pathway, through the upregulation of cell surface receptors, FAS and DR5 (Fridman & Lowe 2003; Zilfou & Lowe 2009).

1.9.2.4 p53 mediated regulation of mTOR signalling

Transcriptional networks under the influence of p53 are not limited to the DDR and cell death pathways. p53 is an important sensor of metabolic stress, and is activated in response to stimuli such as low oxygen and low nutrients, by AMPK (Jones et al. 2005). Through this mechanism, p53 is able to exert significant control over various metabolic processes (Vousden & Ryan 2009).

Integral to the role of p53 as a tumour suppressor is the inhibition of growth and proliferation, but these roles are also utilised to protect the cell from stress. Cell growth and proliferation is extensively regulated by mTOR signalling. mTOR signalling has been shown to be regulated by p53, as the loss of p53 leads to mTORC1 activation (Agarwal et al. 2015; Akeno et al. 2015). Furthermore,

enhanced p53 activity was shown to lead to diminished phosphorylation of 4E-BP1 and p70-S6K (Horton et al. 2002). p53 induces the expression of a number of negative regulators of mTOR signalling (Figure 1-12). The expression of PTEN, TSC2 and AMPK, are all enhanced by p53 in response to DNA damage (Feng et al. 2005; Feng et al. 2007). PTEN inhibits Akt activation, subsequently enhancing TSC activity, whereas AMPK directly enhances TSC activity through phosphorylation events. p53 also induces the expression of TSC2, enhancing TSC activity, and inhibiting mTORC1 in a similar manner to TSC overexpression (Inoki et al. 2002). p53 also regulates IGF-BP3, a protein that binds to IGF and diminishes PI3K signalling (Figure 1-12). Reduced levels of PI3K activation diminishes Akt activation, and enhances TSC activity (Buckbinder et al. 1995). Sestrin 1 and sestrin 2 are negative regulators of mTOR signalling, that are also induced by p53. Sestrin proteins have been shown to inhibit mTORC1 activity through the direct activation AMPK (Budanov & Karin 2008). Furthermore, sestrin proteins were shown to mediate the suppression of mTORC1 dependent 4E-BP1 phosphorylation, in combination with REDD1, in response to DNA damage (Cam et al. 2014). Interestingly, sestrin proteins have also been shown to regulate mTORC1 independently of AMPK by inhibiting mTORC1 translocation to the lysosome (Parmigiani et al. 2014) (Figure 1-12).

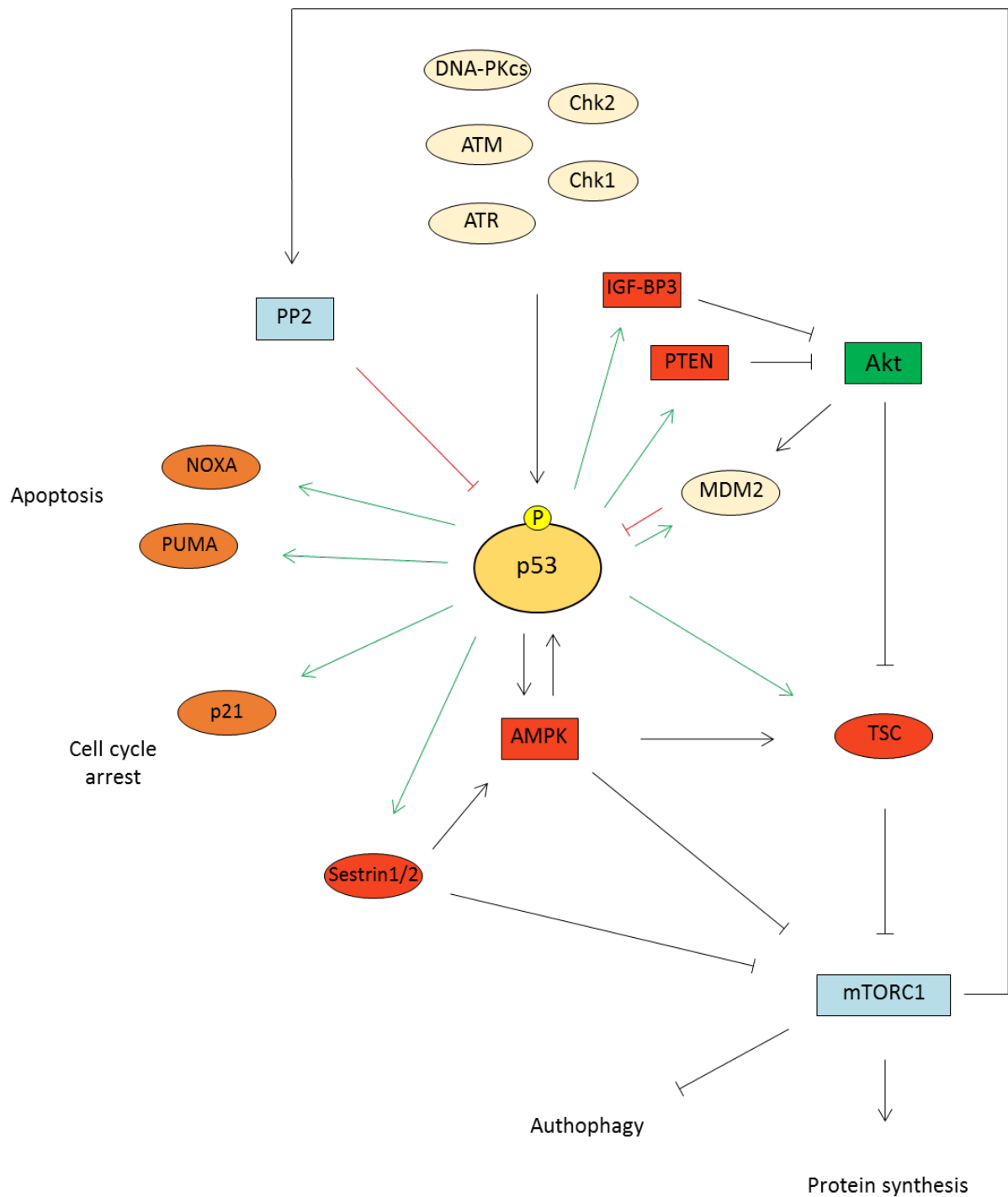


Figure 1-12. p53 dependent regulation of mTOR signalling

DDR signalling and AMPK activation of p53. Green arrows indicate transcriptional target genes of p53 signalling. Orange boxes indicate proteins involved in cell death and cell cycle arrest. Red boxes indicate inhibitors of mTORC1 signalling, whereas green boxes indicate activators of mTORC1 signalling. Red blocked arrows indicate inhibitors of p53 activity.

mTORC1 signalling is negatively regulated by p53. Conversely, p53 is negatively regulated by mTORC1, through the activation of protein phosphatase 2A (PP2A). PP2A de-phosphorylates p53 at Ser 15, a key modification in the stabilisation of p53, and this was shown to repress apoptosis (Kong et al. 2004) (Figure 1-12).

p53 activity is controlled by a number of positive and negative feedback mechanisms. Akt diminishes p53 activity by activating MDM2 and enhancing the degradation of p53 (Ashcroft et al. 2002). However, in response to stress, p53 dependent expression of PTEN represses MDM2 activity, through the inhibition of Akt, in a positive feedback mechanism that maintains p53 activity (Figure 1-12). Conversely, p53 negatively regulates itself through transactivation of MDM2 expression (Barak et al. 1993) (Figure 1-12). For a cell, the consequence of abnormal p53 activity could be catastrophic. These feedback mechanisms ensure p53 activity is tightly regulated to ensure cell survival.

1.10 Aims of thesis

Doxorubicin is an effective chemotherapeutic but it has been implicated in long-term toxicity in non-cancerous cells, such as cardiomyocytes.

Upon DNA damage, the DDR cell cycle checkpoints are activated to enable DNA repair. Additionally, global protein synthesis is inhibited to conserve energy and enable the selective translation of the mRNA of proteins involved in the repair process. Therefore, it might be expected that doxorubicin-induced DNA damage may lead to the rapid inhibition of global protein synthesis, possibly through the phosphorylation of eIF2 α , as has been observed with other DNA damaging agents. However, unpublished data generated within the Willis laboratory has shown that in the non-transformed breast epithelial cell line, MCF10A, doxorubicin induced DNA damage rapidly, but eIF2 α was not phosphorylated until 16 hours. Delayed phosphorylation of eIF2 α in response to doxorubicin is in stark contrast to UVB-induced DNA damage, when eIF2 α phosphorylation was observed within one hour (Willis laboratory data, unpublished). Interestingly, a delay of 12 hours between doxorubicin-induced DNA damage and eIF2 α phosphorylation has been observed in MEFs (Peidis et

al. 2011), suggesting that eIF2 α phosphorylation may regulate protein synthesis in response to doxorubicin-induced DNA damage.

The aim of this thesis was to characterise the mechanism of doxorubicin-induced protein synthesis inhibition, in the non-transformed cell line, MCF10A. Initially, the role of doxorubicin-induced eIF2 α phosphorylation was investigated with regard to the regulation of global protein synthesis. Furthermore, translation initiation is additionally regulated by the mTORC1 target protein, 4E-BP1, therefore, the regulation of mTORC1 activity in response to doxorubicin-induced DNA damage was also studied.

2 Materials and methods

2.1 Chemicals and reagents

Unless otherwise stated, all analytical grade chemicals were acquired from Sigma (Poole, UK). All reagents were acquired from Life Technologies (Paisley, UK) and ThermoFisher scientific (Loughborough, UK).

2.1.1 Buffers

RIPA buffer: 50 mM Tris pH 7.5, 150 mM sodium chloride, 1% Triton X-100, 0.1% SDS, 0.5% sodium deoxycholate, 1X Roche protease inhibitor cocktail and 1X Roche PhosStop phosphatase inhibitor cocktail.

5X SDS loading buffer: 312 mM Tris pH 6.8, 10% SDS, 50% glycerol, 0.1% bromophenol blue, 50 mM DTT.

Trypsin: PBS, 0.05% trypsin, 0.53 mM EDTA.

4X SDS-PAGE resolving buffer: 1.5 M Tris pH 8.8, 1% SDS.

2X SDS-PAGE stacking buffer: 0.25 M Tris pH 6.8, 0.2% SDS.

SDS-PAGE running buffer: 25 mM Tris pH 8.8, 192 mM glycine, 0.1% SDS.

SDS-PAGE transfer buffer: 50 mM Tris pH 8.8, 192 mM glycine, 20% methanol.

2.2 Cell culture techniques

2.2.1 Cell lines

MCF10A p53^{+/+}: Non-transformed human breast epithelial cell line.

MCF10A p53^{-/-}: p53 null non-transformed human breast epithelial cell line.

2.2.2 Cell maintenance

Cell lines were typically cultured in the appropriate media (Table 2-1), at 37°C and 5% CO₂, within a humidified atmosphere.

2.2.2.1 MCF10A p53^{+/+} cells

p53^{+/+} cells were trypsinised by incubation with 5 ml trypsin for 15 minutes at 37°C. Trypsin was deactivated by the addition of pre-warmed re-suspension media and cells were pelleted at 900 rpm. The cell pellet was re-suspended in the appropriate volume of growth media.

2.2.2.2 MCF10A p53^{-/-} cells

p53^{-/-} cells were trypsinised by incubation with 5 ml for 10 minutes at 37°C. Trypsin was deactivated by the addition of pre-warmed re-suspension media and cells were pelleted at 900 rpm. The cell pellet was re-suspended in the appropriate volume of growth media.

2.2.2.3 Synchronisation of MCF10A cells

MCF10A cells were synchronised to G0/G1 by serum and growth factor starvation. Cells were grown in MCF10A synchronisation media (Table 2-1) for 24 hours and released from synchronisation by replacing media with growth media (Table 2-1).

MCF10A (p53^{+/+} and p53^{-/-}) cell culture media: Dulbeccos modified eagles medium (DMEM) / F12 (1:1)			
Supplement	Growth media	Re-suspension media	Synchronisation media
Horse serum	5%	10%	0.1%
EGF	20 ng/ml	-	-
Insulin	10 µg/ml	-	-
Hydrocortisone	500 ng/ml	-	-
Cholera toxin	10 ng/ml	-	-

Table 2-1. MCF10A cell culture media

Table of cell culture media used for MCF10A cells. All media was prepared in Dulbeccos modified eagles medium (DMEM) / F12 (1:1), with the appropriate concentration of supplement.

2.2.2.4 Cryopreservation of cell lines

Cells were cultured to 80% confluence in a T-175 flask and re-suspended in 4 ml freezing mix (appropriate growth media, 20% FBS, 7.5% DMSO). Re-suspended cells were aliquoted into 1 ml volumes, and frozen slowly at -80°C prior to transfer to liquid nitrogen for long term storage.

2.2.2.5 Reviving frozen cell stocks

Frozen cells were thawed quickly in a 37°C water bath and transferred to 10 ml of the appropriate supplemented growth media. Cells were pelleted to remove DMSO and re-suspended in 37°C pre-warmed growth media equilibrated to 5% CO₂.

2.2.3 Cell transfection

2.2.3.1 Plasmid DNA transfection

Plasmid DNA was transfected into cells using lipofectamine LTX PLUSTM reagent. Cells were typically seeded onto a 6 well plate at a density of 6×10^5 in 2 ml growth media.

For each transfection, Lipofectamine LTX reagent was diluted in 150 µl Opti-MEM medium at a ratio of 3:1 with DNA (3 µl LTX per 1 µg DNA). The desired concentration of plasmid DNA was diluted in 150 µl Opti-MEM, and PLUSTM reagent was added to a ratio of 1:1 with DNA (1 µl PLUSTM reagent per 1 µg DNA). Diluted LTX transfection reagent was combined with diluted DNA/PLUSTM reagent and incubated for 5 minutes at room temperature. The transfection mix was added to the cells in a drop wise manner within 20 minutes of cell seeding.

2.2.3.2 siRNA transfection

Cells were transfected with siRNA using lipofectamine RNAiMAX reagent. Cells were typically seeded onto a 6 well plate at a density of 6×10^5 in 2 ml growth media.

For each transfection, 2 µl Lipofectamine RNAiMAX reagent was diluted in 100 µl opti-MEM medium, and the appropriate concentration of siRNA was diluted in 100 µl opti-MEM. Diluted transfection reagent was combined with diluted siRNA, mixed gently and incubated at room temperature for 10 minutes. siRNA

transfection mix was added to cells in a drop wise manner within 20 minutes of seeding.

siRNA sequences:		
Target protein	Manufacturer	Catalogue number
PKR	Dharmacon	LQ-003527-00-0002
PERK	Dharmacon	LQ-004883-00-0002
GCN2	Dharmacon	LQ-005314-00-0002
TSC2	Dharmacon	LQ-003029-00-0002
4EBP1	Dharmacon	LQ-003005-00-0002
4EBP2	Dharmacon	LQ-018671-00-002
PP6c	Dharmacon	LQ-009935-00-0002
DNA-PKcs	Dharmacon	LQ-005030-00-0002
ATM	Dharmacon	L-003201-00-0005
p53	Thermo Fisher	4390825, ID:s605
Non-targeting #1	Dharmacon	D-001810-01-05

Table 2-2. siRNA target sequences

siRNAs used to deplete proteins of interest.

2.2.4 Treatment with doxorubicin

Cells were typically seeded onto a 6 cm plate at a density of 1×10^6 , or onto 6 well plates at a density of 6×10^5 per well, 24 hours prior to treatment.

Doxorubicin (Sigma, Poole, UK) was dissolved in water and stored at 4°C, protected from light. Doxorubicin was spiked into media at the appropriate concentration.

2.2.5 Treatment with small molecule inhibitors

Cells were typically seeded onto 6 well plates at a density of 6×10^5 , 24 hours prior to treatment. AZD8055 (Selleckchem, Newmarket, UK), rapamycin (Cell Signaling Technologies), ISRIB (Sigma, Poole, UK), NU7026 (Sigma, Poole, UK), nutlin-3a (Sigma, Poole, UK) and VE-821 (Sigma, Poole, UK) were dissolved in DMSO, whereas KU55933 (Selleckchem, Newmarket, UK) was dissolved in water (Table 2-2).

Inhibitor	Target	Solubility	Stock concentration	Working concentration	Supplier
AZD8055	mTORC1/2	DMSO	1 μ M	100 nM	Selleck
Rapamycin	mTORC1	DMSO	100 μ M	100 nM	CST
ISRIB	ISR (eIF2B)	DMSO	2 mM	200 nM	Sigma
NU7026	DNA-PKcs	DMSO	10 mM	10 μ M	Sigma
KU55933	ATM	Water	10 mM	10 μ M	Selleck
VE-821	ATR	DMSO	10 mM	3 μ M	Sigma
Nutlin-3a	MDM2	DMSO	10 mM	10 μ M	Sigma

Table 2-3. Small molecule inhibitors

Small molecule inhibitors used to treat MCF10A cells.

2.2.6 Flow cytometry

6×10^5 cells were seeded on 6 well plates 24 hours prior to treatment. All cell staining was measured and quantified using a BD FACS Aria II flow cytometer (BD bioscience, Oxford, UK).

2.2.6.1 Cell death analysis

Cell death was measured through Annexin V-FITC (eBioscience, Altrincham, UK) and Draq7 (Abcam, Cambridge, UK) staining. All media (and any detached cells) was removed and stored at 37°C. Cells were washed in PBS and trypsinised for 15 minutes at 37°C. Trypsinised cells were combined with detached cells and allowed to recover for 15 minutes at 37°C. Cells were pelleted at 900 rpm for 5 minutes and re-suspended in 400 µl 1X annexin buffer (BD bioscience, Oxford, UK). Re-suspended cells were incubated with Draq 7 (1:1000) and annexin V-FITC (1:100) at room temperature for 10 minutes.

2.2.6.2 Cell cycle analysis of live cells

Cell cycle analysis of live cells was measured by Hoechst staining. Cells were incubated in media with Hoechst 33342 (16 µM) for 45 minutes prior to cell death analysis protocol (2.2.6.1 Cell death analysis).

2.2.6.3 Ethanol fixation of cells

All media (and detached cells) was removed and stored at 37°C. Cells were washed in PBS and trypsinised in 500 µl trypsin for 15 minutes. Trypsinised cells were combined with detached cells and allowed to recover for 15 minutes at 37°C. Cells were pelleted at 900 rpm for 5 minutes, re-suspended in 1 ml 70% ethanol and left at 4°C overnight.

2.2.6.4 Cell cycle analysis of fixed cells

FxCycle violet stain (4', 6-diamidino-2-phenylindole, dihydrochloride) preferentially binds dsDNA and fluoresces upon excitation with a violet laser. After ethanol fixation, cells were washed and re-suspended in 500 µl PBS/1% BSA. Cells were incubated with 1 µl FxCycle Violet stain, 16 hours prior to FACS analysis, to quantify populations of cells in G1 and G2 phases of the cell cycle.

2.2.6.5 Quantification of S-phase cells

5-ethynyl-2'-deoxyuridine (EdU) is an analogue of thymidine incorporated during DNA synthesis. EdU incorporation and staining was carried out using Click-iT EdU Flow Cytometry Assay Alexa Fluor 647 azide (Life technologies). Cells were incubated with EdU (10 μ M) for 1.5 hours prior to ethanol fixation.

After fixation, cells were washed in PBS/BSA 1% and re-suspended in 100 μ l 1X Click-iT saponin-based permeabilisation and wash reagent. To detect the incorporation of EdU, 500 μ l staining reaction cocktail (Table 2-3) was added to each sample and incubated in the dark at room temperature for 30 minutes. All samples were washed and re-suspended in 500 μ l 1X Click-iT saponin-based permeabilisation and wash reagent. To better characterise cell cycle state, EdU incorporated cells were subsequently incubated with FxCycle violet dye to additionally quantify G1 and G2 populations.

Reaction components	Volume per reaction
PBS	483 µl
CuSO ₄	10 µl
Fluorescent dye azide	2.5 µl
1X Reaction buffer additive	50 µl
Total volume	500 µl

Table 2-4. EdU reaction cocktail

Components of the EdU detection reaction cocktail.

2.2.6.6 Quantification of reactive oxygen species

Cells were incubated with 20 μ M 2',7'-Dichlorofluorescein diacetate (DCFH-DA) 30 minutes prior to collection. All media (and any detached cells) was removed and stored at 37°C. Adherent cells were washed in PBS and trypsinised in 500 μ l trypsin for 15 minutes. Trypsinised cells were combined with previously removed detached cells, pelleted at 900 rpm for 5 minutes and re-suspended in PBS.

2.2.6.7 Analysis of flow cytometry data

All data generated from the BD FACS Aria II flow cytometer was analysed with FlowJo data analysis software package version 10.1 (FlowJo LLC, Ashland, USA). Cell debris (Figure 2-1A) and doublets (Figure 2-1C) were removed from analysis by gating cell populations. Cell cycle state was quantified using the Watson Pragmatic algorithm (Watson et al. 1987) (Figure 2-1D), or manual gating following EdU incorporation and FxCycle staining (Figure 2-1E).

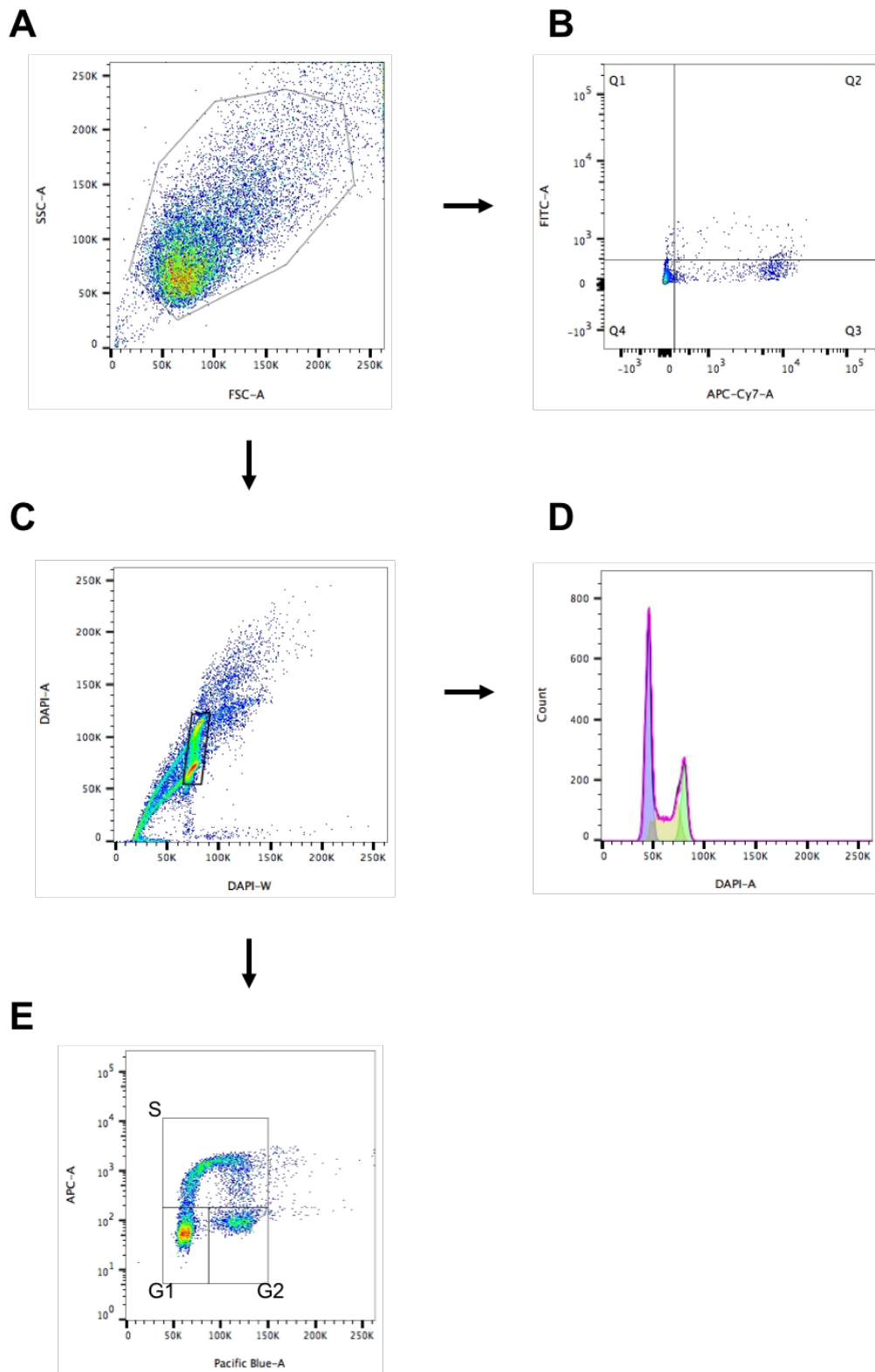


Figure 2-1. Gating of FACS analysis

Example of the gating of cells analysed by FACS to remove debris (A) and doublets (C) from analysis. Examples of gating used to analyse cell death (B), cell cycle using Watson analysis (D) and EdU/FxCycle detection (E).

2.2.7 Low resolution, high content fluorescent microscopy

DCFH-DA fluorescence was quantified in live cell populations by low-resolution, high throughput fluorescent microscopy, using Cellomics ArrayScan VTI HCS reader (ThermoFisher scientific).

2.2.8 β -Galactosidase senescence staining

Cellular senescence was measured using acidic β -Galactosidase staining kit (Cell Signalling Technology).

Cells were typically seeded onto a 6 well plate at a density of 6×10^5 per well, 24 hours prior to treatment with doxorubicin. All media was removed and cells were washed with PBS prior to fixation (1 ml fixative solution) for 15 minutes, at room temperature. After fixation, cells were washed with PBS and incubated with a staining solution (1X staining solution, 10 μ l supplement A and B, 1 mg/ml X-gal) at 37°C for 16 hours.

2.2.9 Microscopy

All microscopy images were acquired with bright field optics using Zeiss Axiovert 135 or Zeiss Axiovert 200M microscopes. All images were acquired with AxioCam HRc and analysed using Zeiss AxioVision software.

2.3 Protein techniques

2.3.1 Preparation of protein samples

2.3.1.1 Whole cell lysis

Media was removed and cells were washed with 1X PBS. Whole cell lysates were prepared by lysing cells directly in the culture plate plates in RIPA buffer. To digest all chromatin, 10 units of Benzonase (Millipore, Hertfordshire, UK) was added per 200 µl lysis buffer. Cell lysates were incubated on ice for 30 minutes to allow for nucleic acid digestion. Lysates were snap frozen in liquid nitrogen and stored at -80°C until required.

2.3.1.2 Protein quantification

The protein concentration of all lysates was quantified using Pierce BCA protein assay kit (ThermoFisher scientific, Loughborough, UK). 10 µl of each sample was incubated with 200 µl BCA solution (50:1 dilution of reagent A to B) in a microtitre plate. Plates were incubated at 37°C in the dark for 30 minutes before cooling to room temperature. The absorbance was measured using a plate reader (BioTek, Swindon, UK) at 562 nm. The protein concentrations of all samples were calculated in duplicate.

2.3.2 Western blotting

2.3.2.1 Protein sample preparation

All protein samples were diluted in 5X SDS sample buffer (312 mM Tris pH 6.8, 10% SDS, 50% glycerol, 0.1% bromophenol blue, 50 mM DTT) prior to heating at 75°C for 10 minutes.

1X 1.5 mm SDS-PAGE gel resolving gels				
	6%	10%	12.5%	15%
Resolving buffer (4X)	2.5 ml	2.5 ml	2.5 ml	2.5 ml
Acrylamide (30%)	2 ml	3.34 ml	4.2 ml	5 ml
Water	5.5 ml	4.06 ml	3.2 ml	2.4 ml
25% APS	100 µl			
TEMED	6 µl			
5 ml stacking gel				
Stacking buffer (2X)	2.5 ml			
Acrylamide (30%)	0.67 ml			
Water	1.8 ml			
25% APS	50 µl			
TEMED	3 µl			

Table 2-5. Recipes for SDS-PAGE gels

Recipe for SDS-PAGE gels. Depending on the resolution required, SDS-PAGE resolving gels were prepared with differing percentages of acrylamide.

2.3.2.2 SDS-polyacrylamide gel electrophoresis

Proteins were separated according to mass using sodium dodecyl sulphate polyacrylamide gel electrophoresis (SDS-PAGE). Gels were cast using the appropriate resolving gel polyacrylamide percentage and stacking layer of polyacrylamide (Table 2-4) and run using a Bio-Rad mini-protean tetra cell system (Bio-Rad, Hertfordshire, UK). 20 µg of protein was typically loaded in each well for each sample. Gels were run in 1X SDS running buffer at 80 volts for 45 minutes (to allow samples to clear the stacking gel), prior to increasing to 105 volts until the sample buffer passed through the gel.

Pre-cast NuPAGE bis-tris (4-12%) or tris-acetate (3-8%) gels were run using the XCell SureLock system and the provided 1X running buffer. Gels were run at 150 volts until the sample buffer passed through the gel.

2.3.2.3 Protein transfer to PVDF membrane

Proteins were transferred to PVDF membranes using wet transfer. Transfer cassettes were layered with a sponge, 3 pieces of chromatography paper, SDS-PAGE gel, PVDF membrane (pre-soaked in methanol), 3 pieces of chromatography paper and another sponge. Transfer cassettes were placed into a transfer block and submerged in SDS transfer buffer. Protein transfers were typically run at 100 volts for 1 hour at 4°C.

2.3.2.4 Ponceau staining

Protein bands were visualised on PVDF membranes using Ponceau S solution (0.5% w/v in 5% w/v/TCA) to determine the quality of protein transfer.

Membranes were incubated with Ponceau S solution for 5 minutes at room temperature, and washed in water to detect protein bands.

2.3.2.5 Primary antibody incubation

Non-specific binding was blocked by incubation of PVDF membranes in 5% skimmed milk powder in TBST, for 1 hour. Primary antibodies for non-phosphorylated target proteins were diluted in 5% skimmed milk powder in 1X TBST (Table 2-5), whereas primary antibodies for phosphorylated target proteins were diluted in 5% BSA in 1X TBST (Table 2-6). Membranes were incubated with primary antibodies on a rotator at 4°C, for approximately 16 hours.

2.3.2.6 Secondary antibody incubation and ECL detection

After the removal of the primary antibody, PVDF membranes were washed 3 times for 10 minutes in 1X TBST. The appropriate concentration of secondary antibody (Table 2-7) was diluted in 5% skimmed milk powder in 1X TBST and incubated with the membrane on a rotator for 2 hours at room temperature. Following three further 10 minute washes with 1X TBST, ECL-prime solution (GE healthcare, Buckinghamshire, UK) was prepared and incubated on the membrane for 5 minutes. X-ray film was exposed to the membrane to visualise luminescence.

2.3.2.7 Secondary antibody incubation and LI-COR detection

LI-COR specific secondary antibodies (Table 2-7) were diluted in 5% skimmed milk powder in TBST and incubated on a rotator for 2 hours, protected from light. Membranes were washed three times for 10 minutes in TBST and stored in PBS at 4°C until detection.

Fluorescent signal was detected using LI-COR Odyssey imaging system and images analysed with LI-COR image studio software package version 5.2.5 (LI-COR Biosciences, Nebraska, USA).

Target	Source	Band size (kDa)	Dilution	Supplier
Akt	Rb	60	1:1000	Cell signaling #9272
ATF-4	Rb	49	1:1000	Cell signaling #11815
ATM	Rb	350	1:1000	Abcam #32420
Cyclin A	Ms	55	1:1000	Cell signalling #4656
Cyclin D1	Ms	36	1:1000	Cell Signalling #2926
Cyclin E1	Ms	47	1:1000	Cell signalling #4129S
DNA-PKcs	Rb	460	1:3000	Abcam #70250
eEF2	Rb	95	1:3000	Cell signaling #2332
eEF2K	Rb	105	1:1000	Cell signaling #3692
eIF2 α	Rb	38	1:1000	Cell signaling #9772
eIF4E-BP1	Rb	15-20	1:4000	Cell signaling #9644
eIF4E-BP2	Rb	15-20	1:1000	Cell signaling #2845
GCN2	Rb	220	1:1000	Cell signaling #3302
MDM2	Ms	90	1:1000	Sigma #M4308
p21	Rb	21	1:1000	Cell signaling #2947
p27	Rb	27	1:1000	Cell Signalling #2552
p53	Ms	53	1:1000	Dako #M7001
p70 S6 Kinase	Rb	70	1:1000	Cell signaling #2708
PARP	Rb	89-116	1:1000	Cell signaling #9542
PERK	Rb	140	1:1000	Cell signaling #3192
PKR	Rb	74	1:1000	Cell signaling #12297
PP6c	Rb	37	1:1000	Abcam #131335
RPS6	Rb	32	1:2000	Cell signaling #2217
TSC2	Rb	200	1:1000	Cell signaling #4308S
β -tubulin	Rb	55	1:1000	Cell signaling #2146

Table 2-6. Primary antibodies for non-phosphorylated target proteins

Table of primary antibodies used for western blot analysis. Source of antibodies were mouse (Ms) or rabbit (Rb). All antibodies were diluted in 5% milk/TBST.

Target	Source	Band size (kDa)	Dilution	Supplier
p-Akt (S-473)	Rb	60	1:1000	Cell signaling #4058
p-AMPK (T-172)	Rb	62	1:1000	Cell signaling #2535
p-ATM (S-1981)	Ms	350	1:1000	Abcam #81292
p-Chk 1 (S-345)	Rb	56	1:1000	Cell signaling #2348
p-Chk 2 (T-68)	Rb	56	1:1000	Cell signaling #2661
p-DNA-PKcs (S-2056)	Rb	460	1:1000	Abcam #18192
p-eEF2 (T-56)	Rb	95	1:3000	Cell signaling #2331
p-eEF2K (S-366)	Rb	105	1:1000	Cell signaling #3691
p-eIF2 α (S-51)	Rb	38	1:2000	Abcam #32157
p-eIF4E-BP1 (S-65)	Rb	15-20	1:4000	Cell signaling #9456
p-H3 (S-10)	Rb	17	1:1000	Cell Signalling #9701S
p-p38 (T-180/Y-182)	Rb	38	1:1000	Cell signaling #9215
p-p53 (S-15)	Ms	53	1:1000	Cell signaling #9286
p-p70 S6 Kinase (T-389)	Rb	70	1:1000	Cell signaling #9205
p-RPS6 (S-240/S-244)	Rb	32	1:2000	Cell signaling #2215
p-TSC2 (T-1462)	Rb	200	1:1000	Cell signaling #3617S
γ H2A.X (S-139)	Rb	15	1:1000	Cell signaling #9718

Table 2-7. Primary antibodies for phosphorylated target proteins

Table of primary antibodies used for western blot analysis. Phosphorylated residue or residues are indicated in brackets. Source of antibodies were mouse (Ms) or rabbit (Rb). All antibodies were diluted in 5% BSA/TBST.

Antibody	Dilution used	Supplier
ECL α -Mouse HRP	1:5000	Dako #PO447
ECL α -Rabbit HRP	1:10000	GE healthcare #NA934V
LI-COR α -Mouse	1:2000	LI-COR IR 800CW #925-32210
LI-COR α -Rabbit	1:2000	LI-COR IR 680RD #925-68071

Table 2-8. Secondary antibodies

Table of secondary antibodies used for western blot analysis. Secondary antibodies for ECL or LI-COR western blot detection systems. All antibodies were diluted in 5% milk/TBST. LI-COR secondary antibodies were protected from light.

2.3.2.8 Removal of antigens from PVDF membranes

Antigens were removed from membranes after incubation with Restore™ western blot stripping buffer (ThermoFisher scientific) for 15 minutes. Stripped membranes were washed three times for 10 minutes in TBST prior to re-blocking in 5% skimmed milk powder TBST and primary antibody incubation (2.3.2.5 Primary antibody incubation).

2.3.2.9 Quantification of band intensity

Luminescence from all ECL western blots were quantified using Image Studio software package version 5.2.5 (LI-COR Biosciences, Nebraska, USA). All values were typically normalised to β -tubulin.

2.3.3 Radiolabelling

2.3.3.1 ^{35}S methionine incorporation

Cells were typically seeded in a six well plate at a density of 6×10^5 , 24 hours prior to incorporation. Media was supplemented with 1.11 MBq/ml ^{35}S methionine label (Hartman Analytical, Germany) for 30 minutes at 37°C. Cells were washed with chilled PBS prior to lysis in 400 μl passive lysis buffer (Promega, Southampton, UK).

2.3.3.2 ^3H uridine incorporation

Cells were typically seeded in a six well plate at a density of 6×10^5 , 24 hours prior to incorporation. 750 μl of media was supplemented with 0.14 MBq/ml ^3H Uridine (Hartman Analytical, Germany) for 30 minutes at 37°C. Media was removed and cells washed with chilled PBS prior to lysis in 400 μl RIPA buffer.

2.3.3.3 Radioisotope precipitation and quantification

Protein was precipitated using trichloroacetic acid (TCA) at a final concentration of 25%. Precipitated protein was captured on glass fibre filter paper (GE Healthcare, Buckinghamshire, UK) using a vacuum manifold. Captured protein was washed with 70% IMS and acetone. 2 ml ecoscint scintillation cocktail (National Diagnostics) was added to the filter paper in a scintillation vial.

Incorporation of ^{35}S and ^3H radioisotopes were quantified using a Wallac winspectral 1414 liquid scintillation counter. Each sample was carried out in triplicate.

2.3.3.4 Normalisation of spectral counts

Quantified spectral counts per minute were normalised to the total amount of protein for each sample, using a Bradford assay prior to TCA precipitation. 5 µl of each lysate was added to 170 µl of Bradford reagent (Bio-Rad, Hertfordshire, UK) in a microtitre plate, in triplicate. The absorbance of each sample was measured at 595 nm on a plate reader (BioTek, Swindon, UK).

2.3.4 Polysome profiling

2.3.4.1 Preparation of cell lysate

Cells were typically seeded at a density of 10×10^6 in a 15 cm plate, 24 hours prior to treatment. Cycloheximide (final volume 100 µg/ml) was added to cells at 37°C, 5 minutes prior to harvest. Plates were transferred onto ice and washed twice with 1X PBS-cycloheximide (100 µg/ml). Cells were lysed directly on the plate in 500 µl lysis buffer (300 mM NaCl₂, 15 mM MgCl₂, 15 mM tris-HCL pH 7.5, 1 mM DTT, 0.2 M sucrose, 0.1 mg/ml cycloheximide, 0.5% IGEPAL, 5 µl RNasin per 1 ml). Cells were incubated on ice for 3 minutes prior to pelleting cells at 1300 x g for 5 minutes. The supernatant was snap frozen in liquid nitrogen and stored at -80°C until required.

2.3.4.2 Sucrose density centrifugation

Sucrose gradients were prepared using differing concentrations of sucrose (w/v) in gradient buffer (300 mM NaCl₂, 15 mM MgCl₂, 15 mM tris-HCL pH 7.5, 1 mM DTT, 0.1 mg/ml cycloheximide). For example, sucrose concentrations of 50%, 40%, 30%, 20% and 10% (w/v) were layered sequentially in 12 ml ultracentrifuge tubes. 2 ml of each solution was added in order of decreasing sucrose concentration and frozen at -80°C prior to the addition of the next layer. Gradients were completely thawed at 4°C prior to use. Cell lysates were layered onto of the sucrose gradient tube prior to centrifugation at 38,000 rpm (acceleration 9, deceleration 6) for 2 hours at 4°C, using a Beckman Coulter ultracentrifuge.

A solution of 65% sucrose was injected into the base of the gradient tube at a flow rate 1 ml/min. Gradients were fractionated using a gradient fractionation system (Presearch Ltd, Hampshire, UK) and fractions were collected at 1 minute intervals using FOXY Jr collection system (Presearch Ltd, Hampshire,

UK). Absorbance was measured constantly at 254 nm using a UA-6 UV-VIS detector (Presearch Ltd, Hampshire, UK).

2.3.5 Statistical analysis

All statistical analysis testing for significance used a two-tailed student's *t* test, assuming unequal variances, in Microsoft excel (version 15.23). A *P* value below 0.05 was considered to be statistically significant.

2.4 Bacterial Techniques

2.4.1 Bacterial cell transformation

DH5 α competent cells were thawed on ice and transformed with 100 ng DNA per 80 μ l cells. DNA/competent cells were incubated together on ice for 15 minutes prior to heat shock at 42°C for 1 minute and incubation on ice for 2 minutes. 1 ml of LB media was added to transformed cells and incubated at 37°C for 1 hour. 100 μ l was spread on LB agar with the appropriate antibiotic and incubated at 37°C overnight.

2.4.2 Bacterial culture

For mini-prep cultures, one colony was picked from LB agar plates (prepared above) and grown in 5 ml LB media containing the appropriate antibiotic overnight at 37°C in a bacterial shaker. For maxi-prep cultures, 100 μ l of a 5 ml culture was added per 50 ml LB media containing the appropriate antibiotic and incubated overnight at 37°C in a bacterial shaker.

Each culture was processed using Wizard plus sv mini-prep DNA purification system (Promega, Southampton, UK) or Hi-speed maxi-prep kit (QIAGEN, Manchester, UK), to isolate transformed DNA.

2.4.3 Bacterial glycerol stocks

Glycerol stocks of transformed bacterial colonies were generated by the addition of 500 μ l sterile glycerol to 1 ml of a mini-prep culture. Cultures were frozen in liquid nitrogen and stored at -80°C.

3 Doxorubicin-induced eIF2 α phosphorylation and inhibition of translation initiation

3.1 Introduction

3.1.1 eIF2 α dependent regulation of protein synthesis

Cells modulate protein synthesis in response to cellular stress in order to conserve energy and selectively translate mRNA, which encode proteins required for the stress response. As highlighted in the introduction, the majority of regulation occurs at the initiation stage and is controlled by two key proteins, eIF2, that recruits the initiator Met-tRNA_i to the 40S ribosomal subunit, and 4E-BP, which binds eIF4E to prevent eIF4F complex formation.

eIF2 is comprised of three subunits (α , β and γ) and forms the eIF2-GTP-Met-tRNA ternary complex, delivering the initiator Met-tRNA_i to the 40S ribosome during translation initiation. Translation can be inhibited through the phosphorylation of eIF2 α subunit at serine 51. Phosphorylation of eIF2 α converts eIF2-GDP to an inhibitor of its guanine nucleotide exchange factor, eIF2B, decreasing the availability of eIF2-GTP and inhibiting translation initiation. The family of proteins responsible for this modulation are eIF2 kinases (eIF2Ks), and comprise of PERK, PKR, GCN2 and HRI. eIF2Ks phosphorylate eIF2 α in response to a range of stress stimuli including, endoplasmic reticulum stress (PERK), viral infection (PKR), amino acid deprivation (GCN2) and heme deficiency (HRI).

3.1.2 DNA damage dependent protein synthesis inhibition

DNA damage stimuli, such as UV and cisplatin, rapidly inhibit global protein synthesis (Deng et al. 2002; Powley et al. 2009; Somers et al. 2015; Wu et al. 2002), and enables the selective translation of mRNA involved in the DNA damage response, such as p53 (Takagi et al. 2005) and NER proteins (Powley et al. 2009). In response to UV, eIF2 α phosphorylation has been shown to be the primary inhibitor of protein synthesis, and eIF2 α phosphorylation was shown to be dependent on GCN2 (Deng et al. 2002; Wu et al. 2002; Jiang & Wek 2005; Powley et al. 2009) and PERK (Wu et al. 2002). In addition, UV induced

eIF2 α phosphorylation has been shown to be dependent on the degradation of the eIF2 α protein phosphatase, CReP (Loveless et al. 2015).

3.1.3 Inhibition of Topoisomerase II by doxorubicin

During transcription and replication, DNA strands are separated to enable access of RNA and DNA polymerases. Consequently, tension builds either side of the separation site, and would eventually block the progression of the polymerases. Supercoiling is relieved by topoisomerases that cut the DNA backbone to facilitate the unwinding of DNA. In human cells, there are two key types of topoisomerases that cleave a single strand (type I, Top I), or both strands (type II, Top II) of the DNA backbone, to facilitate the unwinding of supercoiled DNA (reviewed extensively in (Nitiss 2009a; Pommier et al. 2010; Chen et al. 2013)).

Doxorubicin is an anthracycline antibiotic and a very successful, widely used chemotherapeutic. Doxorubicin induces double strand DNA (dsDNA) breaks, primarily through Top II poisoning (Tewey et al. 1984; Burgess et al. 2008), and this preferentially targets rapidly proliferating cancer cells. Top II generates short-lived dsDNA breaks during its reaction cycle. However, doxorubicin intercalates within the DNA and covalently traps Top II to DNA. It is the processing of this enzyme:DNA covalent complex that generates the dsDNA break (Mao et al. 2001; Fan et al. 2008).

3.1.4 Aims

The phosphorylation of eIF2 α has been shown to rapidly inhibit global protein synthesis in response to varied DNA damage stimuli, such as UVB (Deng et al. 2002; Powley et al. 2009). Unpublished data generated within the Willis laboratory has shown that in the non-transformed breast epithelial cell line, MCF10A, doxorubicin (250 nM) induced DNA damage rapidly, but eIF2 α was not phosphorylated until 16 hours later. Interestingly, in MEFs, eIF2 α phosphorylation was not observed until 12 hours after doxorubicin (1 μ M) induced DNA damage (Peidis et al. 2011), suggesting that the regulation of protein synthesis may differ in response to doxorubicin-induced DNA damage.

The aim of this section was to understand the mechanism of eIF2 α phosphorylation in response to doxorubicin-induced toxicity, and determine its role in the regulation of global protein synthesis in MCF10A cells.

3.2 Results

3.2.1 Optimisation of doxorubicin treatment in MCF10A cells

To investigate the delay between DNA damage and eIF2 α phosphorylation, a time course experiment was carried out to optimise doxorubicin treatment in MCF10A cells, using a range of physiologically and non-physiologically relevant concentrations. Three concentrations of doxorubicin were used: 250 nM; 500 nM; and 1 μ M. In cell culture, a concentration of 250 nM is comparable to the plasma concentration observed in patients, within 1 hour of treatment by continuous infusion (Gewirtz 1999). Importantly, doxorubicin has been identified to function as a Top 2 poison at concentrations in excess of 400 nM (Gewirtz 1999). A concentration of 1 μ M was also chosen as this is widely used in many studies, and although it still provides valuable insights into doxorubicin's mechanism of action, it is a concentration that should not necessarily be considered physiologically relevant (Gewirtz 1999).

The MCF10A DDR was analysed by western blot (Figure 3-1) and shown to be activated at 1 hour after treatment with doxorubicin. Unsurprisingly, the rate of activation in response to doxorubicin was dose dependent, and most notable when observing Chk2 activity. Chk2 is phosphorylated and activated by ATM in response to DNA damage. In response to 1 μ M doxorubicin, Chk2 was activated at 1 hour, but in response to 250 nM, Chk2 was predominantly activated at 3 hours. Western analysis of ATM phosphorylation and γ -H2AX, could not be used as reliable indicators of early DDR activation due to the poor quality of commercial antibodies. However, longer film exposures showed ATM phosphorylation at 1 hour (not shown), and previous data from within the Willis laboratory, has shown γ -H2AX at 1 hour using fluorescence microscopy.

Although the DDR is activated almost immediately following doxorubicin treatment, eIF2 α phosphorylation was not observed until 16 hours, a considerable delay from the initial recognition of DNA damage. This delay was consistent across all concentrations, but the robustness of eIF2 α phosphorylation was dose dependent, with higher concentrations of doxorubicin enhancing phosphorylation at 16 hours (Figure 3-1).

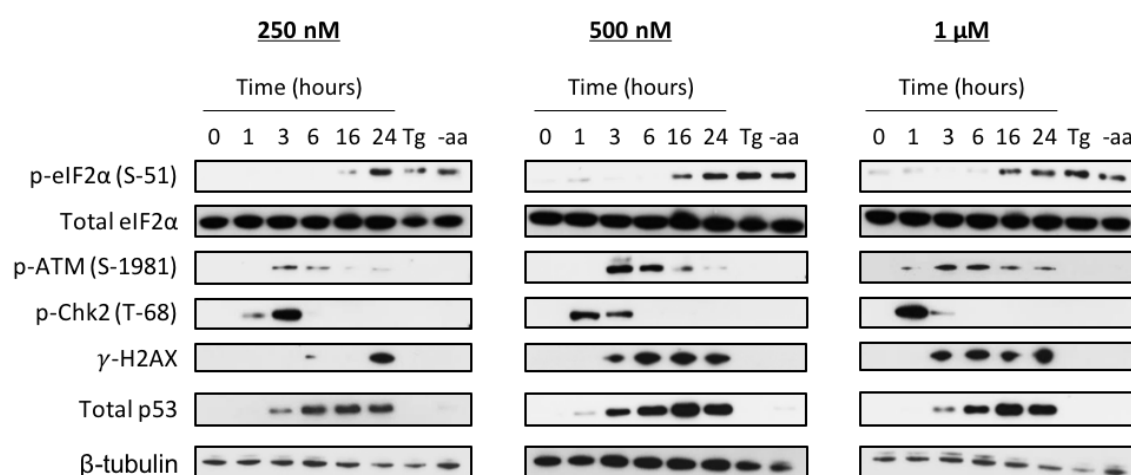


Figure 3-1. DNA damage response in MCF10A cells

Western blot analysis of the DNA damage response and eIF2α phosphorylation in MCF10A cells, treated continuously with three concentrations of doxorubicin for the indicated time period (hours). Tg = thapsigargin (1 μM, for three hours), -a.a = cells grown in media without methionine or cysteine, for 6 hours. Blots shown here were representative of three independent experiments.

eIF2 α phosphorylation is a marker of cellular stress, and can be an indicator of cell death during the unfolded protein response (Armstrong et al. 2010; Aarti et al. 2010; Sano & Reed 2013). To confirm eIF2 α phosphorylation was not due to cell death, FACS analysis was used to quantify apoptosis by staining cells with Annexin-V and Draq7. Annexin-V binds to phosphatidylserine on the plasma membrane of apoptotic cells, whereas Draq7 stains the nuclei of permeabilised and dead cells. Interestingly, only the concentration of 1 μ M doxorubicin significantly enhanced cell death after 24 hours (Figure 3-2A), suggesting that eIF2 α phosphorylation in response to lower concentrations of doxorubicin was not a consequence of cell death. These data are consistent with previously published reports showing that concentrations of doxorubicin above 1 μ M induced apoptosis, whereas lower concentrations induced a senescence-like phenotype (Rebbaa et al. 2003; Jackson & Pereira-smith 2006; Sliwinska et al. 2009), dependent on p53 activity (Elmore et al. 2002; Chang et al. 1999).

Hoechst staining was used to quantify the cell cycle state of live cell populations. Doxorubicin was shown to result in G2/M arrest, but this was not dose dependent at 24 hours (Figure 3-2B). Arrest in G2/M was not surprising as cells will likely not be able to complete DNA replication, due to the inhibition of Top2 by doxorubicin (Tewey et al. 1984; Nitiss 2009a).

Due to the robust DDR, induction of eIF2 α phosphorylation at 16 hours, and lack of cell death after 24 hours, a concentration of 500 nM doxorubicin was chosen for all further experiments presented in this thesis.

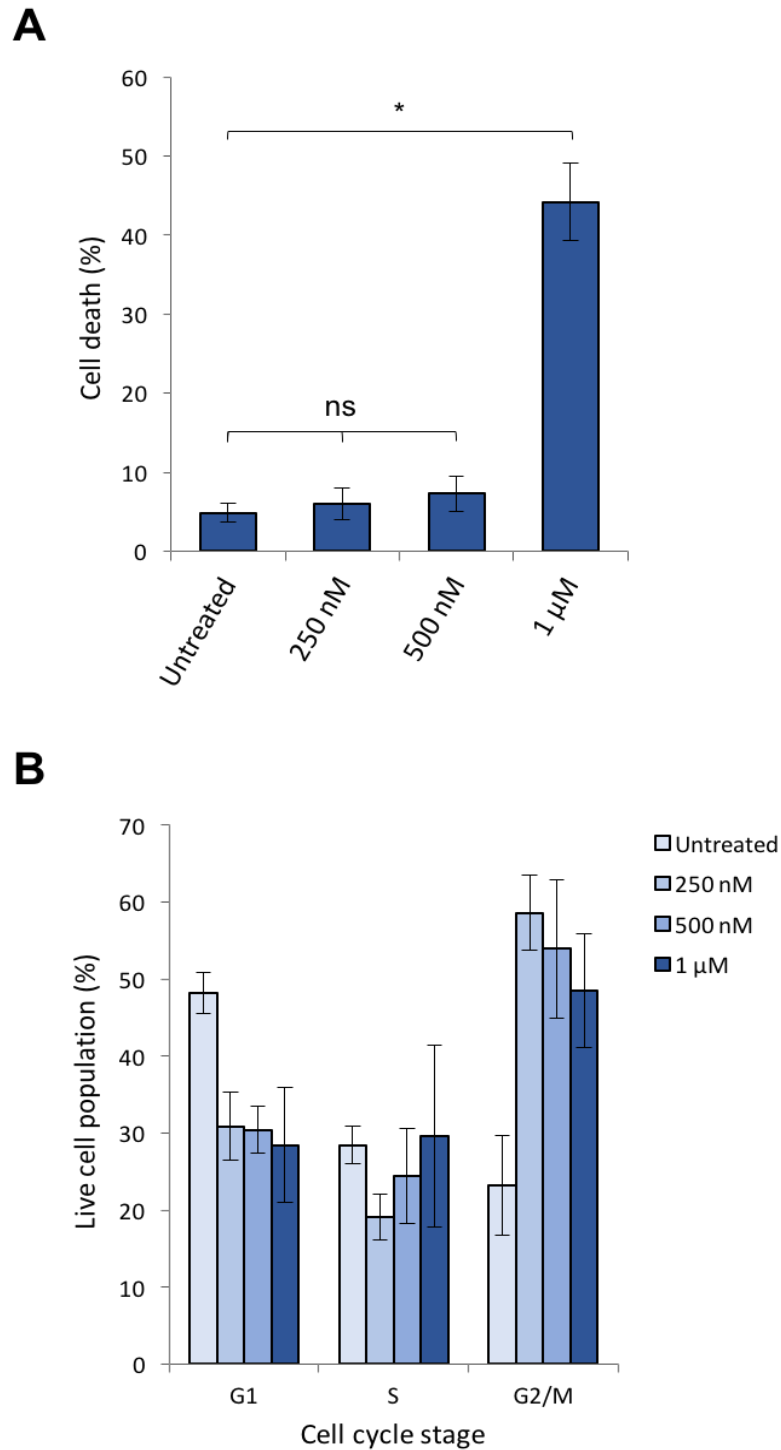


Figure 3-2. Lower concentrations of doxorubicin induced G2/M arrest but not cell death

FACS analysis of MCF10A cells treated continuously with the indicated concentration of doxorubicin for 24 hours. **(A)** Staining with Annexin-FITC and Draq-7 to measure cell death. **(B)** Staining with Hoechst to determine cell cycle state using the Watson Pragmatic algorithm. Data values were an average of three independent experiments, with standard deviation. Significance was calculated using a two-tailed student's *t* test, assuming unequal variances (* = *P* value <0.05, ns = not significant).

3.2.2 Doxorubicin induced G2/M cell cycle arrest

To gain a better understanding of the effect of doxorubicin on the cell cycle, a more in depth doxorubicin time course experiment was carried out using FxCycle violet stain. FxCycle violet stain fluoresces upon DNA binding, enabling quantification of DNA content to determine the cell cycle state in fixed cells. Examination of cell cycle profiles in response to doxorubicin showed that G2/M arrest occurred at 6 hours, whereas the number of cells in S-phase declined at 9 hours (Figure 3-3). Although predicative cell cycle algorithms, such as Watson pragmatic analysis (Watson et al. 1987), are consistent in quantifying cell cycle state, they provide unclear quantification of S-phase cells. A more accurate method to measure proliferation is to quantify the incorporation of EdU (a thymidine analogue) into DNA. Cells were incubated with EdU for 1.5 hours prior to collection. FxCycle was also used to stain DNA content in combination with EdU to quantify G1, G2 and S-phase cells within the same population. EdU fluorescence (APC-A) was plotted against FxCycle fluorescence (Pacific Blue-A) to display the three distinct populations of cells. These populations were quantified during a doxorubicin treatment time course experiment using the gating shown for the untreated sample (Figure 3-4A). These data showed that the population of G1 cells was maintained over the time course. However, the number of S-phase cells decreased substantially from 3-6 hours, mirroring an increase in G2/M cells (Figure 3-4B). These data are consistent with studies that have shown doxorubicin to induce G2/M arrest (Lüpertz et al. 2010; Siu et al. 1999; Xiao et al. 2003), and indicated that cells in G1 arrested prior to the onset of S-phase, whereas cells in S-phase arrested in G2/M.

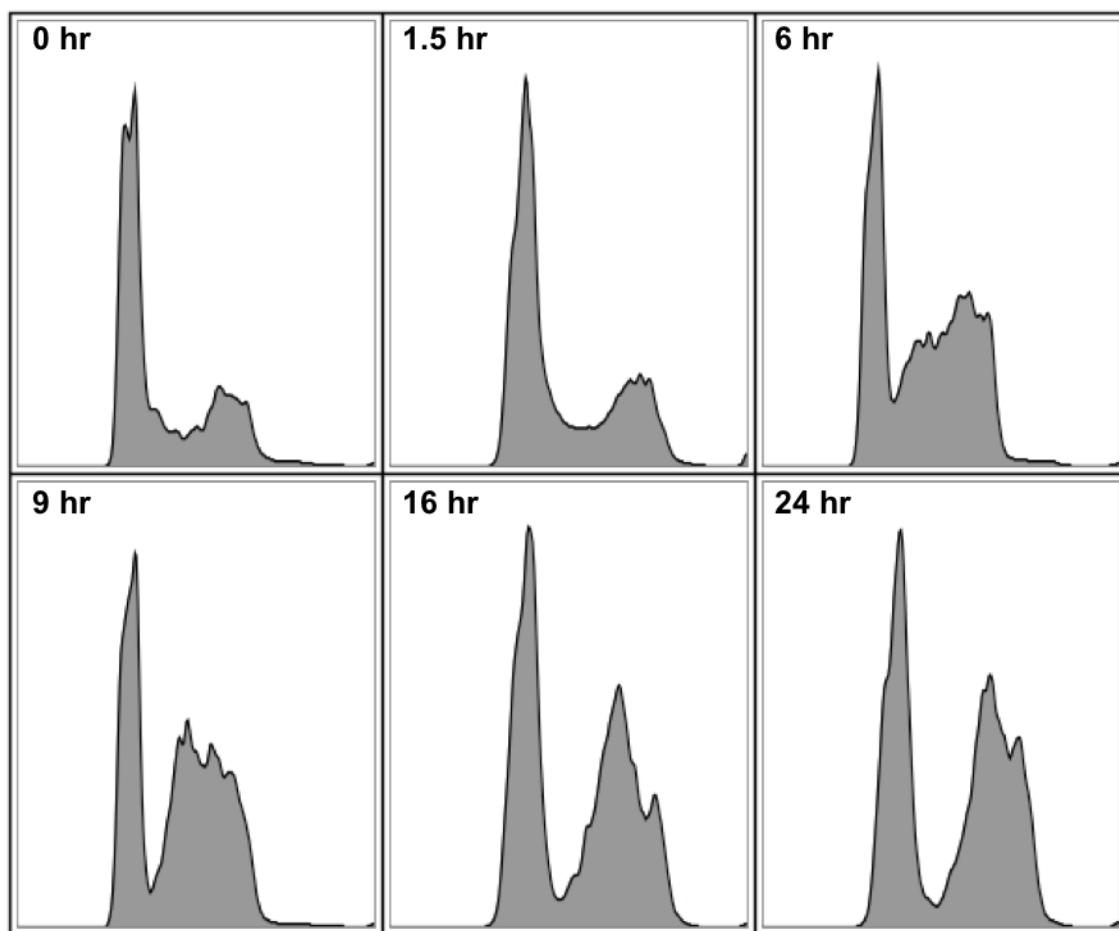


Figure 3-3. Doxorubicin induced G2/M arrest

FACS analysis of MCF10A cells treated continuously with doxorubicin (500 nM) for the indicated time. Cells were fixed in 70% ethanol and stained with FxCycle violet dye. FxCycle signal (Pacific Blue-A) was plotted as a histogram to visualise the cell cycle profile. Histograms were representative profiles from three independent experiments.

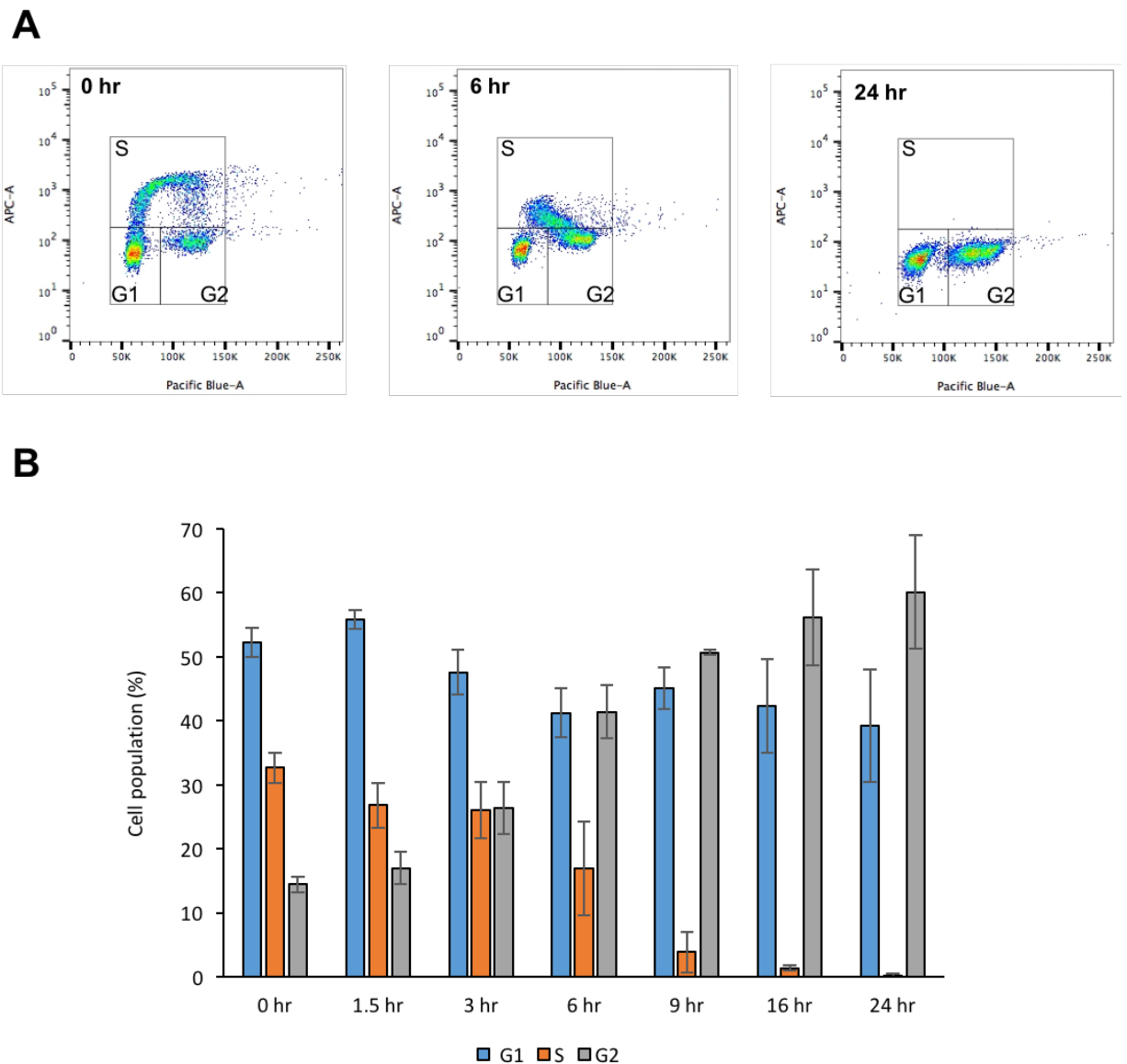


Figure 3-4. Reduction of S-phase cells in response to doxorubicin

FACS analysis of MCF10A cells treated continuously with doxorubicin (500 nM) for the indicated time period (hours). Cells were incubated with EdU (10 μ M) for the final 1.5 hours of treatment and stained with FxCycle violet dye **(A)** EdU incorporation was visualised by plotting EdU fluorescence (APC) against FxCycle fluorescence (Pacific Blue-A), to display three distinct populations of cells in G1, G2 or S-phase (EdU positive counts). Data was representative of three independent experiments. **(B)** Cell cycle distribution following doxorubicin (500 nM) treatment, using the gating system shown in (A). Data values were an average of three independent experiments, and shown with standard deviation.

3.2.3 Doxorubicin inhibited global protein synthesis and translation initiation

eIF2 α phosphorylation was enhanced in response to doxorubicin, suggesting that doxorubicin treatment could reduce the rate of protein synthesis. To determine if protein synthesis was regulated in response to doxorubicin, [³⁵S] methionine incorporation was used to quantify global protein synthesis during a time course experiment (Figure 3-5A).

Initially, protein synthesis rates increased at 3 hours after treatment with doxorubicin. Although doxorubicin was added to cells with fresh growth media, this was not a serum stimulation effect, as the same result was observed when media was not replaced (data not shown). This increase may have been due to the induction of the DDR, requiring rapid translation of mRNA involved in the detection and repair of DNA breaks. In response to IR, protein synthesis was shown to be initially stimulated through activation of mTOR in MCF10A cells (Braunstein et al. 2009).

Doxorubicin significantly inhibited global protein synthesis after 9 hours of treatment, leading to a total reduction of over 50% at 24 hours (Figure 3-5A). One explanation for protein synthesis inhibition would be the lack of mRNA to translate. To determine if protein synthesis inhibition could be due to a lack of newly synthesised mRNA, [³H] uridine incorporation was utilised to quantify global RNA synthesis. Although the level of RNA synthesis was inhibited moderately by 20% in response to doxorubicin at 3 hours, RNA synthesis was only significantly inhibited at 24 hours, where it was inhibited by 50% (Figure 3-5B). These data suggested that doxorubicin induced protein synthesis inhibition, observed at 9-16 hours, was not likely to be due to RNA synthesis inhibition. Interestingly, a delay of 9 hours was observed between DNA damage recognition and protein synthesis inhibition. To investigate whether eIF2 α phosphorylation correlated with protein synthesis inhibition, protein was analysed from samples prepared in parallel to those collected for [³⁵S] methionine incorporation. Surprisingly, the decrease in protein synthesis was shown to precede eIF2 α phosphorylation, and eIF2 α phosphorylation was not observed until 12 hours after doxorubicin treatment, when global protein synthesis was already inhibited by over 40% (Figure 3-5C).

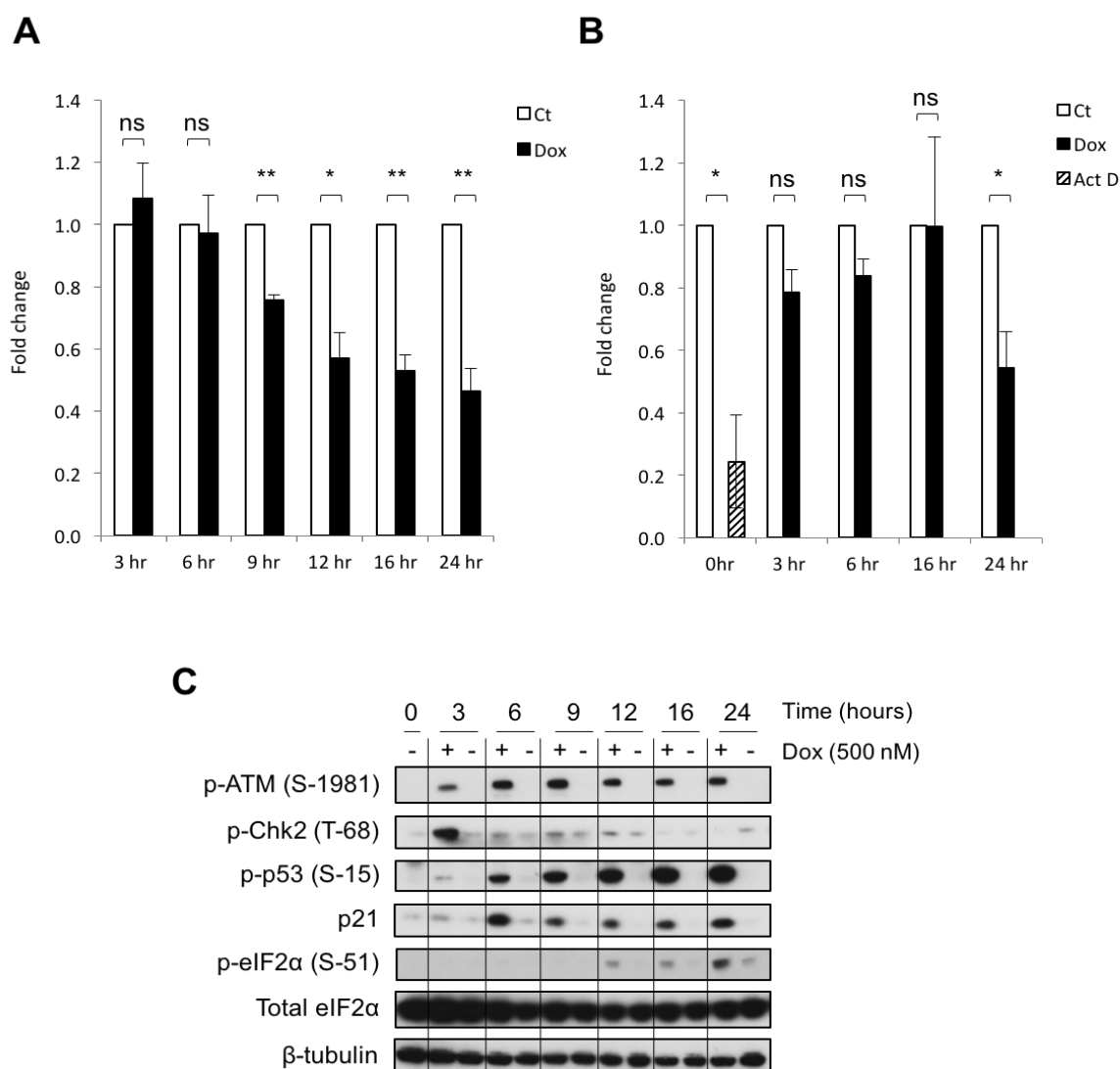


Figure 3-5. Doxorubicin inhibited global protein synthesis

(A) ^{35}S methionine and **(B)** ^3H uridine incorporation, to measure global protein and RNA synthesis respectively. MCF10A cells were treated with 500 nM doxorubicin for the indicated time and pulse-labelled with radioisotope for 30 minutes. Counts per minute were normalised to total protein by Bradford assay and are shown relative to the control for each time point. Data values were an average of three independent experiments, with standard deviation. Statistical significance was calculated using a two-tailed student's *t* test, assuming unequal variances (* = *P* value <0.05, ** = *P* value <0.01, ns = not significant). Act D = Actinomycin D (transcriptional inhibitor), 1 μM for 1 hour. **(C)** Western blot analysis of the DNA damage response and eIF2 α phosphorylation, in protein samples prepared in parallel to ^{35}S methionine incorporation assay. Blots shown here were representative of three independent repeats.

As highlighted earlier, eIF2 α regulates ternary complex formation, functioning as a key regulator of translation initiation. To confirm that the observed reduction in global protein synthesis was due to inhibition of the initiation stage of translation, sucrose density gradients were used to measure the distribution of ribosomes between free ribosomes and polyribosomes. After treatment with doxorubicin for 6 hours, global protein synthesis was not inhibited (Figure 3-5A) and this was reflected in the polysome profiles, where there was a minimal decrease in polysomes and increase in subpolysomes (free ribosomes) (Figure 3-6A). In contrast, when protein synthesis was inhibited at 24 hours, the number of polysomes decreased dramatically, indicating that the inhibition of initiation may reduce the rate of ribosome loading onto mRNA (Figure 3-6B). During a block in translation initiation, ribosomes would ordinarily be seen to dissociate from polysomes and accumulate as free ribosomes in subpolysomes. However, after a 24-hour doxorubicin treatment, ribosomes moving off polysomes did not accumulate in the subpolysomes. Therefore, treatment with doxorubicin did not result in a classic initiation block, such as that observed in response to the mTOR inhibitor, AZD8055 (data not shown). It is possible that prolonged doxorubicin treatment may result in ribosome degradation, or accumulation of ribosomes within stress granules, as has been observed in response to UV (Gaillard & Aguilera 2008; Moutaoufik et al. 2014). However, this phenomena is something that will be investigated in the future.

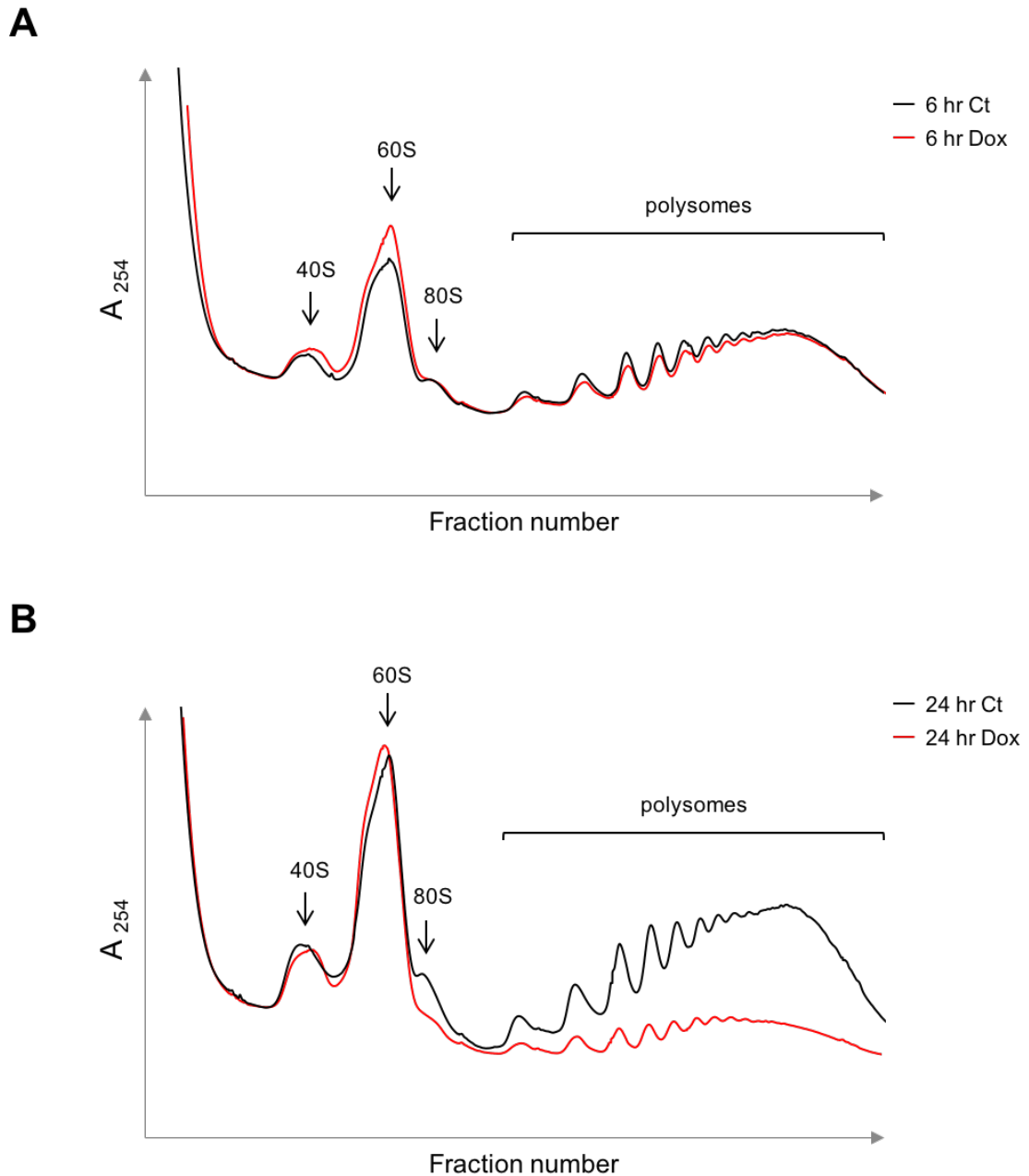


Figure 3-6. Doxorubicin inhibited translation initiation in MCF10A cells

Representative polysome profiles from MCF10A cells, treated continuously with 500 nM doxorubicin for **(A)** 6 hours and **(B)** 24 hours. Traces were obtained by measuring absorbance at 254 nm, after centrifuging cytoplasmic lysates at 38000 rpm, through 10-50% sucrose gradients at 4°C, for 2 hours. Traces were obtained using a flow rate of 1 ml/min. Ct = untreated control sample for each time point.

3.2.4 Combination of eIF2 kinases may regulate doxorubicin-induced eIF2 α phosphorylation

eIF2 α phosphorylation is regulated by a family of eIF2 kinases (eIF2K) comprising of PERK, PKR, GCN2 and HRI, that phosphorylate eIF2 α in response to endoplasmic reticulum stress, viral infection, amino acid deprivation and heme deficiency respectively.

Due to the lack of commercially available antibodies, it was not possible to adequately analyse eIF2K activation by western blot. In order to determine the kinase responsible for doxorubicin-induced eIF2 α phosphorylation, siRNA knockdown of PERK, PKR and GCN2, was utilized prior to doxorubicin treatment. Surprisingly, doxorubicin-induced eIF2 α phosphorylation was only marginally reduced after knockdown of GCN2 (~25%) and PKR (~20%), whereas knockdown of PERK was ineffective (Figure 3-7). It has been shown previously that eIF2 kinases function in combination to co-ordinate a cellular response to stress, and that one can compensate for the other in its absence. For example, in response to prolonged ER stress, PERK acts as the primary kinase, and GCN2 acts as a secondary kinase in the absence of PERK (Jiang et al. 2004). In that study, ER stress induced eIF2 α phosphorylation was still observed in PERK knockout MEFs, however, eIF2 α phosphorylation was almost completely abolished in PERK/GCN2 double knockout MEFs (Jiang et al. 2004). In addition, Nitric oxide can lead to the activation of all four eIF2Ks through direct or indirect mechanisms (Donnelly et al. 2013).

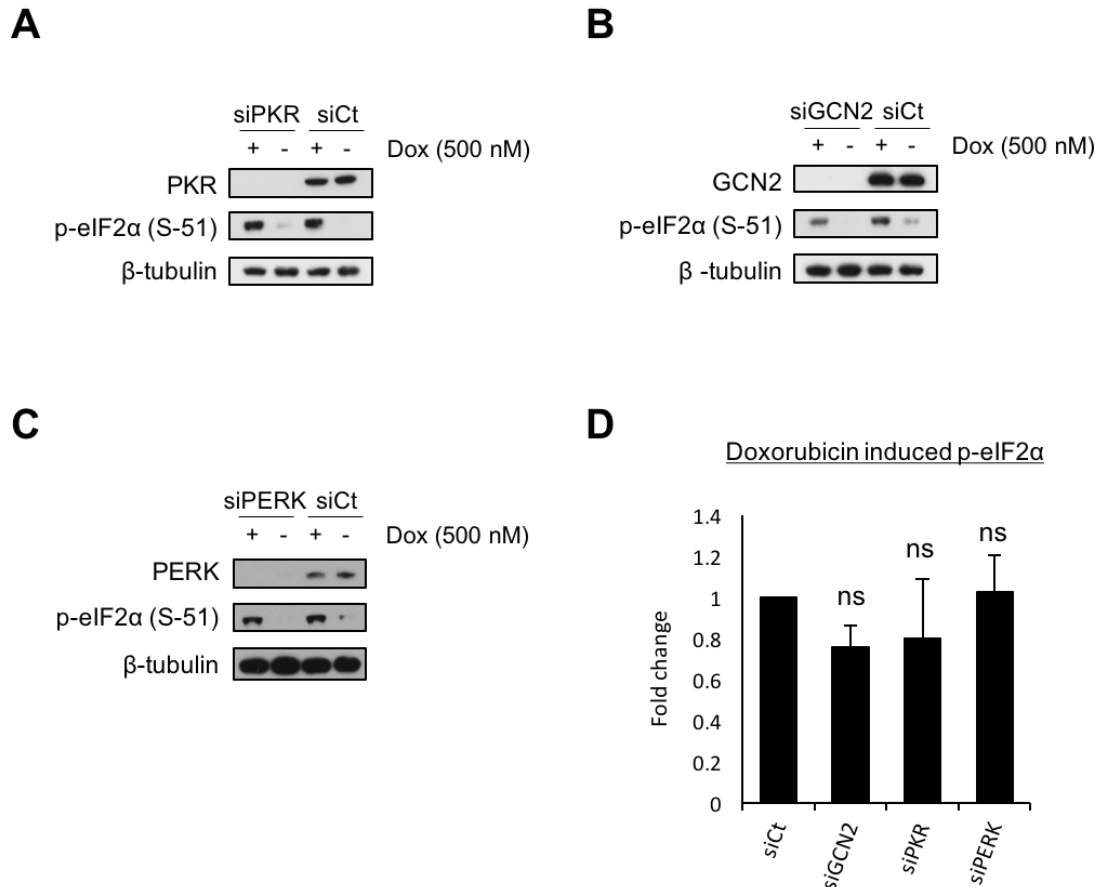


Figure 3-7. Depletion of individual eIF2α kinases had a modest effect on eIF2α phosphorylation induced by doxorubicin

Western blot analysis of eIF2α phosphorylation in response to treatment with doxorubicin, following siRNA knockdown of **(A)** PKR (1 nM), **(B)** GCN2 (2 nM) and **(C)** PERK (1 nM). MCF10A cells were transfected with specific siRNAs for 48 hours. Cells were treated with doxorubicin (500 nM) for a further 24 hours or left untreated. **(D)** Quantification of doxorubicin induced eIF2α phosphorylation following siRNA knockdown (A-C). Level of eIF2α phosphorylation for each knockdown is shown relative to doxorubicin treated siCt cells. Data points were an average of three independent experiments, normalised to β-tubulin levels and displayed with standard deviation. Statistical significance was calculated using a two-tailed student's *t* test, assuming unequal variances (ns = not significant). siCt = non targeting siRNA. Western blots were representative of three independent experiments.

To determine if eIF2Ks could function co-operatively in response to doxorubicin, they were depleted in combination. Combined depletion of GCN2 and PERK significantly reduced doxorubicin-induced eIF2 α phosphorylation by 78%, whereas depletion of GCN2 and PKR significantly reduced eIF2 α phosphorylation by 63% (Figure 3-8B). Combined knockdown of GCN2, PERK and PKR, did not impair eIF2 α phosphorylation further, suggesting that PKR may play a very minor role in the response to doxorubicin. Curiously, individual knockdown of eIF2Ks had minimal effect on eIF2 α phosphorylation, but double eIF2K knockdown greatly reduced eIF2 α phosphorylation. Although it is unlikely that doxorubicin activates all three kinases, it is plausible that knockdown of two or more kinases could limit the capacity for one eIF2K to compensate for the loss of another, and this could result in reduced sensitivity to cellular stress. PERK was not activated in response to doxorubicin (data not shown) and the expression of downstream markers of PERK activation, such as ATF4 and CHOP, were not induced by doxorubicin (data not shown). It would be extremely beneficial to analyse mRNA expression of downstream markers of eIF2K activation, in parallel with protein levels, to gain a greater understanding of eIF2K activation in response to doxorubicin.

The decision to omit HRI was taken due to it having a primary role in response to heme levels in red blood cells (Han et al. 2001), and not breast epithelial cells. However, it has become clear that HRI plays a key role in the regulation of eIF2 α in other cell types and in response to other stimuli, such as oxidative stress (McEwen et al. 2005; Zhan et al. 2002) and ER stress (Acharya et al. 2010). For this reason, HRI will be considered in the future to determine its role in response to doxorubicin in MCF10A cells.

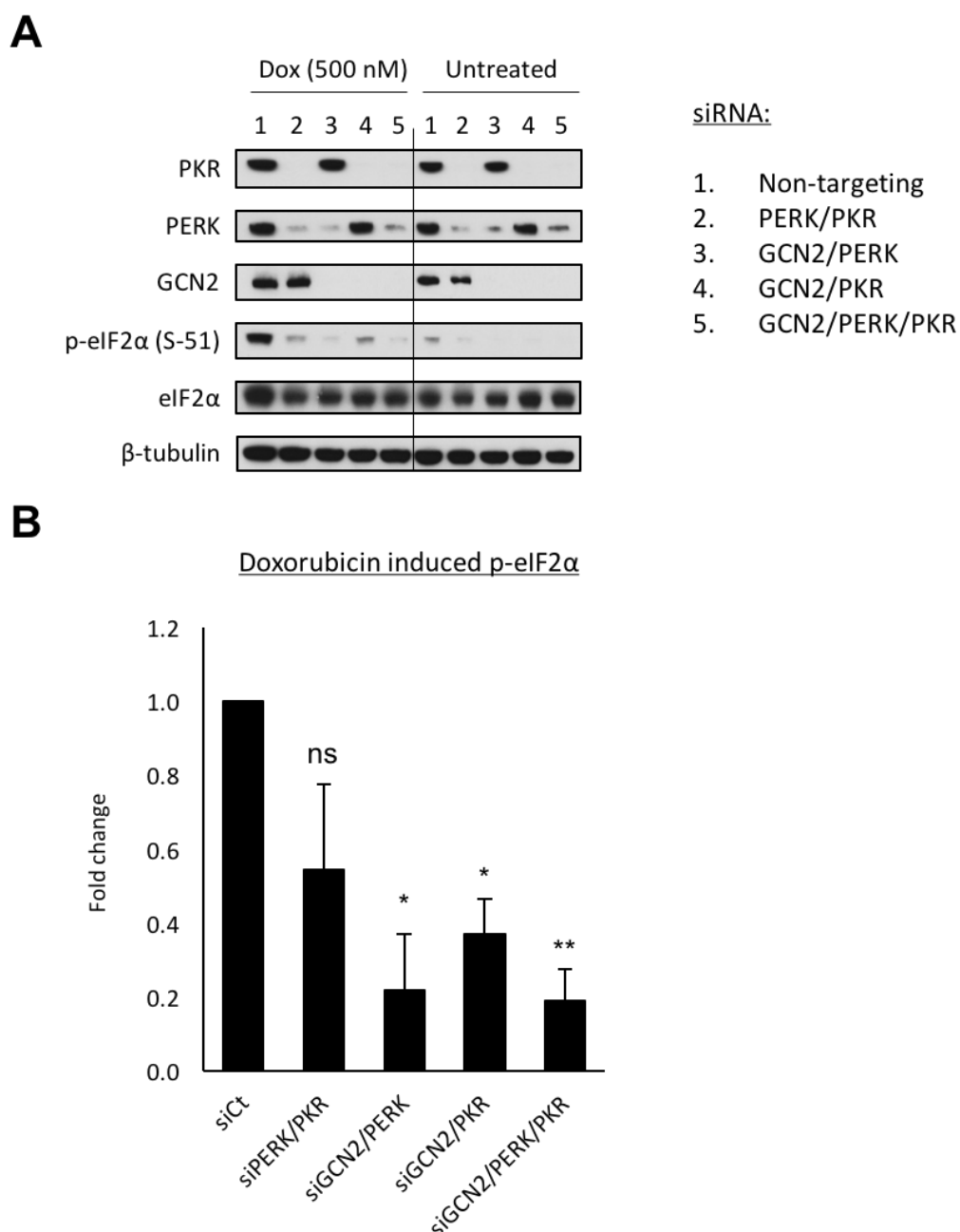


Figure 3-8. Depletion of multiple eIF2α kinases reduced eIF2α phosphorylation induced by doxorubicin

(A) Western blot analysis of eIF2α phosphorylation in response to doxorubicin treatment following eIF2α kinase knockdown. Combinations of siRNAs specific for PKR (1 nM), PERK (1 nM) and GCN2 (2 nM) were transfected into MCF10A cells for 48 hours. Cells were treated with doxorubicin (500 nM) for a further 24 hours or left untreated. **(B)** Quantification of doxorubicin-induced eIF2α phosphorylation (normalised to β-tubulin) from (A) relative to non-targeting siRNA (siCt). An average of three independent experiments, displayed with standard deviation. Statistical significance was calculated using a two-tailed student's *t* test, assuming unequal variances (* = *P* value < 0.05, ** = *P* value < 0.01, ns = not significant).

3.2.5 eIF2 α phosphorylation was not required for doxorubicin-induced inhibition of protein synthesis

eIF2 α is not the only regulator of translation initiation. An interesting question concerned how much of the global inhibition of protein synthesis was dependent on eIF2 α phosphorylation, after treatment with doxorubicin.

Integrated stress response inhibitor (ISRIB), is a compound shown to reverse the inhibitory effect of eIF2 α phosphorylation on global protein synthesis (Sidrauski et al. 2013). Originally identified as an inhibitor of the integrated stress response (ISR), ISRIB does not inhibit PERK activity or eIF2 α phosphorylation (Sidrauski et al. 2013), but relieves all signalling and gene expression downstream of eIF2 α phosphorylation, such as the induction of ATF4 expression (Sidrauski, McGeachy, et al. 2015). ISRIB has been shown to specifically relieve the inhibitory effect of eIF2 α phosphorylation induced by all eIF2Ks (Sidrauski et al. 2013). Although the exact mechanism of ISRIB function is not clear, it has been suggested that ISRIB stabilises eIF2B dimerisation, enhancing eIF2B GEF activity, and desensitising eIF2B to inhibition by eIF2 α phosphorylation (Sekine et al. 2015; Sidrauski, Tsai, et al. 2015). By using ISRIB in combination with doxorubicin, it was possible to reverse the inhibitory effect mediated by doxorubicin-induced eIF2 α phosphorylation, and therefore determine the effect of eIF2 α phosphorylation on global protein synthesis. To confirm that ISRIB rescued ER stress induced protein synthesis inhibition, MCF10A cells were treated with a low concentration of thapsigargin for 1 hour, in combination with ISRIB. Thapsigargin inhibited protein synthesis by 40%, however, the inhibition of protein synthesis was completely rescued by treatment with ISRIB (Figure 3-9A). As expected, after thapsigargin treatment, PERK was activated, eIF2 α phosphorylated and ATF4 protein expression induced. When thapsigargin treated cells were treated with ISRIB, PERK was still activated and eIF2 α phosphorylated, but ATF4 protein expression was not induced (Figure 3-9B). Although treatment with 50 nM ISRIB diminished thapsigargin induced induction of ATF4 expression, it did not completely rescue protein synthesis (not shown), whereas 200 nM ISRIB restored protein synthesis (Figure 3-9A). These data are comparable to published research using 200 nM ISRIB (Sidrauski et al. 2013), and suggested that ISRIB relieved

the inhibitory effect of eIF2 α phosphorylation on protein synthesis in MCF10A cells.

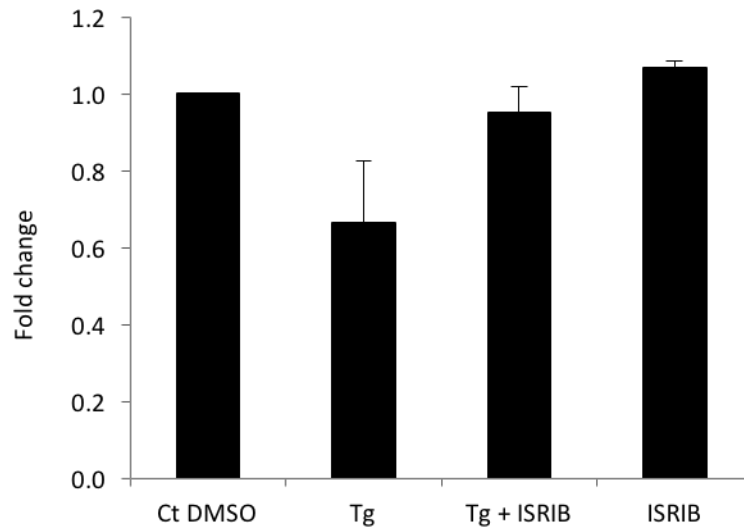
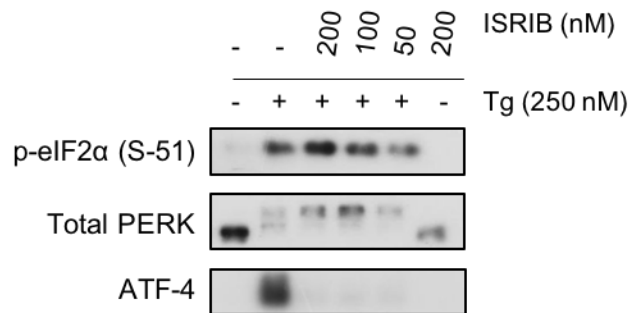
A**B**

Figure 3-9. ISRIB rescued thapsigargin induced protein synthesis inhibition

(A) ^{35}S methionine incorporation in MCF10A cells exposed to thapsigargin (250 nM, 1 hr), with or without ISRIB (200 nM). Counts were normalised to total protein by Bradford assay and shown relative to the untreated control. Data points were an average of three independent experiments, with standard deviation. **(B)** Western blot analysis of proteins involved in the unfolded protein response following exposure to thapsigargin (250 nM, 1 hr), with variable concentrations of ISRIB (200 nM, 100 nM or 50 nM).

Having established that ISRIB functioned in the expected manner, ISRIB was used in combination with doxorubicin to determine if eIF2 α phosphorylation was responsible for the inhibition of protein synthesis.

After doxorubicin treatment for 24-hours, protein synthesis was significantly inhibited by around 60%, but this effect was not rescued by treatment with ISRIB (Figure 3-10A). Interestingly, when analysing protein samples prepared in parallel with ^[35]S incorporated cells, eIF2 α phosphorylation was completely abolished when doxorubicin was used in combination with ISRIB (Figure 3-10B), an effect that had not been observed with ISRIB previously. The loss of eIF2 α phosphorylation could be due to the length of time cells were incubated with ISRIB and doxorubicin. Thapsigargin rapidly induced eIF2 α phosphorylation, therefore incubation with ISRIB was only for 1 hour. However, when treating cells with doxorubicin, cells were incubated with both ISRIB and doxorubicin for 16 hours, in order to observe robust eIF2 α phosphorylation. However, the reduction of eIF2 α phosphorylation induced by doxorubicin and ISRIB was not caused by longer incubations with ISRIB. Data presented in figure 10 showed that thapsigargin induced eIF2 α phosphorylation after pre-treatment with ISRIB for 16 hours. It could be possible that when cells are subjected to prolonged stress in the presence of ISRIB, the compound may lead to off target effects, or modulate the stress response in an alternative way.

Regardless of the effects of ISRIB on eIF2 α phosphorylation, these data strongly suggested that eIF2 α phosphorylation was not responsible for doxorubicin-induced inhibition of protein synthesis.

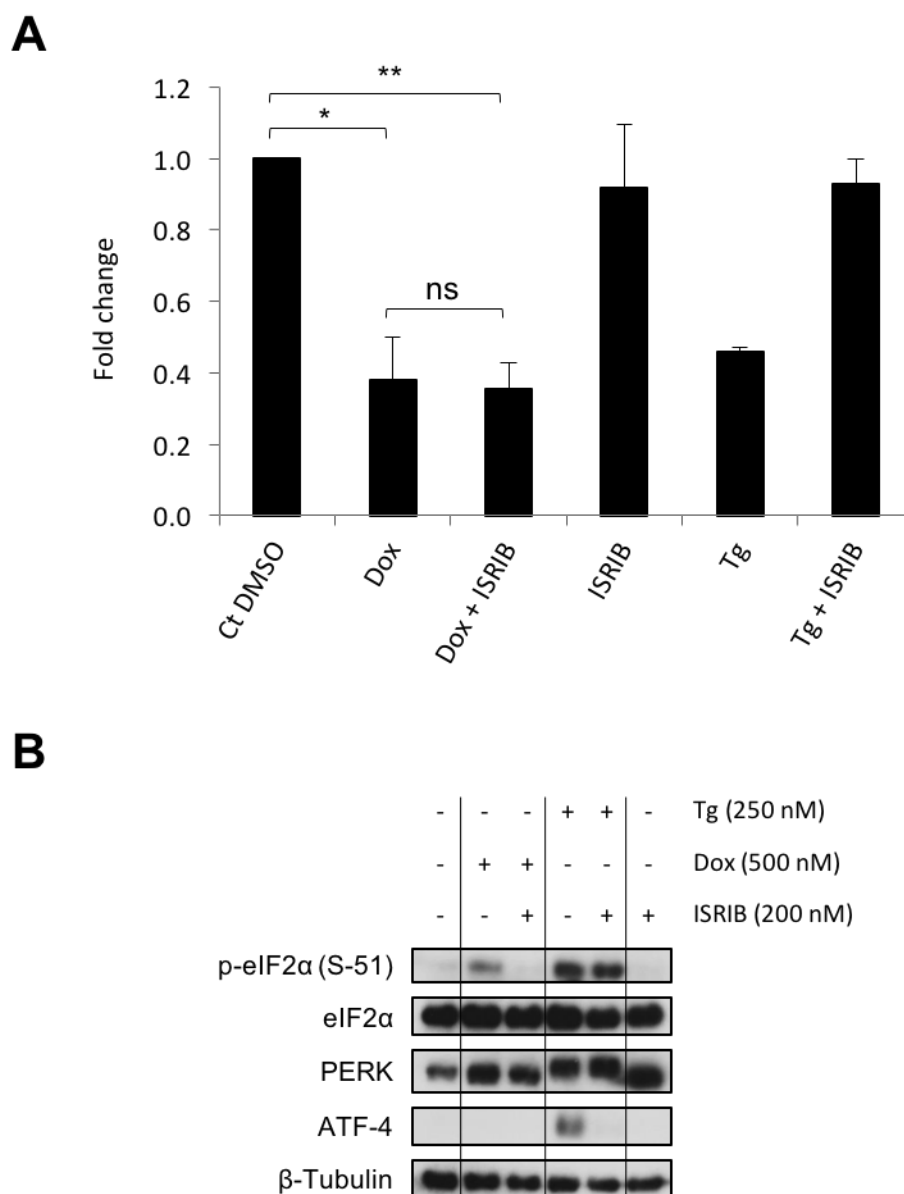


Figure 3-10. ISRIB did not rescue protein synthesis inhibition induced by doxorubicin

(A) ^{35}S methionine incorporation in MCF10A cells treated with doxorubicin (500 nM, 16 hr), or thapsigargin (250 nM, 1 hr), with or without ISRIB (200 nM). Total counts were normalised to total protein by Bradford assay, and shown relative to the untreated control. Data points were an average of three independent experiments, shown with standard deviation. Statistical significance was calculated using a two-tailed student's *t* test, assuming unequal variances (* = *P* value < 0.05, ** = *P* value < 0.01, ns = not significant). **(B)** Western blot analysis of proteins involved in the unfolded protein response, carried out in parallel to ^{35}S methionine incorporation (A). Blots shown here were representative of three independent repeats.

3.3 Discussion

The aim of this section was to determine the link between DNA damage and eIF2 α phosphorylation, in the context of doxorubicin-induced toxicity.

Doxorubicin was shown to activate a robust DDR in MCF10A cells, triggered within one hour of treatment. Of the three concentrations tested, only the higher concentration of doxorubicin (1 μ M) induced significant cell death. Lower concentrations, including 500 nM, did not cause cell death, but induced cell cycle arrest. These data suggested that doxorubicin induced cell cycle arrest at G1/S, thereby preventing DNA replication, and also induced G2/M, preventing entry into mitosis.

Although doxorubicin-induced DNA damage was recognised within 1 hour, inhibition of protein synthesis was not observed until 9 hours, a substantial delay from the activation of the DDR. Doxorubicin inhibited translation initiation, preventing the recruitment of ribosomes to mRNA, and resulted in the loss of polysomes. Typically, inhibition of translation initiation results in a loss of polysomes that accumulate as free ribosomes, in the subpolysomes. In response to treatment with doxorubicin, ribosomes lost from the polysomes did not accumulate in the subpolysomes, suggesting that ribosomes may have been degraded, or sequestered in a form of stress granule (Gaillard & Aguilera 2008; Moutaoufik et al. 2014). Importantly, catalytic inhibition of mTORC1 resulted in a classic translation initiation block, with ribosomes from polysomes accumulating in the subpolysomes. The response to mTORC1 inhibition indicated that the loss of ribosomes observed after treatment with doxorubicin, was likely to be a consequence of doxorubicin toxicity, and not a cell line specific effect. Doxorubicin has been shown to inhibit ribosome biogenesis (Burger et al. 2010), therefore, it is possible that the combined inhibition of translation and ribosome biogenesis, may contribute to the observed effect.

It was possible that protein synthesis inhibition may have been a consequence of a lack of mRNA available to translate. However, inhibition of global RNA synthesis was not observed until 24 hours, suggesting that protein synthesis inhibition at 9 hours was not regulated by mRNA availability. Protein synthesis inhibition was also preceded by cell cycle arrest, suggesting that this response

could be cell cycle dependent, and this question will be addressed in a subsequent chapter.

Although inhibition of global protein synthesis was observed at 9 hours, phosphorylation of eIF2 α was not observed until 12 hours after doxorubicin treatment, when protein synthesis was already inhibited by 40%. Taken together, these data suggested that eIF2 α phosphorylation played a minimal role in the regulation of translation initiation, in response to doxorubicin. Furthermore, after treatment with ISRIB, doxorubicin-induced protein synthesis inhibition was shown to be independent of eIF2 α phosphorylation. ISRIB negated all downstream signalling regulated in response to eIF2 α phosphorylation, and as observed in combination with doxorubicin, completely diminished eIF2 α phosphorylation. Importantly, after treatment with ISRIB and doxorubicin, protein synthesis inhibition was still observed, suggesting that another regulator of translation initiation, such as mTOR signalling, may be responsible for doxorubicin-induced protein synthesis inhibition.

Although eIF2 α was not the predominant regulator of protein synthesis in response to doxorubicin, it was still of value to understand the signalling response that resulted in its phosphorylation. Individual knockdown of eIF2Ks proved inconclusive. In MEFs, it has been shown that treatment with doxorubicin resulted in the PKR dependent phosphorylation of eIF2 α (Peidis et al. 2011). Although a small reduction in doxorubicin-induced eIF2 α phosphorylation was observed after the depletion of PKR (Figure 3-7A), this reduction was not significant, or as substantial as observed in MEFs. A possible explanation for the discrepancy between these two sets of data concerns the concentration of doxorubicin used. In MEFs, PKR was shown to be activated in response to 1 μ M doxorubicin, but this was a concentration that induced cell death in MEFs (Peidis et al. 2011) and MCF10A cells (Figure 3-2A). The data presented here used a concentration of 500 nM that did not induce cell death, raising the possibility that alternative eIF2Ks could be activated in dying population of cells.

The combined depletion of eIF2Ks dramatically diminished eIF2 α phosphorylation induced by doxorubicin. Surprisingly, the greatest reduction of

eIF2 α phosphorylation was observed after depletion of GCN2 and PERK, even though individual depletion did not affect doxorubicin-induced eIF2 α phosphorylation. The absence of HRI from these experiments made the interpretation of these data complicated, and to fully determine the regulation of eIF2 α phosphorylation in response to doxorubicin, HRI must be investigated. Irrespective of the role of HRI, these data suggest that in response to doxorubicin, eIF2 α phosphorylation could be regulated by multiple eIF2Ks.

4 Doxorubicin-induced inhibition of mTORC1 signalling

4.1 Introduction

4.1.1 Regulation of mTORC1 signalling

In mammalian cells, two distinct mTOR complexes have been identified (mTORC1 and mTORC2) that integrate a diverse array of extracellular and intracellular signals. mTORC1 has been extensively studied and shown to regulate protein synthesis, cell growth, proliferation and ribosome biogenesis (Foster & Fingar 2010; Laplante & Sabatini 2009; Shimobayashi & Hall 2014). Essential to the activation of mTORC1 are two GTPases: Rag, which recruits mTORC1 to the lysosome (Sancak et al. 2010); and Rheb, which activates mTORC1 upon translocation to the lysosome (Garami et al. 2003; Long et al. 2005).

TSC is a heterodimer of TSC1 and TSC2 that negatively regulates Rheb activity. TSC2 hydrolyses Rheb-GTP to Rheb-GDP, inhibiting mTORC1 activation (Figure 4-1). TSC is a central regulator of mTOR signalling, mediating the response to a vast array of signals that regulate TSC activity through phosphorylation events. During insulin and growth factor stimulation, TSC is inhibited by Akt (Inoki et al. 2002; Manning et al. 2002), RSK (She et al. 2010) and ERK (Ma et al. 2005). Conversely, TSC activity is enhanced by AMPK mediated phosphorylation in response to low energy (Inoki, Zhu, et al. 2003), and p53 activation (Feng et al. 2005; Wang et al. 2012) (Figure 4-1).

mTORC1 must translocate to the surface of the lysosome for activation by Rheb, in a process mediated by Rag GTPase heterodimers (RagA/B with RagC/D) (Figure 1-5). Rag GTPases were first shown to directly bind to Raptor and relocate mTORC1 to the lysosome, in response to stimulation with amino acids. After mTORC1 translocation to the lysosome, mTORC1 is activated by Rheb (Sancak et al. 2008; Sancak et al. 2010).

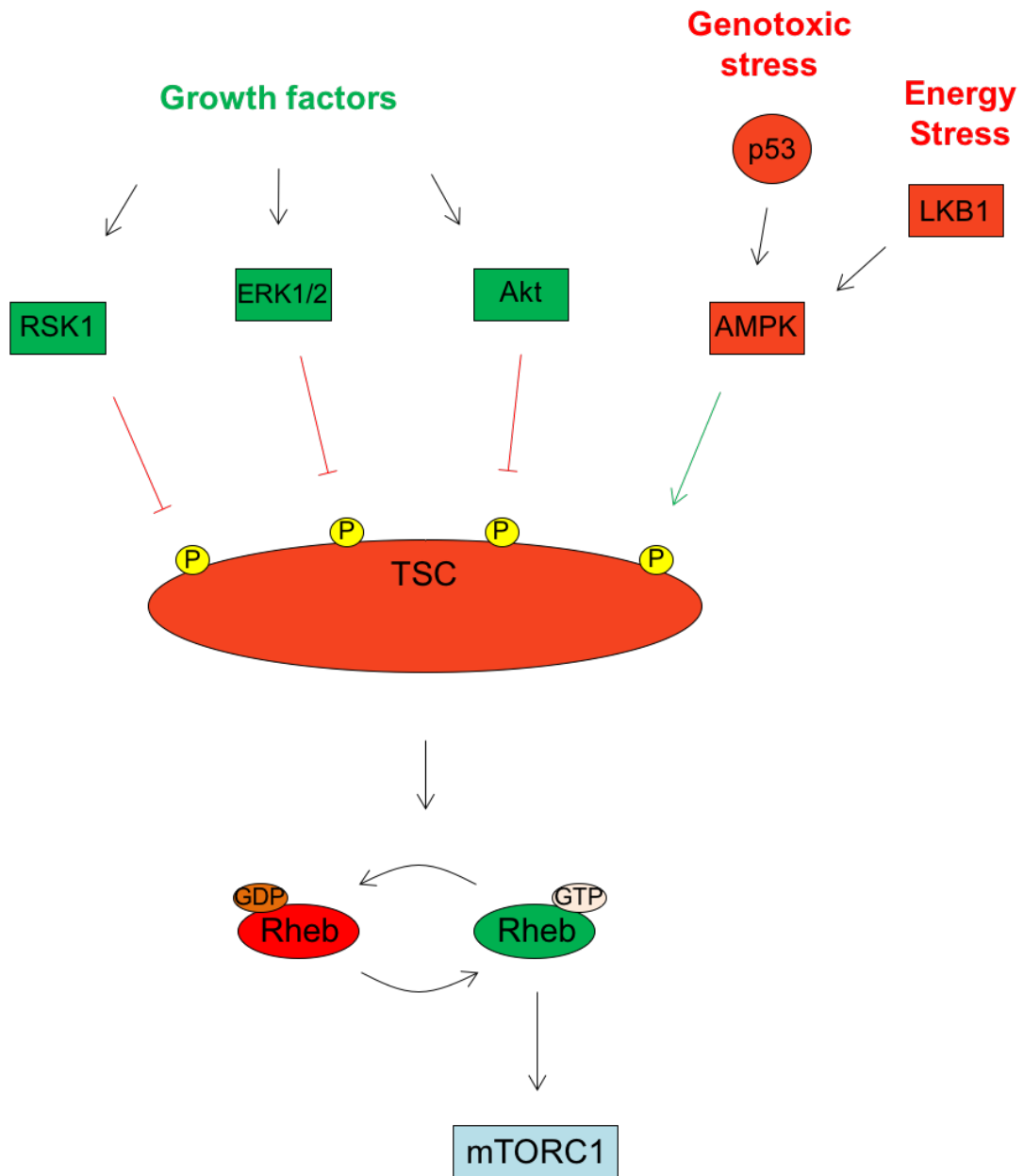


Figure 4-1. Regulation of TSC and mTOR signalling

Schematic representation of the regulation of TSC. Green boxes indicate activators of mTORC1 signalling, whereas red boxes indicate negative regulators of mTORC1 signalling. Red arrows indicate inhibitors of TSC activity and green arrows indicate activators of TSC activity.

4.1.2 mTORC1 regulation of protein synthesis

mTORC1 positively regulates protein synthesis through the inhibition of 4E-BPs and activation of p70 S6K.

As discussed in the introduction, eIF4E is important for recruitment of the 43S PIC to mRNA. 4E-BPs competes with eIF4G for the same binding site on eIF4E (Mader et al. 1995). Upon mTORC1 activation, 4E-BP is hyper-phosphorylated, preventing 4E-BP binding to eIF4E and thereby enabling eIF4F formation. Conversely, in response to mTORC1 inhibition, 4E-BP becomes hypo-phosphorylated, leading to 4E-BP binding to eIF4E and inhibition of eIF4F formation. Three 4E-BP isoforms have been identified in mammalian cells. 4E-BP1 is expressed in most tissues; 4E-BP2 is expressed primarily in the brain, but is present at low levels in most tissue; and 4E-BP3 is primarily expressed in colon and liver (Tsukiyama-Kohara et al. 2001). Importantly, the regulation of all three 4E-BP isoforms are similar, following a pattern of sequential phosphorylation at conserved residues (Hay & Sonenberg 2004).

mTORC1 dependent activation of p70 S6K leads to the phosphorylation of a number of targets that regulate protein synthesis. eEF2K is inactivated upon phosphorylation, enhancing translation elongation by reducing eEF2 phosphorylation (X Wang et al. 2001); eIF4B is activated upon phosphorylation, stimulating the helicase of eIF4A within eIF4F (Raught et al. 2004); and RPS6 phosphorylation has been shown to regulate ribosome biogenesis (Chauvin et al. 2014).

4.1.3 Regulation of mTORC1 by cellular stress

mTORC1 signalling provides a robust response to cellular stress, such as DNA damage and oxidative stress. In response to DNA damage mediated by IR (Braunstein et al. 2009) and etoposide (Tee & Proud 2000; Feng et al. 2005), inhibition of mTORC1 signalling resulted in global protein synthesis inhibition. Oxidative stress has also been shown to inhibit mTORC1 signalling through the ATM dependent activation of TSC2 (Alexander et al. 2010). Interestingly, doxorubicin has been shown to induce oxidative stress through the generation of ROS (Doroshov & Davies 1986), and this effect was suggested to inhibit

mTORC1 signalling in cardiomyocytes (Zhu et al. 2009) and MCF7 cells (Ji et al. 2010).

4.1.4 Aims

The aims of this section were to study mTORC1 activity in response to doxorubicin, and to determine the importance of mTORC1 signalling in the regulation of global protein synthesis. Additionally, doxorubicin toxicity was investigated further by considering the effect of ROS generation, and the consequence of prolonged cell cycle arrest.

4.2 Results

4.2.1 Doxorubicin inhibited mTOR signalling

Doxorubicin was shown to inhibit protein synthesis through the inhibition of translation initiation, and this was independent of eIF2 α . The other key pathway regulating protein synthesis is mTOR. mTOR controls translation initiation through the regulation of 4E-BP binding to eIF4E, therefore, the effect of doxorubicin on mTORC1 signalling was investigated further.

mTORC1 signalling was analysed in response to doxorubicin by western blot (Figure 4-2A). mTORC1 directly phosphorylates both 4E-BP1 and p70 S6K, and therefore both 4E-BP1 and p70 S6K phosphorylation could be used as a measure of mTORC1 activity. In response to doxorubicin, phosphorylation of both p70 S6K (Figure 4-2C) and 4E-BP1 (Figure 4-2D) were reduced by 40% at 6 hours after treatment, suggesting that doxorubicin inhibited mTORC1 signalling. The inhibition of mTORC1 signalling continued up to 24 hours, where phosphorylation of 4E-BP1 and p70 S6K were diminished by 90% and 85% respectively. Interestingly, doxorubicin induced eIF2 α phosphorylation at 9-12 hours, 3-6 hours after the initial inhibition of mTORC1 signalling (Figure 4-2B). mTORC1 inhibition was observed 6 hours from the initial recognition of DNA damage, and importantly, this correlated with protein synthesis inhibition (Figure 3-5A).

p70 S6K is a protein kinase, and its activity can be measured through the phosphorylation status of its target proteins, eEF2K and RPS6. The phosphorylation of both proteins were reduced, indicating mTORC1 signalling was robustly inhibited in response to doxorubicin (Figure 4-2). Taken together, these data suggested that in response to doxorubicin-induced DNA damage, mTOR inhibition may be the primary inhibitor of protein synthesis.

DNA-PKcs is auto-phosphorylated upon recruitment to DSBs (Yajima et al. 2009). Interestingly, DNA-PKcs auto-phosphorylation correlated with the inhibition of protein synthesis inhibition in response to doxorubicin (Figure 4-2A), suggesting that protein synthesis may be regulated in response to the recognition or repair of DNA breaks.

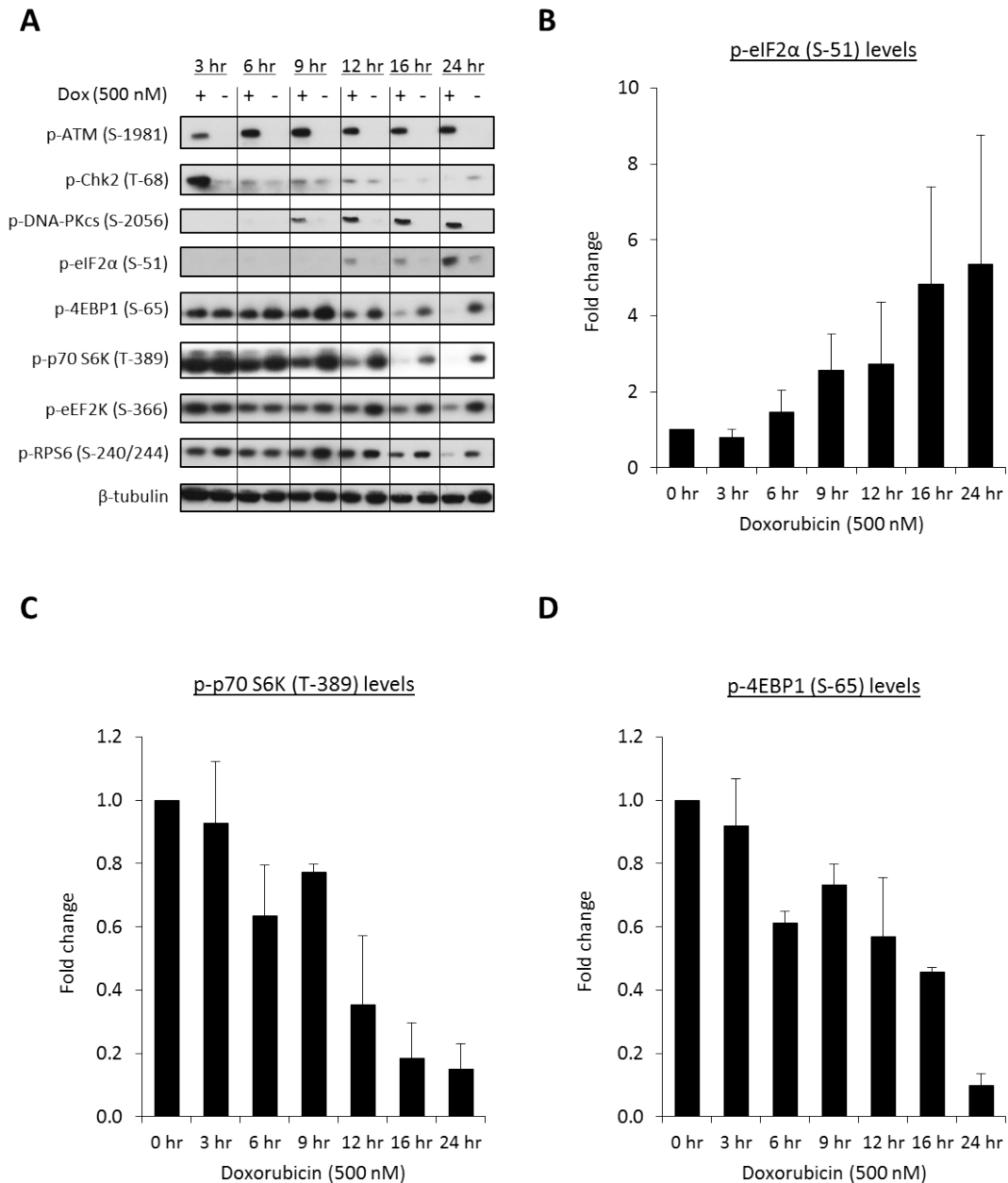


Figure 4-2. Doxorubicin inhibited mTORC1 signalling

(A) Western analysis of mTORC1 signalling in MCF10A cells treated continuously with doxorubicin (500 nM), for the indicated time. Blots were representative of three independent repeats. Quantification of ECL signal from western analysis for **(B)** eIF2α phosphorylation; **(C)** p70 S6K phosphorylation; and **(D)** 4E-BP1 phosphorylation. All values were normalised to β-tubulin levels, and displayed relative to the untreated sample for each time point, with standard deviation.

In order to determine that doxorubicin-induced protein synthesis inhibition was dependent on mTOR inhibition, a number of experiments were attempted to rescue protein synthesis.

The TSC1 and TSC2 heterodimer forms a functional TSC complex, inhibiting mTOR activity through TSC2 dependent regulation of the small GTPase Rheb (Garami et al. 2003) (Figure 4-1). Depletion of TSC2 constitutively activates mTORC1 signalling, and sensitises cells to doxorubicin-induced DNA damage (Ghosh et al. 2006), suggesting that doxorubicin may regulate mTORC1 activity through this pathway. Depletion of TSC2 using siRNA enabled the investigation of two different questions. First, to determine if TSC complex was directly involved in doxorubicin-induced mTORC1 inhibition, and secondly, to determine if constitutive activation of mTORC1 rescued protein synthesis inhibition induced by doxorubicin.

Depletion of TSC2 was analysed by western blot and shown to lead to enhanced p70 S6K activity in untreated samples, when compared to a scrambled control siRNA (Figure 4-3A, lane 4 vs lane 2 and Figure 4-3B). Enhanced phosphorylation of p70 S6K indicated that TSC2 knockdown upregulated mTORC1 signalling. Following doxorubicin treatment of TSC2 knockdown cells, p70 S6K phosphorylation was not abolished (Figure 4-3A, lane 3 vs lane 1 and Figure 4-3B), suggesting that TSC2 knockdown may have alleviated mTORC1 inhibition. Although the basal level of p70 S6K phosphorylation increased following TSC2 knockdown, p70 S6K phosphorylation was still diminished following doxorubicin treatment (Figure 4-3A, lane 3 vs lane 4 and Figure 4-3C). These data suggested that doxorubicin-induced mTORC1 inhibition was maintained in the absence of TSC. Surprisingly, 4E-BP1 phosphorylation was unaffected after TSC2 knockdown (Figure 4-3A, lane 4 vs lane 2 and Figure 4-3C), suggesting that TSC2 knockdown may not be fully activating mTOR signalling.

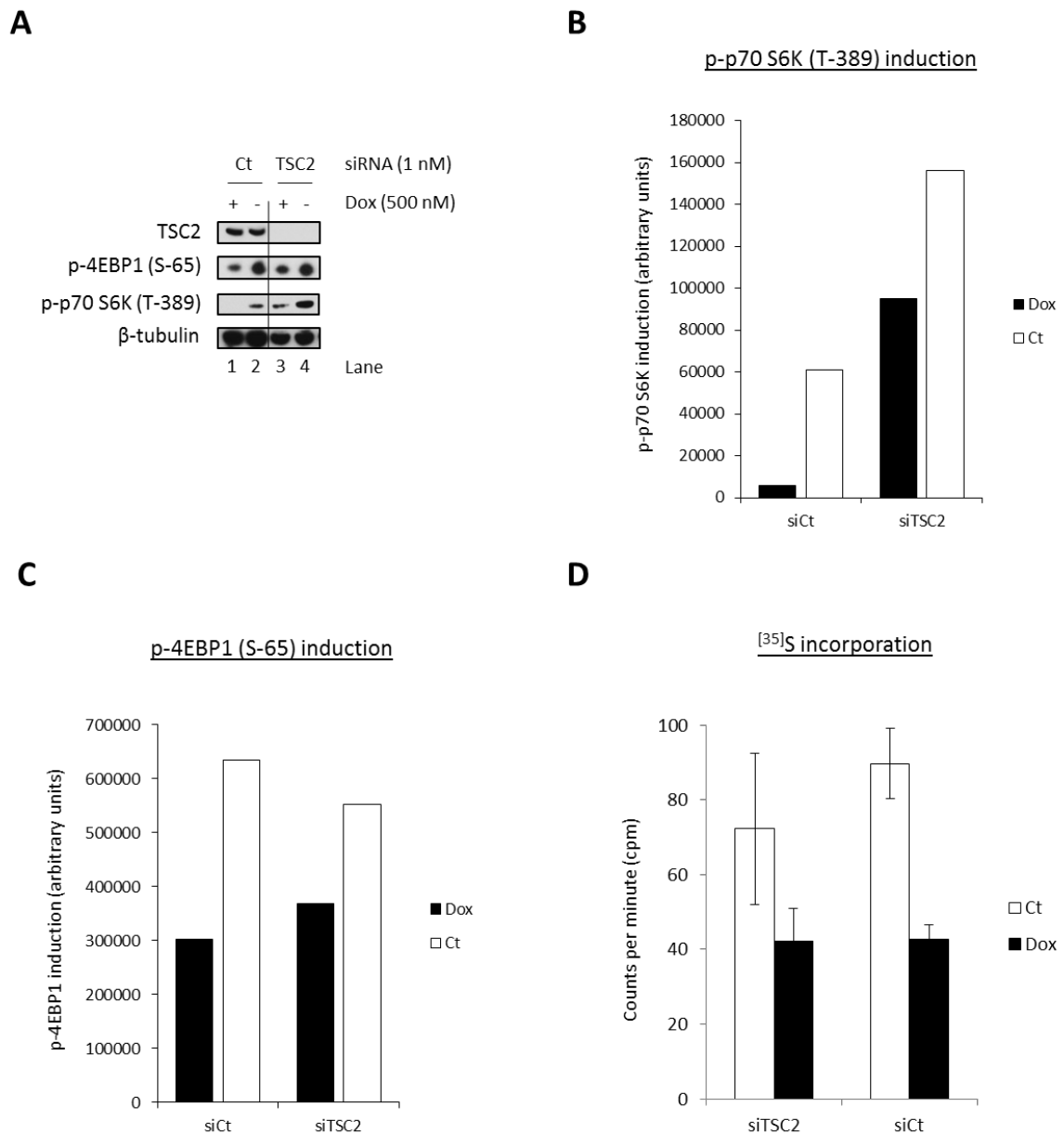


Figure 4-3. Depletion of TSC2 did not rescue doxorubicin-induced protein synthesis inhibition

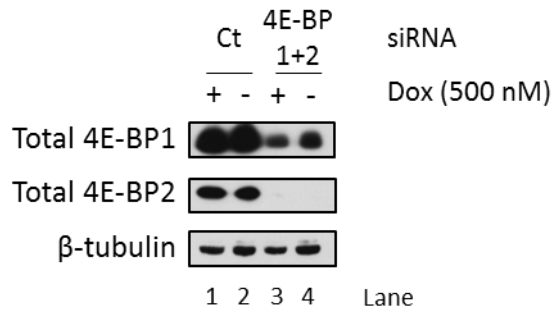
MCF10A cells were transfected with siRNA specific to TSC2 (1 nM) and treated with doxorubicin (500 nM) for 24 hours. **(A)** Western blot analysis following TSC2 knockdown to examine mTOR activity and eIF2α phosphorylation. Quantification of ECL signal from western analysis for **(B)** p70 S6K phosphorylation and **(C)** 4E-BP1 phosphorylation. All values were normalised to β-tubulin levels and shown with standard deviation. **(D)** [³⁵S] methionine incorporation following TSC2 knockdown and doxorubicin (500 nM) treatment. Counts per minute were normalised to total protein by Bradford assay. (B) and (C) were an average of two independent experiments, whereas (D) was an average of three independent experiments, and are shown with standard deviation.

[³⁵S] methionine incorporation was carried out in parallel to western analysis, in order to determine if TSC2 knockdown rescued doxorubicin-induced protein synthesis inhibition. Unfortunately, TSC2 knockdown was not sufficient to rescue protein synthesis inhibition or enhance protein synthesis in untreated samples (Figure 4-3D). The inability of TSC2 knockdown to rescue doxorubicin-induced protein synthesis inhibition indicated that mTORC1 regulation may involve pathways downstream of TSC, such as the regulation of mTORC1 localisation to the lysosome.

As mentioned previously, 4E-BPs regulate translation initiation by binding to eIF4E and preventing eIF4F complex formation. Knockdown of 4E-BP1 has been shown to relieve mTOR dependent protein synthesis inhibition in response to IR (Braunstein et al. 2009). To determine if doxorubicin-induced protein synthesis inhibition was dependent on 4E-BP, siRNA knockdown was again used. As 4E-BPs are extremely similar in activation and function (Hay & Sonenberg 2004), 4E-BP1 and 4E-BP2 were knocked down in combination to limit the capacity for one isoform to compensate for the loss of the other.

Whereas 4E-BP2 was depleted efficiently in these experiments, depletion of 4E-BP1 was only partial (Figure 4-4A). Unfortunately, 4E-BP1/2 depletion failed to rescue doxorubicin-induced protein synthesis inhibition, and also failed to increase protein synthesis in untreated samples (Figure 4-4B). These effects were likely due to the insufficient knockdown of 4E-BP1. To fully determine the role of 4E-BP in doxorubicin-induced protein synthesis inhibition, two consecutive 4E-BP1 knockdowns will be used in an attempt to ensure more efficient 4E-BP1 knockdown. Additionally, PTEN, a negative regulator of PI3K and Akt signalling, could be depleted to upregulate mTORC1 signalling. However, depletion of PTEN would almost certainly upregulate mTORC1 signalling via Akt and TSC activity, and would likely mirror the effect observed after depletion of TSC2.

A



B

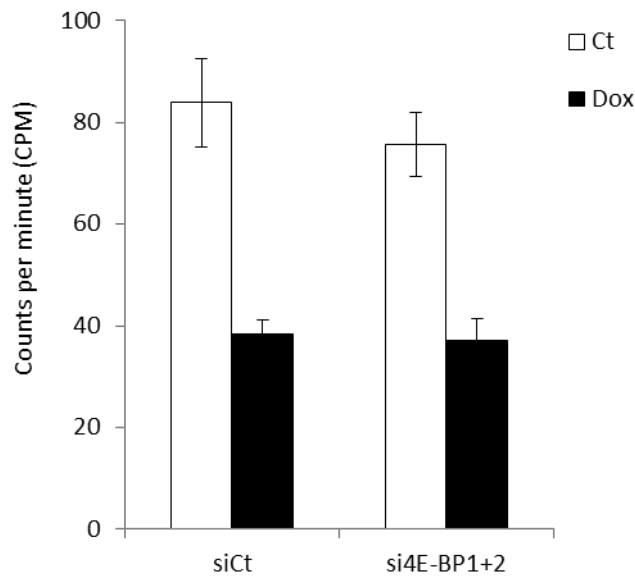


Figure 4-4. Partial depletion of 4E-BP1/4E-BP2 did not rescue doxorubicin-induced protein synthesis inhibition.

MCF10A cells were transfected with siRNA specific to 4E-BP1 (1 nM) and 4E-BP2 (1 nM) for 48 hours, and treated with doxorubicin (500 nM) for 24 hours. Ct = control non-targeting siRNA **(A)** Western blot analysis to examine the level of 4E-BP1/4E-BP2 protein knockdown. **(B)** ^[35]S methionine incorporation following 4E-BP1/4E-BP2 knockdown and doxorubicin (500 nM) treatment. Counts per minute were normalised to total protein by Bradford assay. Data values were an average of three independent experiments, and shown with standard deviation.

4.2.2 Doxorubicin induced crosstalk signalling between mTOR and eIF2

It has become apparent that mTOR signalling can feed into eIF2K signalling and vice versa. It has been shown that catalytic inhibition of mTORC1, using rapamycin (Wengrod et al. 2015) and Torin1 (Gandin, Masvidal, Cargnello, et al. 2016), resulted in an increase in eIF2 α phosphorylation. Conversely, growth factor activation of mTOR signalling resulted in eIF2 α de-phosphorylation (Gandin, Masvidal, Cargnello, et al. 2016). These mechanisms ensure a cell is able to co-ordinate ternary complex and eIF4F formation in response to cellular stress. In response to doxorubicin-induced DNA damage, mTORC1 inhibition preceded eIF2 α phosphorylation (Figure 4-2), and it was hypothesised that mTORC1 inhibition could mediate eIF2 α phosphorylation. To investigate this question, MCF10A cells were treated with AZD8055 (mTORC1 and mTORC2 inhibitor) and rapamycin (mTORC1 inhibitor). mTORC1 activity, measured through the phosphorylation of p70 S6K and 4E-BP1, and eIF2 α phosphorylation, were evaluated by western analysis. In response to two concentrations of AZD8055, mTORC1 signalling was shown to be inhibited at 3 hours (Figure 4-5A). Furthermore, mTORC1 inhibition was observed as early as 1 hour after AZD8055 treatment (data not shown). Intriguingly, eIF2 α phosphorylation was induced at 6 hours after mTORC1 inhibition, a similar time delay to that observed between mTORC1 inhibition and eIF2 α phosphorylation in response to doxorubicin (Figure 4-2). AZD8055 is an ATP-competitive inhibitor of mTOR kinase that binds to the ATP binding cleft (Chresta et al. 2010). As mTOR kinase is a key component of both mTORC1 and mTORC2, AZD8055 selectively inhibits both mTOR complexes. To confirm that eIF2 α phosphorylation was induced in response to solely mTORC1 inhibition, rapamycin was also used. Rapamycin is an allosteric inhibitor of mTORC1. Rapamycin interacts with FKBP12, forming a complex that is able to bind to mTOR kinase near the catalytic site, selectively inhibiting mTORC1 (Brown et al. 1994; Chen et al. 1995). In response to rapamycin, eIF2 α phosphorylation was also observed at 6 hours (Figure 4-5B), strongly suggesting that prolonged mTORC1 inhibition feeds into eIF2K signalling in MCF10A cells. Considering these data, along with the earlier observation that doxorubicin-induced mTORC1 inhibition preceded eIF2 α phosphorylation, it can be hypothesised that eIF2 α phosphorylation was dependent on mTORC1 inhibition.

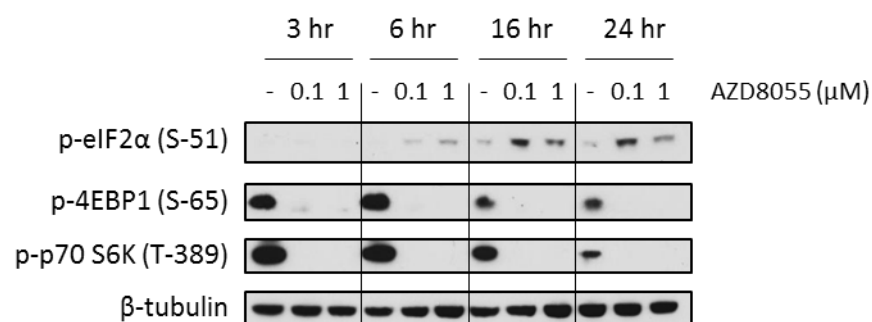
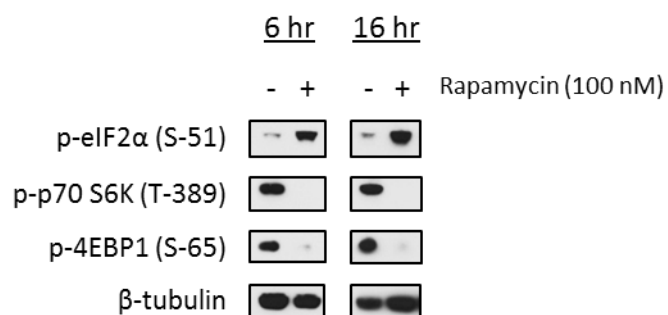
A**B**

Figure 4-5. Catalytic inhibition of mTOR enhanced eIF2α phosphorylation

Western blot analysis of MCF10A cells treated with AZD8055 (**A**) and Rapamycin (**B**) for the indicated time. Blots are representative of three independent repeats.

One mechanism of mTOR-eIF2 crosstalk signalling has been proposed, suggesting that the inhibition of mTORC1 induced eIF2 α phosphorylation by the activation of GCN2. Upon catalytic mTORC1 inhibition, protein phosphatase 6 (PP6) removes an inhibitory phosphorylation site on GCN2, enabling dimerisation and activation of GCN2 (Wengrod et al. 2015). PP6 is a well conserved type 2A serine/threonine protein phosphatase, that has also been shown to bind and activate DNA-PKcs after DSBs (Douglas et al. 2010). Knockdown of the PP6 catalytic component (PP6c) was shown to inactivate its phosphatase activity, reducing IR mediated DNA-PKcs activation (Mi et al. 2009). To determine if these mechanisms may be conserved in MCF10A cells, PP6c was depleted using siRNA. PP6c depleted cells were treated with either doxorubicin or AZD8055, and the level of mTORC1 signalling and eIF2 α phosphorylation was evaluated by western analysis. As a control for PP6c knockdown, DNA-PKcs activation was also monitored using its auto-phosphorylation status. In response to doxorubicin, DNA-PKcs activation was observed, but after depletion of PP6c, DNA-PKcs activation was diminished by 40% (Figure 4-6A, lane 1 vs lane 2 and Figure 4-6B). After treatment with both AZD8055 and doxorubicin, mTORC1 signalling was inhibited in PP6c knockdown cells (Figure 4-6A, lanes 6 and 2 vs lane 4). However, eIF2 α phosphorylation levels were drastically reduced in PP6c knockdown cells when compared to a scrambled control siRNA, in response to both doxorubicin (Figure 4-6A, lane 2 vs lane 1) and AZD8055 (Figure 4-6A, lane 6 vs lane 5). Quantification of the level of eIF2 α phosphorylation induced in response to doxorubicin showed a reduction of 90% in PP6c depleted cells, compared to control siRNA cells (Figure 4-6B). These observations suggested that both catalytic, and DNA damage induced, inhibition of mTOR signalling may feed into eIF2K signalling, and that this response may be dependent on PP6 activity. [³⁵S] methionine incorporation was carried out in parallel to western blot samples to fully determine the effect eIF2 α phosphorylation had on doxorubicin-induced protein synthesis inhibition. Depletion of PP6c did not rescue doxorubicin-induced protein synthesis inhibition (Figure 4-6B), supporting previous data using ISRIB (Figure 1-10B). These data suggested that eIF2 α phosphorylation was not required for protein synthesis inhibition.

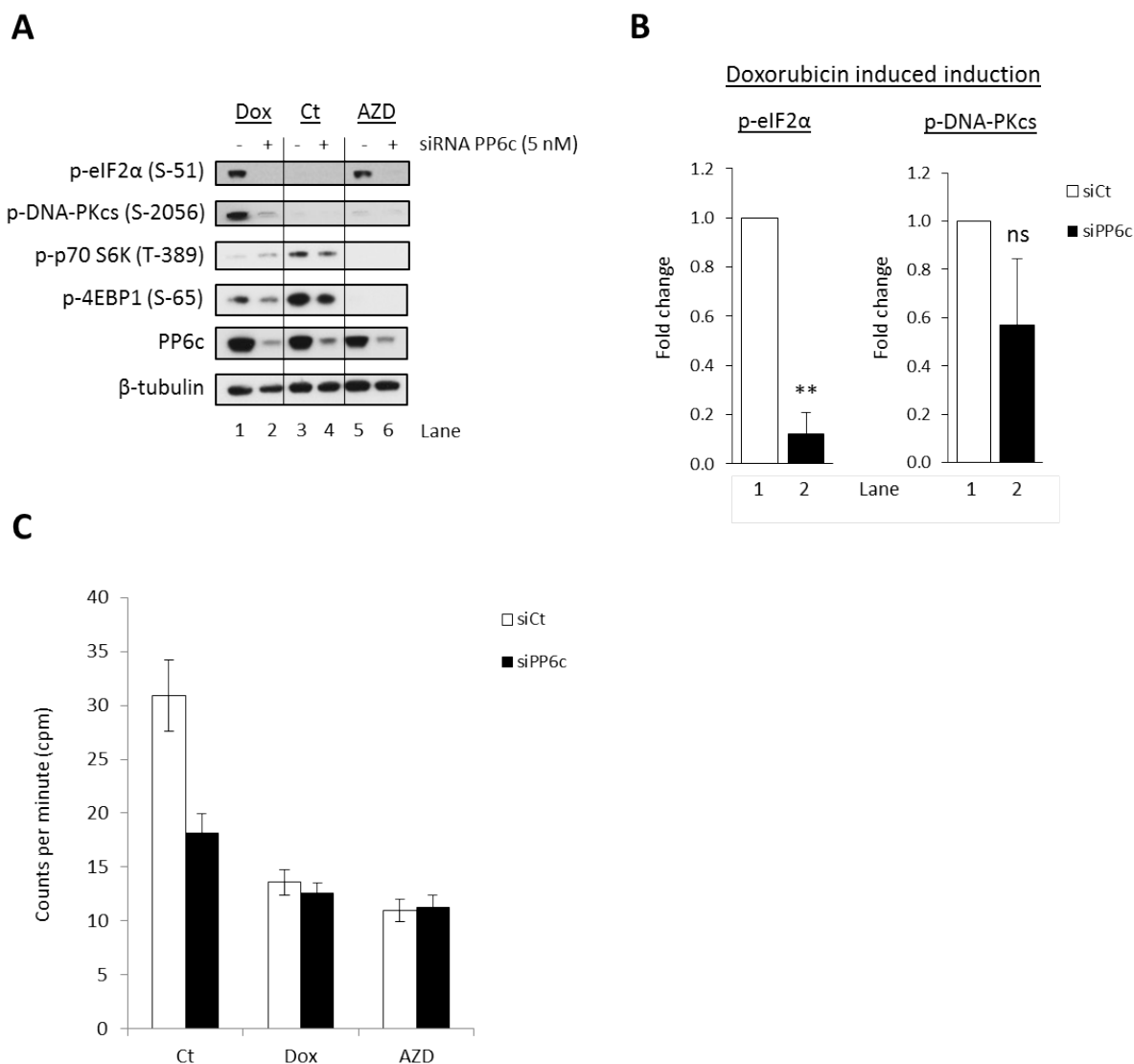


Figure 4-6. Depletion of PP6c diminished doxorubicin and AZD8055 induced eIF2α phosphorylation

MCF10A cells were transfected with siRNA specific for PP6c (5 nM) for 48 hours, and treated with doxorubicin (500 nM) or AZD8055 (100 nM) for 16 hours. **(A)** Western blot analysis following PP6c knockdown and doxorubicin or AZD8055 treatment, examining mTOR activity and eIF2α phosphorylation. **(B)** Quantification of doxorubicin-induced phosphorylation of eIF2α and DNA-PKcs from (A). Quantified values were normalised to β-tubulin levels and shown as fold change relative to siCt. Values were an average of three independent experiments, with standard deviation. Statistical significance was calculated using a two-tailed student's *t* test, assuming unequal variances (** = *P* value <0.01, ns = not significant). **(C)** ³⁵S methionine incorporation following PP6c knockdown and doxorubicin or AZD8055 treatment. Counts per minute were normalised to total protein by Bradford assay. Data points are an average of three individual experiments, with standard deviation.

Unfortunately, knockdown of PP6c resulted in an almost two-fold reduction of global protein synthesis (Figure 4-6B) when compared to a control siRNA, making it difficult to draw any definitive conclusions from these data. Titration of PP6c siRNA from 5 nM to 1 nM, did not inhibit protein synthesis, but knockdown of PP6c protein was still observed (data not shown). In further experiments, PP6c siRNA will be reduced to the lowest concentration that efficiently depletes PP6c without inhibiting global protein synthesis, to determine if PP6c mediates signalling between mTOR and eIF2 α .

Crosstalk signalling from mTORC1 inhibition to eIF2 α phosphorylation has been suggested to be mediated by GCN2. To determine the role played by eIF2Ks in mTORC1 mediated eIF2 α phosphorylation, siRNA knockdown was again used. GCN2, PERK, and PKR were knocked down in combination and treated with AZD8055 for 16 hours, as this was previously shown to provide robust phosphorylation of eIF2 α (Figure 4-5A). These data indicated that depletion of GCN2 and PERK provided the greatest reduction in eIF2 α phosphorylation (Figure 4-7). Intriguingly, combined knockdown of GCN2 and PERK also provided the greatest reduction in eIF2 α phosphorylation in response to doxorubicin (Figure 3-8). These data support the hypothesis that doxorubicin-induced mTORC1 inhibition regulated eIF2 α phosphorylation by signalling to upstream eIF2Ks.

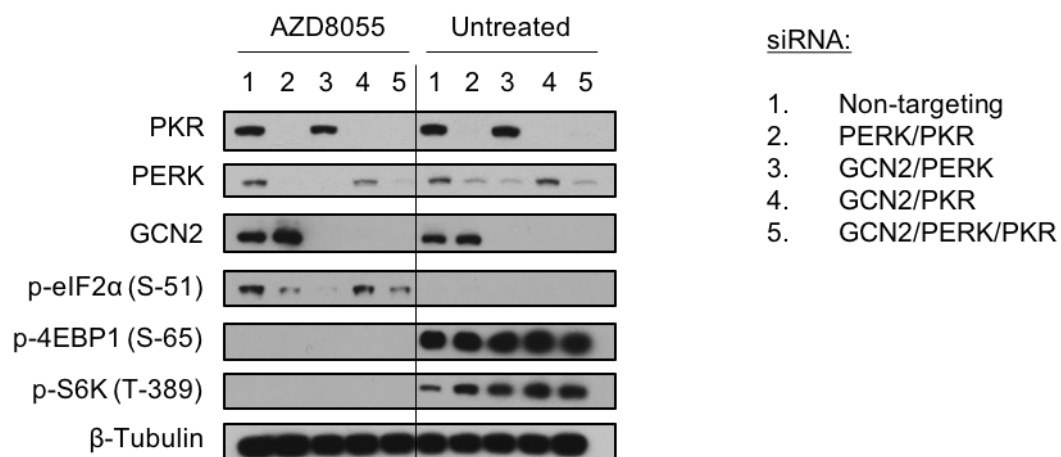


Figure 4-7. Double and triple knockdown of eIF2α kinases diminished AZD8055 induced eIF2α phosphorylation

Western blot analysis of eIF2α phosphorylation in response to AZD8055 following eIF2K knockdown. Combinations of siRNA specific for PKR (1 nM), PERK (1 nM) and GCN2 (2 nM), were transfected into MCF10A cells using RNAiMax lipofectamine reagent, for 48 hours. Cells were treated with AZD8055 (100 nM) for a further 16 hours or left untreated, and the level of eIF2α phosphorylation examined by western blot. siCt = non targeting siRNA.

4.2.3 Treatment with doxorubicin induced a senescence-like phenotype

A 24-hour doxorubicin (500 nM) treatment did not induce significant cell death (Figure 1-2), and it has been suggested that doxorubicin concentrations below 1 μ M induce senescence rather than cell death (Rebbaa et al. 2003; Jackson & Pereira-smith 2006; Sliwinska et al. 2009). Following a 24-hour doxorubicin treatment, cells arrested in G2/M and protein synthesis was inhibited by 50%. Although protein synthesis was significantly inhibited, [³⁵S] methionine incorporation indicated that 50% of global protein synthesis was still functional. It has been suggested that a limited amount of protein synthesis is maintained in cells that have entered a senescence-like phenotype (Young et al. 2009). In an attempt to uncover more information concerning the cellular and metabolic state of doxorubicin arrested MCF10A cells, cells were treated with doxorubicin for 24 hours and allowed to recover in fresh growth media for 24 or 48 hours.

After a 24-hour doxorubicin treatment, western analysis indicated that ATM and p53 were activated as part of the DDR, mTORC1 was inhibited, and eIF2 α phosphorylation was enhanced (Figure 4-8A 0 hr). Upon recovery for 24 hours, p53 phosphorylation (Ser 15) was absent but ATM activation was maintained, as was induction of p21. It has been suggested that the stabilisation of p53 stabilisation, and subsequent expression of p21, are required for sustained G2/M arrest (Bunz et al. 1998). Interestingly, in MCF10A cells, cellular arrest appeared to be sustained in the absence of p53 activation (Figure 4-8A). p53 is stabilised by phosphorylation at Ser 15 in response to DNA damage signalling. However, it is possible that the phosphorylation of other residues may maintain p53 stabilisation in the absence of phosphorylation at Ser 15. To fully determine if p53 stabilisation is maintained after recovery from doxorubicin treatment, total p53 levels must be studied by western analysis.

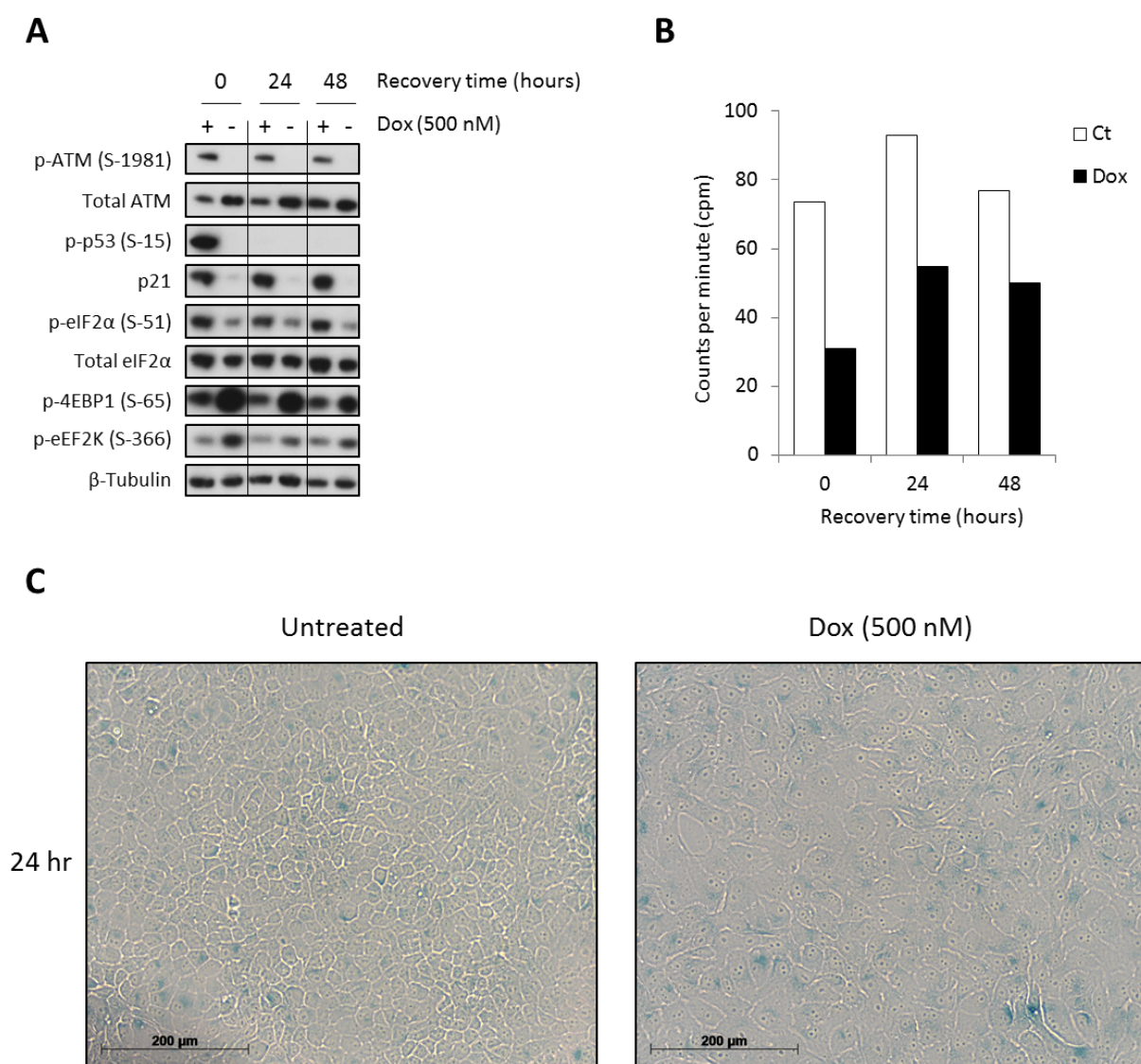


Figure 4-8. MCF10A cells did not immediately recover from doxorubicin treatment

(A) Western blot analysis of the DNA damage response, eIF2α phosphorylation and mTOR activity, after recovery from doxorubicin. Cells were treated with doxorubicin (500 nM) for 24 hours, followed by a recovery period in doxorubicin free media for the indicated time. **(B)** ³⁵S methionine incorporation, carried out in parallel to (A). Counts per minute were normalised to total protein by Bradford assay. The datum included here is preliminary, consisting of 1 experiment. **(C)** Comparison of cell size following doxorubicin treatment (500 nM, 24 hr). Images were acquired using a Zeiss Axiovert 135 microscope, with bright field optics and magnification of 20X.

mTORC1 inhibition and eIF2 α phosphorylation were both maintained in cells allowed to recover from doxorubicin treatment, suggesting protein synthesis did not resume (Figure 4-8A). [³⁵S] methionine incorporation, carried out in parallel to samples analysed by western analysis, indicated that protein synthesis may recover slowly, although protein synthesis was still inhibited by 40% after a 48-hour recovery (Figure 4-8B). It would be interesting to allow cells to recover for longer time periods, to fully determine if protein synthesis rates completely recover. Additionally, cells did not appear to be undergoing cell death due to the absence of detached cells. Taken together, these data suggested that cells do not recover from doxorubicin-induced DNA damage, and do not re-enter the cell cycle. Upon treatment with doxorubicin, cells increase in size compared to untreated cells after 24 hours (Figure 4-8B), and data from within the Willis laboratory has shown that cells continue to increase in size without dividing, for up to 7 days.

DNA damage has been shown to induce a senescence-like phenotype in a number of cell types (Chen & Ames 1994; Di Leonardo et al. 1994; Maya-Mendoza et al. 2014; Cho et al. 2011). Markers of cellular senescence include: cell cycle arrest, while maintaining metabolic activity; lack of replication; and large cell morphology (Chen & Ames 1994; Campisi & d'Adda di Fagagna 2007; Kuilman et al. 2010). As these were all characteristics observed in MCF10A cells in response to doxorubicin, acidic β -galactosidase staining was analysed to measure cellular senescence. Senescent cells overexpress lysosomal β -galactosidase, defined as senescence-associated β -galactosidase activity (SA- β -gal), that can be detected by measuring X-gal cleavage at pH 6 (Dimri et al. 1995; Lee et al. 2006). MCF10A cells were treated with doxorubicin for 24-hours and allowed to recover in fresh growth media for a further 48 hours prior to SA- β -gal staining. SA- β -gal activity was observed in doxorubicin treated cells (Figure 4-9), indicating that doxorubicin may be inducing a senescent-like phenotype.

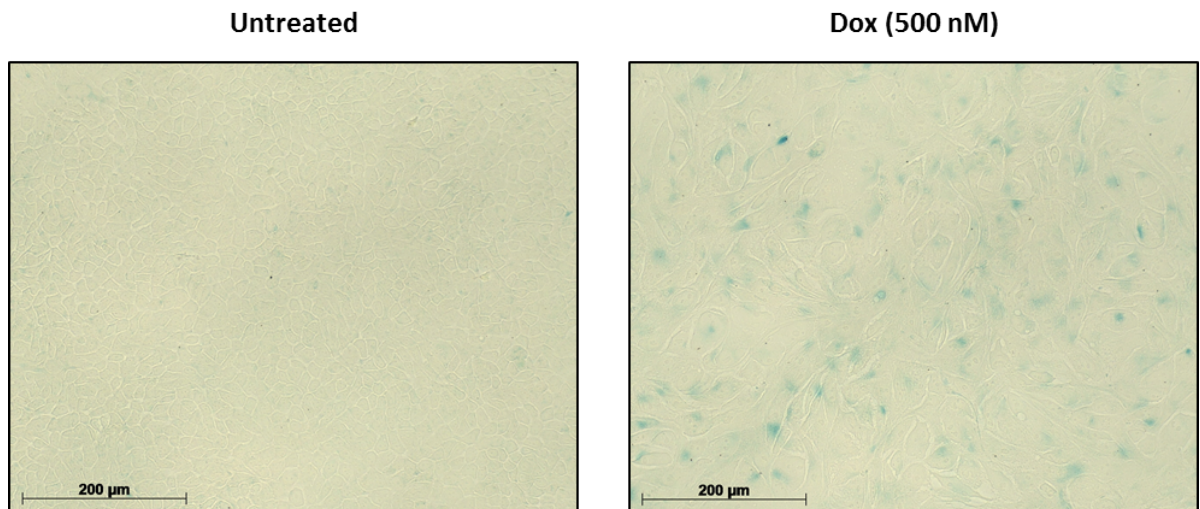


Figure 4-9. Doxorubicin rapidly induced a senescence-like phenotype

β -galactosidase staining assay. Cells were treated with doxorubicin (500 nM) for 24 hours, followed by a recovery period in doxorubicin free media for 48 hours prior to SA- β -gal activity assay. Images were acquired using a Zeiss Axiovert 200M microscope, with bright field optics and magnification of 20X.

4.2.4 Doxorubicin did not induce substantial ROS generation

Although doxorubicin functions primarily as a Top2 poison, it has the capacity to generate reactive oxygen species (ROS) in the presence of iron. Doxorubicin reversibly oxidises to a semiquinone, cycling within mitochondria to generate ROS (Doroshov & Davies 1986). A major side effect of using doxorubicin as a chemotherapeutic drug is cardiotoxicity (Zhou et al. 2001; Nitiss & Nitiss 2014). It has been hypothesised that cardiotoxicity is caused by mitochondrial iron accumulation and ROS generation (Berthiaume & Wallace 2007). Dexrazoxane is an iron chelator used in combination with doxorubicin, that has been shown to protect cardiac cells from doxorubicin toxicity (Martin et al. 2009; Lebrecht et al. 2007), by reducing iron and ROS generation within mitochondria (Ichikawa et al. 2014). These studies support the hypothesis that doxorubicin toxicity could be mediated by ROS generation, leading to damage within the cell. ROS generation can result in DNA damage, protein damage, kinase activation, impaired mitochondrial function (Deavall et al. 2012), and has been implicated in doxorubicin toxicity in non-cardiac cell lines. ROS has been shown to directly activate ATM (Guo et al. 2010), furthermore, doxorubicin enhanced ATM signalling and AMPK activation were greatly reduced in the presence of a ROS scavenger, N-acetyl cysteine (NAC) (Kurz et al. 2004; Ji et al. 2010).

To examine the possibility that ROS generation may be responsible for doxorubicin-induced mTOR inhibition and protein synthesis inhibition, cellular ROS levels were quantified using DCFH-DA. DCFH-DA is a cell permeable probe that fluoresces upon oxidation (Keston & Brandt 1965). Cells were treated with doxorubicin for 24 hours, incubated with DCFH-DA for the final 30 minutes, and Hoechst 33342 for the final 5 minutes to stain nuclei. To minimise cell stress, DCFH-DA fluorescence was initially measured using low-resolution fluorescent imaging, enabling the analysis of fluorescent compounds in live cell populations without the need for trypsinisation. Using H₂O₂ as a positive control for oxidative stress, DCFH-DA fluorescence was observed throughout the population of cells (Figure 4-10A). After treatment with doxorubicin, DCFH-DA fluorescence was also observed throughout the cytoplasm in a similar to pattern to that observed for H₂O₂, suggesting that doxorubicin may induce the generation of ROS (Figure 4-10A).

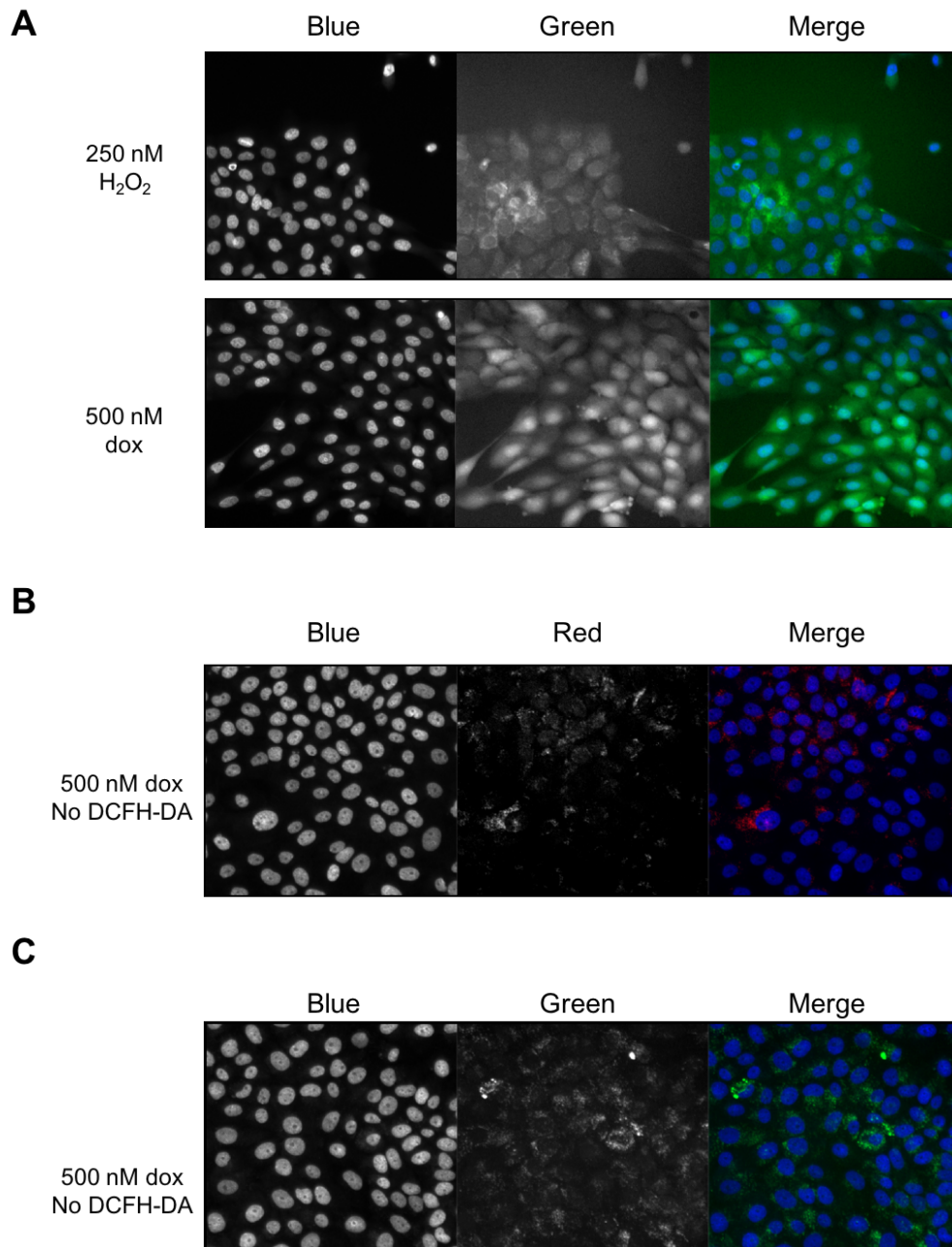


Figure 4-10. Quantification of reactive oxygen species using low resolution, high content fluorescent microscopy

Cells were analysed using Cellomics ArrayScan VTI HCS reader **(A)** MCF10A cells treated with doxorubicin (500 nM, 24 hours) or H_2O_2 (250 nM, 6 hours) prior to incubation with DCFH-DA (20 μ M) for 30 minutes. Cells were analysed using blue (Hoechst) and green (DCFH-DA) channels **(B)** MCF10A cells were treated with doxorubicin (500 nM, 24 hours) in the absence of DCFH-DA and analysed using blue (Hoechst) and green (DCFH-DA) channels. **(C)** MCF10A cells were treated with doxorubicin (500 nM, 24 hours) in the absence of DCFH-DA and analysed using blue (Hoechst) and red (doxorubicin) channels.

Doxorubicin auto-fluoresces red, so it was possible to visualise the cellular distribution of doxorubicin using the appropriate laser and filter. Analysis of cells treated with doxorubicin in the absence of DCFH-DA indicated that doxorubicin might localise to the mitochondria (Figure 4-10B), where doxorubicin could generate ROS. The wavelength of green and red are relatively close to each other on the visible light spectrum, so it was plausible that the emission of DCFH-DA could spill over into the emission of doxorubicin, and vice-versa. This could result in an overlap of the observed signal, providing false positive data. To determine if the overlap of emissions were a factor, cells were treated with doxorubicin in the absence of DCFH-DA and analysed using low-resolution fluorescent imaging. Unfortunately, when viewed using the green laser, doxorubicin auto-fluorescence was observed within the green channel (Figure 4-10C), implying that the DCFH-DA signal observed previously may be partly background doxorubicin fluorescence.

To overcome the issue of doxorubicin auto-fluorescence, DCFH-DA fluorescence was quantified using FACS analysis. The flow cytometer, BD FACS aria II, had separate red and green lasers, as well separate detectors, dramatically reducing the capacity for emission overlap. For FACS analysis, cells were treated identically as for low-resolution fluorescent imaging, except cells were trypsinised and allowed to recover for 15 minutes prior to analysis. Unfortunately, the population of H₂O₂ treated cells did not increase DCFH-DA fluorescence when compared to untreated cells (Figure 4-11A). Upon doxorubicin treatment, DCFH-DA fluorescence only increased moderately, as shown by the enhanced FITC-A signal, however, this was not enough to form two distinct populations of cells (Figure 4-11A). Although the quantification of DCFH-DA fluorescence indicated a significant increase in ROS generation (Figure 4-11B), the lack of a positive control for DCFH-DA fluorescence makes interpretation of these data challenging. The absence of a positive DCFH-DA population of cells in response to doxorubicin suggested that ROS generation was minimal in MCF10A cells, but it has been suggested that the ability of DCFH-DA to quantify ROS is limited. DCFH-DA is subject to redox cycling and generating false positive fluorescence (Kalyanaraman et al. 2012), and DCFH-DA does not directly react with H₂O₂, meaning that DCFH-DA cannot be used

as a direct measure of H_2O_2 (Kalyanaraman et al. 2012). Furthermore, these experiments were carried out using a time point of 24 hours, where it was possible that the mitochondria may be damaged and ceased to function correctly (Kuznetsov et al. 2011). To determine the impact of doxorubicin-induced ROS generation, alternative methods of ROS quantification should be used in parallel and analysed over a time course experiment.

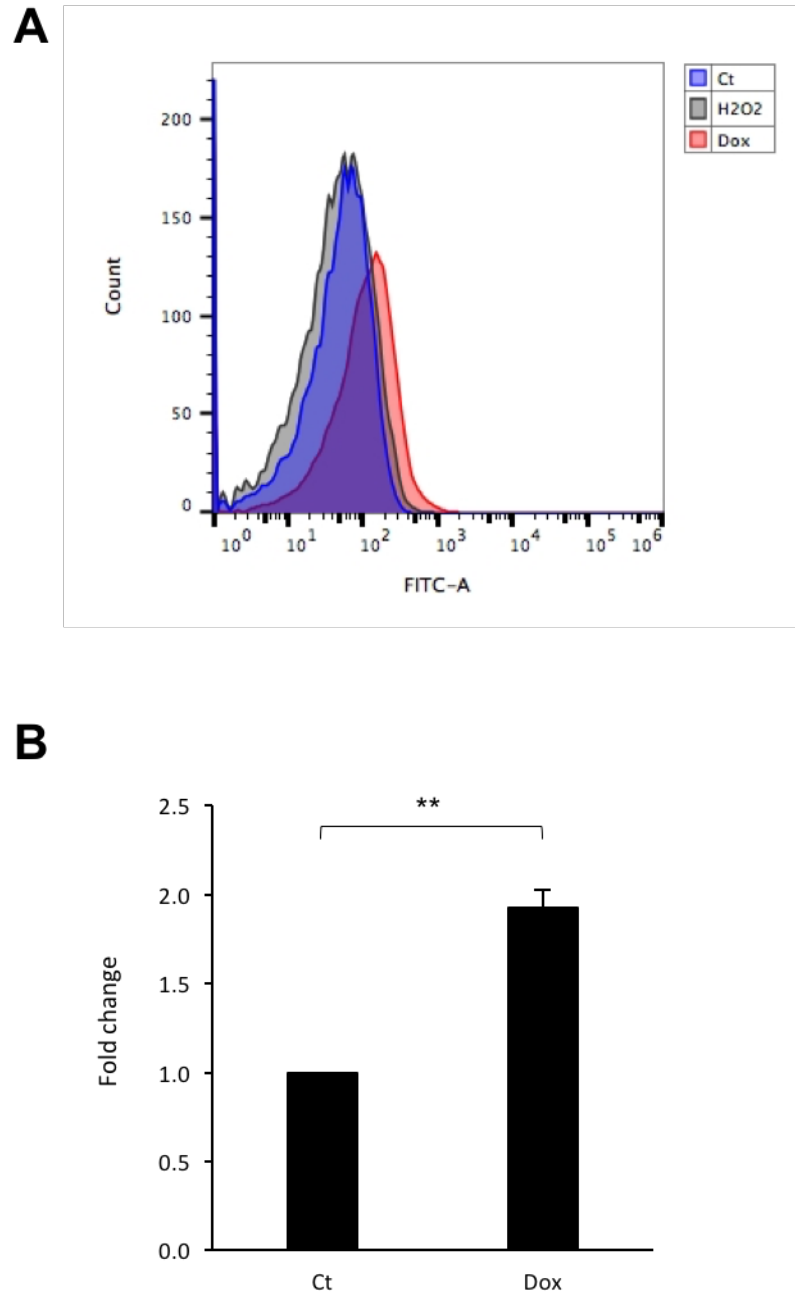


Figure 4-11. FACS quantification of reactive oxygen species after treatment with doxorubicin

(A) FACS analysis of MCF10A cells treated with doxorubicin (500 nM, 24 hr) or H_2O_2 (250 nM, 6 hr), prior to incubation with DCFH-DA (20 μ M) for 30 minutes. DCFH-DA signal (FITC-A) was visualized as a histogram. Increase in DCFH-DA signal corresponds to an increase in reactive oxygen species. **(B)** Quantification of DCFH-DA signal in doxorubicin treated cells. Data points were an average of three individual experiments, shown with standard deviation. Statistical significance was calculated using a two-tailed student's *t* test, assuming unequal variances (** = *p*-value <0.01).

4.3 Discussion

The aim of this chapter was to determine the role of mTOR inhibition in doxorubicin-induced protein synthesis inhibition.

Treatment with doxorubicin induced the inhibition of mTORC1 signalling at 6 hours. Importantly, mTORC1 inhibition correlated with global protein synthesis inhibition and preceded eIF2 α phosphorylation by 3-6 hours. These data suggested that mTOR signalling may be the predominant negative regulator of protein synthesis, in response to doxorubicin-induced DNA damage. To determine if mTORC1 inhibition was responsible for global protein synthesis inhibition, a series of rescue experiments were attempted. Firstly, the negative regulator of mTORC1 signalling, TSC2, was depleted by siRNA knockdown. Although depletion of TSC2 upregulated mTORC1 mediated p70 S6K phosphorylation, it did not rescue protein synthesis inhibition. These data indicated that doxorubicin may inhibit mTORC1 activity by a mechanism independent of TSC activity, such as the regulation of mTORC1 localisation. Secondly, 4E-BPs were depleted to minimise mTORC1 dependent inhibition of translation initiation. Unfortunately, combined depletion of 4E-BP1 and 4E-BP2 did not rescue protein synthesis inhibition induced by doxorubicin, due to the insufficient knockdown of 4E-BP1. If mTORC1 inhibition was regulating protein synthesis inhibition, it would most likely mediate this effect through the regulation of 4E-BPs. Consequently, siRNA depletion of 4E-BP1 will be improved by the application of sequential 24 hour knockdowns, in an effort to fully determine the role of 4E-BPs in doxorubicin-induced protein synthesis inhibition.

Prolonged catalytic inhibition of mTORC1 resulted in the phosphorylation of eIF2 α , suggesting that mTOR signalling may communicate with eIF2 signalling. Using western blot analysis, catalytic mTORC1 inhibition was shown to induce eIF2 α phosphorylation at 6 hours. Interestingly, a delay of 6 hours was observed between doxorubicin-induced mTORC1 inhibition and eIF2 α phosphorylation. Therefore, these data suggested that mTORC1 inhibition could mediate the subsequent phosphorylation of eIF2 α . Crosstalk signalling from mTORC1 to eIF2 has been previously reported, and it was suggested to be mediated by PP6 (Wengrod et al. 2015). Here, depletion of PP6 activity

diminished doxorubicin and AZD8055 induced eIF2 α phosphorylation, indicating that PP6 could mediate crosstalk signalling. Additionally, depletion of PP6 activity diminished doxorubicin-induced DNA-PKcs activation, suggesting that DNA-PKcs could also play a role in doxorubicin-induced eIF2 α phosphorylation. Unfortunately, depletion of PP6c resulted in the inhibition of global protein synthesis, suggesting that the siRNA may have undesired, non-specific effects. To fully determine the role of PP6 in mTOR-eIF2 crosstalk signalling, the siRNA will be titrated down to a concentration that does not inhibit protein synthesis, but that does provide efficient depletion of PP6c.

PP6 has been suggested to mediate the activation of GCN2 by the removal of an inhibitory phosphorylation site (Wengrod et al. 2015). Combined knockdown of eIF2Ks were used in an attempt to determine the kinases response for AZD8055 induced eIF2 α phosphorylation. Interestingly, combined knockdown of GCN2 and PERK resulted in the greatest depletion of AZD8055 induced eIF2 α phosphorylation, mirroring the response observed after doxorubicin treatment (Figure 3-8). These data indicated that GCN2 and PERK may mediate the phosphorylation of eIF2 α in response to prolonged mTORC1 inhibition, however, this response must be shown to be reproducible before definitive conclusion can be made.

Doxorubicin treated cells displayed markers of a senescence-like phenotype. Cells did not appear to recover from doxorubicin treatment after incubation in drug free media for 48 hours. However, mTORC1 inhibition, eIF2 α phosphorylation, and protein synthesis inhibition were all maintained. Furthermore, enhanced SA- β -gal activity suggested that cells rapidly entered a senescence-like phenotype, after treatment with doxorubicin for only 24 hours.

In addition to the induction of strand breaks by Top2 poisoning, doxorubicin also induces toxicity through the generation of ROS. By quantifying levels of ROS, using the fluorescent probe DCFH-DA, ROS generation after treatment with doxorubicin was shown to be minimal, due to the lack of a distinct population of fluorescent cells. However, ROS generation was quantified after a 24-hour doxorubicin treatment, a time when the mitochondria could be damaged and have ceased to function correctly. To fully determine the role of ROS generation

in doxorubicin-induced toxicity, ROS production should be quantified through a time course experiment. In addition, it may be beneficial to analyse mitochondrial function in parallel to the quantification of ROS, to ensure that damaged mitochondria are not concealing doxorubicin-induced ROS generation.

5 Doxorubicin-induced inhibition of mTORC1 signalling was mediated by p53

5.1 Introduction

5.1.1 DNA damage signalling

The DDR is mediated by the phosphoinositide 3-kinase (PI3K) related kinases ATM, ATR, and DNA-PKcs. ATM, ATR, and DNA-PKcs are recruited to DNA breaks through protein-protein interactions with DNA damage sensors, MRE11-RAD50-NBS1 (MRN) complex, ATR interacting protein (ATRIP) and Ku70/80, respectively (Uziel et al. 2003; Zou & Elledge 2003; Gottlieb & Jackson 1993). ATM and DNA-PKcs are activated in response to double strand DNA breaks (DSBs), whereas ATR is activated to a broad range of damage, including single strand breaks (SSBs) and replication stress. Recruitment to the DNA break site is essential for the activation of each kinase, and the subsequent activation of DDR effectors (Falck et al. 2005). DDR effectors regulate cell cycle arrest, DNA damage repair, and programmed cell death (reviewed extensively in (Polo & Jackson 2011; Dasika et al. 1999; Sirbu & Cortez 2013)). DDR signalling protects cells by ensuring damaged DNA is not replicated or passed onto daughter cells, by activating cell cycle arrest checkpoints and initiating DNA repair pathways.

ATM and ATR are DDR signalling kinases that activate DNA damage effectors, Chk2 and Chk1 respectively. ATM and ATR share a number of downstream target proteins (Wang et al. 2006), including p53 (Shieh et al. 2000). The recruitment of ATR to DNA damage is mediated by ATRIP binding to replication protein A (RPA) at SSBs (Zou & Elledge 2003). Conversely, ATM is recruited to DNA breaks through interactions with MRN complex, which binds to exposed DSBs (Uziel et al. 2003).

DNA-PKcs was first identified as a core component of NHEJ DNA repair machinery and is essential for DNA repair (Kurimasa et al. 1999). Ku70/Ku80 recruits DNA-PKcs to DSB sites, leading to DNA-PKcs auto-phosphorylation and activation (Gottlieb & Jackson 1993). DNA-PKcs has also been shown to activate Chk2 in response to DNA damage (Jack et al. 2004; Li & Stern 2005),

indicating that it too shares downstream targets with ATM and ATR. Importantly, ATM, ATR and DNA-PKcs have all been suggested to directly phosphorylate p53 at Ser 15 (Lees-Miller et al. 1992; Banin et al. 1998; Tibbetts et al. 1999), suggesting that all three pathways signal as part of the DDR.

5.1.2 p53 dependent DNA damage cell cycle checkpoints

p53 is regulated by post-translational modifications, and implicated in the control of hundreds of genes in response to DNA damage and metabolic stress (Riley et al. 2008). After exposure to stress, p53 regulates cell cycle arrest, apoptosis, and DNA repair (Wade Harper et al. 1993; Waldman et al. 1995; Oren 2003; Haupt et al. 2003; Menendez et al. 2009). Mutations inactivating p53 function are common in human cancers, reducing anti-proliferative properties and enhancing tumorigenesis (Hollstein et al. 1991). Under basal conditions, p53 has an extremely short half-life and is degraded through a ubiquitin-proteasome dependent pathway, mediated by MDM2 (Kubbutat et al. 1997). In response to stress such as DNA damage, activated Chk1 and Chk2 phosphorylate p53 (Shieh et al. 2000), disrupting the interaction with MDM2 and stabilising p53 (Shieh et al. 1997). Cell cycle arrest in G1 is regulated by the p53 dependent expression of p21. p21 disrupts cyclin D-cdk4 binding to Rb, thereby enhancing Rb inhibition of EF2 and preventing progression into S-phase (Shiyanov et al. 1996) (Figure 1-11). p53 regulates cell cycle arrest in G2 by the inhibition of cyclin B-cdk1 formation, and preventing progression into M-phase (Bates et al. 1998; Zhan et al. 1999) (Figure 1-11). p53 also induces cell death pathways by regulating the transcriptional control of pro-apoptotic factors, including Bax, Puma, Bid and Noxa (Yu & Zhang 2005). Upon p53 activation, cell fate is likely to be dependent on a combination of factors, such as cell type and strength of stimuli (i.e. amount of DNA damage).

5.1.3 Aims

The aims of this section were to determine the importance of cell cycle progression in the DDR induced by doxorubicin. Signalling from DNA damage was also studied in greater detail by examining the roles played by ATM, ATR and DNA-PKcs. As p53 is a shared target of each DDR kinase, the role of p53 in doxorubicin-induced toxicity was examined in a p53 null cell line.

5.2 Results

5.2.1 Doxorubicin-induced eIF2 α phosphorylation and mTOR inhibition was not dependent on cell cycle state

Many signalling pathways integrate to regulate cell cycle progression, and conversely, the cell cycle regulates the activity of these signalling pathways. For example, during mitosis, eEF2K is inactivated by cdc2-cyclin B (Smith & Proud 2008), and 4E-BP1 is hypo-phosphorylated (Pyronnet et al. 2001). Proliferation has been shown to be closely linked to the rate of protein synthesis (Johnson et al. 1976), and in *Saccharomyces cerevisiae*, it has been suggested that DNA damage is only fully recognised during DNA synthesis (Palou et al. 2010). Furthermore, cell cycle state has been shown to affect DNA repair efficiency (Ambrosio et al. 2015; Orthwein et al. 2014). Taking these factors into account, it was possible that the delayed inhibition of protein synthesis could be a consequence of cell cycle regulation. To determine if cell cycle state was responsible for doxorubicin-induced mTORC1 inhibition and eIF2 α phosphorylation, MCF10A cells were synchronised in G0. Synchronisation of MCF10A cells was possible through growth factor starvation for 24 hours (Zimmerman & Erikson 2007). Cells were released from synchronisation by the re-stimulation with growth factors and analysed by FACS, using EdU incorporation to quantify S-phase, and FxCycle to quantify G1 and G2 populations. After synchronisation, 90% of cells accumulated in G0/G1, as shown by the FxCycle histogram profile (Figure 5-1A). After release from synchronisation, FxCycle staining indicated that it took cells 16 hours to progress into S-phase (Figure 5-1A). Cell cycle analysis with FxCycle was supported by EdU incorporation, suggesting cells entered S-phase between 12-16 hours after release (Figure 5-1B). By 24-28 hours, many cells had progressed through S-phase into G2, or completed a cycle back to G1 as the population became asynchronous.

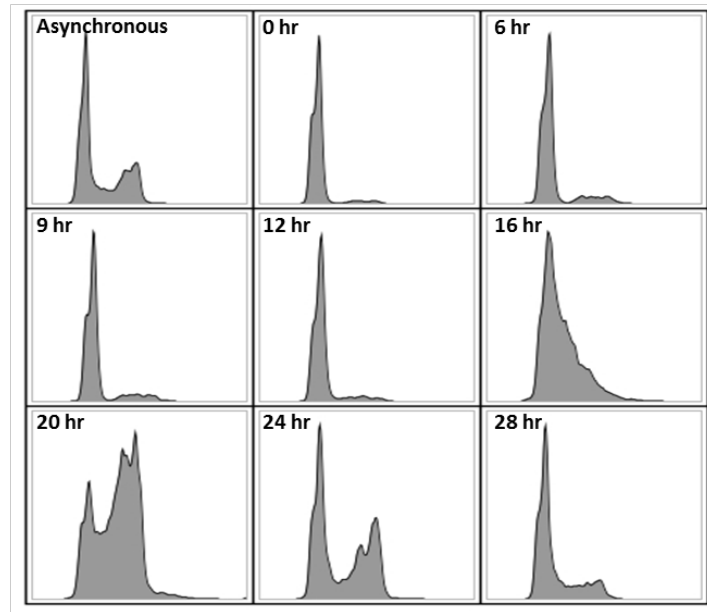
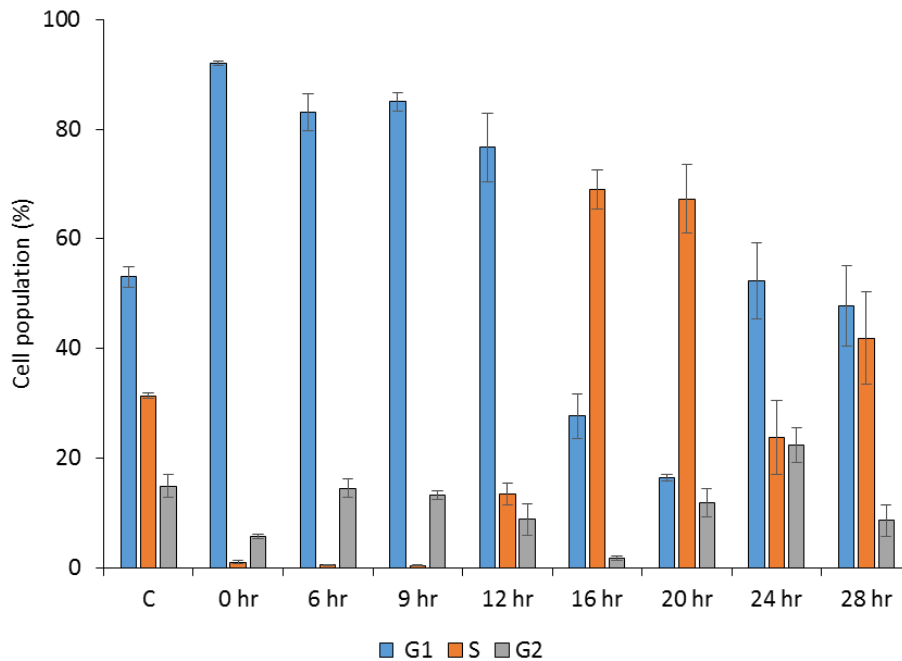
A**B**

Figure 5-1. Synchronisation of MCF10A cells

FACS analysis of MCF10A cells synchronised by growth factor starvation for 24 hours and released by re-stimulation with growth factors for the indicated time. Cells were incubated with EdU (10 μ M) for the final 1.5 hour of treatment and stained with FxCycle violet dye. **(A)** FxCycle signal (Pacific Blue-A) plotted as a histogram to visualise the cell cycle profile. Histograms were representative data from three individual experiments. **(B)** Cell cycle distribution following release from starvation, using EdU to quantify S-phase cells and FxCycle to quantify G1/G2 cell populations. Data point were an average of three individual experiments with standard deviation.

To determine the effect that doxorubicin had on the cell cycle, MCF10A cells were synchronised for 24 hours and treated with doxorubicin during re-stimulation with growth factors. Using FxCycle histograms (Figure 5-2A) and EdU incorporation (Figure 5-2B) cells were again shown to accumulate in G0/G1. However, following doxorubicin treatment, cells remained in G1 for up to 28 hours, and importantly, cells did not appear to be undergoing cell death due to the lack of detached cells.

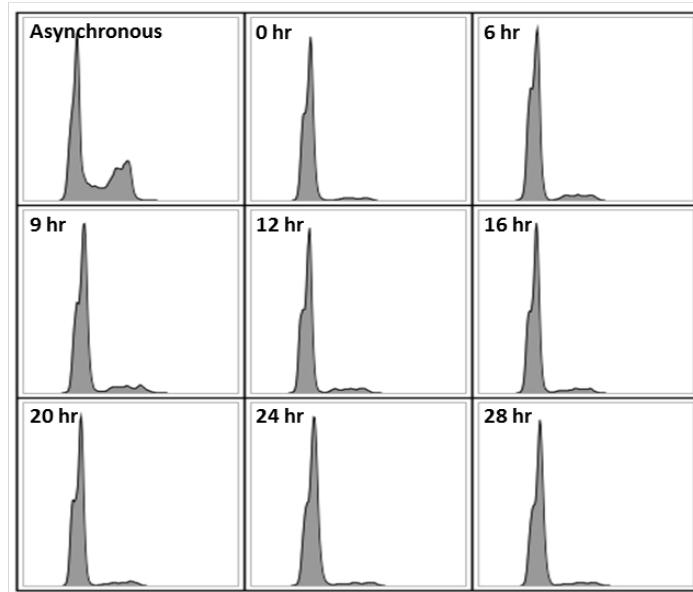
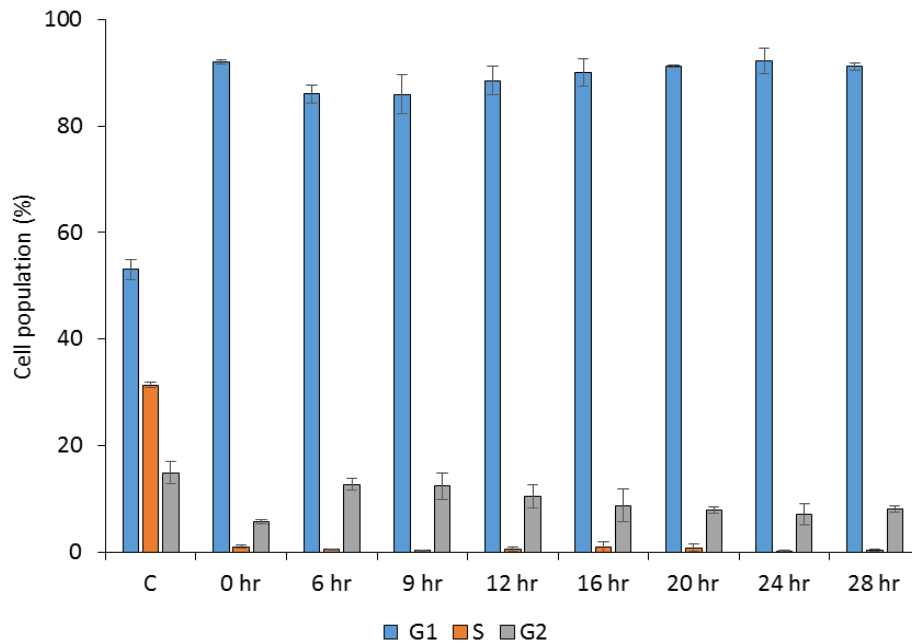
A**B**

Figure 5-2. Doxorubicin inhibited cell cycle progression following release from synchronisation

FACS analysis of MCF10A cells synchronised by starvation for 24 hours and released with fresh growth media, with or without doxorubicin (500 nM) for the indicated time. Cells were incubated with EdU (10 μ M) for the final 1.5 hour of treatment, fixed in 70% ethanol and stained with FxCycle violet dye. **(A)** FxCycle signal (Pacific Blue-A) is plotted as a histogram to visualise the cell cycle profile. Histograms were representative data from three individual experiments. **(B)** Cell cycle distribution following release from starvation, using EdU to quantify S-phase cells and FxCycle to quantify G1/G2 cell populations. Data points were an average of three individual experiments with standard deviation.

The cell cycle is regulated through differential expression of cyclin proteins, which mediate cell cycle progression by regulating cdks. The relative abundance of individual cyclin proteins indicates cell cycle state. As summarised in the introduction, cyclin D is expressed in G1; cyclin E is expressed in G1/S-phase; cyclin A is expressed during S-phase; and cyclin B is expressed during mitosis (Figure 1-11). Protein samples were collected in parallel with FACS samples that were synchronised and released, with or without doxorubicin treatment. To determine if the abundance of cyclin proteins correlated with FACS analysis, cyclin D, cyclin E and cyclin A were analysed by western blot. Due to the poor quality of commercially available cyclin B antibodies, phosphorylation of histone 3 was used as a marker of mitosis (Hans & Dimitrov 2001).

In untreated synchronised and released cells, the expression of cyclin D1 and cyclin E were induced at 6-12 hours (Figure 5-3A), indicating entry into S-phase. Cyclin A expression was observed at 16-24 hours, suggesting that cells were in S-phase and progressing into G2 (Figure 5-3A). Finally, histone 3 phosphorylation was observed at 24 hours, indicating that cells were entering mitosis (Figure 5-3A). In doxorubicin treated synchronised and released cells, the absence of cyclin D1, cyclin A, and histone 3 phosphorylation, as well as the induction of p21 expression, suggested a lack of cell cycle progression (Figure 5-3A). Cyclin E expression was induced at 6 hours but its expression was maintained throughout the time course. Sustained expression of cyclin E suggested that doxorubicin treated cells re-entered the cell cycle, but did not progress into S-phase (Figure 5-3A). In summary, western blot analysis of cyclin protein expression correlated well with EdU incorporation and FxCycle cell cycle analysis.

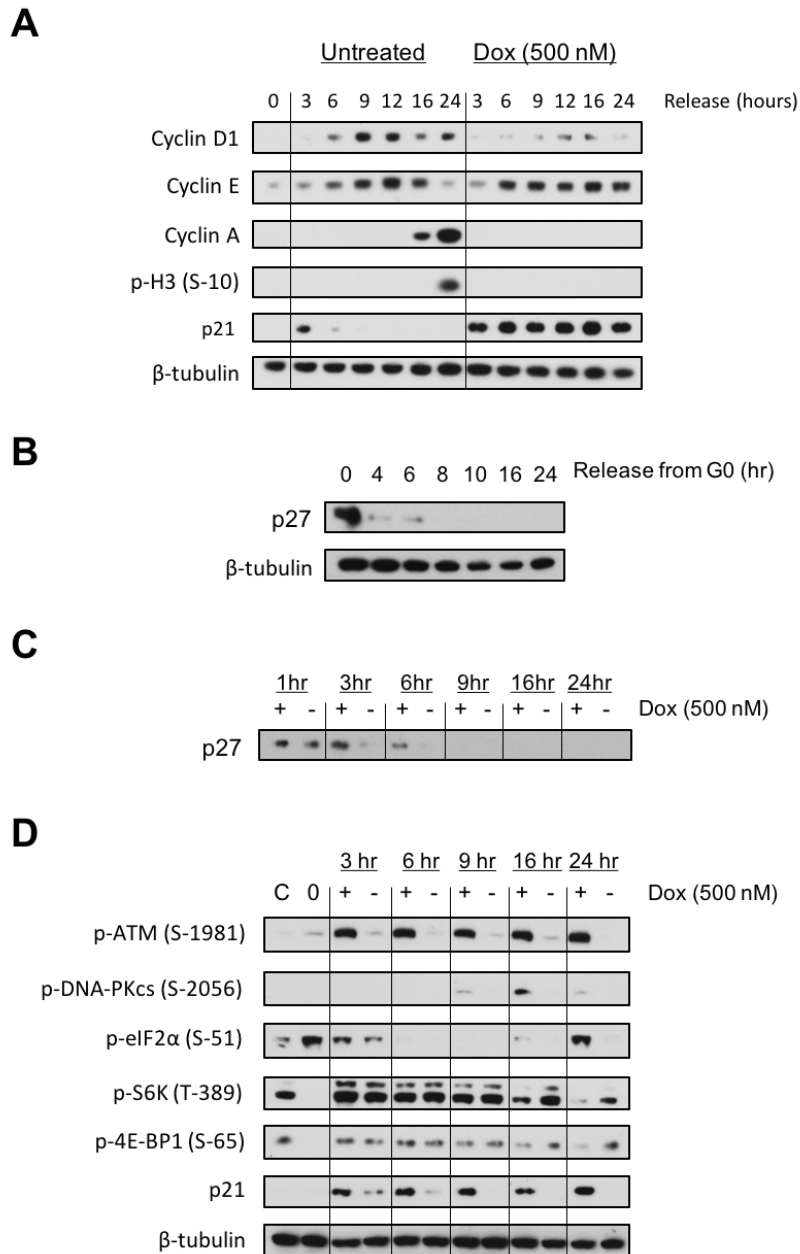


Figure 5-3. eIF2α phosphorylation and mTORC1 inhibition were observed in synchronised cells treated with doxorubicin

Cells were synchronised by starvation for 24 hours and released with fresh growth media, with or without doxorubicin (500 nM) for the indicated time. **(A)** Western blot analysis of cyclins and markers of cell cycle progression. **(B)** Expression of p27 in synchronised and released cells in the absence of doxorubicin. **(C)** Expression of p27 in synchronised and released cells with or without doxorubicin (500 nM) for the indicated time. **(D)** Western blot analysis of mTORC1 activity and eIF2α phosphorylation upon release from synchronisation, untreated or treated with doxorubicin (500 nM) for the indicated time.

Western blot analysis was carried out on synchronised cells, released with or without doxorubicin, to determine if doxorubicin-induced mTORC1 inhibition and eIF2 α phosphorylation were dependent on cell cycle state. p27 is a negative regulator of the cell cycle and its expression is indicative of G0 cell cycle arrest (Pagano et al. 1995; Deng et al. 2004). In untreated cells, p27 expression was enhanced after synchronisation (Figure 5-3B) and diminished at 3 hours after release (Figure 5-3C), indicating that cells had re-entered the cell cycle. However, p27 expression was maintained in doxorubicin treated cells for up to 6 hours (Figure 5-3C), suggesting that DNA damage delayed re-entry into the cell cycle. Importantly, these data suggested that doxorubicin treated cells were re-entering the cell cycle, but were arrested at the G1 checkpoint. Although 90% of cells were arrested at 1-3 hours (Figure 5-2B), doxorubicin activated ATM at 1 hour, indicating that strand breaks were recognised in arrested cells (Figure 5-3D). Furthermore, DNA-PKcs was shown to be activated from 9 hours (Figure 5-3D). eIF2 α phosphorylation was initially elevated at 3 hours after synchronisation release, irrespective of treatment. It was likely that eIF2 α phosphorylation was enhanced during G0 arrest as this correlated with p27 expression (Figure 5-3C). eIF2 α phosphorylation diminished upon cell cycle re-entry (Figure 5-3D) but was induced from 16 hours after treatment with doxorubicin. mTOR signalling was inhibited after synchronisation and activated upon re-stimulation with growth factors (Figure 5-3D). mTORC1 signalling also appeared to be inhibited in response to doxorubicin at 16 hours, shown by a reduction in p70 S6K and 4E-BP1 phosphorylation (Figure 5-3D).

These data suggested that doxorubicin-induced mTORC1 inhibition, and eIF2 α phosphorylation, were independent of cell cycle state or arrest, indicating they may be direct consequences of DDR signalling.

5.2.2 The role of DNA damage signalling pathways in doxorubicin-induced mTOR inhibition was unclear

As the delay between DNA damage and protein synthesis inhibition did not appear to be dependent on cell cycle progression or arrest, the role of DDR kinases were examined further. In response to DNA damage, ATM, DNA-PKcs and ATR regulate DNA damage site recognition, growth arrest, and initiate repair (Polo & Jackson 2011; Marechal & Zou 2013; Shiloh & Ziv 2013). Both ATM and DNA-PKcs were shown to be activated after treatment with doxorubicin (Figure 4-2). Importantly, protein synthesis inhibition was shown to correlate with DNA-PKcs activation (Figure 4-2), indicating that protein synthesis inhibition could be a direct consequence of the DDR.

Small molecule ATP competitive inhibitors were used to determine the relative contribution of each pathway in response to doxorubicin-induced DNA damage.

KU55933 is a potent ATP-competitive inhibitor of ATM, shown to relieve activation and downstream signalling in response to IR (Hickson et al. 2004). Cells were treated with KU55933 for 1 hour prior to treatment with doxorubicin, and the activation of the DDR and eIF2 α phosphorylation was analysed by western blot. ATM activation and Chk2 phosphorylation were absent at 3 hours following treatment with doxorubicin and KU55933 (Figure 5-4A), suggesting KU55933 inhibited the activation of ATM after treatment with doxorubicin. In order to study eIF2 α phosphorylation, longer incubations were required. Unfortunately, longer incubations with doxorubicin and KU55933 induced cell death and PARP cleavage. In addition, longer incubations with KU55933 induced eIF2 α phosphorylation in the absence of doxorubicin, suggesting the inhibitor may be toxic to the cell (Figure 5-4A).

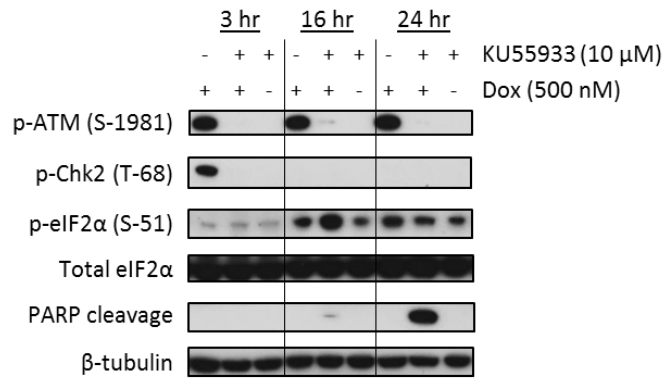
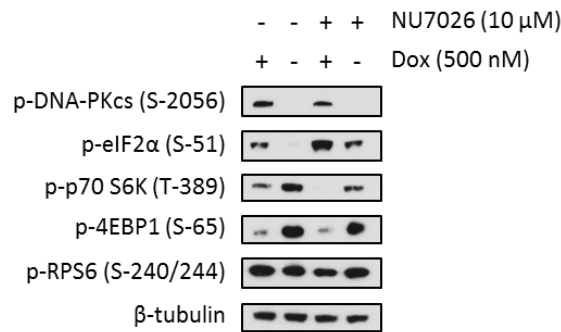
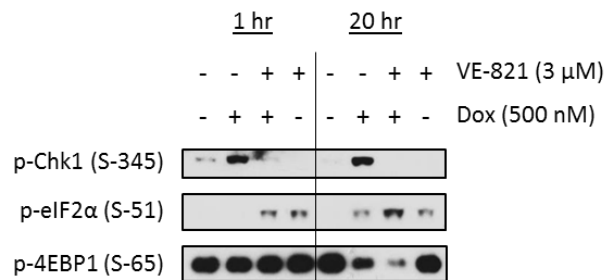
A**B****C**

Figure 5-4. DNA damage signalling inhibitors did not alleviate mTOR inhibition or eIF2 α phosphorylation

Representative western blot analysis of mTORC1 inhibition and eIF2 α phosphorylation in response to doxorubicin treatment and DDR kinase inhibition. **(A)** ATM inhibitor, KU55933. Cells were pre-treated with KU55933 for 1 hour prior to doxorubicin treatment for the indicated time. **(B)** DNA-PKcs inhibitor, NU7026. Cells were treated with doxorubicin for 6 hours prior to the addition of NU7026 for a further 5 hours. **(C)** ATR Inhibitor, VE821. Cells were pre-treated with VE821 for 1 hour prior to doxorubicin treatment for the indicated time.

NU7026 is an ATP-competitive inhibitor of DNA-PKcs, shown to inhibit dsDNA break repair in response to IR (Veuger et al. 2003). Due to suspected toxicity with longer NU7026 incubations (data not shown), cells were treated with doxorubicin for 6 hours prior to incubation with NU7026 for a further 5 hours. These timings were chosen because DNA-PKcs was activated in response to doxorubicin at 9 hours (Figure 4-2). DNA-PKcs activation, mTORC1 inhibition and eIF2 α phosphorylation were analysed by western blot. NU7026 minimally reduced DNA-PKcs auto-phosphorylation in response to doxorubicin. However, NU7026 enhanced doxorubicin-induced eIF2 α phosphorylation and inhibition of mTORC1 signalling (Figure 5-4B). Unfortunately, cells incubated with NU7026 alone for 5 hours also showed elevated levels of eIF2 α phosphorylation and reduced mTORC1 signalling (Figure 5-4B). mTOR and DNA-PKcs are both members of the PI3K family, so it was possible that NU7026 may also inhibit mTOR. In MCF10A cells, it was determined that a concentration of 10 μ M NU7026 was required to inhibit DNA-PKcs activation (data not shown). However, the IC₅₀ of NU7026 toward mTOR was 6.4 μ M (Leahy et al. 2004), indicating that the concentrations of NU7026 required for DNA-PKcs inhibition also inhibit mTOR. Therefore, NU7026 was not a specific enough inhibitor to use in this manner.

VE-821 is a selective ATP-competitive inhibitor of ATR, shown to relieve downstream ATR signalling in response to DNA damage stimuli (Reaper et al. 2011). Cells were treated with VE-821 for 1 hour prior to treatment with doxorubicin. ATR activity, mTORC1 activity and eIF2 α phosphorylation were analysed by western blot. ATR was activated by doxorubicin, as demonstrated by the phosphorylation of a downstream kinase, Chk1. However, Chk1 activation was inhibited after pre-treatment with VE-821 (Figure 5-4C). After treatment with doxorubicin for 20 hours, VE-821 enhanced mTORC1 inhibition and eIF2 α phosphorylation. Unfortunately, eIF2 α phosphorylation was also elevated in cells incubated with only VE-821, suggesting that VE-821 may also be toxic to the cell. It should be noted that this was preliminary datum and the role of ATR in doxorubicin-induced toxicity will be addressed in the future.

It was not practical to study signalling pathways that respond to cell stress with inhibitors that induce underlying levels of cell stress, as this could generate unreliable data. To overcome this problem, ATM and DNA-PKcs were depleted using siRNA, in an effort to uncover more detail about the role of DNA damage kinases.

It has been shown that ATM enhances the accuracy of DNA repair but is dispensable for the repair process (Caron et al. 2015). ATM depleted cells were treated with doxorubicin and analysed by western blot, to identify if ATM signalling was required for mTOR inhibition or eIF2 α phosphorylation. The knockdown of ATM was efficient and reduced downstream ATM signalling, as demonstrated by diminished Chk2 phosphorylation at 3 hours (Figure 5-5A). Depletion of ATM did not affect the level of mTORC1 inhibition or eIF2 α phosphorylation, when compared to a scrambled control siRNA, suggesting that ATM signalling was not required for doxorubicin-induced mTORC1 inhibition.

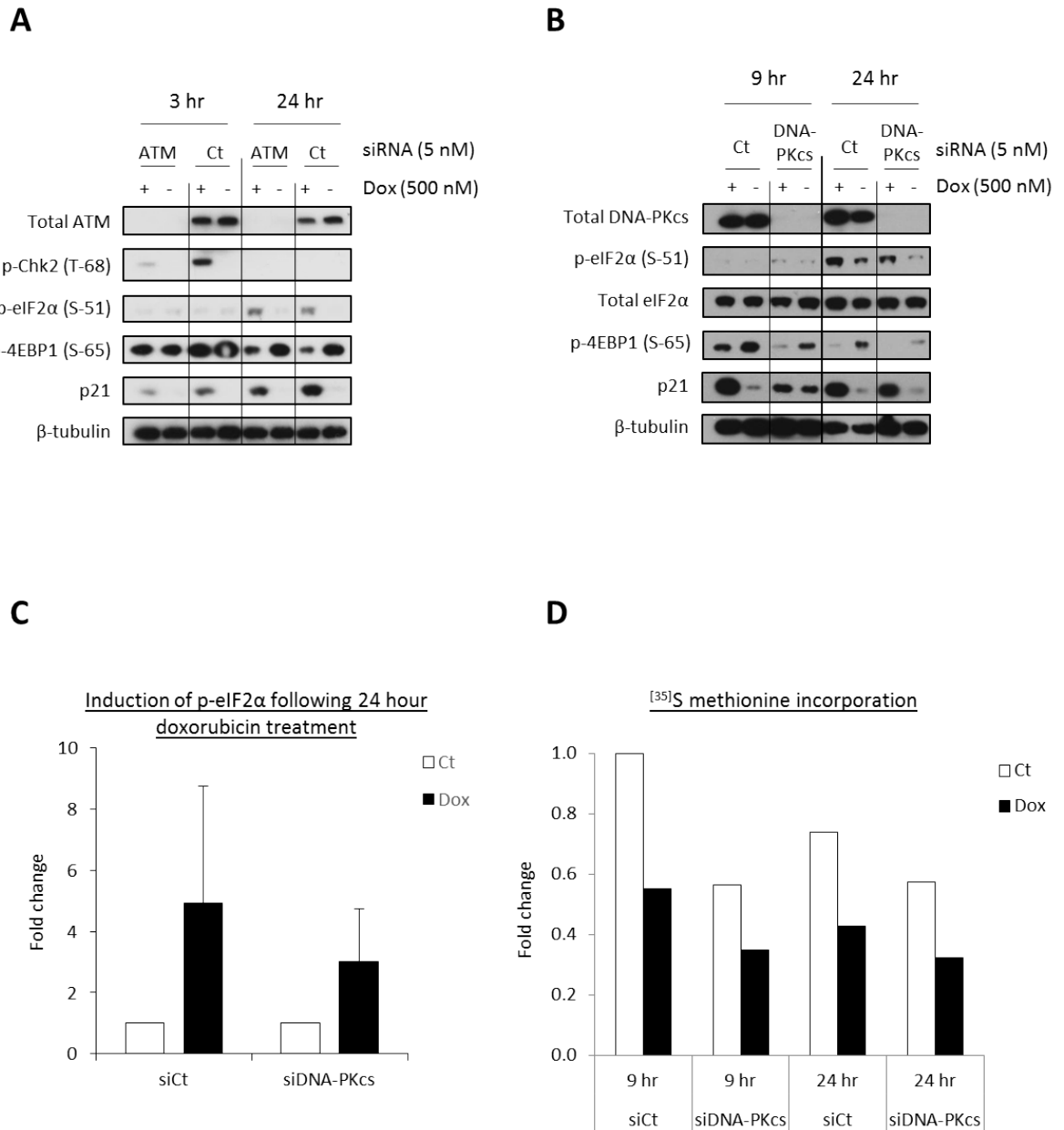


Figure 5-5. Analysis of doxorubicin-induced mTOR inhibition and eIF2α phosphorylation following depletion of ATM and DNA-PKcs

(A) ATM siRNA was transfected into MCF10A cells for 48 hours. **(B)** DNA-PKcs siRNA was transfected into MCF10A cells by two back-to-back 72 hour transfections. Cells were treated with doxorubicin (500 nM) for the indicated time and mTORC1 activity and eIF2α phosphorylation was analysed by western blot. **(C)** Quantification of eIF2α phosphorylation from (B). Data was an average of three independent experiments, shown with standard deviation. **(D)** ³⁵S methionine incorporation following DNA-PKcs knockdown and doxorubicin treatment. Counts per minute were normalised to total protein by Bradford assay. Data points were an average of two individual experiments.

DNA-PKcs has been shown to be crucial for DNA repair (Caron et al. 2015) as a central component of the NHEJ machinery (Kurimasa et al. 1999). DNA-PKcs was also depleted using siRNA, to determine the importance of DNA-PKcs in the regulation of doxorubicin-induced mTORC1 inhibition and eIF2 α phosphorylation. DNA-PKcs is an extremely stable protein with a half-life in excess of 5 days (Ajmani et al. 1995). To fully deplete DNA-PKcs, two consecutive 72-hour siRNA knockdowns were carried out prior to treatment with doxorubicin. Knockdown of DNA-PKcs was effective and reduced eIF2 α phosphorylation following a 24-hour doxorubicin treatment (Figure 5-5B AND C). However, 4E-BP1 phosphorylation was also reduced in untreated DNA-PKcs depleted cells (Figure 5-5B), and depletion of DNA-PKcs appeared to reduce the growth rate of cells (data not shown). [³⁵S] methionine incorporation was used to quantify global protein synthesis in DNA-PKcs depleted cells. Unfortunately, after knockdown of DNA-PKcs, global protein synthesis was reduced by 40% when compared to a scrambled control siRNA (Figure 5-5D). In addition to being a key factor in NHEJ, DNA-PKcs has also been identified an important regulator of telomere maintenance (Bailey et al. 1999), and DNA-PKcs deficiency has previously been shown to lead to stalling and collapsing replication forks (Shimura et al. 2007). It was likely that depletion of DNA-PKcs was having undesired off-target effects, leading to cell cycle arrest and metabolic shutdown. For this reason, data indicating a reduction of eIF2 α phosphorylation after doxorubicin treatment in DNA-PKcs depleted cells are difficult to interpret. Therefore, the depletion of DNA-PKcs was not an option to study this mechanism further. A more specific DNA-PKcs inhibitor has been identified (Leahy et al. 2004), and will be used in the future to further elucidate the role of DNA-PKcs.

5.2.3 Doxorubicin-induced mTORC1 inhibition was mediated by p53

As p53 is a key mediator of the DNA damage response, an MCF10A cell line with a p53 deletion ($p53^{-/-}$) was used to determine the role of p53 after doxorubicin-induced DNA damage. Initially $p53^{-/-}$ cells were treated with doxorubicin in parallel to MCF10A $p53^{+/+}$ ($p53^{+/+}$) cells, and mTORC1 signalling and eIF2 α phosphorylation was analysed by western blot. As expected, $p53^{-/-}$ cells did not express p53 and showed no induction of p21 expression upon treatment with doxorubicin. However, DNA damage was still recognised, as indicated by ATM activation (Figure 5-6A). Interestingly, in $p53^{+/+}$ cells, doxorubicin inhibited mTORC1 activation and induced of eIF2 α phosphorylation, but these responses were not present in $p53^{-/-}$ cells (Figure 5-6A). Although eIF2 α phosphorylation was generally enhanced in untreated $p53^{-/-}$ cells, eIF2 α phosphorylation was not induced further upon treatment with doxorubicin (Figure 5-6B). Additionally, 4E-BP1 phosphorylation was diminished after treatment with doxorubicin in $p53^{+/+}$ cells, whereas $p53^{-/-}$ cells had elevated levels of 4E-BP1 phosphorylation that were enhanced upon treatment with doxorubicin (Figure 5-6C). Elevated levels of eIF2 α phosphorylation indicated that $p53^{-/-}$ cells may be experiencing underlying stress, potentially as a consequence of the p53 deletion. In $p53^{+/+}$ cells, protein synthesis was regulated by an inhibition in translation initiation that was likely to be the consequence of mTORC1 inhibition. However, in $p53^{-/-}$ cells, mTORC1 signalling was not inhibited and eIF2 α was not further phosphorylated, indicating that protein synthesis may not have been affected. ^[35]S methionine incorporation was used to quantify protein synthesis in response to doxorubicin in both cell lines. In untreated samples, global protein synthesis was enhanced in $p53^{-/-}$ cells by around 20% when compared to $p53^{+/+}$ cells (Figure 5-6D). After treatment with doxorubicin, protein synthesis was still inhibited in $p53^{-/-}$ cells, although this was not to the same extent as observed in $p53^{+/+}$ cells (Figure 5-6B). These data suggested that protein synthesis may be inhibited through some other form of regulation, such as at translation elongation.

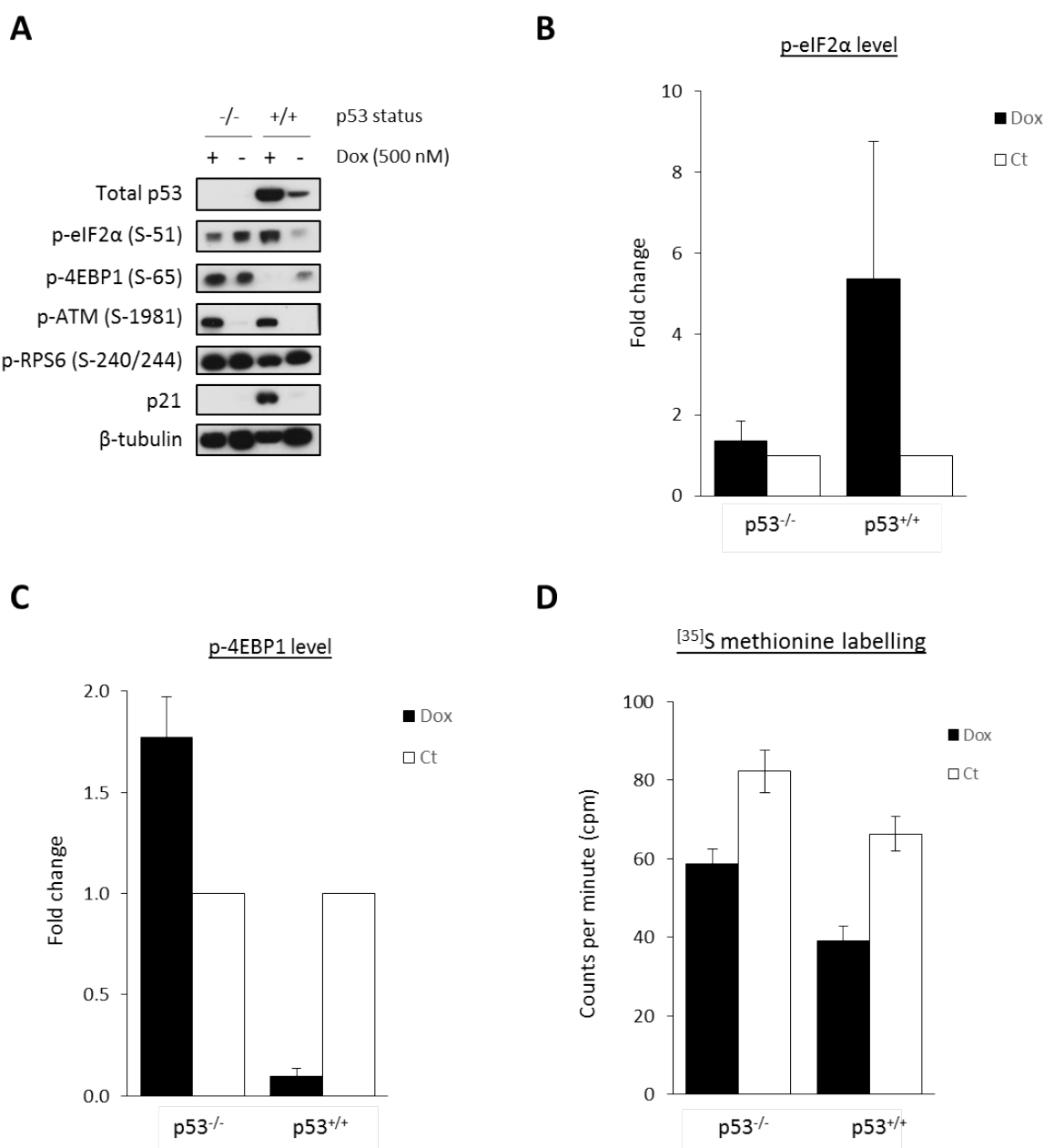


Figure 5-6. Doxorubicin did not inhibit mTORC1 signalling or induce eIF2α phosphorylation in MCF10A p53^{-/-} cells

Comparison between MCF10A p53^{-/-} and p53^{+/+} cells after a 24-hour doxorubicin (500 nM) treatment. **(A)** Western blot analysis of DDR, mTORC1 signalling and eIF2α phosphorylation. Blots were representative of three individual experiments. **(B)** and **(C)** Quantification of p-eIF2α induction (B) and 4E-BP1 phosphorylation (C) from western blots shown in (A). Values shown as a fold change relative to the untreated sample, for each cell line, with standard deviation. **(D)** [³⁵S] methionine incorporation carried out in parallel to samples in (A). Counts per minute were normalised to total protein by Bradford assay. Data presented was an average of three individual experiments with standard deviation.

5.2.4 p53^{-/-} cells were less sensitive to doxorubicin-induced inhibition of translation initiation

To determine if p53^{-/-} cells also regulated protein synthesis at the level of translation initiation, sucrose density centrifugation was used to analyse ribosome distribution in response to doxorubicin. p53^{-/-} cells showed a similar ribosome profile to p53^{+/+} cells at 6 hours (Figure 5-7). Interestingly in p53^{-/-} cells, treatment with doxorubicin for 24 hours also resulted in a loss of polysomes, although this was not to the same degree as observed in p53^{+/+} cells. Additionally, ribosomes lost from the polysomes did not accumulate within the subpolysomes (Figure 5-7B), mirroring the response in p53^{+/+} cells. These data indicated that translation initiation was inhibited in p53^{-/-} cells, but not the same extent as p53^{+/+} cells, and correlated well with protein synthesis rates. Halfmers were observed in p53^{-/-} cells and these were accentuated upon doxorubicin treatment. Halfmers are polyribosomes with an additional 40S subunit attached to mRNA and are indicative of defects in subunit joining and ribosome biogenesis (Helser et al. 1981; Adams et al. 2002). Interestingly, perturbation of ribosome biogenesis, such as during nucleolar stress, has been shown to activate p53. Ribosomal proteins such as RPL5, RPL11 and RPL23, enter the nucleoplasm to bind and inhibit MDM2, subsequently leading to the stabilisation and activation p53, and p53 dependent cell cycle arrest (Zhang & Lu 2009). It is possible that these mechanisms are absent from p53^{-/-} cells, leading to defective ribosome biogenesis. Furthermore, doxorubicin has been shown to inhibit ribosome biogenesis (Burger et al. 2010). It is possible that the loss of subpolysomes in MCF10A cells after treatment doxorubicin for 24 hours (Figure 5-7) was due to the inhibition of ribosome biogenesis, and could also contribute to the activation of p53.

A direct comparison between untreated p53^{-/-} and p53^{+/+} cells showed that p53^{-/-} cells had fewer subpolysomes, and hence fewer free ribosomes (Figure 5-7C). Interestingly, the level of polysomes were comparable, indicating that under non-stressed conditions, p53^{-/-} cells translated as efficiently as p53^{+/+} cells (Figure 5-7C). When comparing traces from doxorubicin treated p53^{+/+} and p53^{-/-} cells, it became apparent that the reduction of polysomes in p53^{-/-} cells was not as substantial as in p53^{+/+} cells (Figure 5-7D). These data suggested that

translation initiation was not as robustly inhibited in p53^{-/-} cells, supporting western blot and [³⁵S] incorporation data.

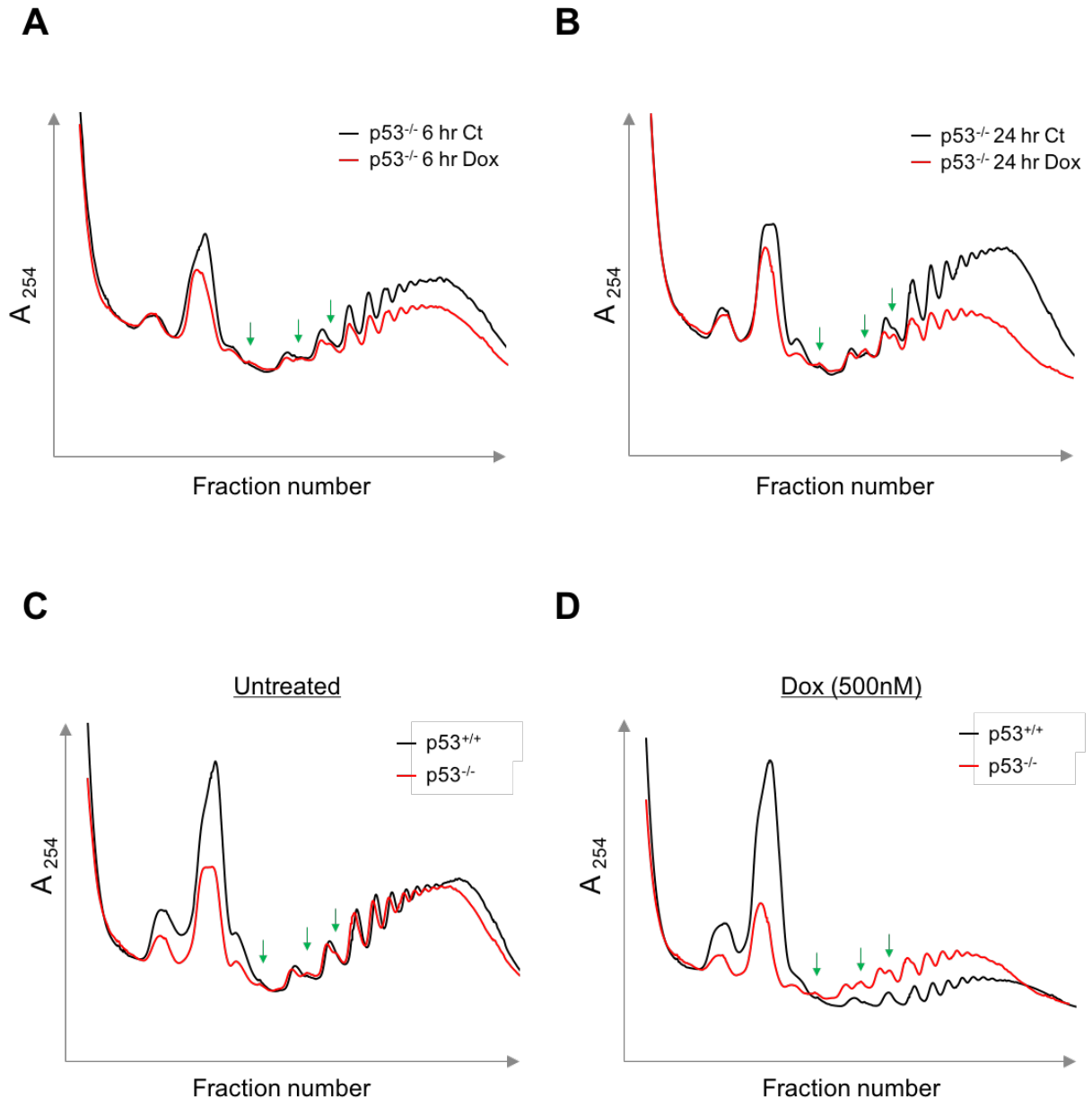


Figure 5-7. Doxorubicin inhibited translation initiation in p53^{-/-} cells less robustly than in p53^{+/+} cells

Representative polysome profiles from MCF10A p53^{-/-} cells, treated continuously with 500 nM doxorubicin for **(A)** 6 hours and **(B)** 24 hours. Traces were obtained by measuring absorbance at 254 nM after centrifuging cytoplasmic lysates at 38000 rpm through 10-50% sucrose gradients at 4°C for 2 hours, with a flow rate of 1 ml/min. Ct = untreated control sample. **(C)** Comparison of polysome profiles from untreated MCF10A p53^{+/+} and p53^{-/-} **(D)** Comparison of polysome profiles from doxorubicin (500 nM, 24 hours) treated MCF10A p53^{+/+} and p53^{-/-} cells. Halfmer polysomes are marked by green arrows.

5.2.5 Doxorubicin-induced eIF2 α phosphorylation was dependent on p53 mediated mTORC1 inhibition

p53 has been shown to inhibit mTORC1 activity through the activation of AMPK and regulation of TSC2 (Feng et al. 2005). However, TSC2 knockdown failed to rescue doxorubicin-induced protein synthesis inhibition, mTORC1 inhibition, and eIF2 α phosphorylation (Figure 4-3). While the work within this thesis was in progress, the p53 dependent expression of sestrin 2 was shown to negatively regulate mTORC1 signalling in response to a range of DNA damage agents (Cam et al. 2014). Interestingly, sestrin 2 expression was not induced in p53^{-/-} cells after treatment with doxorubicin (Figure 5-8), suggesting that p53 may inhibit mTORC1 signalling indirectly, through the upregulation of its transcriptional targets.

Prolonged mTORC1 inhibition was also shown to enhance eIF2 α phosphorylation in p53^{+/+} cells, via crosstalk signalling (Figure 4-5). To determine if p53 played a role in mTOR-eIF2K signalling, p53^{+/+} and p53^{-/-} cells were treated with AZD8055, rapamycin, and doxorubicin.

Treatment of p53^{+/+} cells with doxorubicin resulted in mTORC1 inhibition and enhanced eIF2 α phosphorylation. Additionally, AZD8055 and rapamycin both induced eIF2 α phosphorylation in p53^{+/+} cells (Figure 5-8). Importantly, in p53^{-/-} cells, AZD8055 and rapamycin also induced mTORC1 inhibition and eIF2 α phosphorylation, however, doxorubicin did not inhibit mTORC1 or enhance eIF2 α phosphorylation (Figure 5-8). p53^{-/-} cells also displayed enhanced mTORC1 activity, as demonstrated by the increased phosphorylation of 4E-BP1 and p70 S6K, suggesting that p53 was negatively regulating mTOR signalling (Figure 5-8). These data also suggested that crosstalk signalling from mTORC1 inhibition to eIF2 α , was likely to be mediated by downstream signalling from mTORC1, because catalytic inhibition of mTORC1 still enhanced eIF2 α phosphorylation in p53^{-/-} cells. The absence of mTORC1 inhibition in p53^{-/-} cells treated with doxorubicin suggested that p53 may mediate DDR induced mTORC1 inhibition. Taken together, these data strongly suggested that mTORC1 inhibition was required for eIF2 α phosphorylation in response to DNA damage, and mTORC1 inhibition was mediated by p53.

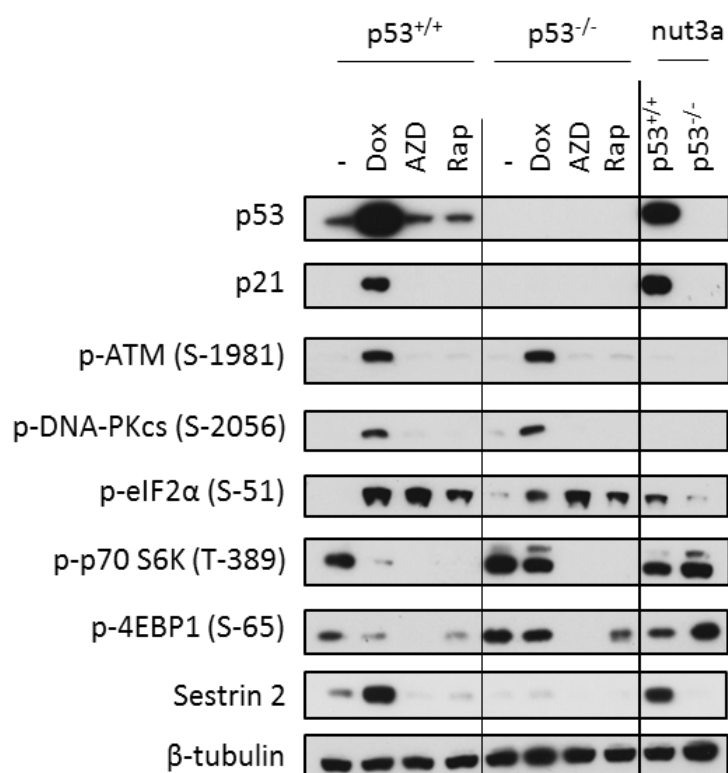


Figure 5-8. p53 mediated mTORC1 inhibition and eIF2α phosphorylation in response to doxorubicin

Western blot analysis of mTORC1 signalling and eIF2α phosphorylation in MCF10A p53^{+/+} and p53^{-/-} after treatment with doxorubicin (500 nM), AZD8055 (100 nM), rapamycin (100 nM) and Nutlin-3a (Nut) (10 μM) for 16 hours. Blots were representative of two independent experiments.

The DDR is complex and requires input from many signalling pathways. To determine that mTORC1 inhibition and subsequent eIF2 α phosphorylation was dependent on p53 activation, nutlin-3a was used to activate p53 in the absence of DNA damage. Nutlin-3a selectively inhibits the interaction between p53 and MDM2, leading to p53 stabilisation (Vassilev et al. 2004). Upon treatment of p53^{+/+} cells with nutlin-3a, p53 was stabilised and p21 expression was induced (Figure 5-8). Treatment with nutlin-3a moderately diminished p70 S6K phosphorylation and increased eIF2 α phosphorylation (Figure 5-8). Unsurprisingly, nutlin-3a did not induce p21 expression, mTORC1 inhibition, or eIF2 α phosphorylation in p53^{-/-} cells. These data suggested that mTORC1 inhibition was mediated by p53 stabilisation, and this was crucial for the induction of eIF2 α phosphorylation. Furthermore, these findings support the notion that one function of p53 is the regulation of mTORC1 signalling.

5.2.6 Knockdown of endogenous p53 recapitulated the response in p53^{-/-} cells

MCF10A p53^{-/-} cells would have been subject to a rigorous selection process during their creation. It is possible that some of the effects being attributed to p53 knockout are in fact artefacts of the cell selection process. p53 was depleted using siRNA knockdown in p53^{+/+} cells, in an attempt to recapitulate the effect observed in p53^{-/-} cells. The depletion of p53 became problematic when subsequently treating cells with a DNA damage agent, due to the induction of p53 expression. To overcome this problem, p53^{+/+} cells were subjected to two back-to-back 24-hour transfections. After treatment with doxorubicin, ATM was shown to be activated, indicating that DNA damage was being recognised, however, p53 was efficiently depleted and the induction of sestrin 2 was diminished (Figure 5-9). Importantly, depletion of p53 relieved doxorubicin-induced mTORC1 inhibition and diminished eIF2 α phosphorylation, when compared to the control non-targeting siRNA (Figure 5-9), suggesting that sestrin 2 may mediate the inhibition of mTORC1 activity. eIF2 α phosphorylation was also induced in untreated p53 depleted cells, indicating that knockdown of p53 was recapitulating the response observed in the p53^{-/-} cell line (Figure 5-9). These data suggested that p53 may be a mediator of mTORC1 inhibition in response to doxorubicin-induced DNA damage.

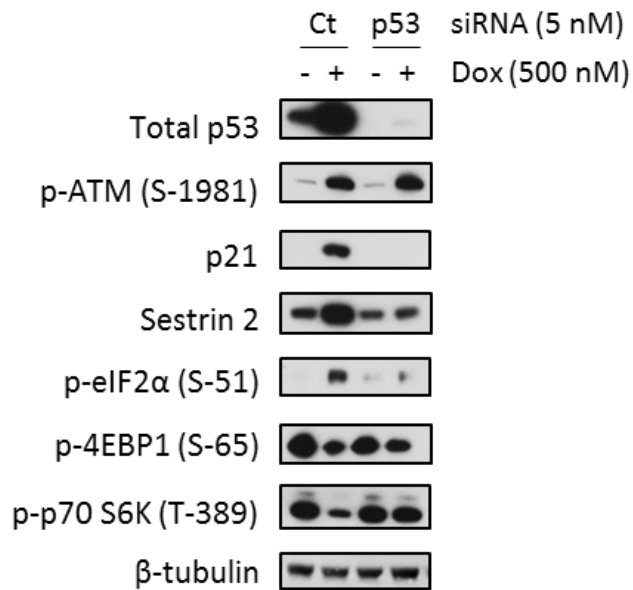


Figure 5-9. siRNA depletion of p53 recapitulated the response observed in p53^{-/-} cells

siRNA specific to p53 (5 nM) were transfected into MCF10A p53^{+/+} cells using RNAiMax lipofectamine reagent by two consecutive 24-hour transfections. Cells were treated with doxorubicin (500 nM) for 14 hours and mTORC1 activity and eIF2α phosphorylation analysed by western blot.

5.2.7 p53 was required for doxorubicin-induced G1 arrest

p53 has been shown to regulate cell cycle arrest in G1 (Waldman et al. 1995; Hyun & Jang 2015) and G2 (Agarwal et al. 1995; Levesque et al. 2005), and in MCF10A cells, doxorubicin was previously shown to induce cell cycle arrest at both checkpoints (Figure 3-2B). To determine if cell cycle arrest was dependent on p53, FACS analysis was carried out on p53^{-/-} cells using FxCycle violet stain to quantify G1/G2 cells, and EdU incorporation to quantify S-phase cells. A direct comparison of cell cycle profiles from p53^{+/+} and p53^{-/-} cells indicated that the cell cycle of untreated cells were similar. After treatment with doxorubicin, p53^{+/+} cells arrested in G1 and G2 within 9 hours (Figure 5-10A and B). Conversely, p53^{-/-} cells bypassed G1 arrest after treatment with doxorubicin and arrested in G2 (Figure 5-10A and B). Furthermore, the impaired G1 checkpoint in p53^{-/-} cells resulted in the detection of S-phase cells throughout the time course (Figure 5-10B). These data strongly suggested that p53 was required for doxorubicin-induced G1 arrest, but arrest in G2 appeared to be p53 independent.

As p53 mediated cell cycle arrest following treatment with doxorubicin, it was reasonable to suggest that p53 may also play a role in protection from cell death. To address this question, Annexin-FITC and Draq7 staining was used to quantify cell death after a 24-hour doxorubicin treatment. 500 nM doxorubicin was previously shown to induce minimal cell death in p53^{+/+} cells when compared to untreated cells (Figure 3-2A). However, cell death observed in doxorubicin treated p53^{-/-} cells was more than double that observed in untreated cells (Figure 5-11), indicating that p53 may protect cells from doxorubicin-induced cell death.

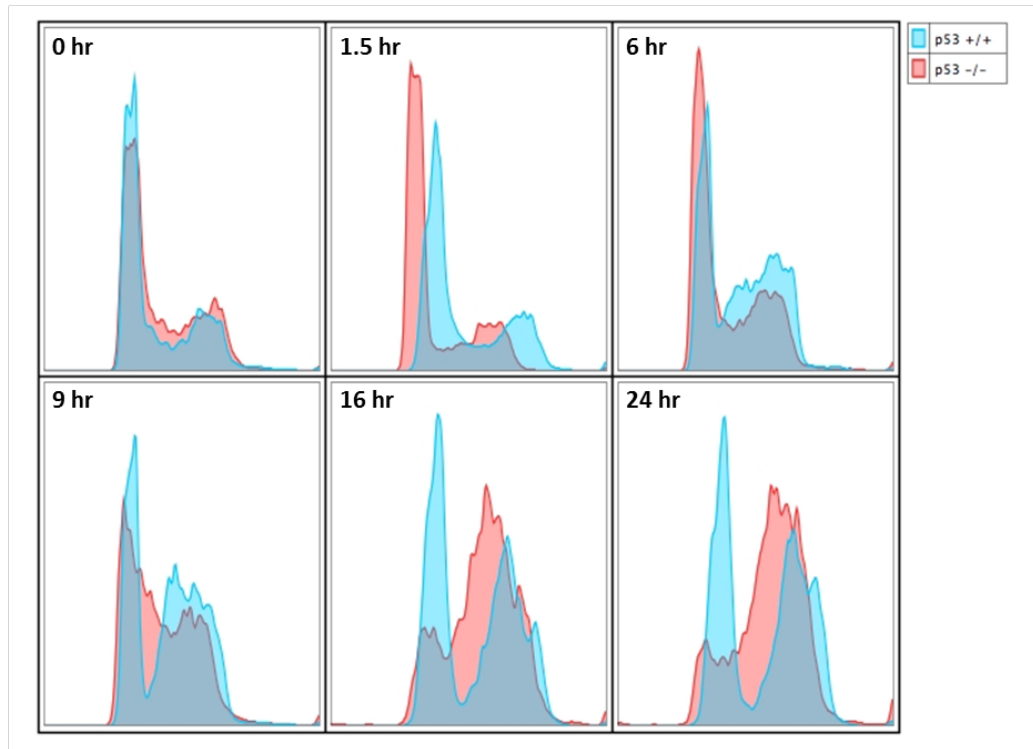
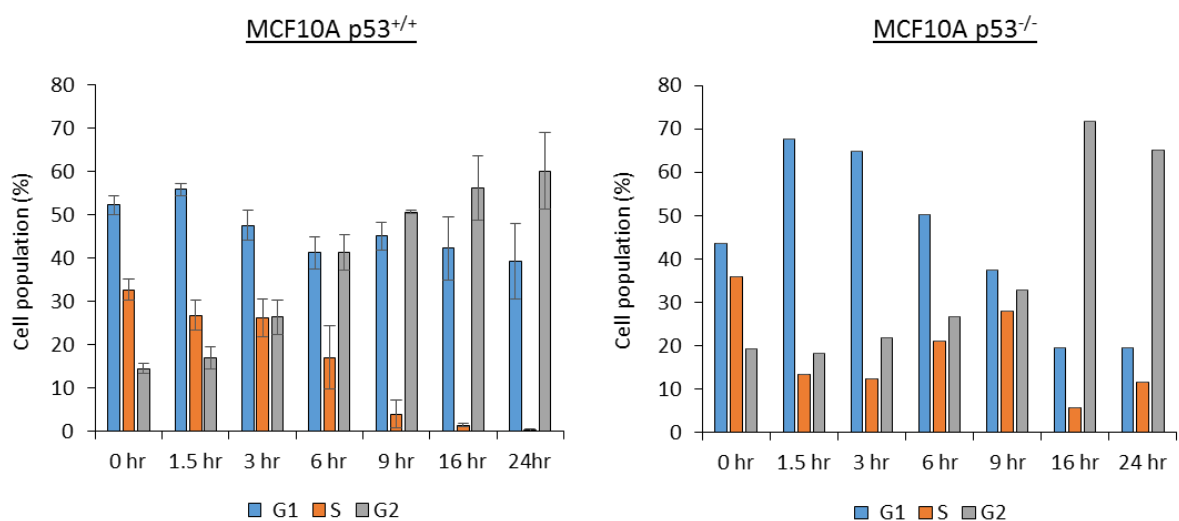
A**B**

Figure 5-10. p53 mediated doxorubicin-induced G1 cell cycle arrest

FACS analysis of MCF10A p53^{+/+} and p53^{-/-} cells treated continuously with doxorubicin (500 nM) for the indicated time. **(A)** Cell cycle analysis by staining with FxCycle violet dye. FxCycle signal (Pacific Blue-A) plotted as a histogram to visualise the cell cycle profile. **(B)** Quantification of cell cycle distribution using FxCycle and EdU incorporation (10 μ M, 1.5 hr). p53^{-/-} data was representative of one experiment.

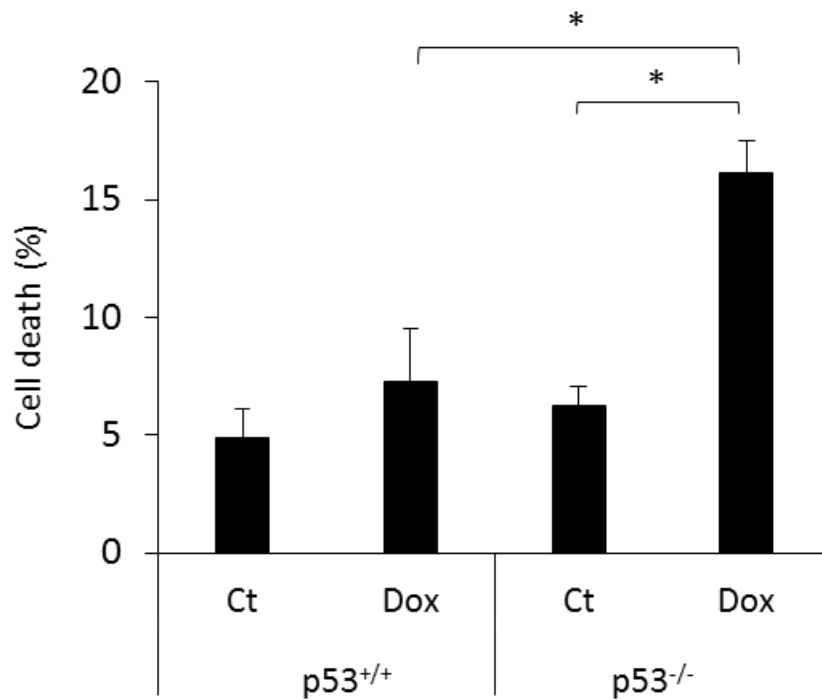


Figure 5-11. p53^{-/-} cells were more sensitive to doxorubicin-induced cell death

Quantification of cell death in MCF10A p53^{-/-} and p53^{+/+} cells by Annexin-FITC and Draq-7 staining following a continuous 24-hour doxorubicin (500 nM) treatment. An average of two individual experiments, with standard deviation. Statistical significance was calculated using a two-tailed student's *t* test, assuming unequal variances (* = *P* value <0.05).

5.3 Discussion

The aim of this chapter was to determine the role of cell cycle progression and DDR signalling, in doxorubicin-induced mTORC1 inhibition and eIF2 α phosphorylation.

In *Saccharomyces cerevisiae*, it has been suggested that DNA damage is only fully recognised during DNA synthesis (Palou et al. 2010). If this response was conserved in MCF10A cells, delayed mTORC1 inhibition and eIF2 α phosphorylation could have been dependent on progression to S-phase. Subsequently, inhibition of protein synthesis could be a direct consequence of cell cycle arrest. By synchronising cells in G0 prior to treatment with doxorubicin, cells were shown to immediately arrest in G1. Importantly, mTORC1 signalling was still shown to be inhibited in response to doxorubicin at 16 hours. Furthermore, eIF2 α phosphorylation was shown to be enhanced at 16 hours, and DNA-PKcs was shown to be activated at 9 hours. These data strongly indicated that doxorubicin-induced mTORC1 inhibition and eIF2 α phosphorylation, were not a consequence of cell cycle progression or arrest, suggesting that they may be regulated directly in response to DDR signalling.

To investigate the role of the DDR kinases in doxorubicin-induced protein synthesis inhibition, small molecule ATP competitive inhibitors of ATM, DNA-PKcs, and ATR were used. Unfortunately, all three inhibitors appeared to induce underlying levels of cellular stress. It was most likely that these inhibitors were not specific enough to be incubated with cells for the long periods required to observe robust eIF2 α phosphorylation, so it was not practical to use them further. Depletion of ATM suggested that signalling through this pathway was not required for doxorubicin-induced mTORC1 inhibition or eIF2 α phosphorylation. Although depletion of DNA-PKcs also diminished doxorubicin-induced eIF2 α phosphorylation, knockdown of DNA-PKcs also resulted in substantial off-target effects, including the inhibition of protein synthesis. Subsequently, it was not possible to deduce many conclusions from these experiments. Off-target effects of DNA-PKcs depletion were potentially due to disturbing the role of DNA-PKcs in telomere maintenance, leading to stalling replication forks and cell cycle arrest (Bailey et al. 1999; Shimura et al. 2007). Although the DDR mediated inhibition of mTORC1 signalling was unlikely to be

mediated by ATM, further analysis will be required to fully determine the roles of DNA-PKcs and ATR.

The role of p53 was investigated using an MCF10A cell line with a deletion of p53. In p53^{+/+} cells, doxorubicin treatment induced mTORC1 inhibition and eIF2 α phosphorylation, however both of these responses were absent in the p53^{-/-} cell line. Additionally, translation initiation and protein synthesis were not inhibited as robustly in the p53^{-/-} cell line, and the basal level of eIF2 α phosphorylation was also enhanced in p53^{-/-} cells, suggesting an underlying level of cellular stress. Although doxorubicin did not further induce the phosphorylation of eIF2 α in the p53^{-/-} cell line, catalytic inhibition of mTORC1 induced eIF2 α phosphorylation. These data suggested that p53 was required for doxorubicin-induced mTORC1 inhibition, but not for subsequent crosstalk signalling to eIF2. Furthermore, mTORC1 activity was greatly enhanced in p53^{-/-} cells, supporting the notion that p53 may function as a negative regulator of mTORC1 activity.

Depletion of p53 from p53^{+/+} cells appeared to recapitulate the response observed in p53^{-/-} cells, enhancing mTORC1 activity and eIF2 α phosphorylation. During their production, p53^{-/-} cells would have been subject to a severe single cell selection process that could have altered the stress response, or induced underlying cellular stress. Consequently, p53 depletion in p53^{+/+} cells will be used to determine if the response to doxorubicin, and catalytic mTORC1 inhibition, is similar to that observed in the p53^{-/-} cells. Additionally, p53 could be transfected back into the p53^{-/-} cell line, to determine if this reverses the effects observed in response to doxorubicin.

Doxorubicin does not only induce DNA strand breaks by Top2 poisoning, but also damages the cell through various other mechanisms, such as the generation of ROS. Consequently, DNA damage induced by doxorubicin is relatively complex. To gain further insight into the mechanism induced by doxorubicin, stabilisation of p53 was induced in the absence of DNA damage by treatment with nutlin-3a. Intriguingly, stabilisation of p53 in the absence of strand breaks induced mTORC1 inhibition and eIF2 α phosphorylation, further suggesting that p53 may be a negative regulator of mTORC1 signalling. These

data support the hypothesis that doxorubicin-induced mTORC1 inhibition was mediated by the DDR activation of p53.

In response to doxorubicin, p53 was also shown to be essential for the activation of the DNA damage checkpoint in G1, however, the DNA damage checkpoint in G2 was shown to be independent of p53 activity. Furthermore, p53^{-/-} cells were more sensitive to doxorubicin induced cell death, indicating that p53 may play an important role in cell survival through the expression of pro-survival genes. It would be extremely beneficial to determine if p53^{-/-} cells bypass a senescence-like phenotype, and instead initiate cell death pathways in the absence of p53.

6 Discussion

Doxorubicin is an effective chemotherapeutic that is listed as an essential medicine by the World Health Organisation (WHO, model list of essential medicines, 2015). Unfortunately, long-term toxicity has been observed in patients treated with doxorubicin, leading to cardiotoxicity (Gewirtz 1999) and the development of secondary cancers (Azim et al. 2011). As long-term toxicity is often observed in non-cancerous cells, an intriguing question concerned how non-cancerous cells respond to doxorubicin-induced toxicity. Unpublished data from the Willis laboratory has shown that DNA damage induced by UVB rapidly inhibits protein synthesis in non-transformed MCF10A cells. Contrastingly, doxorubicin did not inhibit protein synthesis, or induce eIF2 α phosphorylation, until 16 hours, indicating a delayed response to DNA damage.

Within this thesis, doxorubicin-induced protein synthesis inhibition was shown to be independent of eIF2 α phosphorylation and likely mediated by p53 dependent mTORC1 inhibition. Furthermore, mTORC1 inhibition was subsequently shown to enhance eIF2 α phosphorylation in a signalling mechanism mediated by PP6 activity, and eIF2 α phosphorylation is hypothesised to mediate cell fate.

6.1 Proposed model for doxorubicin-induced protein synthesis inhibition

Treatment with doxorubicin resulted in p53 mediated inhibition of mTORC1 signalling. Importantly, mTORC1 inhibition was likely to be independent of TSC activity and possibly a direct consequence of p53 mediated gene transcription. Furthermore, doxorubicin-induced protein synthesis inhibition was shown to be independent of eIF2 α , and most likely to be regulated by mTORC1 dependent regulation of 4E-BP1 (Figure 6-1).

Doxorubicin activated ATM, ATR and DNA-PKcs, resulting in the phosphorylation of p53. Although the exact mechanism of p53 activation was unclear, ATM was shown to be dispensable in doxorubicin-induced mTORC1 inhibition. Due to its role as a sensor of DSBs, the most likely candidate to regulate p53 activity in response to doxorubicin would be DNA-PKcs (Figure 6-1).

Prolonged mTORC1 inhibition was shown to enhance eIF2 α phosphorylation, through signalling mechanisms that were potentially mediated by PP6 and potentially cytoplasmic DNA-PKcs. Although the exact mechanism is not yet clear, mTORC1 inhibition may induce eIF2 α phosphorylation by the activation of GCN2 and/or PERK. It is hypothesised that in addition to co-ordinating protein synthesis shutdown, eIF2 α phosphorylation may regulate cell fate (Figure 6-1).

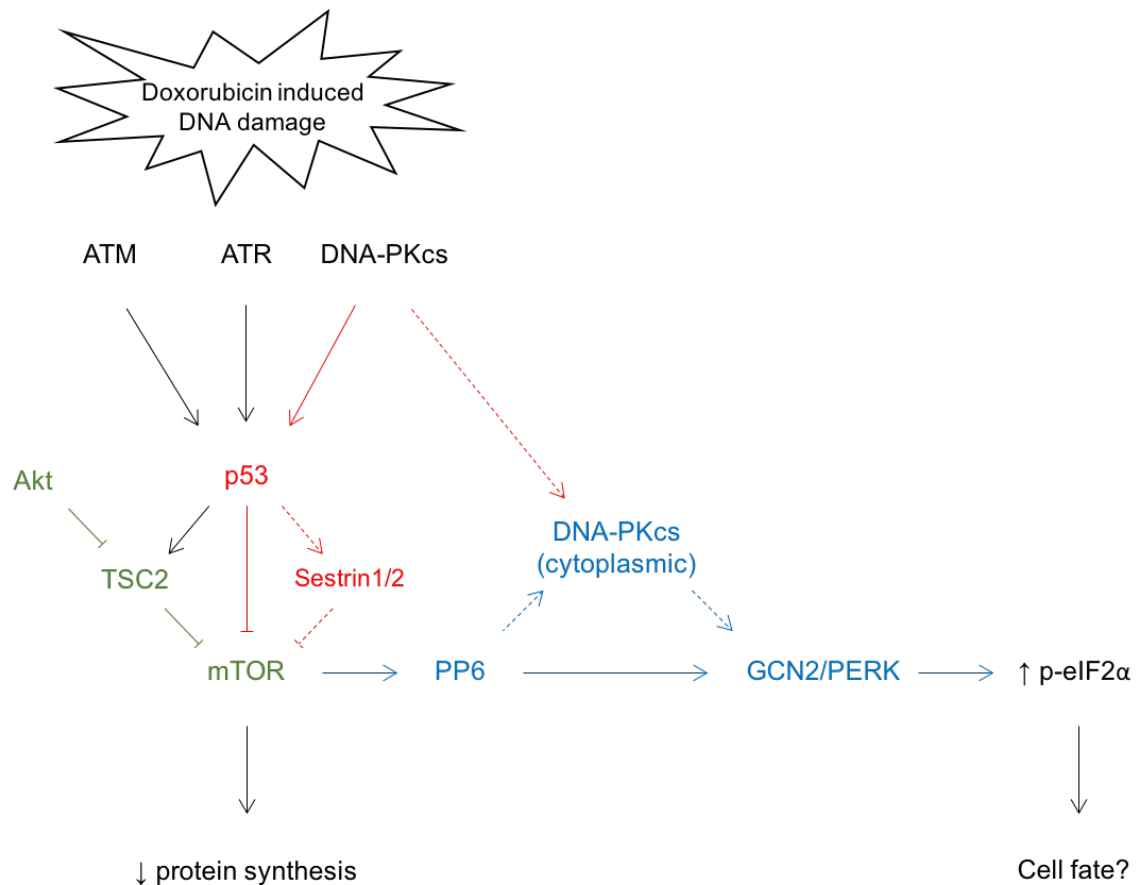


Figure 6-1. Proposed model of doxorubicin-induced mTORC1 inhibition and eIF2α phosphorylation

Schematic representation of a proposed model of doxorubicin-induced protein synthesis inhibition. Solid lines indicate known steps, whereas broken lines indicate unclear steps. Proposed doxorubicin-induced signalling is shown in red, Akt dependent mTOR signalling is shown in green, and mTOR-eIF2K crosstalk signalling is shown in blue.

6.2 Role of eIF2 α in doxorubicin-induced toxicity

UVB-induced DNA damage has been shown to rapidly inhibit global protein synthesis through enhanced eIF2 α phosphorylation (Deng et al. 2002; Wu et al. 2002). In MEFs, protein synthesis inhibition was observed within 30 minutes of UVB treatment (Deng et al. 2002), whereas data from the Willis laboratory has shown that in MCF10A cells, protein synthesis inhibition is observed within 15 minutes. Furthermore, UVB induced eIF2 α phosphorylation was shown to regulate the preferential translation of mRNAs required for the DDR (Powley et al. 2009). Unpublished data from the Willis laboratory suggested that doxorubicin enhanced eIF2 α phosphorylation in MCF10A cells. Furthermore, doxorubicin was shown to induce eIF2 α phosphorylation in MEFs (Peidis et al. 2011), suggesting that eIF2 α may regulate protein synthesis in response to doxorubicin-induced DNA damage. Interestingly, eIF2 α phosphorylation was observed at 12 hours after treatment with doxorubicin in MCF10A cells (Figure 3-5C), and this response was also observed in MEFs (Peidis et al. 2011). These studies indicated that eIF2 α phosphorylation may regulate protein synthesis inhibition in response to doxorubicin, so the signalling to eIF2 α was explored further.

Individual depletion of GCN2 or PKR did not reduce doxorubicin-induced eIF2 α phosphorylation in MCF10A cells. In MEFs, UVB-induced eIF2 α phosphorylation was shown to be dependent on GCN2 (Deng et al. 2002; Powley et al. 2009), whereas doxorubicin-induced eIF2 α phosphorylation was shown to be dependent on PKR (Peidis et al. 2011). These studies indicated that the regulation of eIF2 α might differ in response to different DNA damage stimuli. In contrast to the regulation observed in MEFs (Peidis et al. 2011), depletion PKR minimally reduced doxorubicin-induced eIF2 α phosphorylation in MCF10A cells (Figure 3-7). The discrepancy between these two sets of data could be explained by the concentration of doxorubicin used. PKR was shown to be activated in response to a concentration of doxorubicin that induced cell death (Peidis et al. 2011), suggesting that the regulation of eIF2 α may also differ in response to the severity of damage.

By using ISRIB in combination with doxorubicin, it was shown that eIF2 α phosphorylation was not the major factor in the inhibition of protein synthesis,

raising the question of what is the function of this modification. A range of transcripts are regulated upon eIF2 α phosphorylation as part of the DDR and UPR (Powley et al. 2009; Baird et al. 2014), suggesting that doxorubicin-induced eIF2 α phosphorylation may preferentially enhance the translation of these target mRNA. Interestingly, translational reprogramming driven by the phosphorylation of eIF2 and subsequent inhibition of eIF2B was shown to enhance the invasiveness and drug resistance of melanoma (Falletta et al. 2017), suggesting that the role of doxorubicin-induced eIF2 α phosphorylation should be considered within the treatment of tumours. It would be useful to analyse the translation of mRNA that are enhanced in response to doxorubicin in combination with ISRIB, to identify the mRNAs that are dependent on doxorubicin-induced eIF2 α phosphorylation. Interestingly, p53^{-/-} cells showed diminished induction of eIF2 α phosphorylation and were more sensitive to doxorubicin-induced cell death. Furthermore, eIF2 α phosphorylation has been suggested to be cytoprotective in MEFs (Peidis et al. 2011; Rajesh et al. 2015), suggesting that eIF2 α phosphorylation may play a role in the regulation of cell fate. As doxorubicin was shown to induce a senescence-like phenotype in MCF10A cells, it would be beneficial to study SA- β -gal activity after dual treatment with ISRIB and doxorubicin to determine the role played by eIF2 α . Furthermore, eIF2 α ^{S51A}, a constitutively non-phosphorylated mutant, or GADD34, a phosphatase that diminishes eIF2 α phosphorylation, could be overexpressed in MCF10A cells to further study the role of eIF2 α phosphorylation on cell fate.

6.3 Doxorubicin-induced protein synthesis inhibition was likely mediated by mTORC1 inhibition

A delay between DNA damage recognition and inhibition of protein synthesis is not common, but has been observed in response to IR in MCF10A cells (Braunstein et al. 2009). In response to IR, inhibition of protein synthesis was mediated by mTOR inhibition and subsequent 4E-BP1 de-phosphorylation (Braunstein et al. 2009). Intriguingly, a number of similarities were observed between cells treated with IR (Braunstein et al. 2009) and doxorubicin. First, polysome profile analysis indicated that doxorubicin and IR inhibited global protein synthesis through the inhibition of translation initiation (Figure 3-6).

Secondly, protein synthesis inhibition was independent of eIF2 α . In response to IR this was shown by the overexpression of the eIF2 α phosphatase, GADD34, whereas in response to doxorubicin, this was shown using ISRIB (Figure 3-10). Thirdly, mTORC1 inhibition preceded eIF2 α phosphorylation and correlated with protein synthesis inhibition in response to both stimuli. These findings suggested that doxorubicin-induced protein synthesis inhibition may be a consequence of mTORC1 inhibition. mTOR activity has been shown to be regulated in response to a range of different DNA damage stimuli. mTOR signalling was enhanced in response to UVB (Carr et al. 2012; Brenneisen et al. 2002) and etoposide (Selvarajah et al. 2014). Contrastingly, etoposide has also been shown to inhibit mTOR signalling (Tee & Proud 2000; Feng et al. 2005), as has cisplatin and mitomycin C (Tee & Proud 2000). Furthermore, mTOR signalling was inhibited in cardiomyocytes isolated from mice treated with doxorubicin (Zhu et al. 2009).

Although the data presented within this thesis suggested that protein synthesis inhibition could be mediated by mTORC1 inhibition, depletion of 4E-BPs or TSC2 did not rescue protein synthesis inhibition (Figure 4-3 and Figure 4-4). Depletion of 4E-BP1 has been shown to reverse IR mediated protein synthesis inhibition (Braunstein et al. 2009). Therefore, the failure of 4E-BP depletion to rescue protein synthesis could have been due to insufficient depletion of 4E-BP1. It will be important to improve the efficiency of 4E-BP1 depletion, to fully uncover its role in doxorubicin induced protein synthesis inhibition. Furthermore, it would be beneficial to use a 4E-BP1 and 4E-BP2 knockout cell line to confirm the regulatory effect of 4E-BPs in doxorubicin-induced toxicity.

Although the depletion of TSC2 was efficient and enhanced mTORC1 activity, it did not rescue doxorubicin-induced protein synthesis inhibition. Furthermore, TSC2 depletion did not reverse doxorubicin-induced mTORC1 inhibition. These data suggested that doxorubicin might inhibit mTORC1 independently of TSC activity, such as through the regulation of mTORC1 localisation. Interestingly, p53-induced sestrin proteins have been identified to inhibit mTORC1 localisation to the lysosome, through the regulation of GATOR and Rag proteins, independently of TSC activity (Parmigiani et al. 2014). p53 was stabilised and activated following treatment with doxorubicin, so it is plausible

that the sestrin proteins could inhibit mTORC1 activity in a similar manner. Furthermore, silencing of sestrin proteins rescued IR-induced protein synthesis inhibition (Braunstein et al. 2009), suggesting that the role of sestrin proteins in response to doxorubicin should be considered. While the work within this thesis was in progress, it was shown that sestrin 2 regulates the de-phosphorylation of 4E-BP1 in response to a range of DNA damage agents (Cam et al. 2014). However, the role of sestrin 2 was not shown in the context of protein synthesis inhibition, or any other downstream mTORC1 targets. Here, sestrin 2 expression was shown to be induced after treatment with doxorubicin in MCF10A cells. Importantly, the induction of sestrin 2 was absent in p53^{-/-} cells, and reduced after depletion of endogenous p53 in p53^{+/+} cells, suggesting that the regulatory mechanism of sestrin proteins may be conserved in response to DNA damage. It may be beneficial to diminish the induction of sestrin proteins prior to the induction of doxorubicin-induced DNA damage, and analyse global protein synthesis rates.

6.4 Doxorubicin-induced mTORC1 inhibition was mediated by p53 activity

In MCF10A cells, p53 was shown to mediate the diminished phosphorylation of both 4E-BP1 and p70 S6K in response to doxorubicin (Figure 5-8). It is hypothesised that this response could be mediated by the expression of sestrin proteins, however sestrin 2 was shown to only diminish 4E-BP1 phosphorylation (Cam et al. 2014). Sestrin 2 did not regulate the reduction of p70 S6K phosphorylation, which was shown to be mediated by DNA-PKcs dependent Akt activation (Cam et al. 2014). Importantly, using temperature sensitive cell lines, p53 induced in the absence of DNA damage was shown to negatively regulate mTORC1 signalling, and was suggested to inhibit translation initiation through the reduced phosphorylation of 4E-BP1 (Horton et al. 2002). Furthermore, in IR treated MCF10A cells, diminished phosphorylation of both 4E-BP1 and p70 S6K was shown to be dependent on p53 activity (Braunstein et al. 2009), indicating that different cell lines may use alternative mechanisms to regulate mTORC1 in response to different DNA damage stimuli.

Within this thesis, ATM was shown to be dispensable for doxorubicin-induced mTORC1 inhibition (Figure 5-4). However, ATM was identified as the DDR kinase that mediated p53 activation in response to IR (Braunstein et al. 2009). These data indicated that although p53 activation was induced by both doxorubicin and IR, the mechanism of p53 activation may differ in response to each stimulus. The identity of the kinase primarily responsible for doxorubicin-induced p53 stabilisation is currently unknown. However, DNA-PKcs is activated in response to DSBs and therefore is the most likely candidate to activate p53 in the absence of ATM. To identify the role played by DNA-PKcs in doxorubicin-induced p53 activation, a more specific DNA-PKcs inhibitor will be used. It would also be beneficial to use a human cell line with defective DNA-PKcs function and DNA-PKcs null MEFs, to confirm any data obtained with inhibitors. Additionally, it should not be discounted that p53 may stabilise independently of DDR phosphorylation, as has been observed in response to nutlin-3a (Vassilev et al. 2004).

p53^{-/-} cells were shown to have enhanced mTORC1 activity (Figure 5-8), suggesting that p53 functions as a negative regulator of mTORC1 activity. mTORC1 activity was enhanced in p53^{-/-} tumours (Akeno et al. 2015), and the deletion of p53 has been shown to enhance mTORC1 signalling (Agarwal et al. 2015; Leontieva et al. 2013; Horton et al. 2002). Additionally, p53 has been shown to enhance the expression of negative regulators of mTOR signalling, PTEN and TSC2 (Feng et al. 2005). Intriguingly, enhanced mTORC1 activity following the deletion of p53 was attributed to the down regulation of TSC2 and sestrin proteins, diminishing mTORC1 localisation to the lysosome (Agarwal et al. 2015). Activation of p53 in the absence of DNA damage also induced mTORC1 inhibition and eIF2 α phosphorylation (Figure 5-8), supporting the hypothesis that p53 activation inhibits mTORC1 signalling. It would be advantageous to study a panel of cell lines with different p53 status, to gain a better understanding of the role of p53 in doxorubicin-induced mTORC1 inhibition.

Many studies examining doxorubicin-induced toxicity use transformed cell lines, that are treated with high concentrations of doxorubicin in combination with kinase inhibitors, to sensitise cells to death. For example, catalytic mTOR

inhibitors sensitise tumours to doxorubicin (Piguet et al. 2008; Shi et al. 2012; Romano et al. 2004) and reverse doxorubicin resistance in PTEN knockout cells (Grunwald et al. 2002). In the context of using doxorubicin as a chemotherapeutic drug, this approach may be effective, however, many transformed cell lines harbour mutations or deletions affecting p53 activity. Subsequently, the cellular response in transformed cell lines differs substantially to non-transformed MCF10A cells, so it is difficult to deduce too much from these studies. Data presented within this thesis, suggested that the p53 status of a tumour or cell line might be a key determinant of the efficiency of doxorubicin to inhibit cell growth, through the inhibition mTORC1. A panel of transformed human cell lines were shown to lose the capacity to inhibit protein synthesis in response to IR (Braunstein et al. 2009). Additionally, rapamycin-induced inhibition of cell proliferation is reduced in transformed MCF10A cell lines, due to enhanced mTOR signalling (Kim et al. 2009). These studies suggested that if the response to doxorubicin were to be expanded to encompass transformed cell lines, they would be unlikely to mediate the response observed in MCF10A cells. Furthermore, mTORC1 activity was enhanced in MCF7 cells, and doxorubicin did not induce protein synthesis inhibition (data not shown). However, MCF7 cells express wild-type p53, suggesting that the deregulation of mTORC1 signalling in transformed cell lines may not be solely regulated by p53 status.

6.5 Crosstalk signalling from mTORC1 inhibition mediated eIF2 α phosphorylation

A number of studies have reported signalling between mTOR to eIF2 α , providing a platform to co-ordinate eIF4F formation and ternary complex availability. Upon the catalytic inhibition of mTOR, eIF2 α is phosphorylated after the PP6-dependent activation of GCN2 (Wengrod et al. 2015). Conversely, after insulin stimulation of mTOR signalling, eIF2 α phosphorylation is diminished by the recruitment of an unidentified phosphatase, in a mechanism dependent on eIF2 β phosphorylation (Gandin, Masvidal, Cargnello, et al. 2016). Furthermore, a series of studies have indicated that mTOR and eIF2K signalling may be closely interlinked. eIF2 α phosphorylation induced by ROS was shown to diminish mTORC1 activity (Rajesh et al. 2015), whereas prolonged ER stress

leading to eIF2 α phosphorylation subsequently suppressed mTORC2 activity (Chen et al. 2011). Additionally, activated Akt has been implicated in maintaining an inhibitory phosphorylation site on PERK, preventing its activation (Tenkerian et al. 2015). These studies suggested that mTOR and eIF2 signalling communicate with each other in response to cellular stress. Additionally, a number of mRNA are regulated upon the phosphorylation of eIF2 α , as part of the DDR and UPR (Powley et al. 2009; Baird et al. 2014). Therefore, crosstalk signalling from mTOR to eIF2 could provide a mechanism whereby mTOR signalling can regulate eIF2 α sensitive mRNA, in addition to 5'TOP mRNAs.

DNA-PKcs was activated at 9 hours after treatment with doxorubicin, correlating with mTORC1 inhibition (Figure 4-2), and DNA-PKcs activation was diminished after depletion of PP6c. Although DNA-PKcs primarily regulates DNA repair in the nucleus, it has been shown to be localised in the cytoplasm (Frasca et al. 2001; Mi et al. 2009) and lipid rafts (Lucero et al. 2003). Cytoplasmic DNA-PKcs has been implicated in the activation of Akt at the plasma membrane (Feng et al. 2004) and subsequently down regulates p70 S6K signalling in response to DNA damage (Cam et al. 2014). Furthermore, cytoplasmic DNA-PKcs has been implicated in the activation of GCN2 during translational reprogramming in response to UVB induced DNA damage (Powley et al. 2009). Interestingly, PP6 has been shown to directly bind and activate DNA-PKcs (Mi et al. 2009) and GCN2 (Wengrod et al. 2015). Although DNA-PKcs and GCN2 have not been shown to inhabit the same complexes, here, it was observed that depletion of PP6c reduced doxorubicin-induced DNA-PKcs activation and eIF2 α phosphorylation (Figure 4-6), suggesting that they could form part of a common mechanism mediating eIF2 α phosphorylation.

The delay between doxorubicin-induced mTORC1 inhibition and eIF2 α phosphorylation was extensive, indicating that the mechanism of crosstalk signalling may be an extremely complex process. Unfortunately, the role of eIF2 β (Gandin, Masvidal, Cargnello, et al. 2016) could not be investigated due to the poor quality of commercially available eIF2 β antibodies. It would be extremely interesting to determine if crosstalk signalling mediated by PP6 and

eIF2 β occur in parallel in response to doxorubicin, and this question will be considered in any further investigations.

References

- Aarti, I., Rajesh, K. & Ramaiah, K.V.A., 2010. Phosphorylation of eIF2 alpha in Sf9 cells: A stress, survival and suicidal signal. *Apoptosis*, 15(6), pp.679–692.
- Acharya, P., Chen, J.-J. & Correia, M.A., 2010. Hepatic heme-regulated inhibitor (HRI) eukaryotic initiation factor 2alpha kinase: a protagonist of heme-mediated translational control of CYP2B enzymes and a modulator of basal endoplasmic reticulum stress tone. *Molecular pharmacology*, 77(4), pp.575–92.
- Adams, C.C. et al., 2002. Saccharomyces cerevisiae nucleolar protein Nop7p is necessary for biogenesis of 60S ribosomal subunits. *RNA*, 8(2), pp.150–65.
- Agarwal, M.L. et al., 1995. p53 controls both the G2/M and the G1 cell cycle checkpoints and mediates reversible growth arrest in human fibroblasts. *Proceedings of the National Academy of Sciences of the United States of America*, 92(18), pp.8493–8497.
- Agarwal, S. et al., 2015. p53 Deletion or Hot-spot Mutations Enhance mTORC1 Activity by Altering Lysosomal Dynamics of TSC2 and Rheb. *Molecular Cancer Research*, 14(January), pp.66–78.
- Ahnesorg, P., Smith, P. & Jackson, S.P., 2006. XLF interacts with the XRCC4-DNA Ligase IV complex to promote DNA nonhomologous end-joining. *Cell*, 124(2), pp.301–313.
- Aitken, C.E. & Lorsch, J.R., 2012. A mechanistic overview of translation initiation in eukaryotes. *Nature structural & molecular biology*, 19(6), pp.568–76.
- Ajmani, B.A.K. et al., 1995. Absence of Autoantigen Ku in Mature Human Neutrophils and Human Promyelocytic Leukemia Line (HL-60) Cells and Lymphocytes Undergoing Apoptosis. *The Journal of Experimental Medicine* *Journal of Experimental Medicine*, 181(June).
- Akeno, N. et al., 2015. p53 suppresses carcinoma progression by inhibiting mTOR pathway activation. *Oncogene*, 34(October 2013), pp.1–11.
- Alexander, A. et al., 2010. ATM signals to TSC2 in the cytoplasm to regulate mTORC1 in response to ROS. *Proceedings of the National Academy of Sciences of the United States of America*, 107(9), pp.4153–4158.
- Ambrosio, S. et al., 2015. Cell cycle-dependent resolution of DNA double-strand breaks. *Oncotarget*, 7(4), pp.4949–4960.
- Armstrong, J.L. et al., 2010. Regulation of endoplasmic reticulum stress-induced cell death by ATF4 in neuroectodermal tumor cells. *Journal of Biological Chemistry*, 285(9), pp.6091–6100.
- Asano, K. et al., 2000. A multifactor complex of eukaryotic and initiator tRNA Met is an important translation initiation intermediate in vivo. *Genes & Development*, (14), pp.2534–2546.
- Ashcroft, M. et al., 2002. Phosphorylation of HDM2 by Akt. *Oncogene*, 21, pp.1955–1962.
- Azim, H. a et al., 2011. Long-term toxic effects of adjuvant chemotherapy in breast cancer. *Annals of oncology : official journal of the European Society for Medical Oncology / ESMO*, 22(9), pp.1939–1947.

- Bailey, S.M. et al., 1999. DNA double-strand break repair proteins are required to cap the ends of mammalian chromosomes. *Proceedings of the National Academy of Sciences of the United States of America*, 96(26), pp.14899–14904.
- Baird, T.D. et al., 2014. Selective mRNA translation during eIF2 phosphorylation induces expression of IBTK α . *Molecular biology of the cell*, 25(10), pp.1686–97.
- Bakkenist, C.J. & Kastan, M.B., 2003. DNA damage activates ATM through intermolecular autophosphorylation and dimer dissociation. *Nature*, 421(6922), pp.499–506.
- Banin, S. et al., 1998. Enhanced Phosphorylation of p53 by ATM in Response to DNA Damage. *Science*, 281(5383), pp.1674–1677.
- Barak, Y. et al., 1993. Mdm2 Expression Is Induced By Wild Type P53 Activity. *The EMBO journal*, 12(2), pp.461–8.
- Bar-Peled, L. et al., 2013. A Tumor suppressor complex with GAP activity for the Rag GTPases that signal amino acid sufficiency to mTORC1. *Science*, 340(6136), pp.1100–6.
- Bar-Peled, L. et al., 2012. Ragulator is a GEF for the rag GTPases that signal amino acid levels to mTORC1. *Cell*, 150(6), pp.1196–1208.
- Bates, S. et al., 1998. Cell cycle arrest and DNA endoreduplication following p21 Waf1/Cip1 expression. *Oncogene*, 1.
- Bencheikroun, M.N., Sinha, B.K. & Robert, J., 1993. Doxorubicin-induced oxygen free radical formation in sensitive and doxorubicin-resistant variants of rat glioblastoma cell lines. *FEBS Letters*, 326(1–3), pp.302–305.
- Bergeron, J. et al., 2000. Identification of the interferon-inducible double-stranded RNA-dependent protein kinase as a regulator of cellular response to bulky adducts. *Cancer Research*, 60(24), pp.6800–6804.
- Berthiaume, J.M. & Wallace, K.B., 2007. Adriamycin-induced oxidative mitochondrial cardiotoxicity. *Cell Biology and Toxicology*, 23(1), pp.15–25.
- Bertolotti, A. et al., 2000. Dynamic interaction of BiP and ER stress transducers in the unfolded-protein response. *Nature cell biology*, 2(6), pp.326–332.
- Bonner, W.M. et al., 2008. γ H2AX and cancer. *Nature Reviews Cancer*, 8(12), pp.957–967.
- Boulbles, D.R., Shaiken, T. & Sarbassov, D.D., 2011. Endoplasmic reticulum is a main localization site of mTORC2. *Biochemical and Biophysical Research Communications*, 413(1), pp.46–52.
- Brady, C.A. & Attardi, L.D., 2010. P53 At a Glance. *Journal of Cell Science*, 123(15), pp.2527–2532.
- Braunstein, S. et al., 2009. Regulation of protein synthesis by ionizing radiation. *Molecular and cellular biology*, 29(21), pp.5645–56.
- Brenneisen, P. et al., 2002. Activation of protein kinase CK2 is an early step in the ultraviolet B-mediated increase in interstitial collagenase (matrix metalloproteinase-1; MMP-1) and stromelysin-1 (MMP-3) protein levels in human dermal fibroblasts. *The Biochemical journal*, 365(Pt 1), pp.31–40.

- Brown, E.J. et al., 1994. A mammalian protein targeted by G1-arresting rapamycin-receptor complex. *Nature*, 369, pp.756–758.
- Brown, P.O. & Cozzarelli, N.R., 1981. Catenation and knotting of duplex DNA by type 1 topoisomerases: a mechanistic parallel with type 2 topoisomerases. *Proceedings of the National Academy of Sciences of the United States of America*, 78(2), pp.843–847.
- Browne, G.J. & Proud, C.G., 2004. A Novel mTOR-Regulated Phosphorylation Site in Elongation Factor 2 Kinase Modulates the Activity of the Kinase and Its Binding to Calmodulin. *Molecular and cellular biology*, 24(7), pp.2986–2997.
- Browne, G.J. & Proud, C.G., 2002. Regulation of peptide-chain elongation in mammalian cells. *European Journal of Biochemistry*, 269(22), pp.5360–5368.
- Brunet, A. et al., 2001. Protein kinase SGK mediates survival signals by phosphorylating the forkhead transcription factor FKHRL1 (FOXO3a). *Molecular and cellular biology*, 21(3), pp.952–955.
- Buckbinder, L. et al., 1995. Induction of the growth inhibitor IGF-binding protein 3 by p53. *Nature*, 377, pp.646–649.
- Budanov, A. V. & Karin, M., 2008. p53 Target Genes Sestrin1 and Sestrin2 Connect Genotoxic Stress and mTOR Signaling. *Cell*, 134(3), pp.451–460.
- Bunz, F. et al., 1998. Requirement for p53 and p21 to Sustain G2 Arrest After DNA Damage. *Science*, 282(November), pp.1497–1502.
- Burger, K. et al., 2010. Chemotherapeutic drugs inhibit ribosome biogenesis at various levels. *Journal of Biological Chemistry*, 285(16), pp.12416–12425.
- Burgess, D.J. et al., 2008. Topoisomerase levels determine chemotherapy response in vitro and in vivo. *Proceedings of the National Academy of Sciences of the United States of America*, 105(26), pp.9053–9058.
- Burma, S. et al., 2001. ATM Phosphorylates Histone H2AX in Response to DNA Double-strand Breaks. *Journal of Biological Chemistry*, 276(45), pp.42462–42467.
- Bushell, M. et al., 2001. Disruption of the Interaction of Mammalian Protein Synthesis Eukaryotic Initiation Factor 4B with the Poly(A)-binding Protein by Caspase- and Viral Protease-mediated Cleavages. *Journal of Biological Chemistry*, 276(26), pp.23922–23928.
- Cam, M. et al., 2014. P53/TAp63 and AKT regulate mammalian target of rapamycin complex 1 (mTORC1) signaling through two independent parallel pathways in the presence of DNA damage. *Journal of Biological Chemistry*, 289(7), pp.4083–4094.
- Campisi, J. & d'Adda di Fagagna, F., 2007. Cellular senescence: when bad things happen to good cells. *Nature reviews. Molecular cell biology*, 8(9), pp.729–740.
- Canman, C.E. et al., 1998. Activation of the ATM Kinase by Ionizing Radiation and Phosphorylation of p53. *Science*, 281(5383), pp.1677–1679.
- Carlberg, U., Nilsson, A. & Nygard, O., 1990. Functional properties of phosphorylated elongation factor 2. *Eur J Biochem*, 191(3), pp.639–645.
- Caron, P. et al., 2015. Non-redundant Functions of ATM and DNA-PKcs in Response to DNA Double-Strand Breaks. *Cell Reports*, 13(8), pp.1598–1609.

- Carpenter, A.J. & Porter, A.C.G., 2004. Construction, Characterization, and Complementation of a Conditional-Lethal DNA Topoisomerase II Mutant Human Cell Line. *Molecular biology of the cell*, 15, pp.5700–5711.
- Carr, T.D. et al., 2012. Inhibition of mTOR suppresses UVB-induced keratinocyte proliferation and survival. *Cancer Prevention Research*, 5(12), pp.1394–1404.
- Carracedo, A. et al., 2008. Inhibition of mTORC1 leads to MAPK pathway activation through a PI3K- dependent feedback loop in human cancer. *Journal of Clinical Investigation*, 118(9), pp.3065–3074.
- Chakrabarti, A. & Maitra, U., 1991. Release and recycling of eukaryotic initiation factor 2 in the formation of an 80 S ribosomal polypeptide chain initiation complex. *Journal of Biological Chemistry*, 266(21), pp.14039–14045.
- Champoux, J.J., 2001. DNA Topoisomerases: Structure, Function, and Mechanism. *Annual review of biochemistry*, 70, pp.369–413.
- Chang, B. et al., 1999. Role of p53 and p21waf1/cip1 in senescence-like terminal proliferation arrest induced in human tumor cells by chemotherapeutic drugs. *Oncogene*, 18(July), pp.4808–4818.
- Chauvin, C. et al., 2014. Ribosomal protein S6 kinase activity controls the ribosome biogenesis transcriptional program. *Oncogene*, 33(4), pp.474–83.
- Chen, C.-H. et al., 2011. ER stress inhibits mTORC2 and Akt signaling through GSK-3 β -mediated phosphorylation of rictor. *Science signaling*, 4(161), p.ra10.
- Chen, J. et al., 1995. Identification of an 11-kDa FKBP12-rapamycin-binding domain within the 289-kDa FKBP12-rapamycin-associated protein and characterization of a critical serine residue. *Proceedings of the National Academy of Sciences of the United States of America*, 92(11), pp.4947–51.
- Chen, Q. & Ames, B.N., 1994. Senescence-like growth arrest induced by hydrogen peroxide in human diploid fibroblast F65 cells. *Proceedings of the National Academy of Sciences of the United States of America*, 91(10), pp.4130–4134.
- Chen, S.H., Chan, N.-L. & Hsieh, T., 2013. New mechanistic and functional insights into DNA topoisomerases. *Annual review of biochemistry*, 82, pp.139–70.
- Chiang, G.G. & Abraham, R.T., 2005. Phosphorylation of mammalian target of rapamycin (mTOR) at Ser-2448 is mediated by p70S6 kinase. *Journal of Biological Chemistry*, 280(27), pp.25485–25490.
- Chipuk, J.E. et al., 2005. PUMA Couples the Nuclear and Cytoplasmic Proapoptotic Function of p53. *Science*, 309(1732–1735).
- Cho, S., Park, J. & Hwang, E.S., 2011. Kinetics of the cell biological changes occurring in the progression of DNA damage-induced senescence. *Molecules and Cells*, 31(6), pp.539–546.
- Choo, A.Y. et al., 2008. Rapamycin differentially inhibits S6Ks and 4E-BP1 to mediate cell-type-specific repression of mRNA translation. *Proceedings of the National Academy of Sciences of the United States of America*, 105(45), pp.17414–17419.
- Choy, M.S. et al., 2015. Structural and Functional Analysis of the GADD34:PP1 eIF2 α Phosphatase. *Cell Reports*, 11(12), pp.1885–1891.

- Chresta, C.M. et al., 2010. AZD8055 is a potent, selective, and orally bioavailable ATP-competitive mammalian target of rapamycin kinase inhibitor with in vitro and in vivo antitumor activity. *Cancer Research*, 70(1), pp.288–298.
- Chung, J. et al., 1992. Rapamycin-FKBP specifically blocks growth-dependent activation of and signaling by the 70 kd S6 protein kinases. *Cell*, 69(7), pp.1227–1236.
- Cimprich, K.A. & Cortez, D., 2008. ATR: an essential regulator of genome integrity. *Nature reviews. Molecular cell biology*, 9(8), pp.616–27.
- Close, D.M., Nelson, W.H. & Bernhard, W.A., 2013. DNA damage by the direct effect of ionizing radiation: Products produced by two sequential one-electron oxidations. *Journal of Physical Chemistry A*, 117(47), pp.12608–12615.
- Cooke, M.S. et al., 2003. Oxidative DNA damage: mechanisms, mutation, and disease. *Faseb J*, 17(10), pp.1195–214.
- Cowling, V.H., 2010. Regulation of mRNA cap methylation. *The Biochemical journal*, 425(2), pp.295–302.
- Crosby, J.S. et al., 1994. Erythroid expression of the heme-regulated eIF-2 alpha kinase. *Molecular and cellular biology*, 14(6), pp.3906–14.
- Culjkovic-Kraljacic, B. & Borden, K.L.B., 2013. Aiding and abetting cancer: mRNA export and the nuclear pore. *Trends in cell biology*, 23(7), pp.328–35.
- Dasika, G.K. et al., 1999. DNA damage-induced cell cycle checkpoints and DNA strand break repair in development and tumorigenesis. *Oncogene*, 18(55), pp.7883–99.
- Deavall, D.G. et al., 2012. Drug-induced oxidative stress and toxicity. *Journal of Toxicology*, 2012.
- Deng, J. et al., 2002. Activation of gcn2 in uv-irradiated cells inhibits translation. *Current Biology*, 12(15), pp.1279–1286.
- Deng, S. et al., 2014. Dexrazoxane may prevent doxorubicin-induced DNA damage via depleting both topoisomerase II isoforms. *BMC cancer*, 14, p.842.
- Deng, X. et al., 2004. The cyclin-dependent kinase inhibitor p27Kip1 is stabilized in G0 by Mirk/dyrk1B Kinase. *Journal of Biological Chemistry*, 279(21), pp.22498–22504.
- Dibble, C.C., Asara, J.M. & Manning, B.D., 2009. Characterization of Rictor phosphorylation sites reveals direct regulation of mTOR complex 2 by S6K1. *Molecular and cellular biology*, 29(21), pp.5657–70.
- Dimri, G.P. et al., 1995. A Biomarker That Identifies Senescent Human-Cells in Culture and in Aging Skin in-Vivo. *Proceedings of the National Academy of Sciences of the United States of America*, 92(20), pp.9363–9367.
- Dizdaroglu, M. & Jaruga, P., 2012. Mechanisms of free radical-induced damage to DNA. *Free Radical Research*, 46(4), pp.382–419.
- Dmitriev, S.E. et al., 2003. Assembly of 48S translation initiation complexes from purified components with mRNAs that have some base pairing within their 5' untranslated regions. *Molecular and cellular biology*, 23(24), pp.8925–33.

- Donahue, B.A. et al., 1994. Transcript cleavage by RNA polymerase II arrested by a cyclobutane pyrimidine dimer in the DNA template. *Proceedings of the National Academy of Sciences of the United States of America*, 91(18), pp.8502–6.
- Dong, J. et al., 2000. Uncharged tRNA activates GCN2 by displacing the protein kinase moiety from a bipartite tRNA-binding domain. *Molecular Cell*, 6(2), pp.269–279.
- Donnelly, N. et al., 2013. The eIF2 α kinases: Their structures and functions. *Cellular and Molecular Life Sciences*, 70(19), pp.3493–3511.
- Doroshov, J.H. & Davies, K.J.A., 1986. Redox cycling of anthracyclines by cardiac mitochondria. II. Formation of superoxide anion, hydrogen peroxide, and hydroxyl radical. *Journal of Biological Chemistry*, 261(7), pp.3068–3074.
- Douglas, P. et al., 2010. Protein Phosphatase 6 Interacts with the DNA-Dependent Protein Kinase Catalytic Subunit and Dephosphorylates -H2AX. *Molecular and cellular biology*, 30(6), pp.1368–1381.
- Dowling, R.J.O. et al., 2010. mTORC1-Mediated Cell Proliferation, But Not Cell Growth, Controlled by the 4E-BPs. *Science*, 328(May).
- Dreyfus, M. & Régnier, P., 2002. The poly(A) tail of mRNAs: Bodyguard in eukaryotes, scavenger in bacteria. *Cell*, 111(5), pp.611–613.
- Dulic, V. et al., 1994. p53-dependent inhibition of cyclin-dependent kinase activities in human fibroblasts during radiation-induced G1 arrest. *Cell*, 76(6), pp.1013–1023.
- Dyson, N., 1998. The regulation of E2F by pRB-family?proteins. *Genes & Development*, 12(617), pp.2245–2262.
- Efeyan, A. & Sabatini, D.M., 2010. MTOR and cancer: Many loops in one pathway. *Current Opinion in Cell Biology*, 22(2), pp.169–176.
- El-Deiry, W.S. et al., 1993. WAF1, a potential mediator of p53 tumour suppression. *Cell*, 75(4), pp.817–825.
- Elmore, L.W. et al., 2002. Adriamycin-induced senescence in breast tumor cells involves functional p53 and telomere dysfunction. *The Journal of biological chemistry*, 277(38), pp.35509–15.
- Falck, J., Coates, J. & Jackson, S.P., 2005. Conserved modes of recruitment of ATM, ATR and DNA-PKcs to sites of DNA damage. *Nature*, 434(7033), pp.605–611.
- Faller, W.J. et al., 2014. mTORC1-mediated translational elongation limits intestinal tumour initiation and growth. *Nature*, 517(7535), pp.497–500.
- Falletta, P. et al., 2017. Translation reprogramming is an evolutionarily conserved driver of phenotypic plasticity and therapeutic resistance in melanoma. *Genes & Development*, 31, pp.18–33.
- Fan, J.R. et al., 2008. Cellular processing pathways contribute to the activation of etoposide-induced DNA damage responses. *DNA Repair*, 7(3), pp.452–463.
- Feng, J. et al., 2004. Identification of a PKB/Akt hydrophobic motif Ser-473 kinase as DNA-dependent protein kinase. *Journal of Biological Chemistry*, 279(39), pp.41189–41196.
- Feng, Z. et al., 2005. The coordinate regulation of the p53 and mTOR pathways in

- cells. *Proceedings of the National Academy of Sciences of the United States of America*, pp.3–8.
- Feng, Z. et al., 2007. The regulation of AMPK B1, TSC2, and PTEN expression by p53: Stress, cell and tissue specificity, and the role of these gene products in modulating the IGF-1-AKT-mTOR pathways. *Cancer Research*, 67(7), pp.3043–3053.
- Feoktistova, K. et al., 2013. Human eIF4E promotes mRNA restructuring by stimulating eIF4A helicase activity. *Proceedings of the National Academy of Sciences of the United States of America*, 110(33), pp.13339–44.
- Finch, R. a et al., 2002. mdmx Is a Negative Regulator of p53 Activity in Vivo mdmx Is a Negative Regulator of p53 Activity in Vivo. *Cancer Research*, (62), pp.3221–3225.
- Foster, K.G. &ingar, D.C., 2010. Mammalian target of rapamycin (mTOR): Conducting the cellular signaling symphony. *Journal of Biological Chemistry*, 285(19), pp.14071–14077.
- Frasca, D. et al., 2001. Role of DNA-dependent protein kinase in recognition of radiation-induced DNA damage in human peripheral blood mononuclear cells. *Int Immunol*, 13(6), pp.791–797.
- Frias, M.A. et al., 2006. mSin1 Is Necessary for Akt/PKB Phosphorylation, and Its Isoforms Define Three Distinct mTORC2s. *Current Biology*, 16(18), pp.1865–1870.
- Fridman, J.S. & Lowe, S.W., 2003. Control of apoptosis by p53. *Oncogene*, 22(56), pp.9030–9040.
- Gaillard, H. & Aguilera, A., 2008. A Novel Class of mRNA-containing Cytoplasmic Granules Are Produced in Response to UV-Irradiation. *Molecular biology of the cell*, 19, pp.4980–4992.
- Gandin, V., Masvidal, L., Cargnello, M., et al., 2016. mTORC1 and CK2 coordinate ternary and eIF4F complex assembly. *Nature communications*, 7, p.11127.
- Gandin, V., Masvidal, L., Hulea, L., et al., 2016. nanoCAGE reveals 5' UTR features that define specific modes of translation of functionally related MTOR-sensitive mRNAs. *Genome Res*, 26(5), pp.636–648.
- Garami, A. et al., 2003. Insulin activation of Rheb, a mediator of mTOR/S6K/4E-BP signaling, is inhibited by TSC1 and 2. *Molecular cell*, 11(6), pp.1457–1466.
- García-Martínez, J.M. & Alessi, D.R., 2008. mTOR complex 2 (mTORC2) controls hydrophobic motif phosphorylation and activation of serum- and glucocorticoid-induced protein kinase 1 (SGK1). *The Biochemical journal*, 416(3), pp.375–385.
- Gewirtz, D.A., 1999. A critical evaluation of the mechanisms of action proposed for the antitumor effects of the anthracycline antibiotics adriamycin and daunorubicin. *Biochemical Pharmacology*, 57(7), pp.727–741.
- Ghilarov, D.A. & Shkundina, I.S., 2012. DNA-topoisomerases and their functions in cell. *Molecular Biology*, 46(1), pp.52–63.
- Ghosh, S. et al., 2006. Essential role of tuberous sclerosis genes TSC1 and TSC2 in NF-kappaB activation and cell survival. *Cancer cell*, 10(3), pp.215–26.

- Giacinti, C. & Giordano, a, 2006. RB and cell cycle progression. *Oncogene*, 25(38), pp.5220–7.
- Gingras, A.C. et al., 2001. Hierarchical phosphorylation of the translation inhibitor 4E-BP1. *Genes and Development*, 15(21), pp.2852–2864.
- Gingras, A.C. et al., 1999. Regulation of 4E-BP1 phosphorylation: a novel two-step mechanism. *Genes & development*, 13(11), pp.1422–37.
- Gottlieb, T.M. & Jackson, S.P., 1993. The DNA-dependent protein kinase: Requirement for DNA ends and association with Ku antigen. *Cell*, 72(1), pp.131–142.
- Grunwald, V. et al., 2002. Inhibitors of mTOR reverse doxorubicin resistance conferred by PTEN status in prostate cancer cells. *Cancer Research*, 62(21), pp.6141–6145.
- Gu, J. et al., 2002. Mutual dependence of MDM2 and MDMX in their functional inactivation of p53. *Journal of Biological Chemistry*, 277(22), pp.19251–19254.
- Guo, Z. et al., 2010. ATM activation by oxidative stress. *Science*, 330, pp.517–521.
- Gwinn, D.M. et al., 2008. AMPK Phosphorylation of Raptor Mediates a Metabolic Checkpoint. *Molecular Cell*, 30(2), pp.214–226.
- Haghighat, A. et al., 1995. Repression of cap-dependent translation by 4E-binding protein 1: competition with p220 for binding to eukaryotic initiation factor-4E. *The EMBO journal*, 14(22), pp.5701–9.
- Han, A.P. et al., 2001. Heme-regulated eIF2 α kinase (HRI) is required for translational regulation and survival of erythroid precursors in iron deficiency. *EMBO Journal*, 20(23), pp.6909–6918.
- Hannan, K.M. et al., 2003. mTOR-dependent regulation of ribosomal gene transcription requires S6K1 and is mediated by phosphorylation of the carboxy-terminal activation domain of the nucleolar transcription factor UBF. *Molecular and cellular biology*, 23(23), pp.8862–77.
- Hans, F. & Dimitrov, S., 2001. Histone H3 phosphorylation and cell division. *Oncogene*, 20(24), pp.3021–3027.
- Harding, H.P. et al., 2000. Stress-Induced Gene Expression in Mammalian Cells. *Molecular cell*, 6, pp.1099–1108.
- Harding, H.P., Zhang, Y. & Ron, D., 1999. Protein translation and folding are coupled by an endoplasmic-reticulum-resident kinase. *Nature*, 397(6716), pp.271–274.
- Harrington, L.S. et al., 2004. The TSC1-2 tumor suppressor controls insulin-PI3K signaling via regulation of IRS proteins. *Journal of Cell Biology*, 166(2), pp.213–223.
- Haupt, S. et al., 2003. Apoptosis - the p53 network. *Journal of cell science*, 116(Pt 20), pp.4077–85.
- Haupt, Y. et al., 1997. Mdm2 promotes the rapid degradation of p53. *Nature*, 387, pp.296–299.
- Hay, N. & Sonenberg, N., 2004. Upstream and downstream of mTOR. *Genes and Development*, 18, pp.1926–1945.
- Heitman, J., Movva, N.R. & Hall, M.N., 1991. Targets for cell cycle arrest by the

- immunosuppressant rapamycin in yeast. *Science*, 253(5022), pp.905–909.
- Helser, T.L., Baan, R.A. & Dahlberg, A.E., 1981. Characterization of a 40S ribosomal subunit complex in polyribosomes of *Saccharomyces cerevisiae* treated with cycloheximide. *Molecular and cellular biology*, 1(1), pp.51–57.
- Hermeking, H. et al., 1997. 14-3-3 σ is a p53-Regulated Inhibitor of G2 / M Progression. *Molecular Cell*, 1, pp.3–11.
- Hershey, J.W.B., 1991. Translational control in mammalian cells. *Annual review of biochemistry*, 60, pp.717–755.
- Hetz, C., 2012. The unfolded protein response: controlling cell fate decisions under ER stress and beyond. *Nature reviews. Molecular cell biology*, 13(2), pp.89–102.
- Hickson, I. et al., 2004. Identification and Characterization of a Novel and Specific Inhibitor of the Ataxia-Telangiectasia Mutated Kinase ATM. *Cancer Research*, 64(24), pp.9152–9159.
- Hinnebusch, A.G., 2014. The scanning mechanism of eukaryotic translation initiation. *Annual review of biochemistry*, 83, pp.779–812.
- Hinton, T.M. et al., 2007. Functional analysis of individual binding activities of the scaffold protein eIF4G. *Journal of Biological Chemistry*, 282(3), pp.1695–1708.
- Hollstein, M. et al., 1991. p53 Mutations in Human Cancers. *Science*, 253(5), pp.49–53.
- Holz, M.K. & Blenis, J., 2005. Identification of S6 kinase 1 as a novel mammalian target of rapamycin (mTOR)-phosphorylating kinase. *Journal of Biological Chemistry*, 280(28), pp.26089–26093.
- Honda, R., Tanaka, H. & Yasuda, H., 1997. Oncoprotein MDM2 is a ubiquitin ligase E3 for tumor suppressor p53. *FEBS Letters*, 420(1), pp.25–27.
- Horton, L.E. et al., 2002. p53 activation results in rapid dephosphorylation of the eIF4E-binding protein 4E-BP1, inhibition of ribosomal protein S6 kinase and inhibition of translation initiation. *Oncogene*, 21(34), pp.5325–5334.
- Hsu, P.P. et al., 2011. The mTOR-regulated phosphoproteome reveals a mechanism of mTORC1-mediated inhibition of growth factor signaling. *Science*, 332(6035), pp.1317–22.
- Huang, J. et al., 2008. The TSC1-TSC2 complex is required for proper activation of mTOR complex 2. *Molecular and cellular biology*, 28(12), pp.4104–15.
- Hyun, S.-Y. & Jang, Y.-J., 2015. p53 activates G1 checkpoint following DNA damage by doxorubicin during transient mitotic arrest. *Oncotarget*, 6(7), pp.4804–4815.
- Iadevaia, V. et al., 2012. MTOR signaling regulates the processing of pre-rRNA in human cells. *Nucleic Acids Research*, 40(6), pp.2527–2539.
- Ichikawa, Y. et al., 2014. Cardiotoxicity of doxorubicin is mediated through mitochondrial iron accumulation. *Journal of Clinical Investigation*, 124(2), pp.617–630.
- Imataka, H., Gradi, A. & Sonenberg, N., 1998. A newly identified N-terminal amino acid sequence of human eIF4G binds poly(A)-binding protein and functions in poly(A)-

- dependent translation. *EMBO Journal*, 17(24), pp.7480–7489.
- Imataka, H. & Sonenberg, N., 1997. Human eukaryotic translation initiation factor 4G (eIF4G) possesses two separate and independent binding sites for eIF4A. *Molecular and cellular biology*, 17(12), pp.6940–7.
- Inoki, K., Li, Y., et al., 2003. Rheb GTPase is a direct target of TSC2 GAP activity and regulates mTOR signaling. *Genes and Development*, 17(15), pp.1829–1834.
- Inoki, K. et al., 2006. TSC2 Integrates Wnt and Energy Signals via a Coordinated Phosphorylation by AMPK and GSK3 to Regulate Cell Growth. *Cell*, 126(5), pp.955–968.
- Inoki, K. et al., 2002. TSC2 is phosphorylated and inhibited by Akt and suppresses mTOR signalling. *Nature cell biology*, 4(9), pp.648–57.
- Inoki, K., Zhu, T. & Guan, K.L., 2003. TSC2 mediates cellular energy response to control cell growth and survival. *Cell*, 115(5), pp.577–590.
- Jacinto, E. et al., 2004. Mammalian TOR complex 2 controls the actin cytoskeleton and is rapamycin insensitive. *Nature cell biology*, 6(11), pp.1122–1128.
- Jack, M.T. et al., 2004. DNA-dependent Protein Kinase and Checkpoint Kinase 2 Synergistically Activate a Latent Population of p53 upon DNA Damage. *Journal of Biological Chemistry*, 279(15), pp.15269–15273.
- Jackson, J.G. & Pereira-smith, O.M., 2006. Primary and Compensatory Roles for RB Family Members at Cell Cycle Gene Promoters That Are Deacetylated and Downregulated in Doxorubicin-Induced Senescence of Breast Cancer Cells. *Molecular and cellular biology*.
- Jackson, R., Hellen, C. & Pestova, T., 2012. Termination and post-termination events in eukaryotic translation. *Advances in protein chemistry and structural biology*, 86, pp.45–93.
- Jackson, R.J., Hellen, C.U.T. & Pestova, T. V, 2010. The mechanism of eukaryotic translation initiation and principles of its regulation. *Nature reviews. Molecular cell biology*, 11(2), pp.113–27.
- Jackson, S.P. & Bartek, J., 2009. The DNA-damage response in human biology and disease. *Nature*, 461(7267), pp.1071–8.
- Jefferies, H.B. et al., 1994. Rapamycin selectively represses translation of the “polypyrimidine tract” mRNA family. *Proceedings of the National Academy of Sciences of the United States of America*, 91(10), pp.4441–4445.
- Jenen, P.B. & Sehested, M., 1997. DNA topoisomerase II rescue by catalytic inhibitors. *Biochemical Pharmacology*, 54(7), pp.755–759.
- Ji, C. et al., 2010. Exogenous cell-permeable C6 ceramide sensitizes multiple cancer cell lines to Doxorubicin-induced apoptosis by promoting AMPK activation and mTORC1 inhibition. *Oncogene*, 29(50), pp.6557–68.
- Jiang, H.-Y. et al., 2004. Activating transcription factor 3 is integral to the eukaryotic initiation factor 2 kinase stress response. *Molecular and cellular biology*, 24(3), pp.1365–77.
- Jiang, H.Y. & Wek, R.C., 2005. GCN2 phosphorylation of eIF2 α activates NF- κ B in

- response to UV irradiation. *Biochem J*, 385(Pt 2), pp.371–380.
- Johnson, L.F. et al., 1976. Changes in RNA in relation to growth of the fibroblast. IV. Alterations in the production and processing of mRNA and rRNA in resting and growing cells. *Journal of Cell Biology*, 71(3), pp.933–938.
- Jones, R.G. et al., 2005. AMP-activated protein kinase induces a p53-dependent metabolic checkpoint. *Molecular Cell*, 18(3), pp.283–293.
- Julien, L.A. et al., 2010. mTORC1-activated S6K1 phosphorylates Rictor on threonine 1135 and regulates mTORC2 signaling. *Mol Cell Biol*, 30(4), pp.908–921.
- Kalyanaraman, B. et al., 2012. Measuring reactive oxygen and nitrogen species with fluorescent probes: Challenges and limitations. *Free Radical Biology and Medicine*, 52(1), pp.1–6.
- Kapp, L.D. & Lorsch, J.R., 2004. GTP-dependent Recognition of the Methionine Moiety on Initiator tRNA by Translation Factor eIF2. *Journal of Molecular Biology*, 335(4), pp.923–936.
- Kaul, G., Pattan, G. & Rafeequi, T., 2011. Eukaryotic elongation factor-2 (eEF2): its regulation and peptide chain elongation. *Cell biochemistry and function*, 29(3), pp.227–34.
- Keston, A.S. & Brandt, R., 1965. The fluorometric analysis of ultramicro quantities of hydrogen peroxide. *Analytical Biochemistry*, 11(1), pp.1–5.
- Kim, S.H., Zukowski, K. & Novak, R.F., 2009. Rapamycin effects on mTOR signaling in benign, premalignant and malignant human breast epithelial cells. *Anticancer research*, 29(4), pp.1143–50.
- Knebel, A., Morrice, N. & Cohen, P., 2001. A novel method to identify protein kinase substrates: eEF2 kinase is phosphorylated and inhibited by SAPK4/p38 δ . *EMBO Journal*, 20(16), pp.4360–4369.
- Köhler, A. & Hurt, E., 2007. Exporting RNA from the nucleus to the cytoplasm. *Nature reviews. Molecular cell biology*, 8(10), pp.761–73.
- Kong, J. & Lasko, P., 2012. Translational control in cellular and developmental processes. *Nature reviews. Genetics*, 13(6), pp.383–94.
- Kong, M. et al., 2004. The PP2A-Associated Protein 4 Is an Essential Inhibitor of Apoptosis. *Science*, 306, pp.695–698.
- Kozak, M., 1987. An analysis of 5' -noncoding sequences from 699 vertebrate messenger RNAs. *Nucleic Acids Research*, 15(20), pp.8125–8148.
- Kozak, M., 1991. Structural Features in Eukaryotic Messenger-Rnas That Modulate the Initiation of Translation. *Journal of Biological Chemistry*, 266(30), pp.19867–19870.
- Kubbutat, M.H.G., Jones, S.N. & Vousden, K.H., 1997. Regulation of p53 stability by Mdm2. *Nature*, 387(15), pp.299–303.
- Kuilman, T. et al., 2010. The essence of senescence. *Genes and Development*, 24, pp.2463–2479.
- Kumagai, A. et al., 2006. TopBP1 activates the ATR-ATRIP complex. *Cell*, 124(5),

pp.943–955.

- Kumar, P., Hellen, C.U.T. & Pestova, T. V, 2016. Toward the mechanism of eIF4F-mediated ribosomal attachment to mammalian capped mRNAs. *Genes & development*, 30(13), pp.1573–1588.
- Kunz, J. et al., 1993. Target of rapamycin in yeast, TOR2, is an essential phosphatidylinositol kinase homolog required for G1 progression. *Cell*, 73(3), pp.585–596.
- Kurimasa, A. et al., 1999. Requirement for the Kinase Activity of Human DNA-Dependent Protein Kinase Catalytic Subunit in DNA Strand Break Rejoining. *Molecular and cellular biology*, 19(5), pp.3877–3884.
- Kurz, E.U., Douglas, P. & Lees-Miller, S.P., 2004. Doxorubicin activates ATM-dependent phosphorylation of multiple downstream targets in part through the generation of reactive oxygen species. *The Journal of biological chemistry*, 279(51), pp.53272–81.
- Kuznetsov, A. V. et al., 2011. Changes in mitochondrial redox state, membrane potential and calcium precede mitochondrial dysfunction in doxorubicin-induced cell death. *Biochimica et Biophysica Acta - Molecular Cell Research*, 1813(6), pp.1144–1152.
- Lang, F. & Shumilina, E., 2013. Regulation of ion channels by the serum- and glucocorticoid-inducible kinase SGK1. *FASEB Journal*, 27(1), pp.3–12.
- Laplanche, M. & Sabatini, D.M., 2009. mTOR signaling at a glance. *Journal of cell science*, 122(Pt 20), pp.3589–94.
- Laplanche, M. & Sabatini, D.M., 2012. MTOR signaling in growth control and disease. *Cell*, 149(2), pp.274–293.
- Lavin, M.F. & Gueven, N., 2006. The complexity of p53 stabilization and activation. *Cell death and differentiation*, 13(6), pp.941–950.
- Leahy, J.J.J. et al., 2004. Identification of a highly potent and selective DNA-dependent protein kinase (DNA-PK) inhibitor (NU7441) by screening of chromenone libraries. *Bioorganic and Medicinal Chemistry Letters*, 14(24), pp.6083–6087.
- Lebrecht, D. et al., 2007. Dexrazoxane prevents doxorubicin-induced long-term cardiotoxicity and protects myocardial mitochondria from genetic and functional lesions in rats. *British journal of pharmacology*, 151(6), pp.771–8.
- Lee, B.Y. et al., 2006. Senescence-associated β -galactosidase is lysosomal β -galactosidase. *Aging Cell*, 5(2), pp.187–195.
- Lees-Miller, S.P. et al., 1992. Human DNA-activated protein kinase phosphorylates serines 15 and 37 in the amino-terminal transactivation domain of human p53. *Molecular and cellular biology*, 12(11), pp.5041–5049.
- LeFebvre, A.K. et al., 2006. Translation initiation factor eIF4G-1 binds to eIF3 through the eIF3e subunit. *The Journal of biological chemistry*, 281(32), pp.22917–32.
- Di Leonardo, A. et al., 1994. DNA damage triggers a prolonged p53- dependent G arrest and long-term induction of Cipl in normal human fibroblasts. *Genes and Development*, 8, pp.2540–2551.

- Leontieva, O. V. et al., 2013. Dysregulation of the mTOR pathway in p53-deficient mice. *Cancer Biology and Therapy*, 14(12), pp.1182–1188.
- Levesque, A. a et al., 2005. Distinct roles for p53 transactivation and repression in preventing UCN-01-mediated abrogation of DNA damage-induced arrest at S and G2 cell cycle checkpoints. *Oncogene*, 24, pp.3786–3796.
- Li, J. et al., 1997. PTEN, a putative protein tyrosine phosphatase gene mutated in human brain, breast, and prostate cancer. *Science*, 275(5308), pp.1943–7.
- Li, J. & Stern, D.F., 2005. Regulation of CHK2 by DNA-dependent protein kinase. *Journal of Biological Chemistry*, 280(12), pp.12041–12050.
- Lieber, M.R., 2008. The mechanism of human nonhomologous DNA End joining. *Journal of Biological Chemistry*, 283(1), pp.1–5.
- Lim, S. & Kaldis, P., 2013. Cdks, cyclins and CKIs: roles beyond cell cycle regulation. *Development*, 140(15), pp.3079–93.
- Lindahl, T. & Barnes, D.E., 2000. Repair of Endogenous DNA Damage. *Cold Spring Harbor Symposia on Quantitative Biology*, 65, pp.127–133.
- Liu, P. et al., 2013. Sin1 phosphorylation impairs mTORC2 complex integrity and inhibits downstream Akt signalling to suppress tumorigenesis. *Nature cell biology*, 15(11), pp.1340–50.
- Liu, Q. et al., 2000. Chk1 is an essential kinase that is regulated by Atr and required for the G2/M DNA damage checkpoint. *Genes and Development*, 14(12), pp.1448–1459.
- Lomakin, I.B. & Steitz, T. a, 2013. The initiation of mammalian protein synthesis and mRNA scanning mechanism. *Nature*, 500(7462), pp.307–11.
- Long, X. et al., 2005. Rheb binds and regulates the mTOR kinase. *Current Biology*, 15(8), pp.702–713.
- Loveless, T.B. et al., 2015. DNA Damage Regulates Translation through β -TRCP Targeting of CReP. *PLoS genetics*, 11(6), p.e1005292.
- Lowe, S.W. et al., 1993. p53 is required for radiation-induced apoptosis in mouse thymocytes. *Nature*, 362, pp.847–849.
- Lucero, H., Gae, D. & Taccioli, G.E., 2003. Novel localization of the DNA-PK complex in lipid rafts. A putative role in the signal transduction pathway of the ionizing radiation response. *Journal of Biological Chemistry*, 278(24), pp.22136–22143.
- Lüpertz, R. et al., 2010. Dose- and time-dependent effects of doxorubicin on cytotoxicity, cell cycle and apoptotic cell death in human colon cancer cells. *Toxicology*, 271(3), pp.115–121.
- Ma, L. et al., 2005. Phosphorylation and functional inactivation of TSC2 by Erk: Implications for tuberous sclerosis and cancer pathogenesis. *Cell*, 121(2), pp.179–193.
- Maag, D., Algire, M. a & Lorsch, J.R., 2006. Communication between eukaryotic translation initiation factors 5 and 1A within the ribosomal pre-initiation complex plays a role in start site selection. *Journal of molecular biology*, 356(3), pp.724–37.

- Macejak, D. & Sarnow, P., 1991. Internal initiation of translation mediated by the 5' leader of a cellular mRNA. *Nature*, 353, pp.90–94.
- Mader, S. et al., 1995. The translation initiation factor eIF-4E binds to a common motif shared by the translation factor eIF-4 gamma and the translational repressors 4E-binding proteins. *Molecular and cellular biology*, 15(9), pp.4990–7.
- Major, M.L., Lepe, R. & Costa, R.H., 2004. Forkhead box M1B transcriptional activity requires binding of Cdk-cyclin complexes for phosphorylation-dependent recruitment of p300/CBP coactivators. *Molecular and cellular biology*, 24(7), pp.2649–61.
- Manning, B.D. et al., 2002. Identification of the Tuberous Sclerosis Complex-2 Tumor Suppressor Gene Product Tuberin as a Target of the Phosphoinositide 3-Kinase/Akt Pathway. *Molecular cell*, 10, pp.151–162.
- Mao, Y. et al., 2001. 26 S Proteasome-mediated Degradation of Topoisomerase II Cleavable Complexes. *Journal of Biological Chemistry*, 276(44), pp.40652–40658.
- Marechal, A. & Zou, L., 2013. DNA damage sensing by the ATM and ATR kinases. *Cold Spring Harbor Perspectives in Biology*, 5(9), pp.1–17.
- Martin, E. et al., 2009. Evaluation of the topoisomerase II-inactive bisdioxopiperazine ICRF-161 as a protectant against doxorubicin-induced cardiomyopathy. *Toxicology*, 255(1–2), pp.72–79.
- Matsuoka, S., Huang, M. & Elledge, S.J., 1998. Linkage of ATM to cell cycle regulation by the Chk2 protein kinase. *Science*, 282(5395), pp.1893–1897.
- Maya, R. et al., 2001. ATM-dependent phosphorylation of Mdm2 on serine 394: role in p53 activation by DNA damage. *Genes and Development*, 15, pp.1067–1077.
- Maya-Mendoza, a et al., 2014. Immortalised breast epithelia survive prolonged DNA replication stress and return to cycle from a senescent-like state. *Cell death & disease*, 5(7), p.e1351.
- Mayer, C. et al., 2004. mTOR-dependent activation of the transcription factor TIF-IA links rRNA synthesis to nutrient availability. *Genes and Development*, 18(4), pp.423–434.
- McClendon, A.K., Rodriguez, A.C. & Osheroff, N., 2005. Human topoisomerase II α rapidly relaxes positively supercoiled DNA: Implications for enzyme action ahead of replication forks. *Journal of Biological Chemistry*, 280(47), pp.39337–39345.
- McEwen, E. et al., 2005. Heme-regulated inhibitor kinase-mediated phosphorylation of eukaryotic translation initiation factor 2 inhibits translation, induces stress granule formation, and mediates survival upon arsenite exposure. *Journal of Biological Chemistry*, 280(17), pp.16925–16933.
- Meek, D.W., 2009. Tumour suppression by p53: a role for the DNA damage response? *Nature reviews. Cancer*, 9(10), pp.714–723.
- Menendez, D., Inga, A. & Resnick, M. a, 2009. The expanding universe of p53 targets. *Nature reviews. Cancer*, 9(10), pp.724–737.
- Méthot, N., Song, M.S. & Sonenberg, N., 1996. A region rich in aspartic acid, arginine, tyrosine, and glycine (DRYG) mediates eukaryotic initiation factor 4B (eIF4B) self-association and interaction with eIF3. *Molecular and cellular biology*, 16(10),

pp.5328–5334.

- Mi, J. et al., 2009. Activation of DNA-PK by ionizing radiation is mediated by protein phosphatase 6. *PLoS ONE*, 4(2).
- Mihara, M. et al., 2003. p53 Has a Direct Apoptogenic Role at the Mitochondria Results p53 Rapidly Accumulates at Mitochondria of Primary Thymocytes Undergoing γ IR-. , 11, pp.577–590.
- Miyashita, T. & Reed, J.C., 1995. Tumor suppressor p53 is a direct transcriptional activator of the human bax gene. *Cell*, 80, pp.293–299.
- Moutaoufik, M.T. et al., 2014. UVC-induced stress granules in mammalian cells. *PLoS ONE*, 9(11).
- Nakamura, T. et al., 2015. A critical role for PKR complexes with TRBP in immunometabolic regulation and eIF2 α phosphorylation in obesity. *Cell Reports*, 11(2), pp.295–307.
- Nakamura, T. et al., 2010. Double-Stranded RNA-Dependent Protein Kinase Links Pathogen Sensing with Stress and Metabolic Homeostasis. *Cell*, 140(3), pp.338–348.
- Nakano, K. & Vousden, K.H., 2001. PUMA, a novel proapoptotic gene, is induced by p53. *Molecular Cell*, 7(3), pp.683–694.
- Nitiss, J.L., 2009a. DNA topoisomerase II and its growing repertoire of biological functions. *Nature reviews. Cancer*, 9(5), pp.327–337.
- Nitiss, J.L., 2009b. Targeting DNA topoisomerase II in cancer chemotherapy. *Nature reviews. Cancer*, 9(5), pp.338–350.
- Nitiss, K.C. & Nitiss, J.L., 2014. Twisting and ironing: Doxorubicin cardiotoxicity by mitochondrial DNA damage. *Clinical Cancer Research*, 20(18), pp.4737–4739.
- Novoa, I. et al., 2001. Feedback inhibition of the unfolded protein response by GADD34-mediated dephosphorylation of eIF2 α . *The Journal of cell biology*, 153(5), pp.1011–1022.
- Novoa, I. et al., 2003. Stress-induced gene expression requires programmed recovery from translational repression. *EMBO Journal*, 22(5), pp.1180–1187.
- O'Reilly, K.E. et al., 2006. mTOR inhibition induces upstream receptor tyrosine kinase signaling and activates Akt. *Cancer Research*, 66(3), pp.1500–1508.
- Oberer, M., Marintchev, A. & Wagner, G., 2005. Structural basis for the enhancement of eIF4A helicase activity by eIF4G. *Genes and Development*, 19(18), pp.2212–23.
- Ochi, T. et al., 2015. DNA repair. PAXX, a paralog of XRCC4 and XLF, interacts with Ku to promote DNA double-strand break repair. *Science*, 347(6218), pp.185–188.
- Oda, E. et al., 2000. Noxa, a BH3-Only Member of the Bcl-2 Family and Candidate Mediator of p53-Induced Apoptosis. *Science*, 288(5468), pp.1053–1058.
- Oren, M., 2003. Decision making by p53: life, death and cancer. *Cell Death and Differentiation*, 10(4), pp.431–442.
- Orthwein, A. et al., 2014. Mitosis inhibits DNA double-strand break repair to guard

- against telomere fusions. *Science*, 344(6180), pp.189–93.
- Overholtzer, M. et al., 2003. Structure of the topoisomerase II ATPase region and its mechanism of inhibition by the chemotherapeutic agent ICRF-187. *Proceedings of the National Academy of Sciences of the United States of America*, 100(19), pp.10629–10634.
- Pagano, M. et al., 1995. Role of the ubiquitin-proteasome pathway in regulating abundance of the cyclin-dependent kinase inhibitor p27. *Science*, 269(5224), pp.682–5.
- Palou, G. et al., 2010. Cyclin regulation by the S phase checkpoint. *Journal of Biological Chemistry*, 285(34), pp.26431–26440.
- Parmigiani, A. et al., 2014. Sestrins Inhibit mTORC1 Kinase Activation through the GATOR Complex. *Cell Reports*, 9(4), pp.1281–1291.
- Passmore, L. a et al., 2007. The eukaryotic translation initiation factors eIF1 and eIF1A induce an open conformation of the 40S ribosome. *Molecular cell*, 26(1), pp.41–50.
- Paulin, F. et al., 2001. Eukaryotic translation initiation factor 5 (eIF5) acts as a classical GTPase-activator protein. *Current Biology*, 11(1), pp.55–59.
- Peidis, P. et al., 2011. Doxorubicin bypasses the cytoprotective effects of eIF2 α phosphorylation and promotes PKR-mediated cell death. *Cell death and differentiation*, 18(1), pp.145–54.
- Pelletier, J. & Sonenberg, N., 1988. Internal initiation of translation of eukaryotic mRNA directed by a sequence derived from poliovirus RNA. *Nature*, 334(28), pp.320–325.
- Pende, M. et al., 2004. S6K1-/-/S6K2-/- Mice Exhibit Preinatal Lethality and Rapamycin-Sensitive 5' -Terminal Oligopyrimidine mRNA Translation and Reveal a Mitogen-Activated Protein Kinase-Dependent S6 Kinase Pathway. *Molecular and Cellular Biology*, 24(8), pp.3112–3124.
- Pestova, T. V et al., 2000. The joining of ribosomal subunits in eukaryotes requires eIF5B. *Nature*, 403(6767), pp.332–5.
- Pestova, T. V, Borukhov, S.I. & Hellen, C.U., 1998. Eukaryotic ribosomes require initiation factors 1 and 1A to locate initiation codons. *Nature*, 394(6696), pp.854–859.
- Petroulakis, E. et al., 2009. p53-Dependent Translational Control of Senescence and Transformation via 4E-BPs. *Cancer Cell*, 16(5), pp.439–446.
- Piguet, A.C. et al., 2008. Inhibition of mTOR in combination with doxorubicin in an experimental model of hepatocellular carcinoma. *Journal of Hepatology*, 49(1), pp.78–87.
- Pisareva, V.P. et al., 2008. Translation Initiation on Mammalian mRNAs with Structured 5'UTRs Requires DExH-Box Protein DHX29. *Cell*, 135(7), pp.1237–1250.
- Polo, S.E. & Jackson, S.P., 2011. Dynamics of DNA damage response proteins at DNA breaks: A focus on protein modifications. *Genes and Development*, 25(5), pp.409–433.

- Pommier, Y. et al., 2010. DNA topoisomerases and their poisoning by anticancer and antibacterial drugs. *Chemistry and Biology*, 17(5), pp.421–433.
- Pommier, Y., 2006. Topoisomerase I inhibitors: camptothecins and beyond. *Nature reviews. Cancer*, 6(10), pp.789–802.
- Powley, I.R. et al., 2009. Translational reprogramming following UVB irradiation is mediated by DNA-PKcs and allows selective recruitment to the polysomes of mRNAs encoding DNA repair enzymes. *Genes and Development*, 23(10), pp.1207–20.
- Proudfoot, N.J., 2011. Ending the message : poly (A) signals then and now. *Genes & development*, 25, pp.1770–1782.
- Pullen, N. et al., 1998. Phosphorylation and activation of p70s6k by PDK1. *Science*, 279(5351), pp.707–710.
- Pyronnet, S., Dostie, J. & Sonenberg, N., 2001. Suppression of cap-dependent translation in mitosis. *Genes and Development*, 15(16), pp.2083–2093.
- Qiu, H. et al., 2001. The tRNA-binding moiety in GCN2 contains a dimerization domain that interacts with the kinase domain and is required for tRNA binding and kinase activation. *EMBO Journal*, 20(6), pp.1425–1438.
- Rabl, J. et al., 2011. Crystal structure of the eukaryotic 40S ribosomal subunit in complex with initiation factor 1. *Science*, 331(6018), pp.730–6.
- Rafie-Kolpin, M., Han, A.P. & Chen, J.J., 2003. Autophosphorylation of threonine 485 in the activation loop is essential for attaining eIF2-alpha kinase activity of HRI. *Biochemistry*, 42(21), pp.6536–6544.
- Rajagopalan, S. et al., 1988. Adriamycin-induced Free Radical Formation in the Perfused Rat Heart : Implications for Cardiotoxicity. *Cancer Research*, 48, pp.4766–4769.
- Rajesh, K. et al., 2015. Phosphorylation of the translation initiation factor eIF2 α at serine 51 determines the cell fate decisions of Akt in response to oxidative stress. *Cell death & disease*, 6(1), p.e1591.
- Rastogi, R.P. et al., 2010. Molecular Mechanisms of Ultraviolet Radiation-Induced DNA Damage and Repair. *Journal of Nucleic Acids*, 2010, pp.1–32.
- Raught, B. et al., 2004. Phosphorylation of eucaryotic translation initiation factor 4B Ser422 is modulated by S6 kinases. *The EMBO journal*, 23(8), pp.1761–1769.
- Reaper, P.M. et al., 2011. Selective killing of ATM- or p53-deficient cancer cells through inhibition of ATR. *Nature Chemical Biology*, 7(7), pp.428–430.
- Rebbaa, A. et al., 2003. Caspase inhibition switches doxorubicin-induced apoptosis to senescence. *Oncogene*, 22(18), pp.2805–11.
- Richter, J.D. & Collier, J., 2015. Pausing on Polyribosomes: Make Way for Elongation in Translational Control. *Cell*, 163(2), pp.292–300.
- Riley, T. et al., 2008. Transcriptional control of human p53-regulated genes. *Nature reviews. Molecular cell biology*, 9(5), pp.402–412.
- Rodnina, M. V., 2013. Biochemistry. Translocation in action. *Science*, 340(6140),

pp.1534–5.

- Rogers, G.W. et al., 2001. Modulation of the helicase activity of eIF4A by eIF4B, eIF4H, and eIF4F. *The Journal of biological chemistry*, 276(33), pp.30914–22.
- Rogers, G.W., Richter, N.J. & Merrick, W.C., 1999. Biochemical and kinetic characterization of the RNA helicase activity of eukaryotic initiation factor 4A. *Journal of Biological Chemistry*, 274(18), pp.12236–12244.
- Romano, M.F. et al., 2004. Rapamycin inhibits doxorubicin-induced NF- κ B/Rel nuclear activity and enhances the apoptosis of melanoma cells. *European Journal of Cancer*, 40(18), pp.2829–2836.
- Ron, D. & Harding, H.P., 2012. Protein-folding homeostasis in the endoplasmic reticulum and nutritional regulation. *Cold Spring Harbor Perspectives in Biology*, 4(12).
- Ron, D. & Walter, P., 2007. Signal integration in the endoplasmic reticulum unfolded protein response. *Nat Rev Mol Cell Biol*, 8(7), pp.519–529.
- Roux, P.P. et al., 2007. RAS/ERK signaling promotes site-specific ribosomal protein S6 phosphorylation via RSK and stimulates cap-dependent translation. *The Journal of biological chemistry*, 282(19), pp.14056–64.
- Roy, S. et al., 2015. XRCC4/XLF Interaction Is Variably Required for DNA Repair and Is Not Required for Ligase IV Stimulation. *Molecular and Cellular Biology*, 35(17), pp.3017–3028.
- Rozen, F. et al., 1990. Bidirectional RNA helicase activity of eucaryotic translation initiation factors 4A and 4F. *Molecular and cellular biology*, 10(3), pp.1134–44.
- Ruvinsky, I. et al., 2005. Ribosomal protein S6 phosphorylation is a determinant of cell size and glucose homeostasis. *Genes and Development*, 19(18), pp.2199–2211.
- Sabatini, D.M., 2006. mTOR and cancer: insights into a complex relationship. *Nature Reviews Cancer*, 6(September), pp.729–734.
- Sabatini, D.M. et al., 1994. RAFT1: A mammalian protein that binds to FKBP12 in a rapamycin-dependent fashion and is homologous to yeast TORs. *Cell*, 78(1), pp.35–43.
- Saini, A.K. et al., 2014. Eukaryotic translation initiation factor eIF5 promotes the accuracy of start codon recognition by regulating Pi release and conformational transitions of the preinitiation complex. *Nucleic acids research*, 42(15), pp.9623–9640.
- Sancak, Y. et al., 2010. Ragulator-rag complex targets mTORC1 to the lysosomal surface and is necessary for its activation by amino acids. *Cell*, 141(2), pp.290–303.
- Sancak, Y. et al., 2008. The Rag GTPases bind raptor and mediate amino acid signaling to mTORC1. *Science*, 320(5882), pp.1496–501.
- Sanchez, Y. et al., 1997. Conservation of the Chk1 Checkpoint Pathway in Mammals: Linkage of DNA Damage to Cdk Regulation Through Cdc25. *Science*, 277(5331), pp.1497–1501.
- Sano, R. & Reed, J.C., 2013. ER stress-induced cell death mechanisms. *Biochimica et*

- Biophysica Acta - Molecular Cell Research*, 1833(12), pp.3460–3470.
- Sarbassov, D.D. et al., 2005. Phosphorylation and regulation of Akt/PKB by the rictor-mTOR complex. *Science*, 307(5712), pp.1098–1101.
- Sarbassov, D.D. et al., 2006. Prolonged Rapamycin Treatment Inhibits mTORC2 Assembly and Akt/PKB. *Molecular Cell*, 22(2), pp.159–168.
- Sarbassov, D.D. et al., 2004. Rictor, a Novel Binding Partner of mTOR, Defines a Rapamycin-Insensitive and Raptor-Independent Pathway that Regulates the Cytoskeleton. *Current Biology*, 14, pp.1296–1302.
- Satyanarayana, A. & Kaldis, P., 2009. Mammalian cell-cycle regulation: several Cdk, numerous cyclins and diverse compensatory mechanisms. *Oncogene*, 28(33), pp.2925–39.
- Sekine, Y. et al., 2015. Stress responses. Mutations in a translation initiation factor identify the target of a memory-enhancing compound. *Science*, 348(6238), pp.1027–30.
- Selvarajah, J. et al., 2014. DNA damage-induced S and G2 / M cell cycle arrest requires mTORC2-dependent regulation of Chk1. *Oncotarget*, 6(1), pp.427–440.
- Shah, O.J., Wang, Z. & Hunter, T., 2004. Inappropriate Activation of the TSC/Rheb/mTOR/S6K Cassette Induces IRS1/2 Depletion, Insulin Resistance, and Cell Survival Deficiencies. *Current Biology*, 14, pp.1650–1656.
- Shahbazian, D. et al., 2006. The mTOR/PI3K and MAPK pathways converge on eIF4B to control its phosphorylation and activity. *The EMBO journal*, 25(12), pp.2781–91.
- Shatkin, A.J., 1976. Capping of Eucaryotic mRNAs Review. *Cell*, 1976(December), pp.645–653.
- She, Q.-B. et al., 2010. 4E-BP1 is a key effector of the oncogenic activation of the AKT and ERK signaling pathways that integrates their function in tumors. *Cancer cell*, 18(1), pp.39–51.
- Sherr, C.J. & Roberts, J.M., 1999. CDK inhibitors: positive and negative regulators of G1-phase progression. *Genes and Development*, 13(12), pp.1501–1512.
- Shi, W.-Y. et al., 2012. Therapeutic metformin/AMPK activation blocked lymphoma cell growth via inhibition of mTOR pathway and induction of autophagy. *Cell death & disease*, 3(3), p.e275.
- Shieh, S.Y. et al., 1997. DNA damage-induced phosphorylation of p53 alleviates inhibition by MDM2. *Cell*, 91(3), pp.325–334.
- Shieh, S.Y. et al., 2000. The human homologs of checkpoint kinases Chk1 and Cds1 (Chk2) phosphorylate, p53 at multiple DNA damage-inducible sites. *Genes and Development*, 14(3), pp.289–300.
- Shiloh, Y. & Ziv, Y., 2013. The ATM protein kinase: regulating the cellular response to genotoxic stress, and more. *Nature reviews. Molecular cell biology*, 14(4), pp.197–210.
- Shimobayashi, M. & Hall, M.N., 2014. Making new contacts: the mTOR network in metabolism and signalling crosstalk. *Nature reviews. Molecular cell biology*, 15(3), pp.155–62.

- Shimura, T. et al., 2007. DNA-PK Is Involved in Repairing a Transient Surge of DNA Breaks Induced by Deceleration of DNA Replication. *Journal of molecular biology*, 367(3), pp.665–680.
- Shin, B.-S. et al., 2002. Uncoupling of initiation factor eIF5B/IF2 GTPase and translational activities by mutations that lower ribosome affinity. *Cell*, 111(7), pp.1015–25.
- Shiyanov, P. et al., 1996. p21 Disrupts the interaction between cdk2 and the E2F-p130 complex. *Molecular and cellular biology*, 16(3), pp.737–44.
- Sidrauski, C. et al., 2013. Pharmacological brake-release of mRNA translation enhances cognitive memory. *eLife*, 2013(2), pp.1–22.
- Sidrauski, C., Tsai, J.C., et al., 2015. Pharmacological dimerization and activation of the exchange factor eIF2B antagonizes the integrated stress response. *eLife*, 2015(4), pp.1–27.
- Sidrauski, C., McGeachy, A.M., et al., 2015. The small molecule ISRIB reverses the effects of eIF2 α phosphorylation on translation and stress granule assembly. *eLife*, 4, pp.1–16.
- Sirbu, B.M. & Cortez, D., 2013. DNA damage response: three levels of DNA repair regulation. *Cold Spring Harbor perspectives in biology*, 5(8), pp.1–18.
- Siridechadilok, B. et al., 2005. Structural roles for human translation factor eIF3 in initiation of protein synthesis. *Science*, 310(5753), pp.1513–5.
- Siu, W.Y., Yam, C.H. & Poon, R.Y.C., 1999. G1 versus G2 cell cycle arrest after adriamycin-induced damage in mouse Swiss3T3 cells. *FEBS Letters*, 461(3), pp.299–305.
- Sliwinska, M. a et al., 2009. Induction of senescence with doxorubicin leads to increased genomic instability of HCT116 cells. *Mechanisms of ageing and development*, 130(1–2), pp.24–32.
- Smith, E.M. & Proud, C.G., 2008. cdc2-cyclin B regulates eEF2 kinase activity in a cell cycle- and amino acid-dependent manner. *The EMBO journal*, 27(7), pp.1005–16.
- Sokabe, M. & Fraser, C.S., 2014. Human eukaryotic initiation factor 2 (eIF2)-GTP-Met-tRNAi ternary complex and eIF3 Stabilize the 43 S preinitiation complex. *Journal of Biological Chemistry*, 289(46), pp.31827–31836.
- Somers, J. et al., 2015. A common polymorphism in the 5' UTR of ERCC5 creates an upstream ORF that confers resistance to platinum-based chemotherapy. *Genes and Development*, 29(18), pp.1891–1896.
- Sonenberg, N. et al., 1979. Eukaryotic mRNA cap binding protein: purification by affinity chromatography on sepharose-coupled m7GDP. *Proceedings of the National Academy of Sciences of the United States of America*, 76(9), pp.4345–4349.
- Sonenberg, N. & Hinnebusch, A.G., 2009. Regulation of translation initiation in eukaryotes: mechanisms and biological targets. *Cell*, 136(4), pp.731–45.
- Spahn, C.M.T. et al., 2004. Domain movements of elongation factor eEF2 and the eukaryotic 80S ribosome facilitate tRNA translocation. *The EMBO journal*, 23(5), pp.1008–19.

- Spriggs, K. a et al., 2008. Re-programming of translation following cell stress allows IRES-mediated translation to predominate. *Biology of the cell*, 100(1), pp.27–38.
- Srivastava, S.P., Kumar, K.U. & Kaufman, R.J., 1998. Phosphorylation of Eukaryotic Translation Initiation Factor 2 Mediates Apoptosis in Response to Activation of the Double-stranded RNA-dependent Protein Kinase. *Journal of Biological Chemistry*, 273(4), pp.2416–2423.
- Stephens, L. et al., 1998. Protein kinase B kinases that mediate phosphatidylinositol 3,4,5- trisphosphate-dependent activation of protein kinase B. *Science*, 279(5351), pp.710–714.
- Stommel, J.M. & Wahl, G.M., 2004. Accelerated MDM2 auto-degradation induced by DNA-damage kinases is required for p53 activation. *The EMBO journal*, 23(7), pp.1547–56.
- Takagi, M. et al., 2005. Regulation of p53 translation and induction after DNA damage by ribosomal protein L26 and nucleolin. *Cell*, 123(1), pp.49–63.
- Takano, A. et al., 2001. Mammalian target of rapamycin pathway regulates insulin signaling via subcellular redistribution of insulin receptor substrate 1 and integrates nutritional signals and metabolic signals of insulin. *Molecular and Cellular Biology*, 21(15), pp.5050–62.
- Tee, A.R. & Proud, C.G., 2000. DNA-damaging agents cause inactivation of translational regulators linked to mTOR signalling. *Oncogene*, 1.
- Tenkerian, C. et al., 2015. mTORC2 balances Akt activation and eIF2alpha serine 51 phosphorylation to promote survival under stress. *Molecular Cancer Research*, 1(8), pp.1377–1388.
- Tewey, K. et al., 1984. Adriamycin-induced DNA damage mediated by mammalian DNA topoisomerase II. *Science*, 226, pp.466–468.
- Thoreen, C.C. et al., 2012. A unifying model for mTORC1-mediated regulation of mRNA translation. *Nature*, 485(7396), pp.109–113.
- Thoreen, C.C. et al., 2009. An ATP-competitive mammalian target of rapamycin inhibitor reveals rapamycin-resistant functions of mTORC1. *Journal of Biological Chemistry*, 284(12), pp.8023–8032.
- Tibbetts, R.S. et al., 1999. A role for ATR in the DNA damage-induced phosphorylation of p53. *Genes and Development*, 13(2), pp.152–157.
- Tsukiyama-Kohara, K. et al., 2001. Adipose tissue reduction in mice lacking the translational inhibitor 4E-BP1. *Nature medicine*, 7(10), pp.1128–1132.
- Unbehaun, A. et al., 2004. Release of initiation factors from 48S complexes during ribosomal subunit joining and the link between establishment of codon – anticodon base-pairing and hydrolysis of eIF2-bound GTP. *Genes and Development*, 18, pp.3078–3093.
- Uziel, T. et al., 2003. Requirement of the MRN complex for ATR activation by DNA damage. *The EMBO journal*, 22(20).
- Vassilev, L.T. et al., 2004. In Vivo Activation of the p53 Pathway by Small-Molecule Antagonists of MDM2. *Science*, 303(5659), pp.844–848.

- Vattem, K.M., Staschke, K.A. & Wek, R.C., 2001. Mechanism of activation of the double-stranded-RNA-dependent protein kinase, PKR. *European Journal of Biochemistry*, 268(13), pp.3674–3684.
- Vattem, K.M. & Wek, R.C., 2004. Reinitiation involving upstream ORFs regulates ATF4 mRNA translation in mammalian cells. *Proceedings of the National Academy of Sciences of the United States of America*, 101(31), pp.11269–74.
- Veuger, S.J. et al., 2003. Radiosensitization and DNA Repair Inhibition by the Combined Use of Novel Inhibitors of DNA-dependent Protein Kinase and Poly(ADP-Ribose) Polymerase-1. *Cancer Research*, 63, pp.6008–6015.
- Vousden, K.H. & Ryan, K.M., 2009. P53 and Metabolism. *Nature reviews. Cancer*, 9(10), pp.691–700.
- Wade Harper, J. et al., 1993. The p21 Cdk-Interacting Protein Cip1 Is a Potent Inhibitor of G1 Cyclin-Dependent Kinases. *Cell*, 75, pp.805–816.
- Waga, S. et al., 1994. The p21 inhibitor of cyclin-dependent kinases controls DNA replication by interaction with PCNA. *Nature*, 369, pp.574–578.
- Waldman, T., Kinzler, K.W. & Vogelstein, B., 1995. P21 Is Necessary for the P53-Mediated G(1) Arrest in Human Cancer-Cells. *Cancer Research*, 55(22), pp.5187–5190.
- Wang, H. & Kochevar, I.E., 2005. Involvement of UVB-induced reactive oxygen species in TGF- β biosynthesis and activation in keratinocytes. *Free Radical Biology and Medicine*, 38(7), pp.890–897.
- Wang, J.C., 2002. Cellular roles of DNA topoisomerases: a molecular perspective. *Nature reviews. Molecular cell biology*, 3(6), pp.430–440.
- Wang, S. et al., 2015. Metabolism. Lysosomal amino acid transporter SLC38A9 signals arginine sufficiency to mTORC1. *Science*, 347(6218), pp.188–194.
- Wang, S., Song, P. & Zou, M.H., 2012. Inhibition of AMP-activated protein kinase α (AMPK- α) by doxorubicin accentuates genotoxic stress and cell death in mouse embryonic fibroblasts and cardiomyocytes: Role of p53 and SIRT1. *Journal of Biological Chemistry*, 287(11), pp.8001–8012.
- Wang, X. et al., 2005. Distinct Signaling Events Downstream of mTOR Cooperate To Mediate the Effects of Amino Acids and Insulin on Initiation Factor 4E-Binding Proteins. *Molecular and cellular biology*, 25(7), pp.2558–2572.
- Wang, X. et al., 2001. Regulation of elongation factor 2 kinase by p90(RSK1) and p70 S6 kinase. *The EMBO journal*, 20(16), pp.4370–9.
- Wang, X. et al., 2001. Regulation of elongation factor 2 kinase by p90 RSK1 and p70 S6 kinase. *EMBO Journal*, 20(16).
- Wang, X.Q. et al., 2006. ATR Dependent Activation of Chk2. *Journal of cellular physiology*, 208(1), pp.613–619.
- Watson, J. V, Chambers, S.H. & Smith, P.J., 1987. With a Definable G1 Peak. *Cytometry*, 8, pp.1–8.
- Webb, B.L.J. & Proud, C.G., 1997. Eukaryotic initiation factor 2B (eIF2B). *International Journal of Biochemistry and Cell Biology*, 29(10), pp.1127–1131.

- Wells, S.E. et al., 1998. Circularization of mRNA by eukaryotic translation initiation factors. *Molecular cell*, 2, pp.135–140.
- Wengrod, J. et al., 2015. Phosphorylation of eIF2 α triggered by mTORC1 inhibition and PP6C activation is required for autophagy and is aberrant in PP6C-mutated melanoma. *Science signaling*, 8(367), p.ra27.
- Wu, S. et al., 2002. Ultraviolet light inhibits translation through activation of the unfolded protein response kinase PERK in the lumen of the endoplasmic reticulum. *Journal of Biological Chemistry*, 277(20), pp.18077–18083.
- Xiao, Z. et al., 2003. Chk1 mediates S and G2 arrests through Cdc25A degradation in response to DNA-damaging agents. *Journal of Biological Chemistry*, 278(24), pp.21767–21773.
- Yajima, H. et al., 2009. DNA Double-Strand Break Formation upon UV-Induced Replication Stress Activates ATM and DNA-PKcs Kinases. *Journal of Molecular Biology*, 385(3), pp.800–810.
- Yang, F. et al., 2014. Doxorubicin, DNA torsion, and chromatin dynamics. *Biochimica et Biophysica Acta*, 1845(1), pp.84–89.
- Young, A.R.J. et al., 2009. Autophagy mediates the mitotic senescence transition. *Genes and Development*, 23(7), pp.798–803.
- Yu, J. & Zhang, L., 2005. The transcriptional targets of p53 in apoptosis control. *Biochemical and Biophysical Research Communications*, 331(3), pp.851–858.
- Yu, Y. et al., 2011. Phosphoproteomic Analysis Identifies Grb10 as an mTORC1 Substrate That Negatively Regulates Insulin Signaling. *Science*, 332(6035), pp.1322–1326.
- Yu, Y. et al., 2009. Position of eukaryotic translation initiation factor eIF1A on the 40S ribosomal subunit mapped by directed hydroxyl radical probing. *Nucleic Acids Research*, 37(15), pp.5167–82.
- Zhan, K. et al., 2002. Phosphorylation of eukaryotic initiation factor 2 by heme-regulated inhibitor kinase-related protein kinases in *Schizosaccharomyces pombe* is important for resistance to environmental stresses. *Molecular and cellular biology*, 22(20), pp.7134–46.
- Zhan, Q. et al., 1999. Association with Cdc2 and inhibition of Cdc2/Cyclin B1 kinase activity by the p53-regulated protein Gadd45. *Oncogene*, 18, pp.2892–2900.
- Zhang, H. et al., 2007. PDGFRs are critical for PI3K/Akt activation and negatively regulated by mTOR. *Journal of Clinical Investigation*, 117(3), pp.730–738.
- Zhang, P. et al., 2002. The GCN2 eIF2 α kinase is required for adaptation to amino acid deprivation in mice. *Molecular and cellular biology*, 22(19), pp.6681–8.
- Zhang, Y. & Lu, H., 2009. Signaling to p53: Ribosomal Proteins Find Their Way. *Cancer Cell*, 16(5), pp.369–377.
- Zhou, S., Palmeira, C.M. & Wallace, K.B., 2001. Doxorubicin-induced persistent oxidative stress to cardiac myocytes. *Toxicology Letters*, 121(3), pp.151–157.
- Zhouravleva, G. et al., 1995. Termination of translation in eukaryotes is governed by two interacting polypeptide chain release factors, eRF1 and eRF3. *The EMBO*

- journal*, 14(16), pp.4065–4072.
- Zhu, W. et al., 2009. Acute doxorubicin cardiotoxicity is associated with p53-induced inhibition of the mammalian target of rapamycin pathway. *Circulation*, 119(1), pp.99–106.
- Zilfou, J.T. & Lowe, S.W., 2009. Tumor Suppressive Functions of p53. *Cold Spring Harbor Perspectives in Biology*, pp.1–13.
- Zimmerman, W.C. & Erikson, R.L., 2007. Polo-like kinase 3 is required for entry into S phase. *Proceedings of the National Academy of Sciences of the United States of America*, 104(6), pp.1847–52.
- Zinzalla, V. et al., 2011. Activation of mTORC2 by association with the ribosome. *Cell*, 144(5), pp.757–768.
- Zoncu, R. et al., 2011. mTORC1 Senses Lysosomal Amino Acids Through an Inside-Out Mechanism That Requires the Vacuolar H⁺-ATPase. *Science*, 334(November), pp.678–683.
- Zou, L. & Elledge, S.J., 2003. Sensing DNA damage through ATRIP recognition of RPA-ssDNA complexes. *Science*, 300(June), pp.1542–1548.